




Publicly Accessible Penn Dissertations

1-1-2014

Ebna1-Specific T Cell Responses During Persistent Rhesus Lcv infection and The Development of a Novel Therapeutic Prototype Vaccine for Ebv-Associated Diseases

Rachel Mandy Leskowitz
University of Pennsylvania, RLeskowitz@gmail.com

Follow this and additional works at: <http://repository.upenn.edu/edissertations>

 Part of the [Allergy and Immunology Commons](#), [Cell Biology Commons](#), [Immunology and Infectious Disease Commons](#), [Medical Immunology Commons](#), and the [Virology Commons](#)

Recommended Citation

Leskowitz, Rachel Mandy, "Ebna1-Specific T Cell Responses During Persistent Rhesus Lcv infection and The Development of a Novel Therapeutic Prototype Vaccine for Ebv-Associated Diseases" (2014). *Publicly Accessible Penn Dissertations*. 1343.
<http://repository.upenn.edu/edissertations/1343>

This paper is posted at ScholarlyCommons. <http://repository.upenn.edu/edissertations/1343>
For more information, please contact libraryrepository@pobox.upenn.edu.

Ebna1-Specific T Cell Responses During Persistent Rhesus Lcv infection and The Development of a Novel Therapeutic Prototype Vaccine for Ebv-Associated Diseases

Abstract

The impact of EBV on human health is substantial, but vaccines that prevent primary EBV infections or treat EBV-associated diseases are not yet available. The Epstein-Barr nuclear antigen 1 (EBNA1) is an important target for vaccination because it is the only protein expressed in all forms of latency and in all EBV-associated malignancies. The overarching goal throughout this dissertation was to determine if EBNA1 is a suitable target for vaccine development. This was addressed in two ways. First, because an improved understanding of EBNA1-specific T cell responses benefits EBV vaccine development, we characterized responses against EBNA1 of the EBV-homologous rhesus lymphocryptovirus (rhLCV) in naturally infected rhesus macaques. We assessed frequency, phenotype, and cytokine production profiles of rhesus (rh)EBNA1-specific T cells by intracellular cytokine staining (ICS) and polychromatic flow cytometry. We found that most naturally infected animals had CD4⁺ and/or CD8⁺ T cells against rhEBNA1 and rhBZLF1, an immediate-early lytic phase antigen of rhLCV. Peptide-specific CD8⁺ T cells showed a more activated effector phenotype, while most peptide-specific CD4⁺ T cells exhibited a resting central memory phenotype. T cells were highly functional and produced various combinations of the cytokines IFN- γ , IL-2, and TNF- α . The differentiation status and functional profiles of rhEBNA1-specific T cells suggests they are not impaired by chronic exposure to low levels of antigen, and rhEBNA1-specific T cells therefore represent a viable population to target through vaccination. Similarities between our findings and the human response further validate the rhLCV model for studying chronic EBV infection and for pre-clinical vaccine development. We then asked if vaccination could expand functional rhEBNA1-specific T cells during persistent rhLCV infection. To test this, we developed two serologically distinct replication-defective adenoviral vectors that expressed chimeric rhEBNA1 constructs fused to functional and non-functional versions of Herpes Simplex Virus- glycoprotein D (HSV-gD). HSV-gD has been shown to augment T cell responses by inhibiting the immunosuppressive Herpes Virus Entry Mediator (HVEM) pathway during T cell activation. After confirmation of vaccine specificity and antigenicity *in vitro*, rhesus macaques were vaccinated in a prime-boost regimen, and responses in peripheral blood were measured by ICS and polychromatic flow cytometry. Importantly, we found that vaccination induced the expansion of highly functional rhEBNA1-specific CD8⁺ and CD4⁺ T cells *in vivo*, regardless of HSV-gD binding ability. Vaccination did not increase rhBZLF1-specific T cell responses, thus indicating that rhEBNA1-specific responses were vaccine-driven. Overall, these results serve as important proof-of-principle analyses of a therapeutic EBNA1-based vaccine regimen and demonstrate that EBNA1 is a viable target that warrants exploration in future vaccine studies.

Degree Type

Dissertation

Degree Name

Doctor of Philosophy (PhD)

Graduate Group

Cell & Molecular Biology

First Advisor

Hildegund C. Ertl

Keywords

BZLF1, EBNA1, EBV, EBV vaccine, LCV

Subject Categories

Allergy and Immunology | Cell Biology | Immunology and Infectious Disease | Medical Immunology |
Virology

EBNA1-SPECIFIC T CELL RESPONSES DURING PERSISTENT RHESUS LCV
INFECTION AND THE DEVELOPMENT OF A NOVEL THERAPEUTIC
PROTOTYPE VACCINE FOR EBV-ASSOCIATED DISEASES

Rachel Mandy Leskowitz

A DISSERTATION

in

Cell and Molecular Biology

Presented to the Faculties of the University of Pennsylvania

in

Partial Fulfillment of the Requirements for the

Degree of Doctor of Philosophy

2014

Supervisor of Dissertation

Hildegund C.J. Ertl, M.D.
Caspar Wistar Professor in Vaccine Research

Graduate Group Chairperson

Daniel S. Kessler, Ph.D.
Associate Professor of Cell and Developmental Biology

Dissertation Committee

Michael R. Betts, Ph.D., Associate Professor of Microbiology
Jean D. Boyer, Ph.D., Research Associate Professor of Pathology and Laboratory Medicine
Paul M. Lieberman, Ph.D., Professor of Gene Expression and Regulation, The Wistar Institute
Frederick C. Wang, M.D., Professor of Microbiology and Immunobiology, Harvard Medical School

EBNA1-SPECIFIC T CELL RESPONSES DURING PERSISTENT RHESUS LCV INFECTION
AND THE DEVELOPMENT OF A NOVEL THERAPEUTIC PROTOTYPE VACCINE FOR EBV-
ASSOCIATED DISEASES

COPYRIGHT

2014

Rachel Mandy Leskowitz

This work is licensed under the
Creative Commons Attribution-
NonCommercial-ShareAlike 4.0
International License

To view a copy of this license, visit

<http://creativecommons.org/licenses/by-nc-sa/4.0/>.

This dissertation is dedicated to the many teachers and mentors I've had throughout the years who have fostered my love of science. Thank you for nurturing my endless curiosities, encouraging me to continue asking questions, and exposing me to an exciting world of constant learning and discovery.

In loving memory of my Aunt, Harriet F. Goldfarb, one of the most generous and compassionate people I knew. Her positive attitude towards life, even in the face of so much adversity, was truly inspirational, and I know she would have been proud to see me reach this milestone.

ACKNOWLEDGEMENTS

Pursuing my doctorate degree has in many ways been like running a marathon—enduring hills, valleys, roadblocks, and hurdles along the way. The intense training and preparation has required a tremendous amount of focus, energy, commitment, and perseverance. The process has been physically, emotionally, and mentally challenging, but also extremely rewarding, and I have enjoyed running this race very much. I couldn't have done it without the guidance and support of many individuals.

To my advisor, Gundi Ertl, thank you for your support and mentorship, and for your dedication to training and educating the next generation of scientists. Despite your busy schedule, you are always available for your students—whether reviewing data, discussing experiments, troubleshooting, or initiating stimulating conversation. I feel very fortunate to have an advisor who is genuinely interested in my success. Thank you for giving me the independence to grow as a scientist, while always remaining interested and involved in my academic endeavors. Your passion and enthusiasm are contagious, and you have been a wonderful role model as a strong and powerful woman in science.

I would also like to thank my thesis committee members: Dr. Michael Betts, Dr. Jean Boyer, Dr. Paul Lieberman, and Dr. Frederick Wang. Thanks for all of your helpful advice, insight, feedback, and direction. It was a pleasure working with and getting to know each of you, and I appreciate all of the long hours you spent in my committee meetings. I would especially like to thank Fred, who patiently endured many long hours on the phone with me discussing data, publications, and the art of science writing. Thank you for challenging me to think critically and speak scientifically and for talking me off the ledge during a moment of weakness. Your support, guidance, and enthusiasm have been a source of motivation. This work would also not have been possible without the additional guidance and collaboration from teams at Harvard University, Emory University, and the Wistar Institute- thank you for your various contributions.

To all members of the Ertl lab, past and present, in one way or another you have all helped me reach this point. Thank you for making the Ertl lab a collaborative and fun working

environment and for all of your support throughout the years. To my fellow Ertl lab graduate students, thanks for listening to my presentations to the point that you could recite them back to me. Working towards my doctorate has been both challenging and rewarding, and experiencing this with a group of individuals who can truly relate to every moment of triumph and frustration has been wonderful.

Finally, I feel very lucky to have such wonderful family and friends, all of who supported me throughout this entire process. First and foremost, I'd like to thank my parents for your endless and unconditional love and support. Your continuous and unwavering faith in my abilities as well as your interest and enthusiasm in my graduate career have always been a source of motivation and inspiration. I would also like to thank my siblings, Matt and Ali, who are two of the most brilliant people I know. You've been sources of inspiration for me throughout this journey. Matt, you may have beat me to the title "Dr. Leskowitz" by a few short months, but my degree is better than yours! (Just kidding.) I'd also like to thank all of my friends for being so understanding of my erratic schedule, for picking me up from the lab late at night, and for never questioning my inability to answer the phone while at lab. Ashley, Sydnie, and Rachel, you've been a huge part of my support system these past few years and a wonderful source of encouragement. Sydnie, my forever friend and running partner, thanks for helping me prepare the many delicious treats—from monkey cupcakes to pie-chart cookies—for lab holiday parties and committee meetings. You are one of the most generous people I know, and your support throughout these years has been irreplaceable. Brian, thanks for putting things into perspective during my outbursts of frustration and for being a constant source of calm in my life. I could always count on you to bring me back to reality when stress threatened to sweep me away. And last, but certainly not least, I need to thank a very special man named Jeff, who has been a constant source of love and support for as long as I can remember.

ABSTRACT

EBNA1-SPECIFIC T CELL RESPONSES DURING PERSISTENT RHESUS LCV INFECTION AND THE DEVELOPMENT OF A NOVEL THERAPEUTIC PROTOTYPE VACCINE FOR EBV-ASSOCIATED DISEASES

Rachel M. Leskowitz

Hildegund C.J. Ertl

The impact of EBV on human health is substantial, but vaccines that prevent primary EBV infections or treat EBV-associated diseases are not yet available. The Epstein-Barr nuclear antigen 1 (EBNA1) is an important target for vaccination because it is the only protein expressed in all forms of latency and in all EBV-associated malignancies. The overarching goal throughout this dissertation was to determine if EBNA1 is a suitable target for vaccine development. This was addressed in two ways. First, because an improved understanding of EBNA1-specific T cell responses benefits EBV vaccine development, we characterized responses against EBNA1 of the EBV-homologous rhesus lymphocryptovirus (rhLCV) in naturally infected rhesus macaques. We assessed frequency, phenotype, and cytokine production profiles of rhesus (rh)EBNA1-specific T cells by intracellular cytokine staining (ICS) and polychromatic flow cytometry. We found that most naturally infected animals had CD4⁺ and/or CD8⁺ T cells against rhEBNA1 and rhBZLF1, an immediate-early lytic phase antigen of rhLCV. Peptide-specific CD8⁺ T cells showed a more activated effector phenotype, while most peptide-specific CD4⁺ T cells exhibited a resting central memory phenotype. T cells were highly functional and produced various combinations of the cytokines IFN- γ , IL-2, and TNF- α . The differentiation status and functional profiles of rhEBNA1-specific T cells suggests they are not impaired by chronic exposure to low levels of antigen, and rhEBNA1-specific T cells therefore represent a viable population to target through vaccination. Similarities between our findings and the human response further validate the rhLCV model for

studying chronic EBV infection and for pre-clinical vaccine development. We then asked if vaccination could expand functional rhEBNA1-specific T cells during persistent rhLCV infection. To test this, we developed two serologically distinct replication-defective adenoviral vectors that expressed chimeric rhEBNA1 constructs fused to functional and non-functional versions of Herpes Simplex Virus- glycoprotein D (HSV-gD). HSV-gD has been shown to augment T cell responses by inhibiting the immunosuppressive Herpes Virus Entry Mediator (HVEM) pathway during T cell activation. After confirmation of vaccine specificity and antigenicity *in vitro*, rhesus macaques were vaccinated in a prime-boost regimen, and responses in peripheral blood were measured by ICS and polychromatic flow cytometry. Importantly, we found that vaccination induced the expansion of highly functional rhEBNA1-specific CD8⁺ and CD4⁺ T cells *in vivo*, regardless of HSV-gD binding ability. Vaccination did not increase rhBZLF1-specific T cell responses, thus indicating that rhEBNA1-specific responses were vaccine-driven. Overall, these results serve as important proof-of-principle analyses of a therapeutic EBNA1-based vaccine regimen and demonstrate that EBNA1 is a viable target that warrants exploration in future vaccine studies.

TABLE OF CONTENTS

<u>ACKNOWLEDGEMENTS</u>	<u>IV</u>
<u>ABSTRACT</u>	<u>VI</u>
<u>LIST OF TABLES</u>	<u>X</u>
<u>LIST OF FIGURES</u>	<u>XI</u>
<u>LIST OF ABBREVIATIONS</u>	<u>XIII</u>
<u>CHAPTER 1: INTRODUCTION</u>	<u>1</u>
1.1 EPSTEIN-BARR VIRUS (EBV)	1
1.2 THE ADAPTIVE IMMUNE RESPONSE AGAINST EBV	15
1.3 EBV-ASSOCIATED DISEASES	19
1.4 TREATMENT OF EBV-ASSOCIATED DISEASES	25
1.5 VACCINE STRATEGIES	27
1.6 AN ANIMAL MODEL FOR EBV: RHESUS LYMPHOCRYPTOVIRUS	34
1.7 OBJECTIVES AND SIGNIFICANCE	37
<u>CHAPTER 2: T CELL RESPONSES TO LATENT ANTIGEN EBNA1 AND LYTIC ANTIGEN BZLF1 DURING PERSISTENT RHLCV INFECTION OF RHESUS MACAQUES</u>	<u>40</u>
ABSTRACT	40
INTRODUCTION	42
RESULTS PART I	45
DISCUSSION	54
RESULTS PART II	55
DISCUSSION	71
<u>CHAPTER 3: ADENOVIRUS-BASED VACCINES TO RHESUS LYMPHOCRYPTOVIRUS EBNA1: VECTOR DESIGN, MOUSE STUDIES, <i>IN VITRO</i> TESTING</u>	<u>79</u>
ABSTRACT	79
INTRODUCTION	80
RESULTS	84
DISCUSSION	94
<u>CHAPTER 4: ADENOVIRUS-BASED VACCINES TO RHESUS LYMPHOCRYPTOVIRUS EBNA1 INDUCE EXPANSION OF CD8⁺ AND CD4⁺ T CELLS IN PERSISTENTLY INFECTED RHESUS MACAQUES</u>	<u>96</u>
ABSTRACT	96
INTRODUCTION	98
RESULTS	100
DISCUSSION	119
<u>CHAPTER 5: DISCUSSION</u>	<u>125</u>
SIGNIFICANCE	125
SUMMARY AND CONCLUSIONS	127
FUTURE DIRECTIONS	131

CHAPTER 6: MATERIALS AND METHODS	136
6.1 T CELL RESPONSES TO LATENT ANTIGEN EBNA1 AND LYTIC ANTIGEN BZLF1 DURING PERSISTENT RHLCV INFECTION OF RHESUS MACAQUES	136
6.2 ADENOVIRUS-BASED VACCINES TO RHEBNA1: VECTOR DESIGN, MOUSE STUDIES, <i>IN VITRO</i> TESTING	144
6.3 ADENOVIRUS-BASED VACCINES TO RHEBNA1 INDUCE EXPANSION OF CD8 ⁺ AND CD4 ⁺ T CELLS IN PERSISTENTLY INFECTED RHESUS MACAQUES	152
CHAPTER 7: REFERENCES	156

LIST OF TABLES

CHAPTER 1:

Table 1-1: Subfamily classification of the human herpesviruses	3
Table 1-2: Patterns of latent gene expression and associated diseases.....	9
Table 1-3: Diseases and their approximate association with EBV	20

CHAPTER 2:

Table 2-1: List of rhesus macaques used in this study.....	46
Table 2-2: Numbers of rhEBNA1-specific CD4 ⁺ and CD8 ⁺ T cells	50
Table 2-3: Total cytokine-secreting rhEBNA1- (A) and rhBZLF1- (B) specific CD4 ⁺ and CD8 ⁺ T cells for each animal at both collection points	58

CHAPTER 4:

Table 4-1: Numbers of CD8 ⁺ T Cells/10 ⁶ live CD3 ⁺ cells.....	103
Table 4-2: Numbers of CD4 ⁺ T Cells/10 ⁶ live CD3 ⁺ cells.....	104
Table 4-3: Characteristics and responsiveness of rhesus macaques enrolled in this study.....	105

CHAPTER 6:

Table 6-1: List of antibodies.....	140
Table 6-2: rhEBNA1 peptide sequences	142
Table 6-3: List of antibodies for ICS (mouse studies).....	151

LIST OF FIGURES

CHAPTER 1:

Figure 1-1: The EBV genome in linear and episomal forms	5
Figure 1-2: The EBV life cycle	14
Figure 1-3: EBV and rhLCV ORF homology.....	36

CHAPTER 2:

Figure 2-1: Number of rhEBNA1-specific CD4 ⁺ and CD8 ⁺ T cell responses	49
Figure 2-2: RhEBNA1-specific CD4 ⁺ and CD8 ⁺ T cells over time	53
Figure 2-3: Numbers of rhEBNA1- and rhBZLF1-specific T cells in PBMCs	59
Figure 2-4: Subset analysis of rhEBNA1-specific T cell responses.....	62
Figure 2-5: Subset analysis of rhBZLF1-specific T cell responses.....	63
Figure 2-6: Multi-function analysis of rhEBNA1-specific T cell responses.....	66
Figure 2-7: Multi-function analysis of rhBZLF1-specific T cell responses.....	67
Figure 2-8: PD-1 surface expression on rhEBNA1- and rhBZLF1-specific T cells	70

CHAPTER 3:

Figure 3-1: Enhanced T cell responses to antigens expressed as fusion proteins with HSV-gD..	83
Figure 3-2: <i>In vitro</i> testing of AdC-SgD-rhEBNA1 and AdC-NBEFSgD-rhEBNA1 vaccines.....	86
Figure 3-3: Frequency and number of IFN- γ ⁺ CD8 ⁺ T cells following dose-escalation study	89
Figure 3-4: Kinetics of peptide-specific CD8 ⁺ T cells after vaccination.....	90
Figure 3-5: Peptide-specific CD8 ⁺ T cells after vaccination of C57/Bl6 and ICR mice	91
Figure 3-6: <i>In vitro</i> stimulation of rhEBNA1-specific T cells.....	93

CHAPTER 4:

Figure 4-1: Schedule of vaccinations and blood collection.....	102
--	-----

Figure 4-2: Magnitude of peptide-specific CD8⁺ T cell responses upon vaccination 108

Figure 4-3: Proportions of peptide-specific CD8⁺ and CD4⁺ T cell subsets upon vaccination 109

Figure 4-4: Magnitude of peptide-specific CD4⁺ T cell responses upon vaccination 110

Figure 4-5: Cytokine profiles of rhLCV-specific T cells upon vaccination 113

Figure 4-6: Granzyme B production by rhLCV-specific T cells 117

Figure 4-7: Expression of CCR7 before and after vaccination 118

CHAPTER 6:

Figure 6-1: Gating strategy and representative examples 141

LIST OF ABBREVIATIONS

aa	Amino acid
Ad	Adenovirus
AdHu	Human Adenovirus
APC	Antigen presenting cell
BART	<i>Bam</i> HI A region rightward transcript
BCR	B cell receptor
BL	Burkitt's lymphoma
BTLA	B and T lymphocyte attenuator
CMI	Cell mediated immunity
CNS	Central nervous system
CR2	Complement receptor 2
CTL	Cytotoxic T lymphocyte
DC	Dendritic cell
DLBCL	Diffuse large B cell lymphoma
DMSO	Dimethyl sulfoxide
DRiP	Defective ribosomal product
EBER	Epstein-Barr virus-encoded RNA
EBNA	Epstein-Barr nuclear antigen
EBV	Epstein-Barr virus
FACS	Fluorescence-activated cell sorting
FBS	Fetal bovine serum
GA _r	Glycine-alanine rich repeat domain
GC	Gastric cell carcinoma
g, gp	Glycoprotein
gp42, gp350/220	Glycoprotein 42, 350/220
gH, gL, gD	Glycoprotein H, L, D
HBSS	Hank's balanced salt solution
HCMV	Human cytomegalovirus
HIV	Human Immunodeficiency virus
HL	Hodgkin's lymphoma
HLA	Human leukocyte antigen
HHV	Human herpesvirus
HSV	Herpes simplex virus
HVEM	Herpes virus entry mediator
ICS	Intracellular cytokine staining
IFN- γ	Interferon gamma
IL-2	Interleukin 2
IM	Infectious mononucleosis
im	Intra-muscular
IR	Internal repeat
ITR	Inverted terminal repeat

kb	Kilobase
kDA	Kilo Dalton
KSHV	Kaposi's sarcoma-associated herpesvirus
LCL	Lymphoblastoid cell line
LCV	Lymphocryptovirus
LMP	Latent membrane protein
LP	Leader protein
MHC	Major histocompatibility
MVA	Modified vaccinia Ankara
NBEF	Non-binding effect
NF- κ B	Nuclear factor κ B
NHL	Non-Hodgkin's lymphoma
NHP	Non-human primate
NK	Natural killer
NPC	Nasopharyngeal carcinoma
ORF	Open reading frame
oriP	Origin of plasmid replication
PD-1	Programmed death 1
PMBC	Peripheral blood mononuclear cell
PTLD	Post-transplant lymphoproliferative disease
RBC	Red blood cell
RDV	Rhadinovirus
rhEBNA1	Rhesus Epstein-Barr nuclear antigen 1
rhLCV	Rhesus lymphocryptovirus
SAdV, AdC	Simian, or chimpanzee Adenovirus
SD	Standard deviation
SgD	Super glycoprotein D
SIV	Simian immunodeficiency virus
TCR	T cell receptor
T _{CM} cell	Central memory T cell
T _{EFF} cell	Effector T cell
T _{EM} cell	Effector memory T cell
T _H	T helper cell
TMR	Transmembrane region
TNF- α	Tumor necrosis factor alpha
TR	Terminal repeat
U _L	Unique long
U _S	Unique short
VCA	Viral capsid antigen
VZV	Varicella-zoster virus
XLPD	X-linked lymphoproliferative disease
YNPRC	Yerkes National Primate Research Center

CHAPTER 1: INTRODUCTION

More than 95% of the human population is infected with the Epstein-Barr virus (EBV) by adulthood¹, and EBV contributes to the development of about 1% of all human cancers^{1, 2}. EBV establishes a persistent infection through its latency in B cells, where it can occasionally reactivate, but infections as well as reactivations are controlled by the adaptive immune system³. Although infection is typically benign, EBV is considered a carcinogen due to its strong association with both lymphoid and epithelial cell malignancies, and the incidence of these malignancies is highly elevated during immune suppression. The impact of EBV on human health is substantial, but vaccines that prevent primary EBV infections or treat EBV-associated diseases are not yet available.

1.1 EPSTEIN-BARR VIRUS (EBV)

General properties

Discovery

Denis Burkitt, a surgeon working in East Africa in the late 1950s, was the first to propose that an infectious agent was involved in the etiology of a human malignancy. He was studying a novel childhood tumor, now known as Burkitt's lymphoma (BL), which he noticed was unusually common among areas with similar climatic factors around equatorial Africa^{4, 5}. This idea caught the attention of Dr. Anthony Epstein, who after attending a seminar given by Dr. Burkitt in 1961, arranged to receive BL biopsy specimens. Dr. Epstein and his Ph.D. student Yvonne Barr successfully established a line of BL-derived cells in culture. They examined these cells under an electron microscope and discovered "herpesvirus-like particles in a small proportion [of the cells]"⁶. These particles proved to be biologically and antigenically distinct from other members of

the human herpesvirus (HHV) family, thus marking the discovery of the first candidate human tumor virus, also known as Epstein-Barr virus (EBV), or human herpesvirus 4 (HHV-4).

In the years to follow, serological studies revealed the vast prevalence of EBV worldwide. In 1968, EBV was identified as the cause of infectious mononucleosis (IM) when a lab technician, who had been studying EBV, developed IM and seroconverted⁷. EBV was found to transform human B cells *in vitro* in 1971⁸ and to replicate in human epithelial cells in 1984⁹. Since its initial discovery in BL cells, EBV has been found in a variety of human epithelial and lymphoid malignancies and has also been linked to various autoimmune diseases¹⁰.

Classification

EBV is a member of the *Herpesviridae* family, which is a large group of DNA viruses characterized by their lifelong latency following primary infection. Currently, there are nine herpesviruses known to infect humans¹⁰. These include herpes simplex virus 1 and 2 (HSV1, HHV-1; HSV-2, HHV-2), human cytomegalovirus (HCMV; HHV-5), varicella-zoster virus (VZV; HHV-3), Epstein-Barr virus (EBV; HHV-4), human herpesviruses 6A, 6B, and 7 (HHV-6A, HHV-6B, HHV-7), and Kaposi's sarcoma-associated herpesvirus (KSHV; HHV-8). Herpesviruses are classified into *Alpha-*, *Beta-*, and *Gammaherpesvirinae* subfamilies based on various biological properties such as host range, reproductive cycle, and cell tropism. The gammaherpesviruses, which includes EBV, are lymphotropic and usually establish latency in lymphoid tissue. EBV is distinguished by its latent infection of B lymphocytes and its ability to transform B cells *in vitro* into latently infected, immortalized, B-lymphoblastoid cell lines (LCLs) that proliferate indefinitely in the presence of sufficient growth factors. Subfamily classification of human herpesviruses can be found in **Table 1-1**.

Table 1-1: Subfamily classification of the human herpesviruses

Official name	Common name	Subfamily
<i>Human herpesvirus 1</i>	Herpes simplex virus 1 (HSV-1)	Alpha-
<i>Human herpesvirus 2</i>	Herpes simplex virus 2 (HSV-2)	Alpha-
<i>Human herpesvirus 3</i>	Varicella-zoster virus (VZV)	Alpha-
<i>Human herpesvirus 4</i>	Epstein-Barr virus (EBV)	Gamma-
<i>Human herpesvirus 5</i>	Human cytomegalovirus (CMV)	Beta-
<i>Human herpesvirus 6-A</i>	---	Beta-
<i>Human herpesvirus 6-B</i>	---	Beta-
<i>Human herpesvirus 7</i>	---	Beta-
<i>Human herpesvirus 8</i>	Kaposi's sarcoma-associated herpesvirus (KSHV)	Gamma-

Subfamilies are further divided into a series of genera based on similarities in DNA sequences and genome arrangement as well as immunologic and antigenic similarity of important viral proteins¹⁰. The gammaherpesvirus subfamily consists of the gamma 1 (*Lymphocryptovirus*, *LCV*) genus, which includes EBV and related primate viruses, and the gamma 2 (*Rhadinovirus*, *RDV*) genus, which includes KSHV and other related viruses of primate and non-primate species. EBV is the only human member of the LCV genus, which also includes a number of simian homologs including rhesus lymphocryptovirus (rhLCV), which is the only fully sequenced EBV homolog with a repertoire of lytic and latent genes identical to that of EBV.

Genome and structure

Like all herpesviruses, EBV virions have a protein core that is wrapped by a double stranded DNA viral genome and enclosed within an icosahedral nucleocapsid composed of 162 capsomeres. A protein-rich structure called the tegument separates the nucleocapsid from the envelope and delivers pre-synthesized proteins to newly infected cells. The envelope itself is spiked with several virus-encoded glycoproteins involved in cellular attachment and entry.

The EBV genome is approximately 172 kilobase (kb) pairs long¹⁰, with two distinct programs of gene expression that are broadly characterized as lytic or latent. EBV encodes about 100 proteins as well as multiple non-coding RNAs¹¹ that are organized and expressed in a linear fashion. Therefore, gene overlaps and multiple gene products that result from frame shifts, alternative splicing, and internal translation initiation sites are common. The genome is divided into 15 kb unique short (U_S) and 150 kb unique long (U_L) regions that are separated by multiple tandemly reiterated internal repeats (IRs). Tandemly reiterated terminal repeats (TRs) flank the

genome on both ends (**Figure 1-1A**). During latent infection, the viral genome takes the form of a closed circular molecule from which only a small subset of genes are expressed (**Figure 1-1B**). EBV DNA remains in this circular form during replication in latently infected cells.

Two distinct types of EBV (types 1 and 2) share between 70 to 85% sequence homology¹⁰, and strains within each type are distinguished by the number of genomic repeats. Differences between the two types of EBV are based on sequence polymorphisms in four nuclear proteins expressed during latency (EBNA2, -3A, -3B, and -3C). Both types co-exist in all populations that have been studied¹⁰, but EBV-1 is more prevalent in the developed world than EBV-2, which is common in equatorial Africa and New Guinea¹⁰. Differences between type 1 and 2 are not correlated with human diseases, but it has been shown that EBV-1 isolates transform B cells more efficiently *in vitro*¹⁰. Dual infections and intertypic recombinants are most often observed during immune suppression, and infection with either type results in lifelong persistence.

Figure 1-1: The EBV genome in linear and episomal forms

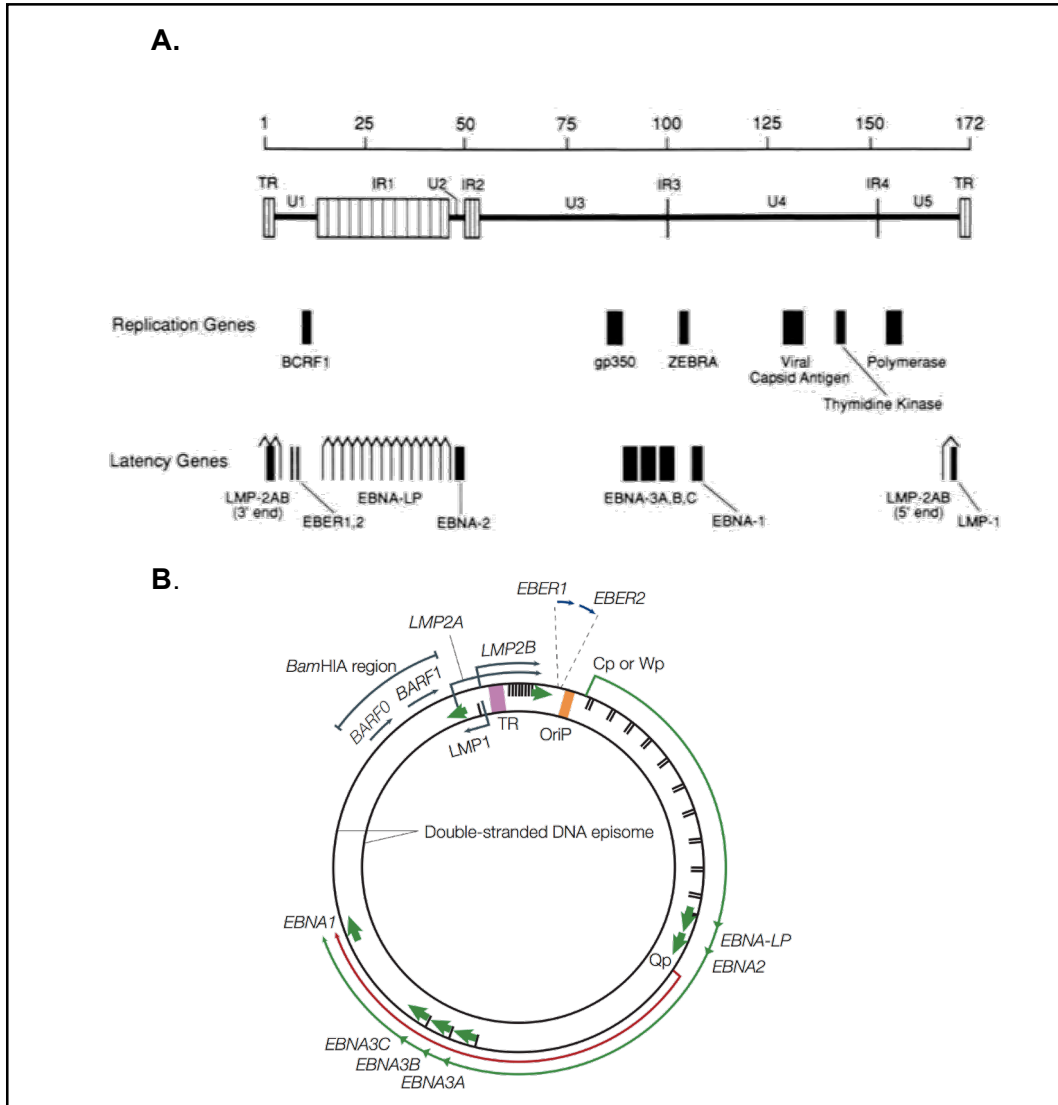


Figure 1-1: (A) Structure of the EBV genome shown in linear form with the location of important lytic and latent genes below. The genome is organized into series of unique short (US) and unique long (UL) regions of internal repeats (IRs) flanked by terminal repeat domains (TRs). Figure was adapted from Straus et al., 1993¹². **(B)** Structure of EBV episome showing location and transcription of latency genes. The origin of plasmid replication is shown in orange (OriP). Arrows indicate the direction of transcription, with larger arrows showing exons. The thin green arrow starting at the Cp or Wp promoters represents transcription of the EBNA proteins during latency III, which are generated by differential splicing. EBNA1 is transcribed from the Qp promoter during latency I and II (red arrow). Figure was adapted from Young et al., 2004¹³. LMP, latent membrane protein; EBNA, Epstein-Barr nuclear antigen; gp, glycoprotein; BCRF1, BamH1 C rightward reading frame; ZEBRA, Z Epstein-Barr virus replication activator, also known as ZTA (Z fragment trans activator) or BZLF1 (BamH1 Z leftward reading frame).

Transmission

EBV is one of the most common known human viruses; 95 to 99% of adults in the U.S. and over 95% of the population worldwide are seropositive¹⁴. Primary infection occurs early in life in most developing countries and is generally asymptomatic or produces only mild clinical symptoms. When infection is delayed until adolescence or adulthood, as is common in developed countries, EBV can cause IM. IM is a benign, self-limited, lymphoproliferative disease characterized by fever, sore throat, cervical lymphadenopathy, and fatigue.

EBV is transmitted orally through saliva; some individuals continue to shed virus even after resolution of primary infection. At any given time, between 20 to 30% of healthy seropositive adults are shedding low concentrations of EBV, and the incidence of shedding increases to 60 to 90% during immunosuppression¹⁵. In addition to oral secretions, EBV can also be transmitted through blood product transfusions and bone marrow or solid organ transplants¹¹. EBV has also been found in genital secretions, which suggests that it can be transmitted sexually¹⁶.

Cell tropism, attachment, and entry

The primary targets of EBV infection are squamous pharyngeal epithelial cells and B cells. Initiation of infection and mechanisms of entry are different for epithelial cells and B cells, which have different cell surface receptors that facilitate binding of EBV. The host range of EBV is therefore partially influenced by receptor availability on target cells. EBV enters epithelial cells via fusion with the plasma membrane and B cells via endocytosis followed by fusion with the endocytic membrane. For B cell entry, EBV virions bind CD21, also known as the complement receptor 2 (CR2), which is highly expressed on B cells. Binding of CD21 to the virus-encoded glycoproteins (gp) 350/220 results in endocytosis. The viral and endocytic membranes fuse via gp42, which binds to human leukocyte antigen (HLA) class II on B cells and forms a three part gp complex with gH and gL (gp42gHgL) that triggers fusion. In contrast, epithelial cell attachment and entry is mediated primarily through interactions between cell surface integrins and the viral protein BMRF2. BMRF2 functions similarly to gp350/220 by tethering virions to target cells and inducing signal transduction pathways. Following attachment, two part complexes (gH/gL) bind to integrins and mediate epithelial cell membrane fusion. Therefore, in addition to surface receptors

on target cells, tropism is also dictated by the composition of glycoproteins on the EBV virion, which can differ depending on the cell in which the virion was produced. Virions produced in B cells are deficient in gp42, as it remains bound to HLA class II. In contrast, virions produced in epithelial cells, which do not express HLA class II, contain high levels of gp42/gH/gL complexes on the surface. As a result, EBV virions produced in B cells are more infectious to epithelial cells, and virions made in epithelial cells are more infectious to B cells¹⁷. While epithelial cells and B cells are the primary targets of EBV, infection of T-cells, monocytes, neutrophils, and natural killer (NK) cells has also been described¹⁷.

Phases of infection

EBV causes both lytic (productive) and latent infections that generally have different primary target cells and express different sets of genes. Initial productive infection is primarily localized to epithelial cells of the oropharynx, where mature infectious virions are assembled and released, resulting in cell lysis. In contrast, latent infection usually occurs in B cells, where the viral genome exists as a stable circular episome, gene expression is restricted, and infectious viral particles are not produced. Latently infected B cells can be detected in peripheral blood, in tonsils and adenoids in the oral cavity, and to a lesser extent in mesenteric lymph nodes and the spleen¹⁸. Latent EBV retains the capacity to reactivate to a lytic state and produce new infectious virions; this can occur in the presence or absence of clinical symptoms.

EBV gene expression during latent infection

Genes expressed during latency are initially growth transforming; infection of naïve B cells results in B cell activation, expansion, and maturation, which allows EBV to spread quickly throughout the B cell compartment¹¹. Although the majority of these lymphoblasts are eventually destroyed by the adaptive immune system, EBV persists within B cells by downregulating gene expression and becoming essentially undetectable to host immune cells. Downregulation of latent gene expression is accompanied by a transition to a resting memory B cell phenotype, and the amount of virus detected in latently infected cells is drastically reduced¹⁹. Latently infected B cells in peripheral blood are present at a rate of about 1 to 60 per million B cells¹⁵. Each cell carries

less than five copies of the latent viral genome^{19, 20}, and the frequency of latently infected cells remains relatively stable over time²¹.

Only a small subset of the nearly 100 EBV-encoded genes is expressed during latency. These include six Epstein-Barr nuclear antigens (EBNAs; 1, 2, 3A, 3B, 3C, leader protein (LP)), three latent membrane proteins (LMPs; 1, 2A, 2B), two EBV-encoded small non-polyadenylated RNAs (EBERs), and rightward transcripts from the *Bam*HI A region of the genome (BARTs). EBNA1 and LMP1 are also expressed during lytic infection¹⁰.

Programs of gene expression

Different programs of gene expression are associated with different phases of latency, and the combination of genes expressed determines the extent of proliferation and the ability of EBV to escape immune surveillance. The growth-transforming properties of latency occur when all of the latency genes are expressed. This is known as latency III. The latency III program of gene expression is also what causes transformation of B cells to LCLs *in vitro*. *In vivo*, pressures of the immune system eventually cause a downregulation of gene expression, which allows EBV to persist in a latent state. In latency II, EBNA1, LMP1, and LMP2 are expressed with the EBERs and *Bam*HI A RNAs. EBNA1 is the only protein expressed during latency I along with the EBERs and *Bam*HI A RNAs. Finally, a fourth program referred to as latency 0 has been used to describe latently infected cells in the blood that do not express any viral genes except the EBERs²². This fourth stage of latency is most common among healthy virus carriers, however, transcripts for EBNA1 and LMP2 have also been detected in the blood of such individuals^{23, 24}.

In addition to establishing lifelong infection, the latency genes and their products are implicated in the pathogenesis of many EBV-associated malignancies. A latency I pattern of gene expression is associated with Burkitt's lymphoma (BL), some diffuse large B cell lymphomas (DLBCLs), and gastric cell carcinomas (GC). Latency II is associated with Hodgkin's lymphoma (HL), T/NK cell lymphomas, and nasopharyngeal carcinoma (NPC). Latency III is found in IM and all EBV-associated Immunoblastic/lymphoproliferative diseases. A list of the different latency programs, genes expressed, and associated diseases can be found in **Table 1-2**. EBV-associated diseases will be discussed in detail in a later section.

Table 1-2: Patterns of latent gene expression and associated diseases

Latency type	Genes expressed	Associated diseases
0	EBER1,2; occasional EBNA1 and/or LMP2	[latently infected B cells in peripheral blood]
I	EBNA1; EBER1,2; <i>BamHI</i> A RNAs	Burkitt's lymphoma Centroblastic diffuse large B cell lymphoma Gastric carcinoma
II	EBNA1; LMP1,2A,2B; EBER1,2; <i>BamHI</i> A RNAs	Chronic active EBV Hodgkin's lymphoma Nasopharyngeal carcinoma T/NK cell lymphoma
III	EBNA1,2,3A,3B,3C,LP; LMP1,2A,2B; EBER1,2; <i>BamHI</i> A RNAs	B cell transformation to LCL <i>in vivo</i> B cell lymphoproliferative disease Immunoblastic diffuse large B cell lymphoma

Function of latency genes

Genes expressed during latency are important for B cell growth transformation, maintaining the viral episome, and preventing apoptosis. The specific functions of these genes and their protein products are reviewed below.

EBNAs: EBNA-LP and EBNA2 are the first proteins expressed during latent EBV infection. EBNA2 is required for B cell transformation and is responsible for activating transcription from various promoters, which results in the expression of additional EBNAs as well as the LMPs^{25, 26}. EBNA2 also activates transcription of several cellular genes including CD21 (EBV receptor), CD23 (B cell activation marker), *c-myc* and *c-fgr* (proto-oncogenes)²⁷⁻²⁹. EBNA-LP enhances EBNA2-dependent transcription of viral and cellular genes and likely plays a role in RNA processing³⁰. The EBNA3 proteins regulate the activity of EBNA2, and they also upregulate cellular and viral gene expression, including CD21 and LMP1 (EBNA3C), CD40 and Bcl-2 (EBNA3B)³¹. EBNA3A and 3C are required for B cell transformation³².

EBNA1 is a DNA binding protein that functions to maintain the viral episome and is therefore essential for EBV persistence. EBNA1 ensures episomal segregation during cell division by binding the origin of plasmid replication (oriP) on the viral genome and tethering it to mitotic chromosomes³³. EBNA1 is also important for B cell transformation during latency and for

activating the expression of additional EBV latent genes¹⁰. Transcription of EBNA1 is autoregulated through its binding to the oriP and various upstream promoters. EBNA1 is the only protein expressed in all of the patterns of latency associated with disease (I, II, III). The importance of EBNA1 and its potential as a vaccine target will be discussed in a later section.

LMPs: LMP1 is an important signaling molecule that is necessary for many of the changes involved in B cell transformation³⁴. Structurally, it mimics proteins of the tumor necrosis factor (TNF)-receptor superfamily by acting as a constitutively active CD40 homolog³⁵. Downstream signaling stimulates two important families (nuclear factor κ B (NF- κ B) and c-jun kinase) of transcriptional activators that are both involved in controlling cell growth^{36, 37}. Additional phenotypic effects include B cell aggregation, the upregulation of activation and adhesion molecules, the activation of cytokine genes, and the induction of cell survival proteins such as Bcl-2^{10, 35}. LMP1 therefore functions as an oncogene for EBV, and the resulting effect is constitutive B cell proliferation. Unlike LMP1, neither LMP2A nor LMP2B are essential for B cell transformation³⁸. LMP2A co-localizes with LMP1 in the plasma membrane of the infected B cell³⁹. Its cytoplasmic tail resembles that of the B cell receptor (BCR), and it competes for binding to molecules involved in BCR downstream signaling. The resulting inhibition of BCR signal transduction allows EBV to prevent and therefore control normal B cell stimulation and activation. This helps promote latency, as normal BCR signaling induces reactivation of the lytic cycle⁴⁰. LMP2A also promotes B cell survival by deregulating transcription factors during B cell development in order to bypass certain developmental checkpoints while driving B cell differentiation to a long-lived memory phenotype⁴¹.

Small RNA molecules: The EBERs are the most abundant EBV RNAs, present at about 50,000 copies per cell¹⁰. Both EBER1 and EBER2 are small, nuclear, non-polyadenylated RNAs whose function is not completely understood. Neither 1 nor 2 are necessary for B cell transformation⁴², but their expression leads to the upregulation of Bcl-2⁴³ and IL-10⁴⁴. The result is increased resistance to apoptosis and enhanced B cell maturation, proliferation, and survival. EBV also encodes a large group of micro RNAs (miRNAs) with a wide range of functions. For example, *BamHI A* transcripts are highly spliced RNAs that most likely influence latent infection

through cell signaling or by regulating promoters, as the transcripts are antisense to many important genes⁴⁵.

EBV gene expression during lytic infection

EBV in infected B cells can remain latent with varying levels of gene expression or it can reactivate to lytic replication. The decision to enter the lytic cycle induces a classic regulatory cascade where about 80 different genes are expressed. Virally-encoded lytic proteins are involved in cell entry, gene expression regulation, nucleotide metabolism, viral DNA synthesis, and virion assembly as well as management of host defenses and cellular metabolism¹⁰. Viral gene expression during lytic infection is defined by the order of expression and the mechanisms that drive it. Gene expression is temporally regulated into three broad phases in which the immediate-early, early, and late genes are sequentially expressed.

Immediate early (IE) gene expression: Viral transactivator proteins incorporated in the viral tegument activate transcription of the IE genes, which encode additional transcriptional transactivators important for early progression of the lytic cycle. IE proteins include BZLF1 and BRLF1, which initiate the switch from latent to lytic infection and downregulate latent gene expression¹⁰.

Early (E) gene expression: Transcription of the E genes is independent of viral DNA synthesis. E proteins such as BSMLF1 and BMRF1 are transactivators of other early genes¹⁰, such as BHRF1 and BALF1, which are homologous to the anti-apoptotic molecule Bcl-2⁴⁶. Additional early genes encode proteins involved in viral DNA replication, such as the major DNA binding protein (BALF2), DNA polymerase (BALF5), ribonucleotide reductases (BORF2 and BaRF1), thymidine kinase (BXLF1), and alkaline exonuclease (BGLF5)¹⁰.

Late (L) gene expression: Expression of the L genes is either augmented by or completely dependent on the onset of viral DNA synthesis. The majority of these genes encode structural proteins such as viral glycoproteins, nucleocapsid proteins, tegument proteins, and a core protein; the majority of the L proteins are therefore required for proper assembly and packaging of EBV virions¹⁰.

The life cycle of EBV

EBV's replication cycle, similar to all herpesviruses, begins after viral fusion and entry in the host cell. Nucleocapsid and tegument are then released into the cytoplasm, where they travel to nuclear pores via the cellular cytoskeleton. Viral DNA is translocated, circularized, and partially chromatinized in the nucleus. Chromatinization is a dynamic form of transcriptional regulation that changes throughout the viral life cycle. The nature of viral DNA chromatinization (and therefore the viral genes accessible) as well as the presence and status of specific viral and cellular regulators of transcription are important factors that influence whether EBV enters lytic replication or establishes latent infection⁴⁷.

It was originally believed that oropharyngeal epithelial cells were the target for primary and productive EBV infection, and that released virions would then latently infect resting naïve (or occasionally memory) B cells that traffic through the oropharynx⁹. However, it has also been shown that viral infection can be entirely restricted to lymphoid cells⁴⁸. This indicates that primary productive infection can occur in B cells, although the majority become latently infected lymphoblasts that display a type III pattern of gene expression¹¹.

Latently infected B cells then typically undergo a phase of maturation and differentiation that is associated with a downregulation of latent gene expression. One proposed pathway in which this occurs is in the germinal centers of lymphoid follicles through similar mechanisms exhibited during normal B cell activation⁴⁹. The latency III program of gene expression induces proliferation of EBV-infected naïve B cells, which eventually migrate to lymphoid follicles to differentiate. This is likely facilitated through a downregulation of gene expression to a type II latency pattern, where LMPs mimic cellular and extracellular factors that may induce class switch recombination, somatic hypermutation, and stimulate BCR signaling. Additional lines of evidence, however, suggest that EBV-infected B cells may not transmit and differentiate through the germinal center^{24, 50}, and not all EBV-infected B cells are isotype-switched⁵¹. Regardless of the mechanism, latently infected B cells differentiate into a resting memory phenotype, where they express even fewer EBV antigens (type I or 0 pattern of latency) and establish a carrier state that persists for life^{19, 22, 24}.

The exact details that lead to viral reactivation remain elusive; however, various contributing factors have been shown to stimulate the transition to lytic replication. For example, latently infected resting memory B cells may encounter their cognate antigen and undergo differentiation into plasma cells⁵². This can trigger re-entry into the EBV lytic cycle, where depending on the location of the B cell, released virions can infect naïve B cells in the periphery, epithelial cells in the oropharynx, or can be shed directly in saliva. Additional factors that may influence reactivation include times of weakened immunity as a result of trauma, infection, or physiological stress associated with increased stress hormones⁵³⁻⁵⁶. The life cycle of EBV is summarized in **Figure 1-2**.

Figure 1-2: The EBV life cycle

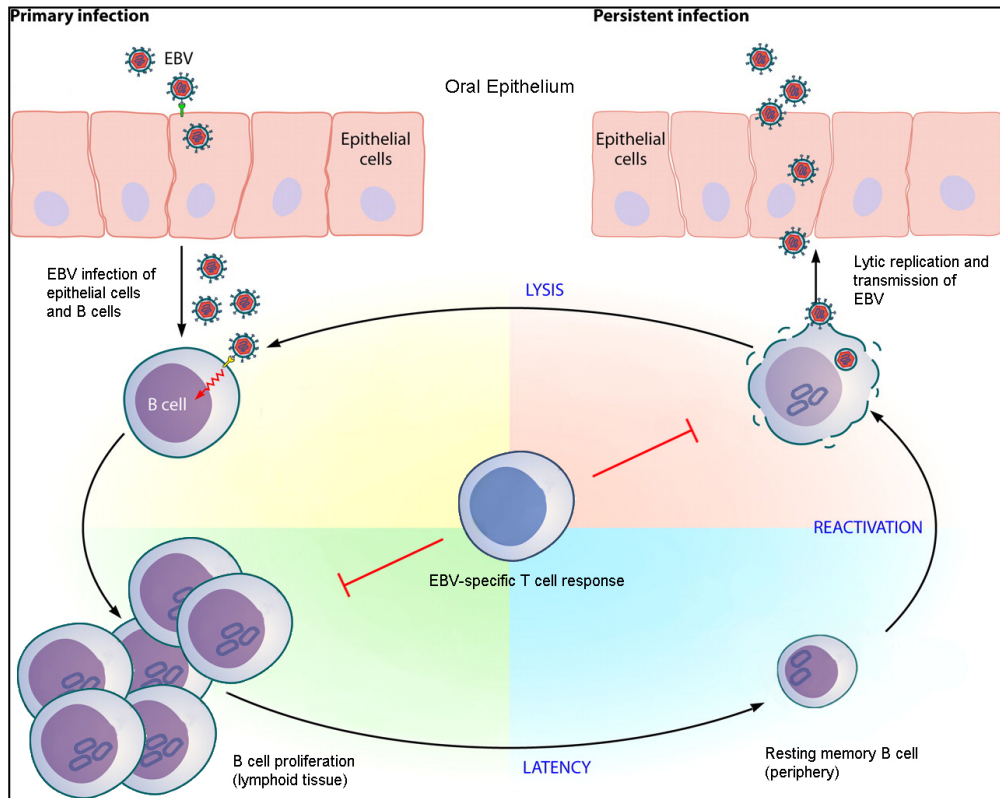


Figure 1-2: Primary EBV infection occurs in epithelial cells and B cells. B cells are infected either directly or with virus released from oral epithelial cells. The majority of EBV-infected B cells undergo latent infection, where the type III program of gene expression induces B cell proliferation and maturation. Some EBV-infected B cells also undergo lytic infection as well. EBV-specific cytotoxic T cells control primary infection and subsequent reactivations, but the virus persists in resting memory B cells. This figure was adapted from Odumade, et al., 2011⁵⁷.

1.2 THE ADAPTIVE IMMUNE RESPONSE AGAINST EBV

The virus-specific immune response is crucial for maintaining a disease-free virus-host equilibrium. The host immune system can easily detect and destroy virus-infected cells during lytic replication, when the vast majority of EBV genes are expressed, but detection is difficult during latency. EBV uses additional mechanisms to hinder or delay host immune responses, which include blocking antigen presentation, mimicking the function of host immunomodulators, and generating orthologs of cellular proteins that mislead infected cells to stimulate desired functions¹⁰. Despite these various mechanisms, healthy individuals mount an effective immune response that regulates and controls infection, but does not completely eliminate the virus. This balance between viral reactivation and host immune surveillance is maintained throughout the lifetime of all healthy seropositive individuals. While components of the innate immune response are certainly important in combating EBV (such as NK cells), the most crucial control comes from the humoral and cell-mediated arms of the adaptive immune system⁵⁸.

The humoral immune response against EBV

The humoral immune response consists of antigen-specific antibodies which target and destroy extracellular pathogens and prevent the spread of intracellular infections⁵⁹. Antibodies can contribute to immunity by binding and therefore blocking infection of host cells (neutralization); by coating pathogen and stimulating phagocyte removal; and by triggering destruction through additional immune mechanisms such as NK cell-mediated killing of antibody-antigen coated cells (antibody-dependent cell-mediated cytotoxicity) or activating the complement system⁵⁹.

EBV elicits a strong humoral immune response. Most EBV-specific antibodies against lytic antigens are generated during acute infection, while EBV-specific antibodies against latent antigens tend to arise during convalescence¹⁵. IgM antibodies against a variety of IE, E, and L lytic antigens arise first, and responses against viral capsid antigen (VCA) are detected most frequently¹⁰. Anti-VCA IgM antibodies are usually present at the onset of symptoms, peak during

the acute phase of infection, and decline to undetectable levels upon resolution of clinical symptoms. VCA IgG arises about three months after the onset of infection, which is around the same time as antibodies to EBNA1 begin to appear¹⁵. IgG antibodies to VCA and EBNA1 persist for life⁶⁰. Antibody responses against other EBV proteins are also detected, including those against the envelope glycoprotein gp350, which can neutralize virus and are important for convalescence and control of reactivation⁶¹. Elevated titers of isotype-specific EBV antibodies can also be used for diagnostic and prognostic characterization of certain EBV-associated diseases, such as BL (VCA, EA)¹⁵, HL (VCA, EA, EBNA2)⁶², NPC (VCA)⁶³, and GC (VCA)⁶⁴.

EBV-induced polyclonal B cell activation also leads to the production of non-EBV-specific heterophile antibodies, which are reactive against antigens expressed on red blood cells (RBCs) of many animals such as sheep, cow, goat, horse, and ox⁷. A standard means of diagnosing IM is by testing the ability of sera from infected patients to agglutinate such cells.

The cell-mediated immune response against EBV

Cell-mediated immunity (CMI) includes CD8⁺ and CD4⁺ T lymphocytes, which interact with peptide derived from viral antigen that is displayed on the surface of antigen presenting cells (APCs) in the context of major histocompatibility (MHC) alleles (in humans these are the HLA alleles). Individuals present different peptides depending on their HLA alleles. As a result of this interaction with MHC molecules, CD8⁺ and CD4⁺ T lymphocytes can be stimulated to proliferate and differentiate into either effector or memory cells⁵⁹. Effector T cells develop quickly, mediate direct or indirect killing of infected cells, and have a more limited lifespan than memory cells, which develop slowly, but confer long-term protection against reinfection⁶⁵.

The typical immune response to an acute infection involves the activation, expansion, and contraction of antigen-specific T cells. Although the majority of expanded cells will die by apoptosis, a minority survives and differentiates into the long-lived memory pool⁶⁶. Upon secondary exposure to cognate antigen, these memory T cells can undergo rapid recall proliferation and can differentiate into secondary effector and memory populations. Memory T cell subsets are quite heterogeneous, but can be broadly classified as either effector memory (T_{EM}) or

central memory (T_{CM}) cells⁶⁵. T_{CM} cells reside primarily in lymphatic tissues and may require further differentiation to attain full effector function, but respond to secondary antigen stimulation with rapid proliferation⁶⁶. In contrast, T_{EM} cells reside primarily in the periphery and have more rapid effector function upon secondary stimulation, but they do not proliferate as well as the T_{CM} compartment⁶⁶. Although both are long-lived, T_{EM} cells have a shorter lifespan than T_{CM} cells, which are stably maintained through homeostatic self-renewal⁶⁶.

T cells are important for controlling acute EBV infection and for long-term control of EBV reactivation⁶⁷. $CD8^+$ T cells recognize viral peptides that are 8 to 11 amino acids (aa) long and are presented by epitope-specific MHC class I molecules on the surface of infected cells⁶⁸. Almost all nucleated cells express MHC class I receptors. EBV-specific cytotoxic T lymphocytes (CTLs) are generated against both lytic and latent antigens, display an effector phenotype during IM, and mediate direct killing of cells infected with intracellular pathogen⁶⁹. CTLs against lytic antigens arise first, while $CD8^+$ T cells against latent antigens arise slightly later during acute infection and can continue to arise for 3 to 4 months following convalescence^{70, 71}. EBV-specific CTLs are generally positive for granzyme and perforin, which correlates with cytotoxic activity, as demonstrated by cytotoxicity and cytokine secretion assays⁷¹⁻⁷⁶. Most EBV-specific CTLs are short-lived and undergo apoptosis once the level of EBV antigen drops. CTLs to IE antigens decline rapidly after infection, while CTLs to latent antigens decline more slowly^{67, 77}. Expression of PD-1, a marker of lymphocyte exhaustion, is elevated on EBV-specific $CD8^+$ T cells during IM, but returns to low levels during convalescence⁶⁷. After resolution of acute infection, lytic antigen responses typically have a T_{EM} cell phenotype, while latent antigen responses have either a T_{EM} or T_{CM} cell phenotype^{67, 70, 74}.

During IM there is a massive expansion of lytic EBV antigen-specific $CD8^+$ T cells. In some individuals, up to 44% of the total $CD8^+$ T cell pool can be directed against a single epitope, and responses are highly HLA type-dependent⁷⁸. IE lytic proteins such as BZLF1 and BRLF1 are highly antigenic and are recognized by more $CD8^+$ T cells than E proteins, which are more antigenic than L proteins⁶⁷. This hierarchy of antigenicity may be due to immune-evasion genes, which are not expressed until later in the lytic cycle. In fact, there is a direct correlation between

lytic protein immunodominance and the efficiency to which those proteins are processed and presented in lytically infected cells⁷⁹. In contrast, up to 5% of CD8⁺ T cells are directed against latent antigens during IM, and EBNA3-specific responses are most common^{67, 80-82}. Other EBV latency proteins that are targets for CD8⁺ T cells include LMP2 followed by EBNA1 and 2^{67, 82-84}. In long-term healthy carriers, the frequency of CTLs directed against EBV antigens can reach 5%, with about 0.2 to 2% of CD8⁺ T cells directed against lytic proteins and 0.05 to 1% of CD8⁺ T cells specific for latent proteins⁶⁷. Thus, a significant proportion of the CD8⁺ T cell pool is devoted to controlling long-term EBV infection. Age-correlated expansion of EBV-specific T cells has also been observed, and responses can constitute up to 14% of total CD8⁺ T cells in healthy individuals over age 60⁸⁵.

In comparison to the CD8⁺ T cell response, less is known about EBV-specific CD4⁺ T cells. CD4⁺ T cells recognize 10 to 18 aa long peptide fragments that are presented by epitope-specific MHC class II molecules after endocytosis rather than de novo synthesis. Only a limited group of cells express MHC class II, including B cells and professional antigen presenting cells (APCs) such as dendritic cells (DCs) and macrophages. CD4⁺ T cells generally have a large repertoire of potential effector activities, and the majority differentiate into various subsets with distinct immunological 'helper' functions (helper T cells (T_H))⁸⁶. CD4⁺ T_H cells can promote the activation of CD8⁺ T cells during inflammatory responses against intracellular pathogens (T_H1), promote B cell activation for antibody secretion in response to extracellular pathogens (T_H2), provide B cell help in lymph node follicles for B cell differentiation (follicular helper, T_{FH}), and help regulate T_{EFF} cells through silence or death signaling (regulatory T cells, T_{regs}). Additionally, CD4⁺ T_H cells can function as CTLs and lyse MHC class II-positive cells that express their cognate antigen.

EBV-specific CD4⁺ T cells produce the inflammatory cytokines interferon gamma (IFN- γ) and tumor necrosis factor alpha (TNF- α), lower levels of interleukin 2 (IL-2), and some clones are perforin positive, cytotoxic, and can inhibit the outgrowth of virus-transformed cells^{67, 87, 88}. EBV-specific CD4⁺ T cell responses against lytic antigens are more evenly distributed across the IE, E, and L proteins compared to CD8⁺ responses^{10, 89, 90}. This is probably because CD4⁺ T cells readily communicate with professional APCs, which process and display extracellular antigen. In

contrast, antigen presented by MHC class I molecules on the surface of virus-infected cells is more likely influenced by EBV immune evasion mechanisms.

During IM, there is large expansion of BZLF1-specific CD4⁺ T cells; responses against BMLF1 and EBNA3A are also commonly detected^{71, 88, 90}. CD4⁺ T cells recognize EBNA3C more than EBNA1 or 2^{71, 90}. After resolution of acute infection, EBV-specific CD4⁺ T cells rapidly decline to less than 1% total frequency after 1 year¹⁰. In healthy carriers, CD4⁺ T cells predominantly recognize EBNA1, with the majority of responses generated against its carboxyl terminus^{91, 92}. CD4⁺ T cells also recognize EBNA2 and 3C, but to a lesser extent than EBNA1^{67, 91, 93}. Other latency proteins (EBNA3A, 3B; LMP1, 2)^{91, 93} and many lytic proteins (BZLF1, BMLF1, BHRF1, BNLF2b, BCRF1, gp110, gp350)^{87, 88, 94-96} are also recognized by CD4⁺ T cells in healthy carriers.

The frequency of EBV-specific CD8⁺ T cells is generally about 10-fold higher than the frequency of EBV-specific memory CD4⁺ T cells in healthy virus carriers^{91, 93}. Studies using B cells with inducible latent gene expression were used to demonstrate that newly infected B cells are better recognized by CD8⁺ T cells, while latently infected B cells are better recognized by CD4⁺ T cells⁹⁷. CD8⁺ T cells recognized latency proteins quickly, but frequencies declined once expression was halted. CD4⁺ T cell recognition of latency proteins was initially delayed, but persisted for several days after expression was suppressed.

1.3 EBV-ASSOCIATED DISEASES

EBV and humans have coevolved for millions of years, during which both virus and host have developed intricate strategies to maintain coexistence in a disease-free setting; a disturbance of the balance between EBV and host immune responses can manifest as a variety of EBV-associated diseases. In the absence of T cells, the oncogenic potential of EBV is demonstrated *in vitro* by its capacity to immortalize B cells. *In vivo*, the incidence of EBV-associated diseases is significantly elevated in individuals with weak or suppressed immune systems. Despite the near ubiquity of EBV worldwide, EBV-associated malignancies are

relatively rare among individuals with intact immune systems. However, there is great geographical variation in incidence, and certain populations of otherwise healthy individuals are at high risk of developing EBV-associated malignancies. This points to a crucial requirement for genetic and environmental cofactors that contribute to the viral tropism and cellular transformation of EBV-associated cancers, but the exact contributions of EBV to the various malignancies are still not clearly understood.

The wide range of EBV-associated diseases can be divided into two broad categories: malignancies of B cell origin (lymphoid) and malignancies of non-B cell/epithelial cell origin. EBV-associated malignant disorders of B cells include a range of immunoblastic lymphomas (that arise during immunosuppression), BL, and a subset of HL. There are also a wide array of non-Hodgkin lymphomas that are positive for EBV to varying degrees¹⁰. Some malignancies of non-B cell origin include NPC, GC, and T cell/NK cell lymphomas. A list of the various diseases and the percent of cases associated with EBV can be found in **Table 1-3**. EBV has also been linked to a number of autoimmune disorders including multiple sclerosis⁹⁸, dermatomyositis⁹⁹, rheumatoid arthritis¹⁰⁰, and systemic lupus erythematosus^{101, 102}; elevated EBV DNA is often detected in the blood of patients with these diseases, but the role of EBV in disease pathogenesis is still unclear^{102, 103}.

Table 1-3: Diseases and their approximate association with EBV

Cellular origin	Disease	Association with EBV	latency type
	IM		III
B cell	B cell lymphoproliferative disease	90%	III
	Immunoblastic diffuse large B cell lymphoma (HIV)	>90%	III
	Chronic active EBV	100%	II
	Burkitt's lymphoma: Endemic	96%	I
	Sporadic	10-70%	
	HIV-associated	30-70%	
	Hodgkin's lymphoma	40-60%	II
	HIV-associated	95%	
Centroblastic diffuse large B cell lymphoma (HIV)	30%	I	
Non-B cell	Nasopharyngeal carcinoma	100%	II
	Gastric carcinoma	10%	I
	T/NK cell lymphomas	10-100%	II

Infectious mononucleosis

IM is a self-limiting lymphoproliferative disease that can be caused by primary EBV infection in adolescents and adults. It is largely a disease of developed countries, where higher standards of hygiene and sanitation result in delayed virus acquisition. Around 50% of adolescents or adults who become infected with EBV will develop IM¹⁰⁴, which is characterized by a massive expansion of latently infected B cells in lymphoid tissue and blood, lytic replication of virus in the oropharynx, and virion shedding into the saliva. Up to 25% of peripheral blood B cells can become infected with EBV during IM, and this stimulates a robust T cell response that can comprise up to 50% of the total T cell pool at its peak⁷⁸. Symptoms of IM are caused by this massive T cell response. Treatment is only supportive, and infection generally resolves on its own.

Malignancies of B cell origin

Immunoblastic lymphomas are a heterogeneous group of latency III-expressing B cell tumors that arise in immune compromised individuals who cannot mount an effective CTL response. Immune suppression can be a result of genetic defects (X-linked lymphoproliferative disease, XLPD), medical treatment (post transplant lymphoproliferative disease, PTLT), or immune-targeting infections (Human Immunodeficiency Virus; HIV)^{105, 106}. XLPD is caused by a mutation in a gene involved in the regulation of T cell activation and homeostasis, which results in an inability to control EBV-driven B cell proliferation¹⁰⁷. PTLT is a heterogeneous group of diseases associated with organ transplant; its development is largely dependent on the degree and duration of immune suppression as well as the type of organ transplanted. Lesions that occur within the first year after transplant are almost always EBV positive¹⁰⁸.

HIV-infected individuals have a 60- to 200-fold increased risk of developing various lymphomas¹⁰⁹. About 10% of all AIDS patients develop B cell malignancies, and EBV is associated with about 60% of cases overall. A small portion of these are considered immunoblastic latency III-expressing tumors, which tend to accompany T cell impairment observed during late stage AIDS. Immunoblastic diffuse large B cell lymphomas (DLBCLs)

comprise 15% of all HIV lymphomas, and >90% are EBV positive¹⁰. Other immunoblastic lymphomas such as primary central nervous system (CNS) lymphomas also occur during the late stages of AIDS and are usually EBV positive. EBV is also associated with cancers that express type I or type II patterns of latency during co-infection with HIV. The most common are BL (35%), HL (5%), and centroblastic DLBCL (25-30%)¹⁰. EBV is present between 30 to 70% (BL), >95% (HL), and in 30% (DLBCL) of cases¹⁰. BL and HL arise early during the course of HIV infection, when immune function is still relatively intact. HIV-infected individuals are also at increased risk for developing Non-Hodgkin lymphomas (NHL) and a variety of lymphomas that involve tissues within the gastrointestinal tract, lungs, liver, and bone marrow¹⁰⁹. NHL during HIV is EBV positive in 50% of cases¹⁰.

The two most common B cell malignancies that occur among immune-competent individuals are BL and HL. BL cells express a type I latency program. Endemic BL is the most common childhood tumor in equatorial Africa and New Guinea, and occurs at an astounding 5 to 20 cases per 100,000 children annually¹¹⁰. This accounts for 74% of all childhood malignancies in equatorial Africa¹¹¹. Non-endemic (sporadic) BL occurs equally across all age groups at a much lower incidence of 0.2 to 3 cases per 100,000 annually throughout the United States and Europe¹¹². While between 20 to 85% of sporadic BL tumors are EBV positive¹⁰, endemic BL is nearly universally positive for EBV¹¹². It is probably not a coincidence that endemic BL is highly prevalent in areas where malaria infection is common, as malaria induces B cell proliferation and may impair EBV-specific CTL activity¹¹³. One indication of a causative role for EBV in BL is that children in endemic regions with the highest antibody titers against VCA are the most at risk for subsequent BL tumor development¹¹⁴. A defining feature of BL is dysregulation of the *c-myc* oncogene caused by a chromosomal translocation into an immunoglobulin locus¹¹⁵. Constitutive expression of the c-MYC protein drives continuous proliferation and inhibits differentiation. EBV may expand the population of B cells at risk for this translocation, or EBV infection may aid in the survival of mutated cells that would have normally undergone apoptosis. Malaria-induced B cell activation would further expand the population of B cells at risk for malignant transformation.

HL is arguably the most common EBV-associated lymphoma worldwide, with about 40% of EBV-positive cases in the western hemisphere and 80% of cases in the developing world¹¹. One indication of EBV's contribution to HL is the 2- to 5-fold increased risk of disease following IM. Risk is highest within the first year after resolution of IM¹¹⁶, and increased antibody titers against EBV antigens have been found prior to the development of HL¹¹⁷. EBV genomes in HL cells are monoclonal, which implies that infection may be a prerequisite for the development of disease¹¹⁸. About 90% of EBV-positive HLs have mutated immunoglobulin genes that cause a loss of function¹⁰. Genes expressed during the type II pattern of EBV latency observed in HL cells may provide the proliferative and anti-apoptotic signals needed for oncogenesis.

Malignancies of non-B cell/epithelial cell origin

NPC and GC are both malignancies of epithelial cell origin that occur in immune competent individuals. NPC occurs worldwide, but it is 10 times more common in Southern China, where it is the most common malignancy in men and the second most common among women¹¹⁹; prevalence is also increased among the Inuit population in the Arctic^{15, 120}. EBV-associated GCs are most prevalent in Central and Eastern Europe as well as some countries in North and South America^{64, 121}. Such geographic variations of incidence imply that both genetic and environmental cofactors have important roles in the etiology of these two diseases. EBV-infected NPC cells typically exhibit a latency II pattern of gene expression, and EBV is more strongly associated with NPC than GC¹²². This is especially true among the undifferentiated subtype that is highly prevalent in China (20-30 cases per 100,000), where nearly all cases are EBV positive¹²⁰. About 10% of all GC cases are associated with EBV¹²³, which may be the most common EBV-associated non-lymphoid malignancy on a global scale, diagnosed in over 90,000 new patients each year¹²⁴. GC tumors express a type I pattern of latency with variable expression of LMP2A¹³. NPC arises from the mucosal epithelium of the nasopharynx, while GC arises from epithelial cells within the gastrointestinal tract. In both malignancies, the accumulation of genetic and epigenetic alterations results in the inactivation of tumor suppressor genes and overexpression of oncogenes, which in the presence of proliferative and anti-apoptotic

signals, leads to tumorigenesis^{64, 125}. EBV also contributes to a variety of other tumors, including carcinomas of the salivary glands, thymomas and thymic carcinomas derived from thymic epithelia cells, laryngeal carcinomas, and lymphoepithelial tumors of the respiratory tract¹⁰.

Atypical EBV infection of cells that are neither B lymphocytes nor epithelial cells is most often observed during immunodeficiency. Individuals with congenital immunodeficiencies, AIDS, or who have undergone transplant surgery occasionally develop leiomyosarcomas with EBV-positive smooth muscle cells expressing various iterations of latency I or II genes^{15, 126}. EBV is also present in virtually all T/NK cell lymphomas, which typically express a type II pattern of latency¹⁰⁹. Additionally, T and NK cells are infected with EBV during chronic active EBV (CAEBV), which is a rare lymphoproliferative disorder of childhood that usually presents after primary EBV infection¹⁰. The etiology of CAEBV is not known, but patients with various genetic mutations have been described, and EBV latency II proteins can be detected in the peripheral blood^{10, 123}.

EBNA1 and EBV-associated disease

One common thread between all EBV-associated diseases is the expression of the EBV latency protein EBNA1, which is the only protein expressed in all types of latency and in all EBV-associated malignancies. EBNA1 is important for initial B cell immortalization. It facilitates EBV genome persistence in latently infected cells, and it initiates the expression of additional latency genes such as the EBERs and small microRNAs, which are involved in cell transformation. The inhibition of EBNA1's DNA-binding ability results in decreased proliferation, loss of episomes, and even apoptosis in certain cell lines^{127, 128}. Conversely, the expression of EBNA1 in EBV-negative cells has been linked to less differentiated, more rapidly growing tumors with increased metastases^{129, 130}. EBNA1 also has several potentially transformative cellular effects that are independent of DNA binding and seem to be essential for EBV-associated carcinogenesis^{11, 131}.

In support of the importance of EBNA1, immune responses directed against the protein are decreased or absent in many EBV-associated malignancies. Furthermore, the loss of such T cells has been linked to the progression of various diseases, including HL, BL, NPC, and NHL⁶².

¹³²⁻¹³⁴. This implies a loss of such responses could contribute to an inability to control infection. HL patients with EBV-positive tumors have a selective loss of EBNA1-specific CD4⁺ T cells compared to patients with EBV-negative tumors and healthy seropositive donors⁶². In one study, 0 of 10 EBV positive, but 9 of 11 EBV negative HL patients had detectable EBNA1-specific CD4⁺ T cells by IFN-γ production or by proliferation assays⁶². Interestingly, the same patients all had detectable EBNA1-specific antibodies. The presence of EBNA1 IgG in the absence of specific CD4⁺ T cell help suggests those T cells were not always absent, but were lost at some point prior to or during tumorigenesis. Similar findings have been described in BL¹³⁴. A selective loss of EBV-specific T cells has also been detected in some HIV-positive individuals, including those under antiretroviral therapy with recovered total CD4⁺ T cell counts¹³³. Additionally, the loss of EBNA1-specific CD4⁺ and CD8⁺ T cells has been associated with the development of NHL¹³³, and a decrease in EBNA1-specific CD8⁺ T cells has been described among patients with EBV-positive NPC¹³². While it is unclear exactly what causes a loss of EBNA1-specific T cells, vaccines that aim to enhance or restore such responses could be a valuable therapeutic approach, as supported by the success of adoptive immune therapies discussed below.

1.4 TREATMENT OF EBV-ASSOCIATED DISEASES

Therapies for immunoblastic lymphomas have a range of effectiveness that is influenced by the source, degree, and duration of immune suppression. Common therapies include those that target viral replication (chemotherapy, radiation, antiviral agents), eliminate B cells nonspecifically (anti-B cell antibodies), or reconstitute EBV-specific immune responses (adoptive transfer). Treatment for PTLD highlights the importance of EBV-specific CTL immunity and function, as reconstitution of EBV-specific immune cells is often an effective therapeutic approach. In fact, between 25 to 63% of adults with early lesions respond well to a reduction of immunosuppression¹⁰⁹. EBV-specific T cells can also be reconstituted through adoptive transfer, where specific T cells are first expanded *in vitro* (using autologous LCLs) and then re-infused into PTLD patients. Activated EBV CTLs are polyclonal, long-lived, have broad reactivity to a range of

latency epitopes, and are able to eradicate tumors upon transfer *in vivo*¹³⁵. EBV-specific CTLs can be expanded from either donor or recipient cells, depending on what cells the PTLD lesions arise from. Both types have successfully been used as prophylaxis in patients with high viral loads after transplant or as treatment for patients with established PTLD^{136, 137}. Even partially HLA-matched donor T cells have demonstrated positive results¹³⁸. The best responses were generated when individuals also received high numbers of CD4⁺ T cells, which have been shown to directly target and kill EBV-transformed B cells in addition to providing helper functions¹⁰⁹.

The success of adoptive therapy for the treatment of PTLD has provoked interest in adapting a similar approach to treat other EBV-related diseases including NPC and HL. This approach has had more limited success due to the restricted expression of latent viral antigens and the various immune suppression/evasion techniques elicited by tumor cells¹⁰⁹. As a result, current strategies aim to target antigen recognition and augment CTL function by altering stimulation protocols, genetically modifying effector cells to render them resistant to certain types of immune suppression, and generating EBV-specific CD4⁺ T cell immunity in conjunction to CD8⁺ CTLs. Additional treatment options are generally the same for EBV positive and negative cancers, and include various combinations of chemotherapy, antiviral drugs, and other compounds that serve to activate viral gene expression in order to sensitize EBV-infected cells, inhibit the growth of cancer cells, or induce apoptosis¹³⁹.

Although adoptive transfer has resulted in sustained clinical responses in some patients, CTL generation is costly, time consuming, and requires access to highly specialized health care facilities. It is therefore an impractical solution for the thousands of patients diagnosed annually with EBV-associated diseases. Further development of strategies that exploit various aspects of EBV biology is warranted; vaccination would be the most cost-effective approach to reach the largest number of people, but there is currently no licensed preventative or therapeutic EBV vaccine.

1.5 VACCINE STRATEGIES

Vaccines have had a substantial impact on disease prevention since Edward Jenner first introduced the concept over 200 years ago. Vaccination has saved more than 700 million cases of disease and more than 150 million deaths¹⁴⁰. Vaccines are responsible for the eradication of smallpox, and diseases that once plagued the world such as poliomyelitis, measles, mumps, and rubella are now practically nonexistent. Vaccines induce protection by stimulating adaptive immune responses and generating functional memory cells that can be rapidly reactivated upon encounter with cognate antigen. The major component of protection for most of these highly successful vaccines is high affinity neutralizing antibodies, which can be generated by many types of vaccines including live attenuated, inactivated, or subunit vaccines¹⁴¹. Most vaccines are given prophylactically to prevent infection, but vaccines can also be used in a therapeutic context after infection has already occurred. Vaccines can limit the spread of a pathogen within infected cells, they can reduce transfer between individuals, and they have even been used to treat or prevent certain cancers.

Conventional vaccines

There are over 70 licensed vaccines that utilize different strategies to induce an immune response¹⁴². Conventional vaccines include live attenuated and inactivated vaccines, purified protein vaccines, peptide/subunit vaccines, DNA vaccines, and recombinant-vectored vaccines. Live attenuated vaccines are most commonly generated through prolonged passage of pathogen in a non-human host so that it can no longer replicate in human cells. Because of their capacity to infect host cells, live attenuated vaccines can induce B and T cell responses; however, the possibility of reversion to virulence is cause for concern. An alternative to live, attenuated vaccines are inactivated (killed) vaccines, which are generated by exposing pathogen to heat, chemicals, or irradiation. Inactivated vaccines do not pose the threat of reversion to virulence, but in exchange they are not as immunogenic and may require multiple exposures to generate long-term immunity. Despite their capacity to elicit broad-ranging potent responses, live

attenuated or killed EBV vaccines are generally not considered a viable option due to the carcinogenic potential of EBV and the capacity for a number of EBV genes to independently transform cells¹⁴³. Protein/subunit vaccines are generated against an immunogenic fragment of the pathogen (typically a protein), either through isolation or using recombinant DNA technology. Immune responses are typically weak, require multiple boosts, and are primarily humoral; synthetic peptides can be used for vaccination in a similar manner. Alone, synthetic peptide vaccines are even less immunogenic than protein/subunit vaccines; however, they can also be incorporated into immune-stimulating complexes with both B and T cell epitopes that induce both humoral and CMI responses. DNA vaccines carry the gene sequence of a specific antigen that is produced inside host cells after vaccination. As a result, DNA vaccines typically favor CMI. Despite the low cost and relative safety of DNA vaccines, delivery and immunogenicity remain a challenge. Recombinant DNA technology can also be used to generate recombinant-vectored vaccines. In this approach, genetically modified viruses such as vaccinia virus and adenovirus serve as vectors for delivering antigen, which is then produced at high levels within the immunized host. Recombinant viral vector vaccines- especially those that infect APCs- have the potential to elicit strong B and T cell responses, and the delivery system itself can even act as a potential adjuvant. Pre-existing immunity and additional safety concerns are challenges for recombinant virus vaccines, but vector modifications, use of viruses that do not commonly infect humans, and development of replication-defective vectors can overcome many of these obstacles¹⁴⁴.

Adenovirus as a vaccine carrier

There are over 50 known human Adenovirus (AdHu) serotypes, which commonly infect humans at a young age. Although relatively non-pathogenic, infection can cause acute respiratory or gastrointestinal illness¹⁴⁵. Adenoviruses (Ad) contain a linear, double stranded DNA genome that is encapsidated in an icosahedral protein shell. The Ad genome can range between 26 to 45 kb pairs long, and contains two inverted terminal repeats (ITRs) at either end¹⁰. Genes are grouped by early, intermediate, and late transcription units¹⁰. The early E1A gene is

expressed first and acts as a transactivator for expression of the remaining early genes. It is therefore necessary for viral replication.

Recombinant Ad-based vectors are an ideal system to deliver antigen for many reasons. First, Ad can be rendered replication-defective by deleting the essential early E1 gene (which is provided in trans during production)¹⁴⁶. Large amounts of foreign DNA can then be incorporated into the deleted E1-domain and expressed off exogenous promoters to ensure high levels of transgene expression¹⁴⁷. Second, Ad vectors express high levels of transgene product in a wide range of cell types, including DCs and macrophages¹⁴⁸. As a result, vectors induce potent and protective transgene product-specific CD8⁺ T cell responses¹⁴⁹. Finally, recombinant Ad vectors are safe, easy to manipulate, and relatively inexpensive to manufacture.

Ad was initially studied as a delivery vehicle for gene transfer, but potent immune responses to both the vector itself as well as the transgene product rapidly cleared Ad-transduced cells and caused serious side effects in some individuals^{150, 151}. The induction of robust T cell responses raised concern for the use of Ad vectors in gene therapy, but was beneficial for the use of Ad vectors as vaccine carriers. The inherent immunogenicity of Ad acts as an adjuvant for stimulating cellular and humoral immune responses, and transgene product-specific responses are sustained over time^{152, 153}. While Ad-transduced cells at the site of vaccination are rapidly cleared by the immune system, very low levels of transcriptionally active vector have been shown to persist in activated T cells and may act as an internal 'boost' for the specific responses¹⁵³.

Several Ad serotypes have been developed for use as vaccine vectors. Early studies focused on AdHu5, which along with AdHu2, are the most prevalent serotypes that infect humans. Mice vaccinated with AdHu5 vectors that expressed rabies glycoprotein (rab.gp) quickly developed protective titers of rab.gp-specific neutralizing antibodies along with antigen-specific CD8⁺ and CD4⁺ T cells¹⁵⁴. Ad vaccine vectors have since been tested with a variety of viral antigen-based transgenes, and they all elicited very high transgene product-specific B and T cell responses¹⁵⁵. Furthermore, the magnitude of transgene-specific T cells is often higher in comparison to responses elicited by other recombinant viral vectors and by DNA vaccines¹⁵⁶.

One potential problem for the use of AdHu5 vaccine vectors is pre-existing immunity. Between 45 to 80% of adults have high titers of neutralizing antibodies specific to AdHu5, which varies depending on geographic region¹⁵⁷. Pre-existing neutralizing antibodies and vector-specific T cells can inhibit adaptive immune responses either by restricting the amount of viral vector that can enter APCs and express transgene (antibodies) or by quickly eliminating vector-transduced cells (CMI)¹⁵⁸. This has been demonstrated in animals that were pre-exposed to AdHu5 prior to immunization with AdHu5 vectors. Transgene product-specific CD8⁺ T cell and B cell responses were reduced in comparison to responses of animals that were not first exposed to AdHu5¹⁵⁸.

Numerous approaches can be used to circumvent the issue of pre-existing immunity. One approach is to increase the vector dosage; however, extremely high doses of Ad vector can induce serious side effects. Alternatively, transgene product-specific responses can be enhanced through prime-boost vaccine strategies that utilize heterologous Ad vectors or additional delivery vehicles¹⁵⁹. Another approach that avoids pre-existing immunity is the use of serologically distinct uncommon human Ads^{160, 161} or Ads that naturally infect non-human species^{157, 162}. Recombinant vectors derived from simian Ad (SAdV, hereon referred to as AdC) are similar to human Ad in terms of genetic organization, structure and cell tropism¹⁶². AdCs have been found to induce strong transgene product-specific T and B cell responses in a similar magnitude as human Ads following systemic vaccination¹⁶³. This has been shown repeatedly in both mice and non-human primates (NHPs) using a variety of transgene products^{159, 164-166}. As a result, several recombinant AdC vectors have been developed as vaccine carriers, including serotypes C68 (AdC68), C6 (AdC6), and C7 (AdC7)¹⁶⁷.

Needs and challenges of an EBV vaccine

Despite their vast impact on public health, current vaccines have their limitations. Vaccines are not yet protective against pathogens with antigenic hypervariation or intracellular pathogens that require T cells for control. Persistent infections with long periods of latency face a unique set of challenges, as the development of -or protection against- clinical disease may not

be feasible endpoints for measuring vaccine efficacy, and traditional correlates of protection may not be sufficient or even desirable outcomes. Neutralizing antibodies are not suited to clear cells that harbor virus. Instead, potent, CTLs are typically responsible for clearing latently infected cells. A thorough understanding of the nature of such antigen-specific T cell responses and appropriate methods of quantification is therefore important for vaccine development. Additional surrogates of protection and biomarkers of disease are also needed, but this information is typically not known until efficacy has been demonstrated in large-scale clinical trials.

A successful EBV vaccine could have numerous applications. The first, and perhaps most obvious use would be to prevent primary EBV infection. However, designing an EBV vaccine that provides sterilizing immunity has been quite challenging—mostly because it is unclear what type of immunity would provide protection from repeated mucosal infections. Furthermore, the natural immune response to EBV may not be sufficient in protecting healthy seropositive individuals from recurrent infections, as repeated infections with different strains of EBV have been described in otherwise healthy individuals^{10, 168}. A second application for a preventative EBV vaccine would be to reduce the incidence of IM, even if the rate of acquisition does not change. The massive expansion of EBV-specific T cells during IM has been described as an “abnormal” immune response that subsequently impairs the immune system¹⁶⁹ and increases the risk of acquiring certain EBV-associated diseases such as HL¹⁷⁰. Furthermore, serum EBV DNA levels are elevated before the onset of PTLD as well as NPC¹⁰⁴. Therefore, a vaccine that prevents IM or facilitates better control of viral DNA in the blood may ultimately decrease the incidence of EBV-associated malignancies. Vaccination to prevent EBV infection or disease would benefit a variety of populations including transplant recipients, individuals in areas with high incidences of NPC and BL, and western societies where there is a high incidence of IM.

EBV vaccines can also be administered to EBV seropositive individuals in the context of therapeutic vaccination to treat or prevent certain malignancies. Currently, the majority of therapies to treat EBV-associated diseases involve an *ex vivo* component, where T cells are stimulated, expanded, and then re-infused. A therapeutic vaccine that is capable of expanding specific immune responses *in vivo* could reach far more individuals than the current adaptive

immune strategies, although adaptive techniques would still be important for individuals where vaccination is not an option. The goal of a therapeutic EBV vaccine would be to restore cellular immunity in diseases where important responses are lacking, such as NPC, HL, and BL. In the presence of disease, vaccination could be administered to elicit or boost T cell responses that limit progression or cause remission. Vaccination could also be used to prevent disease occurrence among high-risk seropositive individuals. Additional groups that would potentially benefit from such a vaccine include those at high risk of acquiring HIV infection as well as HIV-positive individuals with relatively stable CD4⁺ T cells and low HIV loads.

An important factor to consider when designing an EBV vaccine is that of target antigens; but because the immune correlates of protection against EBV infection, IM, and EBV-associated malignancies are not well understood, optimal target antigens are still unclear. The decision of which viral antigens to target through vaccination largely depends on the desired outcome/vaccine application. A preventative EBV vaccine would probably need to elicit neutralizing antibodies; most antigens that elicit neutralizing antibodies are expressed during lytic replication. An effective therapeutic vaccine would need to target the smaller range of proteins expressed during latency, when virus is not replicating. Furthermore, therapeutic EBV vaccine strategies should aim to elicit or boost cellular immune responses against specific EBV antigens that are expressed in the various malignancies. Since different malignancies express different EBV antigens, this is another factor that must be appropriately considered. The work described here focuses on EBNA1 because it is the only latent antigen that is expressed in all EBV-associated malignancies. It is therefore a very promising target for a therapeutic vaccine.

EBV vaccine studies

Most vaccine efforts to date have focused on EBV's gp350, which is the most abundant of the surface antigens, is the main target of virus-neutralizing antibodies, and is also a target for CTLs¹⁰⁴. The potency of gp350 antibodies was demonstrated in immunodeficient mice reconstituted with PBMCs from EBV seronegative individuals¹⁷¹. Monoclonal antibodies to gp350 prevented the development of lymphoma after EBV challenge¹⁷². Recently, two tetrameric gp350

vaccines (a subunit vaccine and a DNA vaccine) were found to be more immunogenic than their monomeric equivalents¹⁷³, however the significance of these results is unknown, as mice were not challenged with tumor after vaccination. Recombinant gp350 in combination with adjuvants or expressed by adenoviral or vaccinia viral vectors also protected cotton-top tamarins and common marmosets from developing EBV-induced lymphomas¹⁷⁴⁻¹⁷⁶. Interestingly, vaccination with the gp350-expressing viral vectors as well as with certain preparations of soluble gp350 did not induce neutralizing antibodies, which suggests a role for CMI^{174, 175, 177}. EBV acquisition in the absence of lymphoma was not a quantified endpoint because these animals do not develop persistent EBV infection.

Vaccines designed to elicit neutralizing antibodies have also been tested in humans, with variable results. A gp350-expressing vaccinia virus induced neutralizing antibodies to EBV when tested in seronegative children in China¹⁷⁸. All 10 children that received the placebo vaccine seroconverted 1.25 years after immunization, while only 3 of 9 vaccinated children became infected in the same time span. In a phase I trial of children with chronic kidney disease, only 33% developed neutralizing antibodies after receiving three doses of soluble gp350, and immune responses declined rapidly¹⁷⁹. Authors concluded that the dosage and adjuvant were likely not optimal. In the only phase II trial of a prophylactic EBV vaccine, vaccination of EBV seronegative adults with three doses of soluble gp350 reduced the rate of EBV IM by 78%, but it did not reduce the rate of EBV acquisition¹⁸⁰. Despite promising results, it is still not clear if a reduction in the rate of IM will reduce the risk of certain malignancies.

Vaccines designed to elicit cellular-based responses have also been studied. The majority of these cell-based therapies have required some sort of *ex vivo* expansion or stimulation phase, but more traditional vaccine designs are under development. In a phase I clinical trial of HLA-matched, EBV seronegative adults, vaccination with an epitope-specific EBNA3A peptide vaccine induced epitope-specific T cells in eight of nine recipients¹⁸¹. Four of those vaccine recipients later became infected with EBV, but none developed IM. In comparison, one of the two placebo recipients who acquired EBV developed IM. Importantly, this study demonstrated that vaccine-driven induction of EBNA3-specific cellular immune responses did not significantly

influence the development of a normal repertoire of EBV-specific T cell responses following seroconversion. This indicates that vaccination will likely not introduce additional risks upon primary exposure to EBV. It also demonstrates the capacity of cell-mediated immunity to protect against IM. Although EBNA3 is highly immunogenic, its expression is limited to lymphoblastic diseases. The challenge now is to devise novel strategies that target other EBV latent antigens expressed during the more restricted phases of latency that are associated with cancers such as NPC, BL, and HL.

Additional vaccine candidates that have induced antibody and/or T cell responses in mice or in human cell lines include an LMP2A-derived peptide-based vaccine, which prolonged survival after tumor challenge and inhibited tumor growth therapeutically¹⁸²; a virus-like particle vaccine expressing EBNA1, LMP2, and nearly all of the EBV lytic genes except BZLF1, which induced neutralizing antibodies and T cell responses in mice and reactivated human T cells lines¹⁸³; and Ad-based vaccines expressing various combinations of EBNA1, LMP1, and LMP2 epitopes, which in one study stimulated T cell responses in healthy EBV seropositive and NPC patient cell lines that inhibited LCL outgrowth¹⁸⁴. This wide array of vaccine candidates serves to explore a variety of options in order to determine the most effective methods for eliciting the most successful responses in the absence of known correlates of protection.

1.6 AN ANIMAL MODEL FOR EBV: RHESUS LYMPHOCRYPTOVIRUS

Because EBV only infects humans, vaccine development has been largely impeded by the lack of an appropriate animal model for EBV research. Humanized mouse models are an alternative system, but the reconstituted immune systems in mice are not identical to those of healthy humans. Despite recent improvements, it is likely that some features of the human immune response will not be accounted for¹⁸⁵. Cotton-top tamarin monkeys can become infected with very high titers of EBV and subsequently develop EBV-induced B cell lymphomas, but the high doses and non-physiologic route of infection (intraperitoneal injection) make it challenging to

translate results to humans. More importantly, these animals are now an endangered species and are therefore not practical as pre-clinical models for vaccine development.

An alternative approach for studying EBV is to use a related virus, rhesus lymphocryptovirus (rhLCV), which naturally infects rhesus macaques (*Macaca mulatta*). The animal model based on rhLCV is a particularly powerful tool for studying various aspects of EBV due to its unusually high degree of biologic, genetic, and pathogenic similarity to EBV and the similarity of the immune responses between humans and non-human primates¹⁸⁶⁻¹⁸⁹. Infection of non-human primates strongly resembles EBV infection of humans¹⁸⁷. Most animals are infected during infancy through the oral route, and a majority of the target population is naturally infected by adulthood^{187, 190}. The virus, which can be detected in blood or upon activation in saliva, persists for life as a latent infection in B cells. As seen with humans, rhLCV infection induces transient lymphoproliferation *in vivo* and immortalizes B cells in tissue culture¹⁸⁷. Animals can develop virus-associated malignancies, and the incidence of these malignancies is increased during immunosuppression^{190, 191}. Furthermore, rhLCV has a high degree of sequence homology to EBV, molecular organization is well conserved between the two viruses, and they have an identical repertoire of latent and lytic genes (**Figure 1-3**)^{190, 192, 193}. In fact, rhLCV is the only fully sequenced gamma-1 herpesvirus with a homolog for every EBV gene, and the functions of the genes are complementary. Thus, the biology, molecular virology, and immunology of rhLCV infection in rhesus macaques are very similar to EBV infection in humans, making this model appropriate for studying EBV immunology as well as for pre-clinical testing of EBV therapeutics.

Figure 1-3: EBV and rhLCV ORF homology

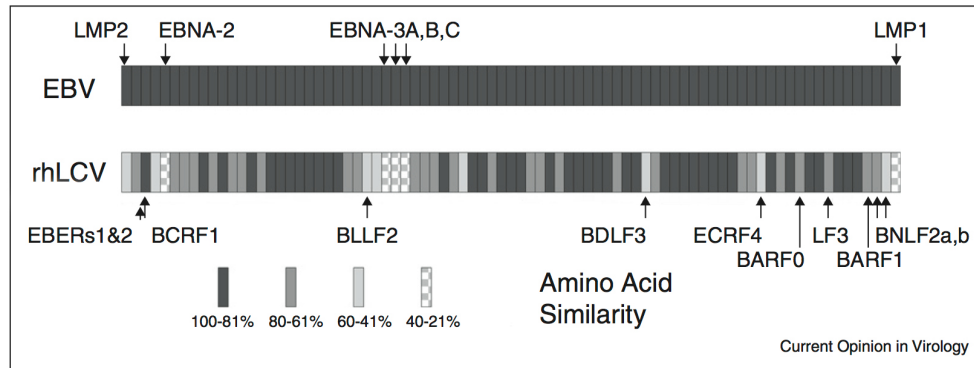


Figure 1-3: Small boxes representing the open reading frames (ORFs) of EBV and rhLCV are aligned in positional order within each genome. EBV and rhLCV share an identical repertoire of ORFs, and genomic arrangements are the same. The degree of amino acid similarity between homologous EBV and rhLCV ORFs ranges between 28% to 98% and is represented by the various shading and patterns within each box. Average homology between all EBV and LCV ORFs is 75.6%. EBNA1 sequence homology falls within the light grey box, at about 46%. BZLF1 sequence homology falls within the medium grey box, at about 71%. Figure was adapted from Wang F., 2013¹⁸⁶.

1.7 OBJECTIVES AND SIGNIFICANCE

Since its discovery over 60 years ago, great strides have been made towards understanding the virology and pathogenesis of EBV. However, translating this information into an effective prophylactic or therapeutic EBV vaccine has proven challenging, and progress towards an EBV vaccine has been slow. Most EBV vaccine efforts to date have focused on decreasing acquisition or reducing the burden of IM. A therapeutic EBV vaccine could also significantly improve public health, but there are still many questions that need to be answered before such a vaccine can reach fruition.

Work described here focuses on EBNA1 as a potential target for a therapeutic EBV vaccine. EBNA1 is an attractive target for vaccination because it is the only EBV protein consistently expressed in all forms of latency and in all EBV associated malignancies. Despite this, EBNA1 has only recently begun to be viewed as an appropriate vaccine antigen. It was originally believed that EBNA1-specific CTL responses were either non-existent or non-functional due to an internal glycine-alanine rich repeat domain (GAR) that had been shown to interfere with antigen presentation by MHC class I molecules¹⁹⁴⁻¹⁹⁶. However, it has since been demonstrated that functional EBNA1-specific T cells are frequently detected in EBV-infected humans¹⁹⁷⁻¹⁹⁹, and a loss of EBNA1-specific CD4⁺ and/or CD8⁺ T cells has been correlated with numerous EBV-associated diseases, including HL, NPC, and BL^{62, 132-134}. These findings suggest that EBNA1 plays an important role in controlling EBV infection.

The overarching goal throughout this dissertation was to determine if EBNA1 is a suitable target for vaccine development. This was addressed with the following aims:

I. Characterize the T cell response to the latent antigen rhEBNA1.

An improved understanding of important immune responses benefits the preclinical development of potential EBV vaccines. Therefore, using the EBV homolog rhLCV as an animal model for EBV, we aimed to characterize the magnitude, phenotype, and functionality of rhesus EBNA1 (rhEBNA1)-specific T cell responses in naturally infected animals. This was done using

some of the most advanced flow cytometry techniques that allow us to precisely characterize responses using a multitude of biological and immunological markers. We hypothesized that most animals would have detectable responses that exhibited a variety of functions. By comparing our findings to the human EBNA1 response, these studies also serve to validate the rhLCV animal model and to establish baseline responses so that we can use this model to develop and test potential vaccines.

II. Develop novel recombinant adenoviral-based vaccine vectors that express rhEBNA1.

EBNA1-specific T cell responses are reduced in a variety of EBV-positive cancers, and a loss of these responses is associated with disease progression. Thus, the primary goal of a therapeutic EBV vaccine would be to restore or enhance EBNA1-specific T cell-mediated immunity directly *in vivo*. Such a vaccine would need to elicit both protective CTL responses as well as a strong central memory component. With that in mind, we developed recombinant Ad-based vaccine vectors that express rhEBNA1 as potential therapeutic prototype vaccines. Ad vectors have been shown to induce potent, multi-specific, and sustained transgene product-specific T cell responses, which is important for targeting cells that are already infected with virus. To further enhance transgene-specific responses, we also included herpes simplex virus glycoprotein D (HSV-gD), which is a known inhibitor of the herpes virus entry mediator - B and T lymphocyte attenuator (HVEM-BTLA) immune inhibitory signaling pathway. Our lab has consistently shown that vaccines that express antigen as fusion protein with HSV-gD elicit more potent T cell responses compared to vaccines that express the antigen alone. These results are independent of antigen or of vaccine carrier. We therefore expected vaccines containing HSV-gD to induce larger transgene-specific responses compared to appropriate controls. Replication-defective Ad vector vaccines expressing rhEBNA1 within functional or non-functional versions of HSV-gD were generated and subsequently tested in a series of *in vitro* and small animal studies for quality control purposes. The main goals of these studies were to demonstrate that all vaccines expressed equal levels of transgene and were capable of inducing EBNA1-specific T cell responses.

III. Vaccinate naturally rhLCV-infected rhesus macaques and evaluate the effect of vaccination on rhEBNA1-specific cellular immunity.

The rhLCV animal model is an excellent tool for the preclinical development of EBV vaccines. Using this system, we sought to evaluate whether vaccination could expand functional rhEBNA1-specific T cells in rhesus macaques with persistent rhLCV infection. Fifteen healthy rhLCV seropositive rhesus macaques were enrolled in the study, and animals were vaccinated in a prime-boost regimen with two serologically distinct replication-defective adenoviral vectors that expressed our chimeric rhEBNA1 constructs. To better understand the effect of vaccination on T cell phenotype and function, we once again conducted in-depth analyses of rhEBNA1-specific T cells using flow cytometry. It has been shown that suboptimal latent EBV T cell responses from both healthy and EBV-positive tumor bearing individuals can be recovered *ex vivo*^{200, 201}. Therefore, our goal was to determine if the induction or expansion of rhEBNA1-specific responses is possible *in vivo* through vaccination. We hypothesized that vaccination with Ad-based rhEBNA1 vectors would lead to the expansion of functional rhEBNA1-specific T cells in the majority of vaccinated animals. This study serves as an important proof-of-principle analysis of a therapeutic rhEBNA1-based vaccine regimen and provides insight into appropriate strategies for therapeutic EBV vaccination. Most importantly, our findings address the critical question of whether EBNA1 is a viable target for vaccination.

CHAPTER 2:

T CELL RESPONSES TO LATENT ANTIGEN EBNA1 AND LYTIC ANTIGEN BZLF1 DURING PERSISTENT RHLCV INFECTION OF RHESUS MACAQUES

ABSTRACT

Epstein Barr virus (EBV) infection leads to life-long viral persistence through its latency in B cells. EBV-specific T cells control reactivations and prevent the development of EBV-associated malignancies in most healthy carriers, but infection can sometimes cause chronic disease and malignant transformation. Epstein-Barr Nuclear Antigen 1 (EBNA1) is the only viral protein consistently expressed during all forms of latency and in all EBV-associated malignancies, and is a promising target for a therapeutic vaccine. Here we studied the EBNA1-specific immune response using the EBV-homologous rhesus lymphocryptovirus (rhLCV) infection in rhesus macaques. We screened 40 animals for rhLCV EBNA1 (rhEBNA1)-specific T cell responses by intracellular cytokine staining (ICS) and flow cytometry. We then assessed the frequency, phenotype, and cytokine production profiles of rhEBNA1-specific T cells in 15 rhesus macaques and compared to the lytic antigen of rhLCV, BZLF1 (rhBZLF1). We were able to detect rhEBNA1-specific CD8⁺ and/or CD4⁺ T cells in 14 of the 15 animals screened. In comparison, all 15 animals had detectable rhBZLF1 responses. Peptide-specific CD8⁺ T cells showed a more

activated phenotype, belonging mainly to the effector cell subset, while most peptide-specific CD4⁺ T cells exhibited a resting phenotype of central memory (T_{CM}). By comparing our results to the human EBV immune response, we demonstrate that the rhLCV model is a valid system for studying chronic EBV infection and for the pre-clinical development of therapeutic vaccines.

Portions of this chapter were adapted from:

Leskowitz RM, Zhou XY, Villinger F, Fogg MH, Kaur A, Lieberman PM, Wang F, and Ertl HC. CD4⁺ and CD8⁺ T cell responses to latent antigen EBNA1 and lytic antigen BZLF1 during persistent lymphocryptovirus infection of rhesus macaques. *Journal of Virology* 2013; 87(15):8351-8362.

INTRODUCTION

The Epstein-Barr Nuclear Antigen 1 is a particularly important target for vaccination, as it is the only protein present during all stages of viral infection including every form of latency, lytic infection, and all EBV-associated cancers²⁰². EBNA1 is a 76 kilo Dalton (kDA) viral-encoded DNA binding phosphoprotein that is essential for the maintenance and replication of viral DNA during latency²⁰³. EBNA1 is therefore tightly linked to EBV persistence³³, and the elimination of EBNA1 from the EBV genome results in a rapid loss of stability^{33, 204}. Furthermore, dominant negative forms of EBNA1 or siRNA depletion of EBNA1 inhibits EBV-dependent B cell proliferation, thus indicating that EBNA1 is also important for B cell transformation during latency^{205, 206}. EBNA1 is separated into C and N terminal domains, which are linked by an internal glycine-alanine rich repeat domain (GAR). The repeat domain stabilizes the protein and inhibits EBNA1's degradation by cellular proteasomes^{194, 195}. As a result, both the generation of peptide sequences for association with MHC class I molecules and the induction of EBNA1-specific CD8⁺ T cells are impaired¹⁹⁵. Furthermore, the mRNA that encodes the GAR is enriched for purines, which causes a lack of secondary structure and reduces the translation efficiency and antigen presentation of EBNA1^{196, 207}. Consequently, despite its obvious importance, EBNA1 was not originally considered a viable target for vaccination, as it was believed to escape immune detection by CTLs.

Nevertheless, recent studies have demonstrated that most EBV-infected humans develop CD8⁺ T cells in response to EBNA1^{197, 198}. The primary source of epitopes is most likely newly synthesized EBNA1 as a result of proteasome-dependent degradation of defective ribosomal products (DRiPs) during translation^{197, 198, 208}. Long-lived, stable EBNA1 has a half life greater than 20 hours in B cells and is therefore not a likely source of epitopes¹⁹⁵. Upon expansion, EBNA1-specific CTLs have been shown to prevent the outgrowth of infected B cells *in vitro* and to secrete IFN- γ in response to stimulation, thus suggesting they play a role in controlling infections *in vivo*¹⁹⁹. Additionally, EBNA1 is an immunodominant target of EBV-specific CD4⁺ T cells that are capable of inhibiting virus-induced B cell proliferation *in vitro*^{92, 209}. In support of the

importance of EBNA1-specific T cell responses, loss of EBNA1-specific CD4⁺ or CD8⁺ T cells has been correlated with numerous diseases, including non-Hodgkin's lymphoma, nasopharyngeal carcinoma, and Burkitt's lymphoma^{62, 132-134}.

While we know that EBNA1-specific CD4⁺ and CD8⁺ T cells develop in response to EBV infection²⁰³, little is known on how persistent, low-level antigen exposure influences the phenotype and functionality of this response *in vivo*. Generally, if antigen is not cleared following primary infection, CD4⁺ and CD8⁺ T cells can develop various degrees of functional exhaustion²¹⁰. Each pathogen and host establish their own unique relationship that varies depending on the duration, magnitude, and location of antigen exposure²¹¹. Chronic viremia and continuous high antigen exposure leads to constant T cell receptor triggering that causes progressive T cell dysfunction and interferes with differentiation into the T_{CM} cell pool²¹². In the most severe situations, this may ultimately result in physical deletion of the responding cells; however, a hierarchical loss of effector functions is more frequently observed²¹². The ability of cytotoxicity, robust proliferation, and IL-2 production are lost at early stages of exhaustion. This is followed by the loss of TNF- α and then IFN- γ production²¹². In contrast, T cells responding to persistent infection with low antigen exposure are not as severely impaired²¹². Studies examining the effect of gammaherpesvirus persistence on the T cell response in mice demonstrate more limited proliferative potential in response to antigen, but the antiviral T cell response is vigorous and exhibits immediate cytotoxic function²¹³. Exhausted T cells also upregulate various cell surface markers, and the number and level of expression appears to be associated with the severity of infection and degree of exhaustion²¹⁴.

A detailed understanding of the immune response to EBNA1 benefits the preclinical development of EBV vaccines. The most common methods for studying EBV-specific T cell responses utilize EBV-specific T cell lines expanded *in vitro* after repetitive antigenic stimulation, which can change T cell function and lead to selective proliferation of specific clones. Instead, we aim to characterize EBNA1-specific T cell responses directly *ex vivo* using intracellular cytokine staining, which offers the ability to both quantitate these responses and to analyze their functional nature directly without expansion.

Using the rhLCV model, we have characterized the magnitude, phenotype, and function of latent rhEBNA1-specific immune responses in healthy rhLCV-infected rhesus macaques. Although some studies have been conducted to assess immune responses to rhLCV^{188, 215}, the scope of such studies has been more limited. Here we screened 40 captivity-kept rhesus macaques for rhEBNA1-specific T cells using ICS followed by multicolor flow cytometry. We then characterized peptide-specific T cell responses in blood from a cohort of 15 captivity-kept rhesus macaques, which allowed us to define dominant CD4⁺ and CD8⁺ T cell subsets and cytokine production profiles. We compared this to responses directed against the highly immunogenic, immediate-early lytic rhBZLF1 protein, which has been studied extensively in humans and to some degree in rhesus macaques. Our results show that most rhLCV seropositive animals carry both rhEBNA1- and rhBZLF1-specific T cells. RhEBNA1-specific CD4⁺ T cells were highly functional, with both T_{CM} and T_{EM} cell subsets and a wide range of cytokine responses, while specific CD8⁺ T cells were composed primarily of more activated IFN- γ -producing effector cells. In contrast, rhBZLF1-specific CD4⁺ T cells maintained a resting phenotype of T_{CM} cells and primarily produced single-cytokine responses. As with rhEBNA1, the CD8⁺ T cell response against rhBZLF1 was more activated than the CD4⁺ T cell response, but contained a large proportion of memory cells as well. The similarities between our findings and the human immune response against these two very important proteins serve to further validate the rhLCV model as a useful and highly relevant animal model for studying various aspects of EBV. Our studies are also fundamentally important for establishing baseline responses so that the rhesus macaque model can be used for exploring potential EBV vaccines.

RESULTS PART I

Characteristics of NHPs

Forty Indian-origin rhesus macaques were enrolled in this study at the Yerkes National Primate Center (YNPC). All animals were female adults ranging from 5-19 years of age at the start of the study. Animals were either housed at a field station or at the main station, and all except ID# 442, PH1019, and PWW were born at YNPC. All animals were SIV negative and all but two animals (RNg7, Rje8) had antibodies to rhLCV. Thus, 95% (38/40) of the rhesus macaques enrolled in our study were rhLCV seropositive. Animals were tested for Mamu-A*01, A*02, A*08, B*01, B*04, B*08, B*17 (YNPC). **Table 2-1** shows housing arrangements, age, rhLCV serology, genotype, and blood collection time points for each animal.

Table 2-1: List of rhesus macaques used in this study

NHP ID #	Housing	Age at start of study	rhLCV serology	MHC Alleles	Blood collection	rhEBNA1		
						CD4 ⁺	CD8 ⁺	
RUu6	MS	10	Y		0, 2M	Y	Y	
442		11	Y	B.01	0	Y	Y	
RDn6		11	Y		0	Y	Y	
RLz5		12	Y		0, 4-6M, 11-13M	Y	Y	
RCv5		13	Y		0, 4-6M, 11-13M	Y	Y	
RTn5		15	Y	A.01, A.08	0, 2M, 4-6M, 11-13M	Y	Y	
RQm7		9	Y		0	Y	N	
RBm7		9	Y	A.01	0	Y	N	
RAT7		9	Y	A.01, A.02	0	Y	N	
RZl7		9	Y	A.01, B.17	0, 4-6M, 11-13M	Y	N	
RCj7		9	Y		0, 4-6M, 11-13M	Y	N	
RFu7		10	Y	A.01	0	Y	N	
RVw6		10	Y	A.01, A.08, B.01	0, 2M, 4-6M, 11-13M	Y	N	
RCa6		12	Y	B.17	0, 2M	Y	N	
RQf7		10	Y	A.01	0	N	N	
PH1019		10	Y	A.08, B.17	0, 2M, 4-6M, 11-13M	N	N	
RMr6		11	Y	A.01, B.01	0	N	N	
RJy5		12	Y	B.17	0	N	N	
RQf6		12	Y	A.02	0	N	N	
RYa6		12	Y	B.01, B.17	0, 4-6M, 11-13M	N	N	
PWw		13	Y	A.02, A.08	0, 2M, 4-6M, 11-13M	N	N	
RKc5		14	Y	B.01	0	N	N	
Rje8		8	N	A.01	0	N/A	N/A	
RNg7		10	N	A.01, B.17(?)	0	N/A	N/A	
RBo10		FS	5	Y	A.01, B.08	0	Y	Y
RLy9			6	Y		0, 4-6M, 11-13M	Y	Y
Ref8			8	Y		0	Y	Y
RDc8			8	Y	A.02	0	Y	Y
RYr9	6		Y	A.01	0	Y	N	
RRi9	7		Y	B.01	0, 4-6M, 11-13M	Y	N	
RQb8	8		Y	A.01	0	Y	N	
RNm8	8		Y		0	Y	N	
RBt7	9		Y	A.01, B.01	0	Y	N	
RQt5	13		Y		0, 4-6M, 11-13M	Y	N	
RTp4	15		Y		0, 4-6M, 11-13M	Y	N	
RJm10	5		Y	B.17	0	N	N	
RNw9	6		Y	A.08	0, 4-6M, 11-13M	N	N	
RTf9	7		Y	A.01, B.01	0	N	N	
RCs7	9		Y		0	N	N	
RYc3	19		Y	A.01	0, 4-6M, 11-13M	N	N	

Abbreviations: NHP, non-human primate; DOB, date of birth; FS, field station; MS, main station. Blood from all 40 animals was collected over a period of two months (time point 0). Additional samples from smaller cohorts were collected at 2 months (6 animals), 4-6 months (15 animals), and 11-13 (15 animals) months after initial bleeds. The two most right-hand columns reflect presence or absence of rhEBNA1-specific CD4⁺ (left) or CD8⁺ (right) T cells detected by ICS at time point 0.

RhEBNA1 responses can be quantitated and characterized directly from the peripheral blood of rhesus macaques

The ability to detect rhEBNA1-specific T cells directly *ex vivo* is important for analyzing intricacies of the immune response and is critical for experiments such as vaccine testing, where the direct effect of vaccination and potential correlates of protection can be assessed. Therefore, our first goal was to determine if rhEBNA1-specific T cells in the peripheral blood of naturally rhLCV infected rhesus macaques can be detected directly *ex vivo* using ICS. To accomplish this, we enrolled a large cohort of 40 animals for testing. The two animals with negative rhLCV serology were excluded from these analyses. To measure rhEBNA1-specific T cell responses, PBMCs were isolated and tested for CD4⁺ and CD8⁺ T cells producing IFN- γ , IL-2, and/or TNF- α in response to a short *in vitro* stimulation with overlapping rhEBNA1 peptide pools. Background activity was measured by culturing cells in medium containing DMSO for the same length of time. Results are expressed as absolute number of cells per 10⁶ live CD3⁺ T cells. To calculate the sum of the peptide-specific response, we subtracted normalized background activity and then summed the seven possible different combinations of functions. We define a positive response as anything greater than the mean plus two standard deviations of total CD4⁺ (183 per 10⁶ CD3⁺ T cells) or CD8⁺ (216 per 10⁶ CD3⁺ T cells) cytokine responses from 5 seronegative animals from the New England Primate Research Center (**Figure 2-1A**). To determine differentiation status, samples were stained for CD95, CD28, and CCR7, where T_{CM} cells are CD95⁺CD28⁺CCR7^{high}, T_{EM} cells are CD95⁺CD28⁺CCR7^{lo}, and T_{EFF} cells are CD95⁺CD28⁻CCR7^{lo}♦.

We were able to detect rhEBNA1-specific CD4⁺ and/or CD8⁺ T cells in 25 of the 38 (66%) rhLCV-seropositive rhesus macaques (**Table 2-1, right-hand columns**). All 25 of the animals had rhEBNA1-specific CD4⁺ T cell responses, while only 10 animals had rhEBNA1-specific CD8⁺ T cell responses (26%). Interestingly, all of the animals with rhEBNA1-specific CD8⁺ T cells also had rhEBNA1-specific CD4⁺ T cells. This could reflect a need for CD4⁺ T helper cells or it could simply be a result of the larger number of MHC class II epitopes within rhEBNA1.

♦ Refer to page 141 for comment on staining panel.

The magnitude of rhEBNA1-specific CD4⁺ and CD8⁺ T cells was quite variable and seemed to fall within three distinct groups based on the number of total CD4⁺ or CD8⁺ specific cells per 10⁶ CD3⁺ T cells. Responses were either (1) less than 1,000, (2) between 1,000-10,000, or (3) greater than 10,000, as seen in **Figure 2-1B** and corresponding shading in **Table 2-2**. The magnitude of CD4⁺ T cell responses ranged between 186 and 42,830 cells per 10⁶ CD3⁺ T cells, but the majority of those responses (19 of 25 animals) were less than 1,000 cells per 10⁶ CD3⁺ T cells. Thus, the median response was 417 cells per 10⁶ CD3⁺ T cells. Subset analyses revealed that rhEBNA1-specific CD4⁺ T cell responses composed of fewer than 1,000 cells per 10⁶ CD3⁺ T cells were evenly distributed between T_{EM} and T_{CM} cell phenotypes (T_{CM} versus T_{EFF}, *P* = 0.007; T_{EM} versus T_{EFF}, *P* = 0.005 by Kruskal-Wallis test), while the majority of rhEBNA1-specific T cell responses composed of greater than 1,000 cells per 10⁶ CD3⁺ T cells were primarily T_{EM} cells (T_{EM} versus T_{EFF}, *P* = 0.03; T_{EM} versus T_{CM}, *P* = 0.027 by Kruskal-Wallis test). Such a large proportion of T_{EM} cells could be reflective of ongoing or recent rhLCV reactivation, which would be expected to increase the proportion of T_{EM} and T_{EFF} cells. This observation is further supported by results for rhEBNA1-specific CD8⁺ T cell responses, which were similarly large in magnitude (258 to 25,264 cells per 10⁶ CD3⁺ T cells). However, in contrast to CD4⁺ T cell responses, only about half of rhEBNA1-specific CD8⁺ T cell responses fell below 1,000 cells per 10⁶ CD3⁺ T cells. The median rhEBNA1-specific CD8⁺ T cell response was therefore significantly larger than the rhEBNA1-specific CD4⁺ T cell response, at 3,213 cells per 10⁶ CD3⁺ T cells (*P* = 0.023, two-sided Mann-Whitney test). This is again suggestive of recent reactivation, as CD8⁺ CTLs rapidly proliferate in order to clear infection, and the observed rhEBNA1-specific CD8⁺ T cells were primarily of an effector phenotype for all animals (T_{EFF} versus T_{CM}, *P* = 0.021; T_{EFF} versus T_{EM}, *P* = 0.035 by Kruskal-Wallis test). Animals with the highest numbers of total rhEBNA1-specific CD8⁺ T cells had the largest proportion effector cells.

Figure 2-1: Number of rhEBNA1-specific CD4⁺ and CD8⁺ T cell responses

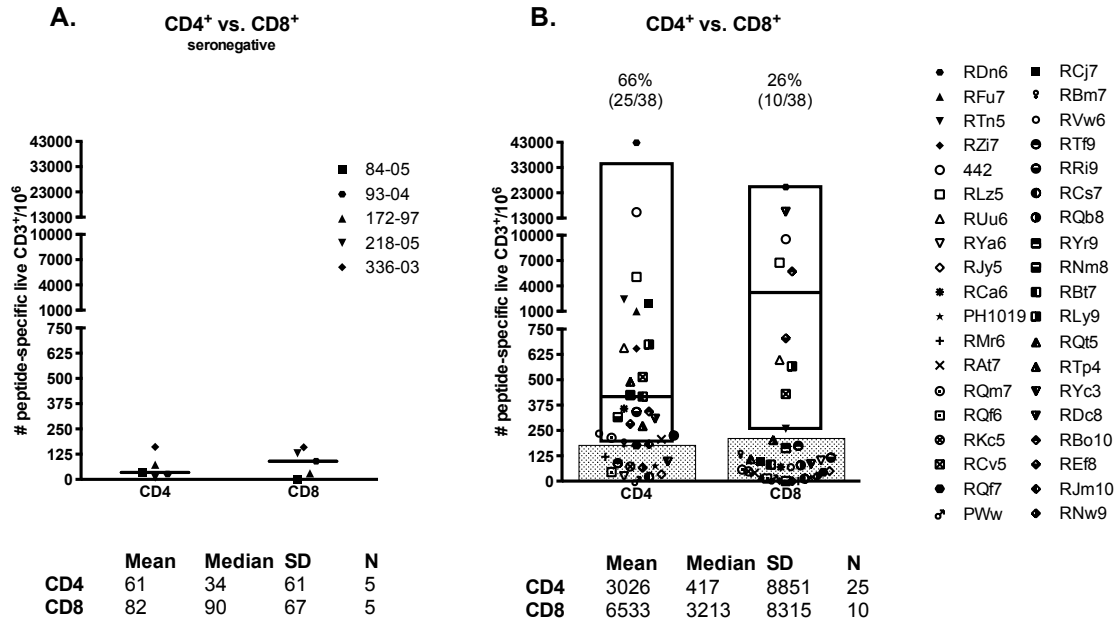


Figure 2-1: PBMCs from rhLCV seronegative (A) and rhLCV seropositive (B) animals were tested by ICS for rhEBNA1-specific CD4⁺ and CD8⁺ T cells producing IFN- γ , IL-2, or TNF- α . Graphs display the total of all cytokine-producing cells per 10⁶ live CD3⁺ T cells after subtraction of normalized background values. (A) Horizontal bars reflect the median response for all rhLCV seronegative samples. The limit of detection is defined as the mean + 2 standard deviations (SD) for total CD4⁺ (183 cells/10⁶ CD3⁺ T cells) and total CD8⁺ (216 cells/10⁶ CD3⁺ T cells) responses from rhLCV seronegative animals. (B) Detection limit cutoffs are represented as shaded bars, and positive responses are displayed as floating bars (5th to 95th percentiles) with lines at the median. The frequency of responding animals is presented above each bar.

Table 2-2: Numbers of rhEBNA1-specific CD4⁺ and CD8⁺ T cells

	Subject	CD4				CD8			
		TOTAL	TCM	TEM	EFF	TOTAL	TCM	TEM	EFF
> 10 ⁴	RDn6	42830	89	32544	2374	25264	0	2245	22661
	442	15353	70	11984	399	9546	17	901	8198
	RDc8	308	208	101	11	15488	1109	104	13145
1,000-10,000	RLz5	5074	567	3464	574	6752	404	414	5427
	RTn5	2406	146	1509	0	258	46	13	100
	RCj7	1865	65	1130	26	-	-	-	-
	RFu7	1012	13	792	0	-	-	-	-
	RBo10	344	138	84	84	5721	458	147	4456
<1,000	RLy9	675	266	138	208	567	21	118	431
	RUu6	657	96	458	50	598	32	53	441
	RCv5	514	355	359	0	430	239	215	120
	REf8	281	201	81	40	704	182	61	280
	RZi7	654	0	459	42	-	-	-	-
	RQt5	490	358	95	3	-	-	-	-
	RYr9	425	238	224	86	-	-	-	-
	RBt7	417	272	43	75	-	-	-	-
	RCa6	358	30	340	19	-	-	-	-
	RRi9	341	104	28	37	-	-	-	-
	RNm8	316	234	65	0	-	-	-	-
	RTp4	272	114	38	96	-	-	-	-
	RVw6	234	85	131	38	-	-	-	-
	RQb8	225	68	30	44	-	-	-	-
	RQm7	214	11	228	4	-	-	-	-
RAt7	206	56	159	24	-	-	-	-	
RBm7	186	136	57	35	-	-	-	-	

Table 2-2: RhEBNA1-specific CD4⁺ (left) and CD8⁺ (right) T cell responses are displayed as counts per 10⁶ live CD3⁺ cells after subtraction of background values. Responses are separated into three groups based on the number of total CD4⁺ or CD8⁺ T cells: light grey, less than 1000 cells; medium grey, between 1,000-10,000 cells; dark grey, greater than 10,000 cells. The number of responses within central memory, effector memory, and effector T cell subsets are listed to the left of the total responses for each animal. Within subsets, all values greater than 100 are in bold, and the largest subset response is highlighted in red; subset responses with 10 or fewer cells difference between them were considered equal.

RhEBNA1-specific T cells decreased and stabilized over time

An outbreak of Human Metapneumovirus at YNPC a few months prior to the onset of these studies may have induced rhLCV reactivation and could therefore be responsible for the large responses observed. Once reactivation was controlled, the magnitude of specific T cell responses would be expected to decline and stabilize. To study this in the context of rhEBNA1, we measured rhEBNA1-specific T cell responses over time in 17 of the 40 rhesus macaques and determined the frequency, magnitude, and phenotype by ICS. Animals included in these studies exhibited a wide range of magnitudes in order to determine if differences were somehow related to response stability. Animals were bled an additional one to three times over a 13-month period in intervals of 2, 4, and 7 months as listed in **Table 2-1**.

The number of animals with rhEBNA1-specific CD4⁺ and/or CD8⁺ T cell responses declined with time. RhEBNA1-specific T cells were initially present in 12 (CD4⁺) and 5 (CD8⁺) of 17 animals at month 0, which decreased to 8 (CD4⁺) and 4 (CD8⁺) of 15 animals by the end of the study (11 to 13 months later). This change could reflect the natural contraction of T cells following re-activation and expansion, or it could simply be a reflection of the small number of animals tested at each time point. Nevertheless, our sample size was too small to conduct powerful statistical analyses, although some important changes did seem to occur. First, the majority of responses tended to decline and stabilize with time, including all CD4⁺ and CD8⁺ responses that were initially greater than 1,000 cells per 10⁶ CD3⁺ T cells (**Figure 2-2**). This reached significance at the 4 to 6 month time point for rhEBNA1-specific total CD4⁺ T cell responses, where the distribution of responses was significantly smaller compared to month 0 ($P = 0.046$, Kolmogorov-Smirnov test) (**Figure 2-2A**). Two animals with responses that did not follow this trend were PH1019 and PWw. In these animals, responses were not detectable at baseline, sharply increased at the second time point, and later decreased. Additionally, the rhEBNA1-specific CD4⁺ T cell responses of RTp4 and RWv6 were relatively stable across all time points, while corresponding CD8⁺ T cell responses were virtually absent. In terms of subsets, CD4⁺ T_{CM} cell responses remained relatively stable (**Figure 2-2B**), while the large CD4⁺ T_{EM} cell responses decreased significantly by 4 to 6 months ($P = 0.041$) and remained stable through

months 11 to 13 ($P = 0.031$, two-sided Mann-Whitney test), as would be expected after resolution or control of reactivation (**Figure 2-2C**). A similar trend was observed within the CD8⁺ T_{EFF} cell responses, and this was most pronounced for animals with the largest magnitudes at the first time point (**Figure 2-2D**).

Figure 2-2: RhEBNA1-specific CD4⁺ and CD8⁺ T cells over time

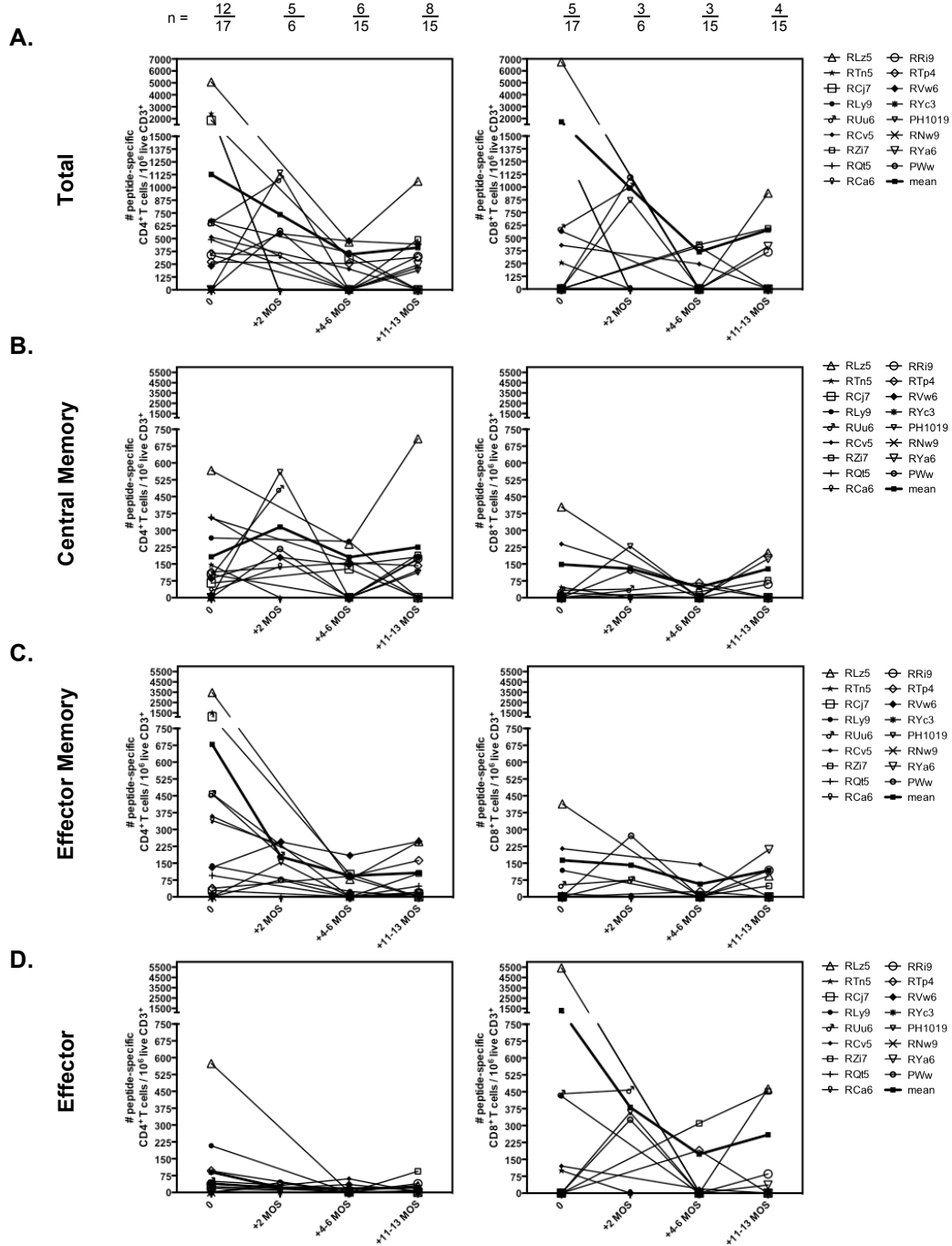


Figure 2-2: RhEBNA1-specific CD4⁺ (left column) and CD8⁺ (right column) T cells detected by ICS at month 0 and then in 2-, 4-, and 7-month intervals are shown using a subcohort of animals from YNPC. Graphs display the total of all cytokine-producing cells per 10⁶ live CD3⁺ T cells after subtraction of normalized background values for (A) total, (B) central memory, (C) effector memory, and (D) effector T cell subsets. Values below the limit of detection are graphed as 0. The number of subjects with positive responses / the total number of subjects tested at each time point is displayed at the top of each column. Responses from RTn5, PH1019, PWw, and RVw6 were measured all four times; RUu-6 and RCa-6 were measured at 0 and +2 MOS; and all remaining animals were measured at 0, +4/6 MOS, and +11/13 MOS.

DISCUSSION

In this study, we assessed the natural immune response to rhEBNA1, which is a highly attractive target for vaccine development. We screened 40 rhesus macaques for rhEBNA1-specific T cells in peripheral blood, and we demonstrate that responses can be detected directly *ex vivo* based on the production of IFN- γ , IL-2, and TNF- α by ICS. The number of animals with rhEBNA1-specific CD4⁺ T cells was larger than CD8⁺ T cells, and the range in magnitude for both subsets was extremely variable. We suspect the largest of those responses is indicative of recent rhLCV reactivation. Animals with fewer than 1,000 rhEBNA1-specific T cells tended to have equal proportions of specific CD4⁺ T_{CM} and CD4⁺ T_{EM} cell responses, with little to no rhEBNA1-specific CD8⁺ T_{EFF} cells. In contrast, animals with more than 1,000 rhEBNA1-specific T cells tended to have mostly rhEBNA1-specific CD4⁺ T_{EM} and CD8⁺ T_{EFF} cells. Chronic infection promotes the differentiation of T_{EM} and T_{EFF} cells, and low-level expression of rhEBNA1 during latent rhLCV infection could therefore be responsible for maintaining relatively equal proportions of rhEBNA1-specific CD4⁺ T_{CM} and T_{EM} cells rather than mostly T_{CM} cells. However, it is also possible that T_{EM} responses in some of these animals are still contracting after recent lytic reactivation. Similarly, the large CD4⁺ T_{EM} and CD8⁺ T_{EFF} cell populations could be indicative of reactivation, or they could be a result of low-level antigen during latent infection.

To determine if rhEBNA1-specific T cells are maintained in this highly activated state, we followed responses over time in a smaller cohort of animals to assess their stability. Our findings provide further evidence of recent rhLCV reactivation, as rhEBNA1-specific T cells tended to decrease and stabilize among those animals with initially high responses. This was especially true within T_{EFF} and T_{EM} cell populations. The presence of rhEBNA1-specific T_{CM} cells and the capacity for expansion and contraction of more activated subsets indicate the potential to successfully target and expand rhEBNA1-specific T cells by vaccination. Our theory of rhLCV reactivation is based on the magnitude and phenotype of rhEBNA1-specific T cell responses, but unfortunately these studies are limited by our lack of data on viral loads. Therefore, we chose not

to characterize the rhEBNA1-specific immune response using these data, as unconfirmed reactivation introduces additional factors that make interpretation quite difficult.

RESULTS PART II

Frequency and magnitude of rhEBNA1- and rhBZLF1-specific T cell responses

The initial goal of these studies was to characterize the frequency, magnitude, phenotype, and function of rhEBNA1-specific T cells in healthy, naturally infected rhesus macaques. However, our original time points may have been influenced by viral infection and possible rhLCV reactivation, as indicated by the magnitude and phenotype of rhEBNA1-specific T cell responses at the first time point. Regardless of the cause of such large responses, our follow-up studies demonstrated that results from month 0 seemed to be atypical, and responses tended to decrease and stabilize with time. We therefore decided to characterize rhEBNA1-specific responses from 15 animals using two additional time points that were collected after responses had stabilized. Furthermore, because it is difficult to characterize immune responses based on such a small sample size, we aimed to increase the number of subjects with detectable rhEBNA1-specific T cells by increasing the degree of overlap within our rhEBNA1 peptide pool from 5 to 10 amino acids. This could potentially increase the number of epitopes that are recognized by T cells. However, increasing the size of the peptide pool creates competition for binding to MHC molecules and could therefore reduce the likelihood of binding a specific peptide during stimulation. This could cause a reduction in T cell responses if there are very few T cell epitopes within the pool. For this reason, PBMCs were stimulated with two different pools that each contained half of the rhEBNA1 peptides from our new larger library, and responses were measured by ICS. For comparison, we also measured T cell responses to the highly immunogenic immediate-early antigen rhBZLF1, which regulates the switch from latent infection to lytic replication and is not expressed during latency^{216, 217}. This also serves as an internal control, as changes caused by reactivation would be detected among rhBZLF1-specific T cells as well. Peptide-specific responses were measured at two time points spaced two months apart,

and analyses were based on the average response of each subject. RhEBNA1- and rhBZLF1-specific total cytokine responses for each time point can be seen in **Tables 2-3A and 2-3B**, respectively.

The number of subjects with detectable rhEBNA1-specific T cells increased after stimulation with the modified rhEBNA1 peptide pools. We were able to detect rhEBNA1-specific CD4⁺ and/or CD8⁺ T cells in 14 of the 15 rhesus macaques (93%) from YNPC (**Figure 2-3A**). Twelve of the 15 animals (80%) had rhEBNA1-specific CD4⁺ T cell responses above the detection limit, with a magnitude that ranged between 238 and 2,190 responding cells per 10⁶ CD3⁺ T cells. Slightly fewer animals had detectable rhEBNA1-specific CD8⁺ T cell responses (10 of the 15, or 67%) with a lower magnitude that ranged from 233 to 693 cells per 10⁶ CD3⁺ T cells. The mean rhEBNA1-specific CD4⁺ T cell response of 638 cells/10⁶ CD3⁺ T cells was significantly higher than the mean CD8⁺ T cell response of 387 cells/10⁶ CD3⁺ T cells ($P = 0.0391$). One subject, RZi7, had neither CD4⁺ nor CD8⁺ rhEBNA1-specific T cells above the detection limit. Eight of the remaining 14 animals had both CD4⁺ and CD8⁺ rhEBNA1-specific T cells; in seven of these animals the CD4⁺ response was higher. We were unable to detect a peptide-specific CD8⁺ T cell response in four animals, and two animals did not have detectable CD4⁺ T cell responses.

In contrast to results for rhEBNA1, we detected rhBZLF1-specific CD4⁺ and/or CD8⁺ T cells in all 15 of the screened animals (**Figure 2-3B**). Fourteen of these macaques (93%) had rhBZLF1-specific CD4⁺ T cell responses above the detection limit, and the magnitude ranged from 226 to 1206 rhBZLF1-specific cells per 10⁶ CD3⁺ T cells. RZi7 was the only animal with no detectable CD4⁺ T cells to rhBZLF1. We were also able to detect rhBZLF1-specific CD8⁺ T cell responses in 14 animals (93%), and the magnitude of the response was larger than the rhBZLF1 CD4⁺ T cell response, ranging from 285 to 2184 rhBZLF1-specific CD8⁺ T cells per 10⁶ CD3⁺ T cells. The one subject with undetectable rhBZLF1 CD8⁺ T cell responses had undetectable rhEBNA1 CD8⁺ T cells as well. While the difference between the mean CD4⁺ (550 cells/10⁶ CD3⁺ T cells) and CD8⁺ (687 cells/10⁶ CD3⁺ T cells) T cell responses was not significant, there seemed to be a trend towards higher CD8⁺ responses, as noted in 7 of the 13 animals with both CD4⁺ and CD8⁺ peptide-specific T cells. Of the remaining six animals, four had larger CD4⁺ than CD8⁺ T

cell responses, and two had similar levels of both CD4⁺ and CD8⁺ rhBZLF1-specific T cells (a difference of fewer than 10 cells per 10⁶ CD3⁺ T cells).

Numbers of rhEBNA1- and rhBZLF1-specific CD4⁺ and CD8⁺ T cells varied between individual animals; some rhesus macaques had over 500 rhEBNA1- or rhBZLF1-specific circulating CD4⁺ or CD8⁺ T cells per 10⁶ CD3⁺ T cells, while the majority of animals had lower numbers averaging 200 to 400 cells. Animals with high rhEBNA1 responses did not necessarily have high rhBZLF1 responses and vice versa. In contrast, those with high responses against one peptide pool tended to have lower responses against the other.

Table 2-3: Total cytokine-secreting rhEBNA1- (A) and rhBZLF1- (B) specific CD4⁺ and CD8⁺ T cells for each animal at both collection points

Subject	Number of T cells by cell population			
	CD4 ⁺		CD8 ⁺	
	Bleed 1	Bleed 2	Bleed 1	Bleed 2
RNw9	461	498	284	235
RQt5	562	294	393	74
RYc3	63	1334	238	410
RRi9	146	538	342	21
RLy9	103	394	44	62
RTp4	739	159	725	34
RCj7	351	744	764	623
RTn5	268	208	0	60
RZi7	67	91	89	14
RLz5	1380	760	450	465
PH1019	71	122	451	458
PWw	158	150	545	149
RVw6	1666	2713	267	603
RCv5	469	714	130	200
RYa6	378	368	457	111

Subject	Number of T cells by cell population			
	CD4 ⁺		CD8 ⁺	
	Bleed 1	Bleed 2	Bleed 1	Bleed 2
RNw9	260	191	2395	1973
RQt5	323	427	324	246
RYc3	32	1893	434	556
RRi9	698	579	1331	614
RLy9	1566	845	0	364
RTp4	152	255	937	610
RCj7	342	254	464	361
RTn5	255	327	352	779
RZi7	137	40	336	294
RLz5	438	178	465	163
PH1019	144	405	1756	1190
PWw	211	730	498	425
RVw6	133	605	411	768
RCv5	1337	957	190	535
RYa6	1007	851	583	234

Peptide-specific responses at both collection points (bleed 1, bleed 2) are displayed as counts per 10⁶ live CD3⁺ cells after subtraction of background values.

Figure 2-3: Numbers of rhEBNA1- and rhBZLF1-specific T cells in PBMCs

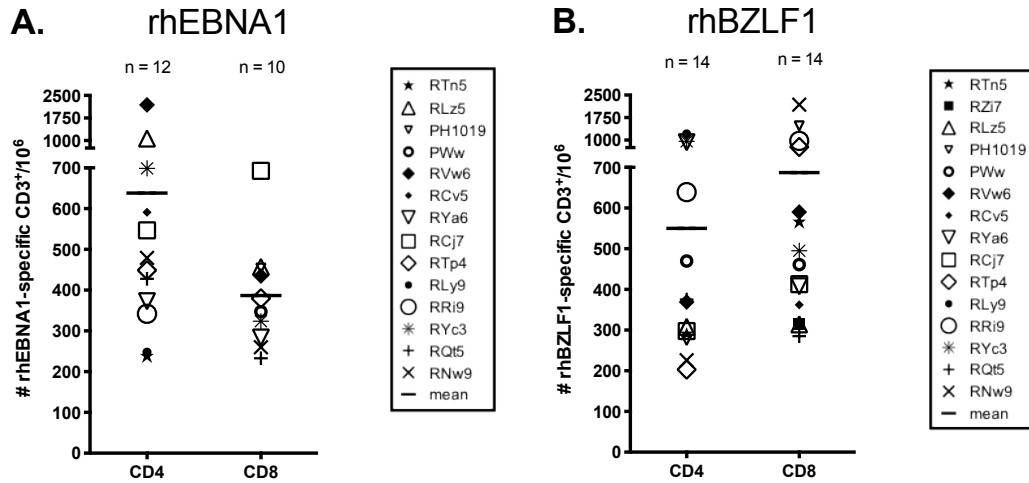


Figure 2-3: We determined the frequency and magnitude of rhEBNA1- and rhBZLF1-specific T cell responses in 15 rhesus macaques by ICS. All values are represented as peptide-specific T cell counts per 10^6 live $CD3^+$ T cells. The average sum of total cytokine secreting rhEBNA1- (**A**) or rhBZLF1- (**B**) specific $CD4^+$ and $CD8^+$ T cells after subtraction of background values is shown. Data for each animal reflect the mean of two time points spaced two months apart; values for each time point can be seen in table 2-3. Bars indicate the mean value of all positive animals within each group. Standard deviations are as follows: rhEBNA1 CD4, 538; rhEBNA1 CD8 134; rhBZLF1 CD4, 358; rhBZLF1 CD8, 538. There was a significant difference between total rhEBNA1 $CD4^+$ and $CD8^+$ T cell cytokine responses ($P = 0.0391$). P -values were calculated using a two-sided Wilcoxon's matched-pairs signed-rank test, with a P -value <0.05 considered significant. All multiple comparisons were Bonferroni-adjusted to control for a type I error rate.

Peptide-specific CD4⁺ and CD8⁺ T cell responses differ in phenotypes and types of cytokine production

We next assessed rhEBNA1- and rhBZLF1-specific subset phenotypes (T_{EFF} , T_{CM} , and T_{EM}) and their corresponding functionalities based on the production of IFN- γ , IL-2, and/or TNF- α . The average CD4⁺ T cell response to rhEBNA1 was composed largely of T_{CM} cells (mean, 426 cells per 10^6 CD3⁺ T cells); T_{EM} cells were detectable at about one-third lower frequency (mean, 138 cells per 10^6 CD3⁺ T cells), and T_{EFF} CD4⁺ T cells were virtually absent (mean, 28 cells per 10^6 CD3⁺ T cells) (**Figure 2-4A**). Differences between each subset were significant (T_{CM} versus T_{EFF} cells, $P = 0.0015$; T_{CM} versus T_{EM} cells, $P = 0.003$; T_{EFF} versus T_{EM} cells, $P = 0.0015$).

Both CD4⁺ T_{CM} and T_{EM} cell populations produced all three cytokines (**Figure 2-4B**). There were subtle differences in the profiles of each. On average, T_{CM} cells produced IL-2 with the highest frequency (IL-2 versus TNF- α , $P = 0.0102$), followed by IFN- γ , and then TNF- α . In contrast, T_{EM} cells most often produced IFN- γ (46%; IFN- γ versus IL-2, $P = 0.006$; IFN- γ versus TNF- α , $P = 0.0117$), followed by IL-2 and TNF- α , which were about the same.

The rhEBNA1 CD8⁺ T cell response differed from the CD4⁺ T cell response in terms of both phenotype and function. In contrast to the large CD4⁺ T_{CM} response, 60% of rhEBNA1-specific CD8⁺ T cells had an effector phenotype with a mean of 237 cells per 10^6 CD3⁺ T cells (**Figure 2-4C**). T cells with a central memory phenotype were detected at about one-half the frequency of the effector response, with a mean of 104 cells per 10^6 CD3⁺ T cells. The T_{EM} cell response was significantly smaller, contributing only 12.5% to the total CD8⁺ response with a mean of 49 cells per 10^6 CD3⁺ T cells (T_{EM} versus T_{EFF} cells, $P = 0.0177$; T_{EM} versus T_{CM} cells, $P = 0.0294$). RhEBNA1-specific CD8⁺ T_{EFF} cells mainly produced IFN- γ (74%; IFN- γ versus TNF- α , $P = 0.006$) (**Figure 2-4D**). Cytokine production within the T_{CM} and T_{EM} cell subsets was low, but the profile of the average response was similar to the rhEBNA1 CD4⁺ T cell response; TNF- α was produced by the fewest T_{CM} cells (TNF- α versus IFN- γ , $P = 0.0411$; TNF- α versus IL-2, $P = 0.0117$), and IFN- γ was produced by the most T_{EM} cells (IFN- γ versus TNF- α , $P = 0.0294$).

The CD4⁺ T cell response to rhBZLF1 was nearly exclusively composed of T_{CM} cells (mean, 467 cells per 10^6 CD3⁺ T cells) (**Figure 2-5A**). The T_{CM} cell response contributed to 88%

of the total rhBZLF1 CD4⁺ T cell response, while T_{EM} and T_{EFF} cell subsets represented only 9% and 3% of the total response, respectively. Differences between each subset were significant (T_{CM} versus T_{EFF} cells, $P = 0.0003$; T_{CM} versus T_{EM} cells, $P = 0.0003$; T_{EFF} versus T_{EM} cells, $P = 0.0018$). The dominant functions of the rhBZLF1 CD4⁺ T_{CM} response differed from that of rhEBNA1. While all three cytokines were still detected, IFN- γ production was significantly lower than both IL-2 (51%) and TNF- α production (37%), comprising only 12% of the total response (IFN- γ versus IL-2, $P = 0.0018$) (**Figure 2-5B**).

The rhBZLF1 CD8⁺ T cell response was larger than the rhEBNA1 CD8⁺ T cell response. It was composed of more equal proportions of T_{EFF} (mean, 226 cells per 10⁶ CD3⁺ T cells), T_{CM} (mean, 214 cells per 10⁶ CD3⁺ T cells), and T_{EM} (mean, 147 cells per 10⁶ CD3⁺ T cells) cell subsets (**Figure 2-5C**). Although there were no significant differences between the average magnitudes of each response, the T_{EM} cell subset contributed only 25% of the total rhBZLF1 CD8⁺ T cell response, while the T_{EFF} and T_{CM} cell subsets were each 38.5% and 36.5% respectively. In terms of cytokine production, all three subsets produced IFN- γ most frequently (in T_{EFF} cells [84%], IFN- γ versus IL-2 and TNF- α , $P = 0.0054$ and 0.0036 , respectively; in T_{CM} cells [58%], IFN- γ versus IL-2 and TNF- α , $P = 0.0006$ and 0.0018 , respectively; in T_{EM} cells [59%], IFN- γ versus IL-2 and TNF- α , $P = 0.003$ and 0.0006 , respectively) (**Figure 2-5D**). IL-2 was produced with a frequency of about 30% within each memory subset, while only 10% of memory responses were positive for TNF- α .

Figure 2-4: Subset analysis of rhEBNA1-specific T cell responses

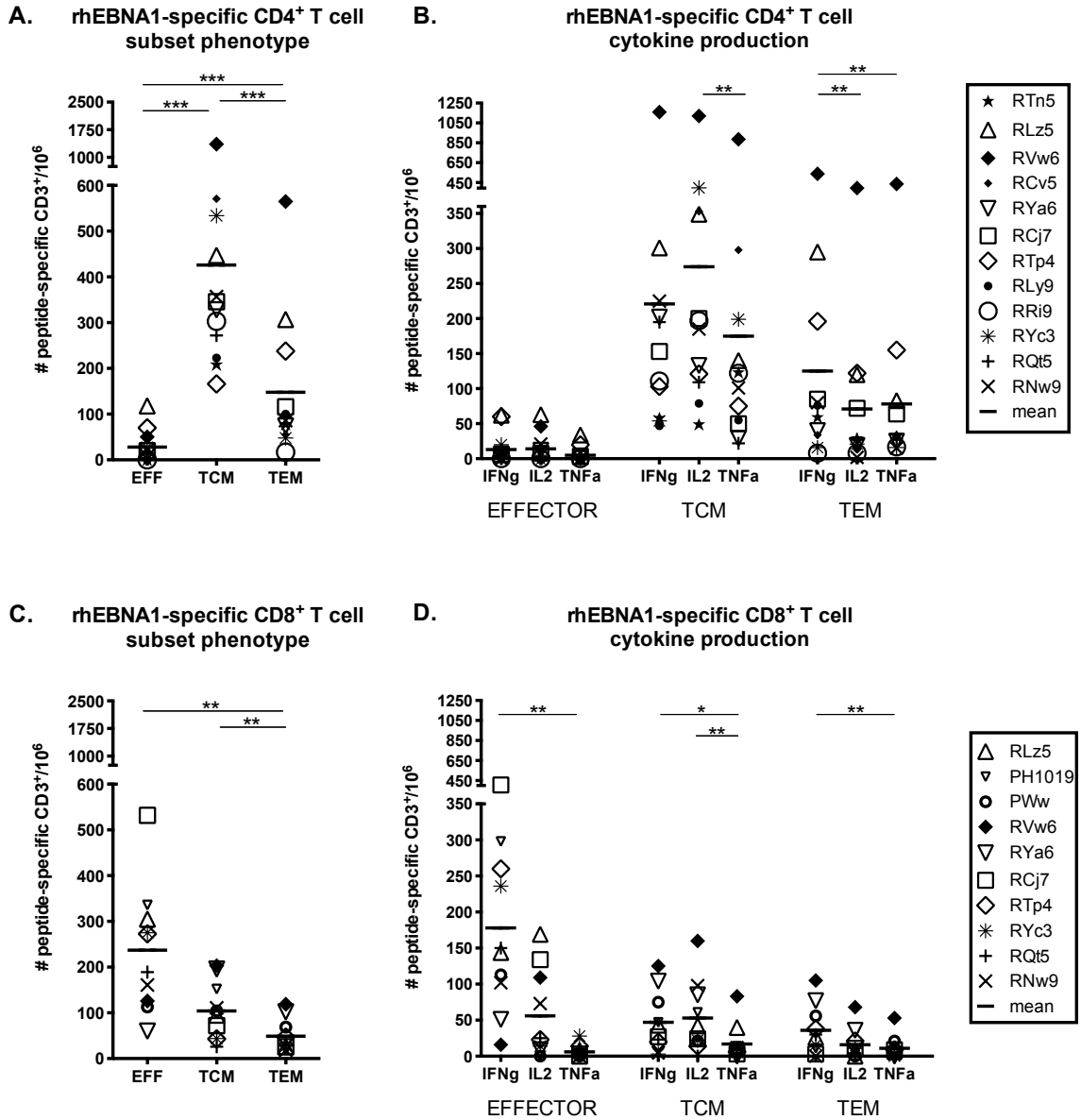


Figure 2-4: The average total counts of rhEBNA1-specific cytokine-producing CD4⁺ (A) and CD8⁺ (C) T cells within the effector (EFF; CD28⁺CD95⁺), central memory (TCM; CD28⁺CD95⁺, CCR7^{hi}), and effector memory (TEM; CD28⁺CD95⁺, CCR7^{lo}) cell populations of all positive animals are shown. The numbers of rhEBNA1-specific CD4⁺ (B) and CD8⁺ (D) effector, TCM, and TEM cells producing IFN- γ , IL-2, and TNF- α were determined. Bars indicate the averages. Significant differences were calculated using a two-sided Wilcoxon's matched-pairs signed-rank test, with a *P*-value <0.05 considered significant (indicated by asterisks). All multiple comparisons were Bonferroni-adjusted to control for type I error rate.

Figure 2-5: Subset analysis of rhBZLF1-specific T cell responses

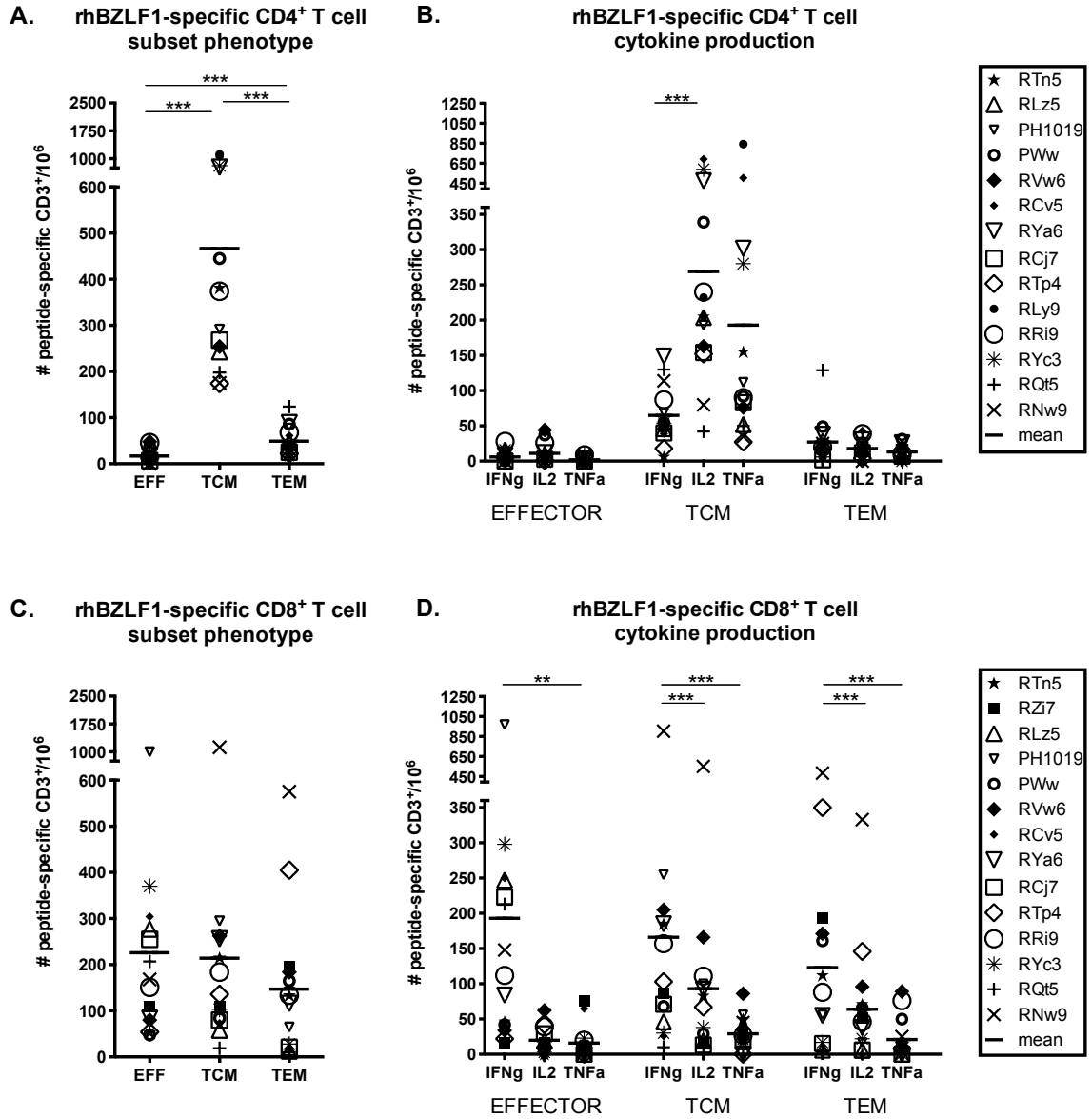


Figure 2-5: The average total counts of rhBZLF1-specific cytokine-producing CD4⁺ (A) and CD8⁺ (C) T cells within the effector (EFF; CD28^{lo}CD95^{hi}), central memory (TCM; CD28^{hi}CD95^{hi}, CCR7^{hi}), and effector memory (TEM; CD28^{hi}CD95^{hi}, CCR7^{lo}) cell populations of all positive animals are shown. The numbers of rhBZLF1-specific CD4⁺ (B) and CD8⁺ (D) effector, TCM, and TEM cells producing IFN- γ , IL-2, and TNF- α were determined. Bars indicate the averages. Significant differences were calculated using a two-sided Wilcoxon's matched-pairs signed-rank test, with a *P*-value <0.05 considered significant (indicated by asterisks). All multiple comparisons were Bonferroni-adjusted to control for type I error rate.

Polyfunctional analyses reveal distinct cytokine combinations within each subpopulation

Because increased polyfunctionality has been associated with increased protection and therefore better control of viral replication in some chronic viral infections^{218, 219}, we further assessed peptide-specific T cell functionality using Boolean gating to analyze the seven possible combinations of IFN- γ , IL-2, and TNF- α production. Comparing the cytokine profiles of the most common rhLCV-specific T cell subsets, rhEBNA1-specific CD4⁺ T_{CM} cells were highly polyfunctional and exhibited an array of different cytokine profiles. While we detected substantial responses within every combination, CD4⁺ T_{CM} cells most often produced either all 3 cytokines or IL-2 alone (**Figure 2-6A**). The rhEBNA1-specific CD4⁺ T_{EM} cell responses were quite similar, producing either all 3 cytokines or IFN- γ alone most often, but the frequency of IL-2 and TNF- α production (either alone or together) was substantially reduced in CD4⁺ T_{EM} cells. In contrast, the majority of rhEBNA1-specific CD8⁺ T_{EFF} cells produced IFN- γ only (**Figure 2-6B**). There was also a small population of IL-2 producing T_{EFF} cells. Based on the degree of double- and triple cytokine-producing cells, the percentage of polyfunctional rhEBNA1-specific CD4⁺ T_{CM} cell responses was significantly larger than the percentage of polyfunctional CD8⁺ T_{CM} cell responses ($P = 0.0021$) (**Figure 2-6C**). A similar trend was observed between CD4⁺ and CD8⁺ T_{EM} cell responses ($P = 0.0519$). Furthermore, CD4⁺ T_{CM} and T_{EM} cell responses were significantly more polyfunctional than CD4⁺ T_{EFF} cell responses (T_{EFF} versus T_{CM}, $P = 0.0366$; T_{EFF} versus T_{EM}, $P = 0.0279$). We observed a similar trend within the rhEBNA1-specific CD8⁺ T cell response as well (T_{EFF} versus T_{CM}, $P = 0.0177$).

In contrast to the high degree of polyfunctionality within the rhEBNA1-specific CD4⁺ memory T cell response, rhBZLF1-specific CD4⁺ T_{CM} cells were largely monofunctional, most often producing only IL-2 or TNF- α (**Figure 2-7A**). RhBZLF1-specific CD8⁺ T_{EFF} cells were strongly dominated by cells producing IFN- γ only (**Figure 2-7B**). While CD8⁺ T_{EFF} cell responses to rhEBNA1 and rhBZLF1 exhibited similar functions, we also detected rhBZLF1-specific CD8⁺ T_{CM} and T_{EM} cells that produced either IFN- γ only, IFN- γ in combination with IL-2, or IL-2 alone. The rhBZLF1 CD8⁺ T_{CM} cell response was significantly more polyfunctional than the CD4⁺ T cell response ($P = 0.0081$), but the majority of both CD4⁺ and CD8⁺ T cell responses were composed

of single-cytokine producing cells and therefore exhibited only a low degree of polyfunctionality **(Figure 2-7C)**.

Figure 2-6: Multi-function analysis of rhEBNA1-specific T cell responses

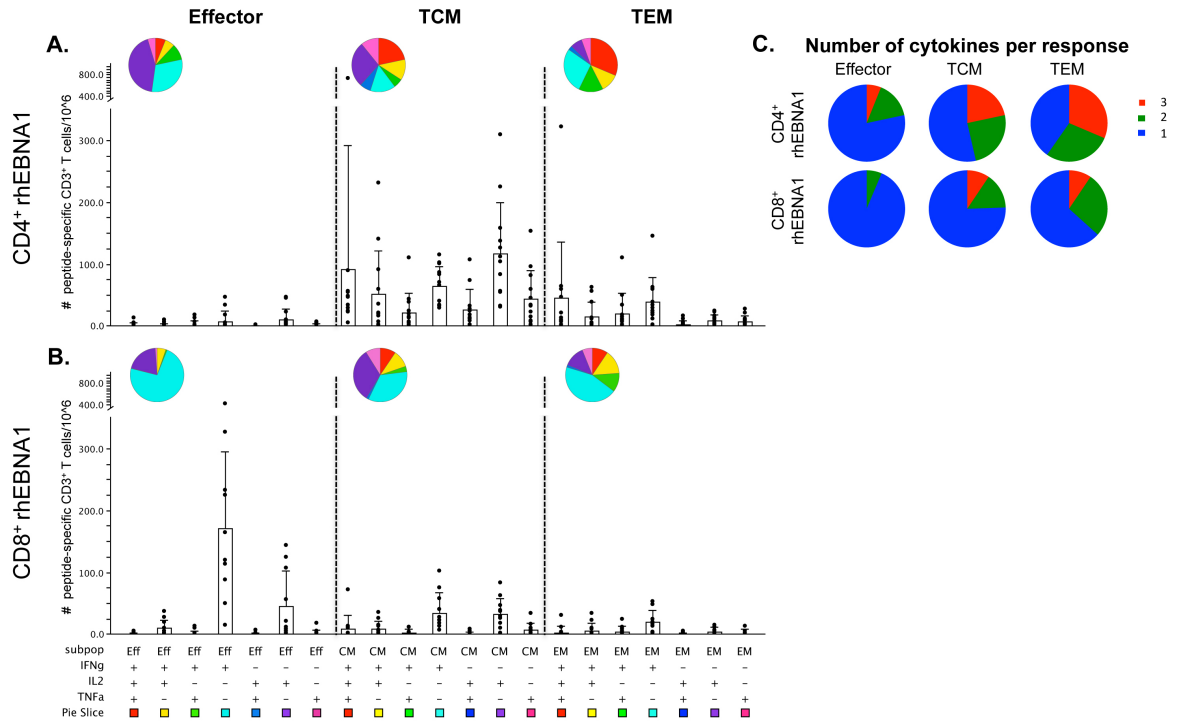


Figure 2-6: Fifteen rhesus macaques were assessed for polyfunctional rhEBNA1-specific T cell responses. Graphs show responses as counts per 10^6 live $CD3^+$ cells after subtraction of background values for all positive animals. **(A and B)** All possible combinations of IFN- γ , IL-2, and TNF- α production by rhEBNA1-specific $CD4^+$ and $CD8^+$ effector, TCM, and TEM cells. Black circles represent the average number of T cells comprising each cytokine combination in a single animal. Bars represent the mean value \pm the standard deviation of each group. Each combination of cytokine responses is represented by plus (+) and minus (-) signs below the x-axis, which is also associated with a pie slice color. The same colors are reflected in the pie charts, which display the average ratio of the various cytokine combinations within each subset. **(C)** Pie charts display the proportion of triple (red), double (green), and single (blue) cytokine-producing $CD4^+$ (top) and $CD8^+$ (bottom) peptide-specific responses based on average production of IFN- γ , IL-2, and/or TNF- α . Percentages of polyfunctional $CD4^+$ TCM and TEM cells were significantly larger than $CD4^+$ effector responses (TCM vs. EFF, $P = 0.0366$; TEM vs. EFF, $P = 0.0279$). The percentage of polyfunctional $CD8^+$ TCM cells was significantly larger than $CD8^+$ effector responses ($P = 0.0177$). $CD4^+$ TCM cells also exhibited a larger degree of polyfunctionality than $CD8^+$ TCM cells ($P = 0.0021$). P -values within groups or between $CD4^+$ and $CD8^+$ responses were calculated using a two-sided Wilcoxon's matched-pairs signed-rank test or two-sided Mann-Whitney test, respectively. A P -value <0.05 was considered significant. All multiple comparisons were Bonferroni-adjusted to control for type I error rate. Graphs were generated using SPICE software (exon.niaid.nih.gov/spice/).

Figure 2-7: Multi-function analysis of rhBZLF1-specific T cell responses

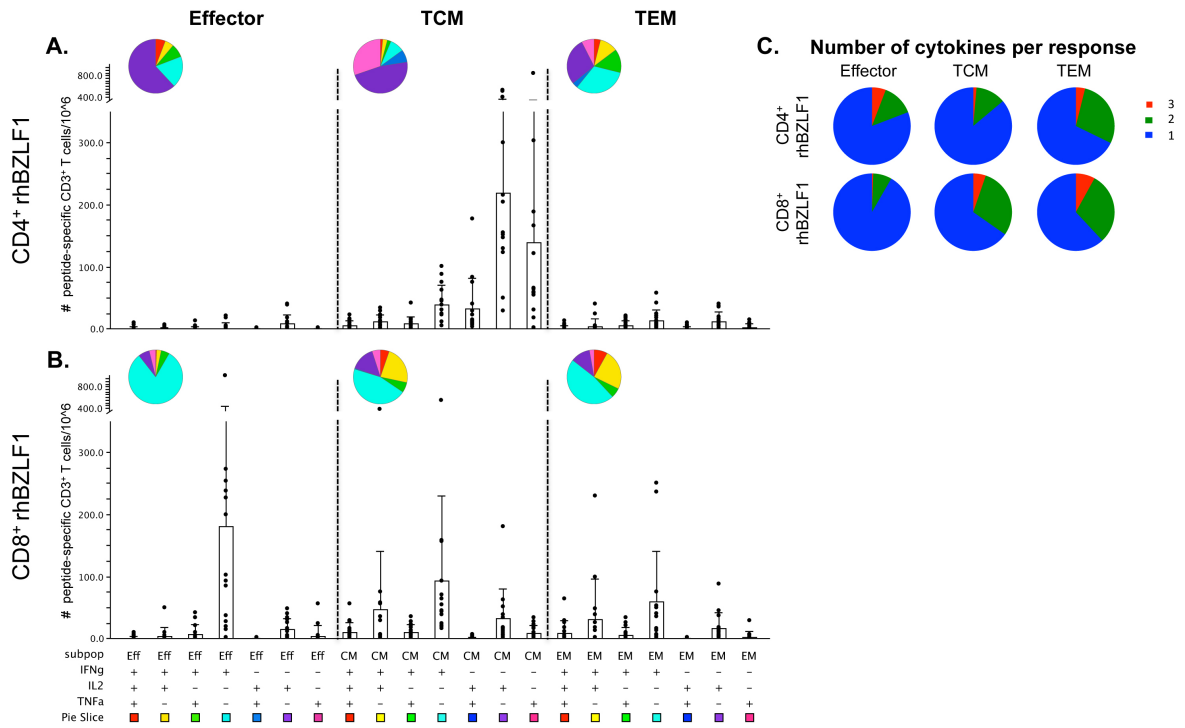


Figure 2-7: Fifteen rhesus macaques were assessed for polyfunctional rhBZLF1-specific T cell responses. Graphs show responses as counts per 10^6 live CD3⁺ cells after subtraction of background values for all positive animals. **(A and B)** All possible combinations of IFN- γ , IL-2, and TNF- α production by rhBZLF1-specific CD4⁺ and CD8⁺ effector, TCM, and TEM cells. Black circles represent the average number of T cells comprising each cytokine combination in a single animal. Bars represent the mean value +/- the standard deviation of each group. Each combination of cytokine responses is represented by plus (+) and minus (-) signs below the x-axis, which is also associated with a pie slice color. The same colors are reflected in the pie charts, which display the average ratio of the various cytokine combinations within each subset. **(C)** Pie charts display the proportion of triple (red), double (green), and single (blue) cytokine-producing CD4⁺ (top) and CD8⁺ (bottom) peptide-specific responses based on average production of IFN- γ , IL-2, and/or TNF- α . CD8⁺ TCM cells exhibited a larger degree of polyfunctionality than CD4⁺ TCM cells ($P = 0.0081$). P -values were calculated using a two-sided Mann-Whitney test, with a P -value <0.05 was considered significant. All multiple comparisons were Bonferroni-adjusted to control for type I error rate. Graphs were generated using SPICE software (exon.niaid.nih.gov/spice/).

Expression of programmed death receptor 1 (PD-1) does not indicate exhaustion

One of the hallmarks of chronic infection is the upregulation of various inhibitory receptors on the cell surface, which can be used to gauge the degree of T cell exhaustion. While the effector-like function and multi-cytokine production by rhEBNA1-specific T cells is not consistent with an exhausted phenotype, the increased proportion of rhEBNA1-specific CD4⁺ T_{EM} cells and IFN- γ production by CD8⁺ T_{EFF} cells could be caused by constant low-level antigen stimulation. Therefore, to determine the activation status of rhEBNA1- and rhBZLF1-specific T cells, we measured cell surface expression of the inhibitory receptor PD-1 by staining cells with a PD-1 antibody prior to stimulation with overlapping peptide pools and ICS. PD-1 is an activation marker of CD4⁺ and CD8⁺ T cells that is upregulated as a negative feedback mechanism to limit immune pathology during infection²²⁰. Upon ligand binding, PD-1 delivers inhibitory signals that downregulate T cell receptor signaling and suppress effector cell functions. During chronic infection, high levels of PD-1 expression have been associated with T cell dysfunction and failure to control infection²²¹. Thus, PD-1 is typically used as a marker of T cell exhaustion.

The percentage of rhEBNA1-specific memory CD4⁺ T cells expressing PD-1 was increased (mean: 55%; range: 23% to 90%) compared to rhBZLF1-specific memory CD4⁺ T cells (mean: 41%; range: 20% to 77%; $P = 0.0186$) and total CD4⁺ memory cells (mean: 35%; range: 28% to 41%) (**Figure 2-8A**; $P = 0.0068$). While the percentage of PD-1⁺ CD4⁺ memory T cells was lower than PD-1⁺ CD8⁺ memory T cells (mean: 54%; range: 41%-66%) ($P = 0.0005$), rhEBNA1-specific T cells did not follow this trend, and there was no significant difference between the two memory subsets. Peptide-specific memory responses were broad, which suggests a range of activation that is highly variable between animals. In contrast, the percentages of both rhEBNA1- (mean: 21%; range: 9% to 49%) and rhBZLF1- (mean: 33%; range: 7% to 68%) specific PD-1⁺ CD8⁺ T_{EFF} cells were significantly lower than total CD8⁺ T_{EFF} cells (mean: 62%; range: 36% to 83%) ($P = 0.0039, 0.0007$, respectively), and the same was true for rhEBNA1-specific PD-1⁺ CD8⁺ effector versus memory cells ($P = 0.039$) (**Figure 2-8B**). There was no correlation between the magnitude of rhEBNA1-specific responses and percentages of PD-1 expression. However, two animals with the highest frequencies of PD-1⁺ CD4⁺ memory cells

(RVw-6) and PD-1⁺ CD8⁺ memory cells (RCj-7) also had some of the largest magnitudes of matching responses. Interestingly, there was a negative correlation for rhBZLF1-specific memory CD4⁺ T cell responses ($r = -0.6$; $P = 0.02$) and a trend towards a positive correlation for rhBZLF1-specific memory CD8⁺ T cell responses ($r = 0.5$; $P = 0.054$), which may encounter antigen more often. As expected, the percentage of PD-1-expressing naïve T cells was significantly lower than all other populations, since PD-1 is expressed upon activation. Similar trends were also observed for the intensity of PD-1 expression (data not shown because inter-experimental values cannot be compared).

Figure 2-8: PD-1 surface expression on rhEBNA1- and rhBZLF1-specific T cells

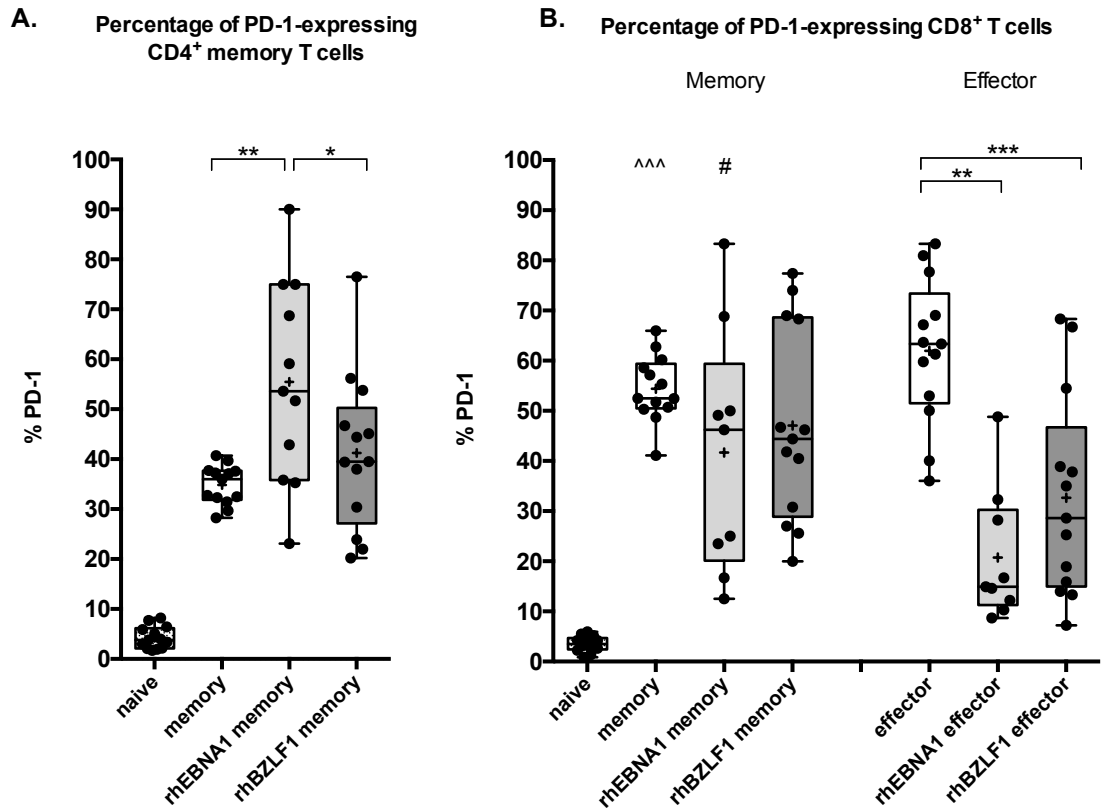


Figure 2-8: The percentages of total, rhEBNA1-, and rhBZLF1-specific CD4⁺ (A) and CD8⁺ (B) T cells expressing PD-1 are shown for memory and effector cell subsets from 14 rhLCV-seropositive rhesus macaques. PBMCs were stained for PD-1 prior to stimulation with overlapping rhEBNA1 or rhBZLF1 peptide pools. The percent of peptide-specific PD-1⁺ T cells was obtained by creating a single Boolean gate that included every combination of cytokines. Animals with peptide-specific responses below the limit of detection were excluded from peptide-specific subsets. Floating bars reflect the interquartile range of responses, with whiskers extending to the minimum and maximum values. Horizontal bars reflect the median response, with a + symbol designating the mean. Significant differences (designated by *) are as follows: total CD4⁺ memory versus total CD8⁺ memory, $P = 0.0005$ (designated by ^) ; rhEBNA1 CD4⁺ memory versus rhBZLF1 CD4⁺ memory, $P = 0.0186$, and total CD4⁺ memory, $P = 0.0068$; rhEBNA1 CD8⁺ memory versus rhEBNA1 CD8⁺ effector, $P = 0.0391$ (designated by #); total CD8⁺ effector versus rhEBNA1 CD8⁺ effector, $P = 0.0039$, and rhBZLF1 CD8⁺ effector, $P = 0.0007$. Additionally, all naïve responses were significantly smaller than every other group. Significance was calculated using Wilcoxon matched-pairs signed rank test, with a P -value <0.05 considered significant. All multiple comparisons were Bonferroni-adjusted to control for type I error rate.

DISCUSSION

The striking similarities between EBV and rhLCV favor the use of rhLCV infection of rhesus macaques as an ideal system for pre-clinical studies aimed at preventing or treating EBV associated malignancies, but a more detailed understanding of rhLCV-specific T cell responses is needed to firmly establish this model. We characterized rhEBNA1-specific T cell responses in 15 rhLCV-seropositive healthy rhesus macaques and compared these responses to rhBZLF1-specific T cells within the same population of animals by ICS. RhEBNA1-specific CD4⁺ T cells were detected at a slightly higher frequency than CD8⁺ T cells, while rhBZLF1-specific CD4⁺ and CD8⁺ T cells were both present in 93% of the animals. Unlike responses in humans²²², responses to rhEBNA1 in macaques did not appear to be influenced by the Mamu-genotype, although additional studies with larger cohorts and more extensive genotyping as well peptide mapping would be required to firmly establish the effects of MHC class I restricting elements on T cell responses.

In addition to frequencies, we also examined subset phenotypes and cytokine production of rhEBNA1- and rhBZLF1-specific T cells. These studies served to determine the effect of persistent low-level antigen on specific T cell responses and to evaluate the capacity of such T cells to respond to vaccination. T cells affected by persistent antigen exposure may be difficult to expand, as T_{CM} cell pools are often depleted and T_{EFF}/T_{EM} cells do not function optimally. We found that rhEBNA1-specific CD4⁺ T cells were composed of both T_{CM} and T_{EM} cell subsets that produced IFN- γ , IL-2, and TNF- α , while rhEBNA1-specific CD8⁺ T cells were primarily IFN- γ -producing T_{EFF} cells. This may suggest that repeated *in situ* reactivation of rhLCV or the persistent presence of latently infected cells expressing rhEBNA1 primarily maintains activation of CD8⁺ rather than CD4⁺ T cells. An alternative explanation could be that rhEBNA1-specific CD8⁺ T cells are exposed to antigen more regularly and are beginning to lose function, but low expression of the inhibitory molecule PD-1 indicates this is most likely not the case. In fact, PD-1 expression was higher on rhEBNA1-specific CD4⁺ memory T cells, which indicates that these T cells probably see antigen more often. In comparison, rhBZLF1-specific CD4⁺ T cells were

primarily of the T_{CM} subset, produced IL-2 and TNF- α , and exhibited significantly lower PD-1 surface expression compared to rhEBNA1-specific memory $CD4^+$ T cells. In contrast, rhBZLF1-specific $CD8^+$ T cells were composed of both effector and memory cell subsets that mainly produced IFN- γ , followed by IL-2. The presence of rhEBNA1-specific T_{CM} cells that produce multiple cytokines in response to stimulation indicates that vaccination could be a feasible approach for expanding this response.

Both rhEBNA1 and rhBZLF1 T cell responses have previously been studied in macaques. Using IFN- γ enzyme-linked immunosorbent spot (ELISpot) assays, Fogg et al.²¹⁵ measured antigen-specific responses to latent rhLCV proteins directly *ex vivo* by culturing PBMCs with recombinant vaccinia viruses. While responses were detected against all latent proteins tested, rhEBNA1-specific $CD8^+$ T cells were identified most frequently in nearly half of the animals (11 of 23) and with the highest mean responses of the latent proteins tested. The same group detected *ex vivo* rhBZLF1-specific $CD8^+$ T cell responses at a frequency of 63% (36 of 57)²¹⁷. Orlova et al.¹⁸⁸ showed by IFN- γ ELISpot assays of T cell lines from healthy seropositive rhesus macaques that rhBZLF1-specific T cells were present in 53% (8 of 15) of the animals tested, 40% of which had specific $CD8^+$ T cells. Using a more sensitive method that allows for simultaneous screening of several T cell cytokines, we show that every rhLCV-seropositive rhesus macaque carries rhBZLF1-specific T cells, while the majority (14 of 15) have circulating rhEBNA1-specific T cells. Such T cells could not be detected at significant frequencies in rhLCV-seronegative animals.

EBNA1- and BZLF1-specific T cells have been studied in more depth in the human system and with a variety of techniques and functional readouts in diverse cohorts. Early studies based on ELISpot assays for IFN- γ revealed EBNA1-specific T cell responses in less than 20% (2 of 13) of healthy human adults, while responses to another latent antigen, EBNA3, were detected in nearly 80% of this cohort²²³. In contrast, Fogg et al.¹³² detected EBNA1-specific T cells *ex vivo* in over 90% (12 of 13) of human adults and about 50% of those responses included EBNA1-specific $CD8^+$ T cells. Bickham et al.²²⁴ studied the EBNA1 $CD4^+$ T cell response and found detectable responses in only 37% (7 of 19) of the tested individuals directly *ex vivo*; upon *in vitro*

expansion EBNA1-specific CD4⁺ T cells became detectable in 95% of those individuals. Similarly, Munz et al.⁹² detected EBNA1-specific CD4⁺ T cell responses in all human adults (10 of 10) upon initial *in vitro* expansion of specific cells.

BZLF1 is considered an immunodominant target of the EBV-specific T cell response^{1, 225}. Prevalence of T cells in response to this antigen within human populations is commonly studied using specific HLA backgrounds and immunodominant epitopes, and so their presence and characteristics in a truly diverse population are not well documented. Houssaint et al.²²⁵ detected BZLF1-specific CD8⁺ T cells in 60% of polyclonal T cell lines from human subjects, but epitope-specific responses have been detected at a much higher rate when cells are tested with the appropriate HLA background. For example, Tan et al.²²⁶ and Woodbury et al.⁷¹ both reported BZLF1-specific responses in all individuals of their HLA-specific cohorts. Less is known about BZLF1-specific CD4⁺ T cells, but Long et al.⁸⁹ used IFN- γ ELISpot assays to detect responses in 79% of EBV-seropositive individuals. The various techniques and corresponding results have been reviewed elsewhere^{1, 89, 217}, but in general, BZLF1 is known to induce a stronger CD8⁺ than CD4⁺ T cell response, which is similar to what we observed in the current study.

Other studies have examined subset phenotypes and cytokine production of human EBV-specific T cells by flow cytometry. Heller et al.²²⁷ reported the presence of proliferation-competent IFN- γ -producing EBNA1-specific CD4⁺ T cells in 90% (18 of 20) of individuals; slightly more than half belonged to the T_{CM} cell subset and the remaining belonged to the T_{EM} cell subset. Both the frequency and subset distribution are quite similar to our findings in rhesus macaques. Guerreiro et al.²²⁸ described responses in eight EBV-seropositive individuals and found the majority of directly *ex vivo*-tested EBNA1-specific CD4⁺ and CD8⁺ T cells and BZLF1-specific CD4⁺ T cells belonged to the T_{CM} cell subset and produced IL-2 and/or TNF- α , while BZLF1-specific CD8⁺ T cells were more activated and produced mainly IFN- γ and TNF- α . While we describe similar subset distributions, we found that rhesus EBNA1 CD4⁺ T cells were more polyfunctional and more commonly produced IFN- γ either alone or in combination with other cytokines. We also detected more activated rhEBNA1 CD8⁺ T cells based on the large effector populations. It is possible that some of these differences are due to the fact that Guerreiro et al. analyzed the

cytokine profiles of only two of the highest responders. Not only may the small sample size sway the response, but also the profile of high responders may naturally differ. Finally, Ning et al.⁸¹ compared BZLF1 polyfunctional responses to a combination of latent EBV antigens, adding MIP1- α and CD107a to the staining panel. Although they did not analyze subset distributions, they found polyfunctional responses within both human CD4⁺ and CD8⁺ T cell populations similar to results of our studies in rhesus macaques. These findings indicate that latent infection has only minor impact on the function of EBNA1-specific T cells.

An additional approach to gauge the degree of T cell exhaustion is to measure the expression of inhibitory receptors on the cell surface. Expression of the inhibitory receptor PD-1 increases after T cell activation, and overexpression of PD-1 has been linked to T cell exhaustion and decreased functional capacity. We had originally planned on measuring PD-1 expression using MHC class I tetramer staining, but the Mamu A*08 specific tetramer developed by our collaborators was not sensitive enough to consistently detect responses directly *ex vivo*. Instead, we stained PBMCs for PD-1 prior to stimulation with peptide pools for ICS. It would have been ideal to stain for multiple inhibitory receptors, but there are only a small number of suitable human antibodies that cross-react with rhesus proteins. Because PD-1 can reflect normal T cell activation as well as T cell dysfunction, our data were interpreted in the context of the phenotypic and functional readouts.

We detected a significantly larger frequency of rhEBNA1-specific PD-1⁺ CD4⁺ memory T cells compared to total and rhBZLF1-specific CD4⁺ memory cells. However, the average percentage of rhEBNA1-specific PD-1⁺ T cells was just above 50%, which is not indicative of exhaustion²²⁹. Salisch et al.²³⁰ used flow cytometry to characterize the distribution of PD-1 expression among T cell subsets in healthy rhesus macaques and found that PD-1 was primarily restricted to memory T cells: between 30% to 45% of CD4⁺ memory T cells expressed PD-1. The increase we observed in PD-1⁺ rhEBNA1-specific CD4⁺ memory T cells relative to total CD4⁺ memory cells could be a result of recent activation or could be caused by low-level rhEBNA1 expression during latency. However, because the frequency of PD-1⁺ rhBZLF1-specific T cells was not elevated in any subset, reactivation is unlikely. Memory responses were broad, which

suggests a range of activation that is highly variable between animals. This could reflect different rates of rhLCV reactivation or the ability of different Mamu genotypes to detect different epitopes.

We were surprised to find consistently low percentages of rhEBNA1- and rhBZLF1-specific PD-1⁺ CD8⁺ T_{EFF} cells compared to total CD8⁺ T_{EFF} cell responses, as effector cells are typically highly activated and are often associated with increased expression of PD-1²³¹. However, Hokey et al.²³¹ found higher PD-1 expression on total CD8⁺ T_{CM} cells compared to T_{EM} and T_{EFF} cells. Similarly, Salisch et al.²³⁰ found that the majority of PD-1⁺ CD8⁺ T cells (between 20-30%) exhibited a memory phenotype. In comparison, we found larger percentages of total PD-1⁺ CD8⁺ memory (54%) and effector cells (62%). Petrovas et al.²³² report a similar percentage of PD-1⁺ CD8⁺ memory T cells in healthy rhesus macaques using an approach similar to ours, however, they stained for PD-1 after stimulating cells for 6 hours, whereas we stained prior to stimulation. The large percentage of total PD-1⁺ CD8⁺ T_{EFF} cells we detected could signify a high degree of general immune activation.

Groups have also studied PD-1 expression on EBV-specific T cells. Day et al.²³³ and Petrovas et al.²³⁴ used a BMLF1 tetramer to detect the percentage of PD1-expressing CD8⁺ T cells, which was about 75% (range: about 50% to 100%). We expected to find a similarly large percentage of rhBZLF1-specific PD-1⁺ CD8⁺ T_{EFF} cells, but instead found the opposite. One explanation is that neither rhEBNA1- nor rhBZLF1-specific CD8⁺ T cells frequently encounter antigen- either due to the rhEBNA1 GAr domain or to a lack of recent reactivation, respectively. Differences in methods of detection and markers used to define various subsets could also be responsible for these discrepancies. Differences could also be a reflection of epitope specificity, as supported by Greenough et al.²²¹, who studied PD-1 expression on EBV-specific CD8⁺ T cells during AIM, convalescence, and chronic infection using tetramers against immediate-early (BRLF1) and early (BMLF1) lytic antigens. They report a percentage of total BRLF1 CD8⁺ T cells expressing PD-1 during convalescence (median: 35.1%; range: 10.3% to 80%) that is quite similar to the percentage of total PD-1⁺ CD8⁺ rhBZLF1 responses in our studies (data not shown, median: 29.8%; range: 12.2% to 70%). They also describe very similar percentages of BMLF1 CD8⁺ T cells as Day et al. and Petrovas et al. Furthermore, they note that PD-1 expression was

highest within the T_{EM} cell compartment, which would be represented within our memory subset (which was also the largest). To our knowledge, we are the first group to study the expression PD-1 on rhLCV-specific T cells. Our results clearly demonstrate that PD-1 is not over-expressed on rhEBNA1- or rhBZLF1-specific T cells, both of which produce multiple cytokines in response to stimulation. Therefore, while antigens may be continually present and could influence the cell phenotypes we observed, they do not appear to cause functional exhaustion.

Trends observed in our studies regarding the immunodominance of lytic and latent proteins parallel responses observed in humans; EBNA1-specific CD4⁺ T cell responses are more dominant than CD8⁺ T cell responses, and the opposite is observed for BZLF1. In concordance with this, we found that rhEBNA1-specific CD4⁺ T cells were more polyfunctional than rhEBNA1-specific CD8⁺ T cells and rhBZLF1-specific CD4⁺ T cells. RhEBNA1- and rhBZLF1-specific CD8⁺ T_{EFF} cells had similar functional properties, but the magnitude of rhBZLF1-specific responses was larger, and rhBZLF1-specific CD8⁺ T_{CM} cells were more polyfunctional. Upon primary infection and subsequent reactivations, BZLF1-specific CD8⁺ T cells are probably seeing more antigen and have a more direct role in controlling reactivations than the CD4⁺ response, which is mostly central memory. On the other hand, EBNA1-specific CD8⁺ T cells may be less sensitive in detecting antigen due to the glycine-alanine repeat domain, and this may somehow trigger a larger and more functional CD4⁺ T cell response.

All of the studies in humans as well as rhesus macaques demonstrate that a natural infection with EBV or rhLCV induces detectable CD4⁺ and CD8⁺ T cell responses to both EBNA1 and BZLF1. Differences in subset distribution or functionality of EBNA1-specific T cell responses in different studies may in part reflect differences in the employed assays. We have chosen to assess antigen-specific responses with overlapping peptide pools and a short 6-hour stimulation because we feel that this method provides the most accurate reflection of the response *in vivo*. Prolonged stimulation of T cells by their *ex vivo* expansion not only changes T cell functions but also leads to selective proliferation of some T cells and concomitant loss of others. Furthermore, studies that use only IFN- γ as an output of response specificity are likely minimizing the actual frequencies of the responses. Variances may also reflect different study populations from diverse

geographic regions, different age ranges, or different underlying diseases. While humans are more frequently exposed to infectious agents and more commonly encounter perturbations of their immune systems that may support EBV reactivation, such as infections²³⁵, autoimmunity²³⁶, or stress^{237, 238}, the non-human primates of our study were housed in a relatively controlled environment. Furthermore, it is important to note that most primates become naturally infected with rhLCV during the first few years of life. Exposure of humans in developed countries is more sporadic and can be delayed until adolescence or even adulthood although infections occur earlier in less developed countries such as Africa²³⁹. Some studies suggest that responses against lytic and latent antigen in healthy seropositive individuals are influenced by the length of time since primary exposure^{71, 240}, and this is much more variable in the human response. Nonetheless, other data failed to demonstrate a correlation between age and magnitude of T cell responses to antigens of EBV using cohorts from Africa²⁴¹.

The immunological responses to EBV are complex yet critical for understanding their role in human carcinogenesis and related diseases. Although primary infection is in general benign, the persistence of this oncogenic virus can lead to multiple cancer types, typically exacerbated by immunological dysfunction or immunosuppression associated with human immunodeficiency virus type 1 (HIV-1) infection or solid-organ transplants. Recent evidence also supports a role for EBV infection in several autoimmune disorders, suggesting that EBV has a complex interaction with the host immune system. The natural rhLCV infection of rhesus macaques provides an ideal animal model to study host immunological responses to EBV-like viruses and is also the system of choice for pre-clinical evaluation of EBV vaccines. Therefore, the importance of this study is twofold: first, by comparing rhesus macaque EBNA1 and BZLF1 T cell responses to human EBNA1 and BZLF1 T cell responses, we have further validated the rhLCV model as an appropriate and useful system for studying EBV. Second, an improved understanding of the rhEBNA1 immune response will benefit the pre-clinical development of vaccines that could potentially prevent or control EBV-associated malignancies.

Our study provides a baseline for future studies of therapeutic interventions in the rhLCV model. We have shown that rhEBNA1-specific T cell responses are present and functional. Next, we will determine if they can be expanded through vaccination.

CHAPTER 3:

ADENOVIRUS-BASED VACCINES TO RHESUS LYMPHOCRYPTOVIRUS EBNA1: VECTOR DESIGN, MOUSE STUDIES, *IN VITRO* TESTING

ABSTRACT

The impact of EBV on human health is substantial, but vaccines that prevent primary EBV infections or treat EBV-associated diseases are not yet available. EBNA1 is an important target for vaccination because it is the only protein expressed in all EBV-associated malignancies. We designed two therapeutic EBV vaccines that express a GAR-deleted rhLCV EBNA1. Vaccines were based on two serotypes of E1-deleted simian adenovirus. To further modulate the response, rhEBNA1 was fused to herpes simplex virus glycoprotein D (gD), which acts to block an inhibitory signaling pathway during T cell activation. Although we were unable to detect rhEBNA1-specific T cell responses in mice, vaccines stimulated IFN- γ production by autologous rhEBNA1-specific T cells *in vitro*. These experiments confirm the specificity and functionality of our novel prototype vaccines.

Portions of this chapter were adapted from:
Leskowitz R, Fogg MH, Zhou XY, Kaur A, Silveira ELV, Villinger F, Lieberman PM, Wang F, and Ertl HC. Adenovirus-based vaccines to rhesus lymphocryptovirus EBNA1 induce expansion of specific CD8⁺ and CD4⁺ T cells in persistently infected rhesus macaques. *Journal of Virology* 2014; 88(9): 4721-4735.

INTRODUCTION

EBV is associated with about 200,000 new cases of cancer annually and around 1% of all human cancers worldwide¹⁰⁴. Although primary infections are in general benign, EBV establishes a persistent infection through its latency in B cells, where it occasionally reactivates. This can lead to EBV-associated malignancies in certain populations⁵². For example, when the immune system becomes compromised, as it does during infection with HIV or immune suppression following organ transplant, its ability to control EBV declines, and EBV-associated malignancies can arise⁵². In Southern China, EBV-associated nasopharyngeal carcinoma afflicts 0.05% of all males over the age of 50²⁴². EBV-associated gastric carcinomas are highly prevalent in Eastern Asia, Eastern Europe and Africa¹⁰⁴, and EBV is tightly linked to endemic forms of Burkitt's lymphoma in Central Africa²⁴³. EBV has also been linked to autoimmune disorders¹⁰². The impact of EBV on human health is thus substantial, but vaccines to prevent primary EBV infections or treat EBV-associated diseases are not yet available.

An effective therapeutic EBV vaccine would need to target antigens produced during latency, when most viral protein expression is down-regulated²⁴⁴. Epstein-Barr nuclear antigen 1 functions to maintain the viral episome and is essential for viral DNA replication during latency. It is the only antigen expressed during all forms of latency²⁴⁵ and in all EBV-associated malignancies²⁴⁶. EBNA1 is thus a primary target for a therapeutic EBV vaccine. However, like many antigens of herpesviruses, EBNA1 subverts CD8⁺ T cell responses, thus potentially enhancing EBVs' ability to persist and escape immune surveillance. EBNA1 mRNA contains a purine-rich domain that encodes a large GAR sequence, which can interfere with EBNA1-specific CD8⁺ T cell responses, either by direct inhibition of GAR-containing protein synthesis or proteasome-mediated degradation, thus leading to reduced antigen presentation¹⁹⁴⁻¹⁹⁶. As a result, induction and effector functions of EBNA1-specific CD8⁺ T cell responses are impaired. Nevertheless, EBNA1-specific CD8⁺ ^{197, 198} and CD4⁺ ⁹² T cells are frequently detected in EBV-infected humans. These T cells are capable of controlling EBV-infected cells *in vitro*^{199, 209}, and the loss of EBNA1-specific T cells has been correlated with numerous EBV-associated

diseases^{62, 132-134}; this suggests that EBNA1-specific T cells play an important role in controlling infections *in vivo*.

Studies described in the following two chapters explore the use of EBNA1 as a potential vaccine target. In the previous chapter, we demonstrated that like humans, rhesus macaques develop EBNA1-specific CD8⁺ and CD4⁺ T cells during persistent rhLCV infection. Here, using the rhLCV model, we developed and tested two prototype vaccines expressing rhesus EBNA1. To facilitate rhEBNA1 processing and antigen presentation, the GAR domain was removed from the coding sequence. To further modulate the response, rhEBNA1 was genetically fused into the C-terminal domain of a modified herpes simplex virus (HSV-1) glycoprotein D (gD), which is a structural envelope protein that is essential for HSV-1 entry into host cells²⁴⁷. HSV-1 gD contains an immunoglobulin fold flanked by an N-terminal hairpin loop, C-terminal extension, and hydrophobic transmembrane region (TMR)²⁴⁸. The N-terminal loop of HSV-gD binds the bimodal herpes virus entry mediator (HVEM)²⁴⁹ and prevents inhibitory molecules from binding HVEM during T cell activation^{247, 250}. Downstream HVEM immunoinhibitory signaling pathways are subsequently blocked²⁵⁰. As we have previously shown, HSV-1 gD thereby enhances T cell responses to antigens fused into its C-terminus²⁴⁷. For example, mice vaccinated with DNA or Ad-based vaccines expressing antigen fused to HSV-1 gD develop significantly larger frequencies of IFN- γ ⁺ CD8⁺ T cells (**Figure 3-1**).

HSV-1 gD-rhEBNA1 chimeric antigens were expressed by E1-deleted Ad vectors of simian serotype 25 (SAdV-25) for priming and serotype 23 (SAdV-23) for booster immunizations. Vectors based on these serotypes are from here on referred to as AdC68 (SAdV-25) and AdC6 (SAdV-23) vectors. We have previously shown that chimpanzee-based Ad vectors induce potent and sustained transgene product-specific T cell responses in rodents^{163, 164} and non-human primates^{159, 251}. Because humans are our eventual target population, we chose simian-derived Ad vectors rather than Ad vectors based on human serotypes in order to prevent neutralization of the vaccine construct by antibodies to the vaccine carrier¹⁶⁷. Heterologous prime-boost vaccine regimens have been shown to elicit high transgene product-specific T cell responses, as they

overcome blocking immunity induced by the first vaccine and allow successful boosting of the memory immune response by the second vaccine^{251, 252}.

This chapter focuses on vaccine production, small animal studies, and *in vitro* experiments designed to test rhEBNA1 transgene expression and the ability of our vaccines to stimulate transgene product-specific T cell responses. Western blotting and cell surface staining experiments confirmed similar levels of transgene expression when rhEBNA1 was fused to various forms of HSV-1 gD. We were unable to detect rhEBNA1-specific T cell responses in mice regardless of the strain of mouse, vaccine dose, or the presence of mutations that destabilized rhEBNA1. However, vaccines stimulated IFN- γ production by autologous rhEBNA1-specific T cells *in vitro*, thus confirming their functionality and specificity.

Figure 3-1: Enhanced T cell responses to antigens expressed as fusion proteins with HSV-gD

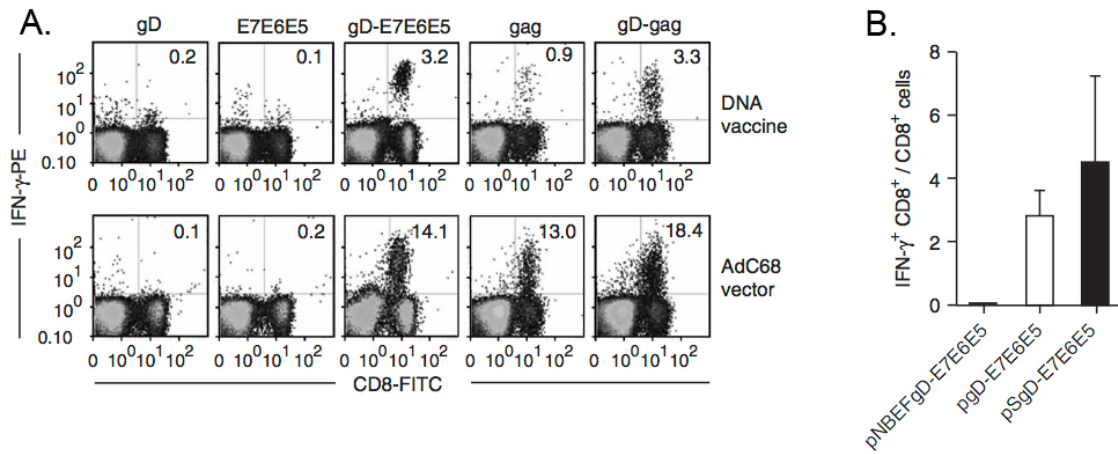


Figure 3-1: (A) PBMCs were stimulated and stained for CD8⁺ surface expression and intracellular IFN- γ 10 days after mice were immunized i.m. with AdC68 vectors (bottom) or DNA vaccines (top) expressing various antigens either alone or fused to gD. Numbers reflect the frequencies of CD8⁺ T cells that produce IFN- γ . **(B)** A comparison of IFN- γ -specific CD8⁺ T cell responses to DNA vaccines expressing antigen fused to wild type gD (center bar), super gD (SgD; black bar), or non-binding gD (NBEFgD) shows enhanced and diminished T cell responses from splenocytes 14 days after immunization. Figure was adapted from Lasaro et al., 2008²⁴⁷.

RESULTS

Vector construction and *in vitro* transgene expression

We developed several Ad-based vaccines expressing rhEBNA1 in which the GAR domain was removed from the coding sequence and a flag tag was inserted. The truncated rhEBNA1 protein was genetically fused into the C-terminal domain of various forms of HSV-1 gD. The GAR-deleted rhEBNA1 was also expressed without a fusion partner (rhEBNA1). Finally, to control for any non-specific effects of vaccination, we used a vaccine that expressed gD fused to an irrelevant antigen, i.e., the nucleoprotein of influenza A virus (gD-NP). Vaccines based on recombinant E1-deleted AdC68 and AdC6 viral vectors were used to deliver the antigens.

The truncated rhEBNA1 was inserted into a mutated version of gD with enhanced HVEM binding (termed super (S)gD; SgD-rhEBNA1). Enhanced binding to HVEM by SgD is the effect of a single amino acid mutation that opens up the HVEM binding domain and results in more potent T cell responses against antigens fused into its C-terminus as compared to wild-type HSV-1 gD²⁴⁸. To control for this effect, we generated a vaccine that expressed the truncated rhEBNA1 within a version of SgD with strongly reduced binding to HVEM (NBEFSgD-rhEBNA1)^{247, 248}. We confirmed rhEBNA1 protein functionality with a DNA binding assay using protein lysates from infected cells (data not shown). Schematic representations of the chimeric proteins are shown in **Figure 3-2A**.

To compare vaccine immunogenicity, it was essential that all vaccines expressed similar amounts of rhEBNA1. We therefore quantified rhEBNA1 expression levels by immunoblotting and cell surface staining of infected CHO-CAR cells. Immunoblots of protein lysates from AdC vector-infected cells confirmed that SgD-rhEBNA1 and NBEFSgD-rhEBNA1 were expressed at similar levels (**Figure 3-2B**). The rhEBNA1 transgene product was detected with antibodies against the flag epitope (**Figure 3-2B**; top), HSV-1 gD (**Figure 3-2B**; center), and rhesus serum reactive to rhEBNA1 (data not shown). As expected, both SgD-rhEBNA1 and NBEFSgD-rhEBNA1 achieved similar levels of expression at the expected size of 90-kDA. The 55-kDA band detected only by the gD antibody is unrelated to rhEBNA1, since it was also expressed by

vectors encoding gD only and therefore reflects either a gD degradation product, an alternative splicing event, or cross-reactivity with an Ad vector-derived protein. It is also possible that gD has been cleaved from the chimeric SgD-rhEBNA1 protein, although full length SgD-rhEBNA1 is still expressed at comparable levels compared to NBEFSgD-rhEBNA1. Cell surface staining of infected CHO-CAR cells for SgD-rhEBNA1 and NBEFSgD-rhEBNA1 with an antibody to flag also revealed similar levels of transgene expression (**Figure 3-2C**). This indicates that the gD transmembrane domain redirected rhEBNA1 from the nucleus to the cell surface at similar levels regardless of the version of gD.

While vectors expressed gD-rhEBNA1 chimeric proteins at similar levels, the AdC-rhEBNA1 vector expressed markedly higher levels of rhEBNA1 (**Figure 3-3A**), which would have made it difficult to determine whether differences in vaccinated animals were due to blockade of the HVEM pathway or to levels of rhEBNA1 expression. We therefore chose the two vectors with similar levels of rhEBNA1 expression but different abilities to block the HVEM pathway (SgD-rhEBNA1, NBEFSgD-rhEBNA1) for *in vivo* comparisons in rhesus macaques.

The chimeric proteins were also tested in an HVEM binding assay to confirm enhanced and reduced binding to SgD and NBEFSgD, respectively. Normalized protein extracts from cells infected with AdC68 vectors encoding SgD-rhEBNA1, NBEFSgD-rhEBNA1 or rhEBNA1 were added to plates coated with HVEM. **Figure 3-2D** shows the enhanced binding of SgD-rhEBNA1 compared to NBEFSgD-rhEBNA1 and rhEBNA1 without gD, both of which failed to bind HVEM at the tested concentrations of protein, as expected.

Figure 3-2: *In vitro* testing of AdC-SgD-rhEBNA1 and AdC-NBEFSgD-rhEBNA1 vaccines

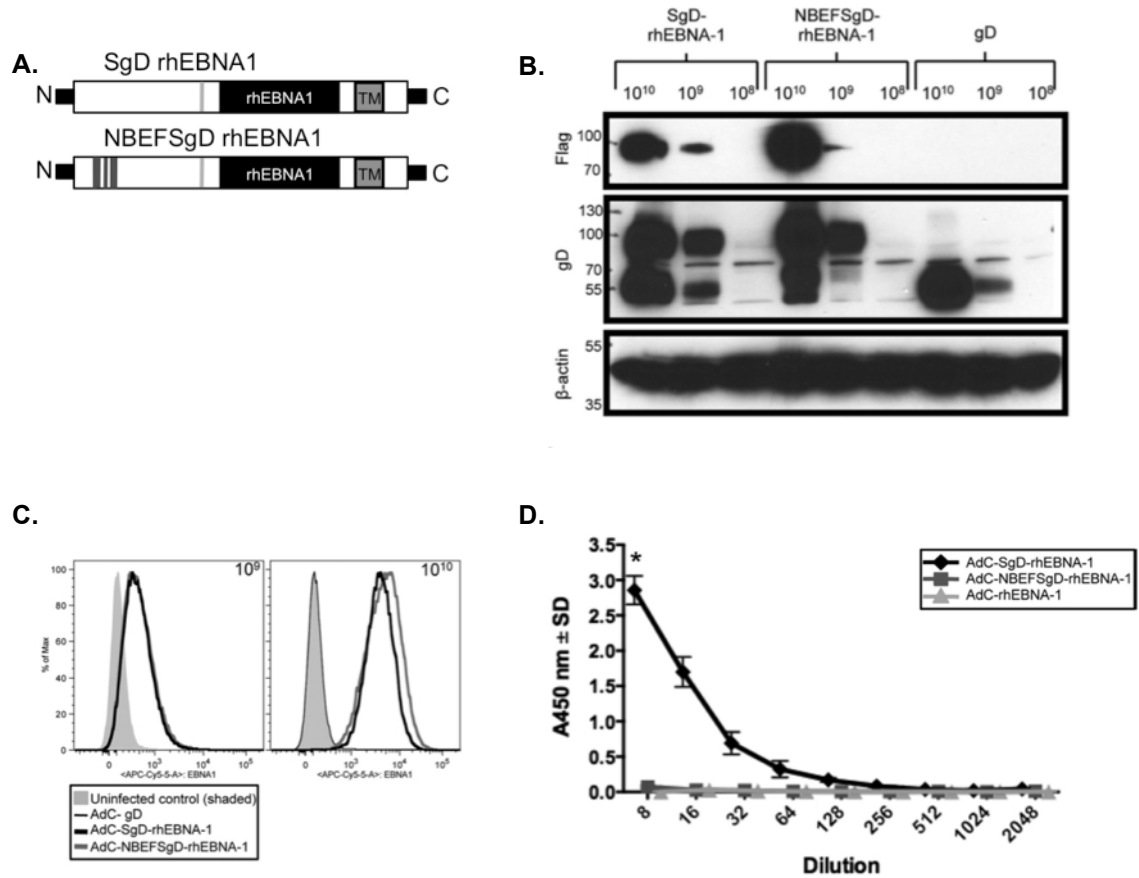


Figure 3-2: (A) Schematic representations of HVEM-binding (top) and non-binding (bottom) gD-rhEBNA1 fusion proteins expressed by AdC-based vaccines. Super (S) gD contains a mutation at position 294 of HSV-1 gD, in which a tryptophan was changed to an alanine (light grey band)²⁴⁸. The result is increased HVEM binding. The non-binding effect (NBEF) gD was generated by replacing seven amino acids at the N-terminus of HSV-1 gD with alanine (dark grey bands)²⁴⁸. These mutations block HVEM binding. **(B)** Western blot analyses of protein lysates harvested from CHO-CAR cells infected with 10^{10} , 10^9 , or 10^8 vps of AdC-based vaccines expressing SgD-rhEBNA1 (left), NBEFSgD-rhEBNA1 (center), or gD alone (right). Transgene products were detected with antibodies against the flag epitope (top row) or HSV-1 gD (center row). Anti β -actin was used as an internal control (bottom row). **(C)** Cell surface staining of infected CHO-CAR cells for SgD-rhEBNA1 and NBEFSgD-rhEBNA1. Cells were infected for 48 hours with 10^{10} or 10^9 vp of AdC68-SgD-rhEBNA1 or AdC68-NBEFSgD-rhEBNA1 or 10^{10} vp of AdC68-gD, stained with mouse anti-flag antibody, and probed with goat anti-mouse IgG-Alexa700. **(D)** An HVEM binding assay was used to test the ability of the chimeric proteins to bind their receptor. Normalized protein extracts from CHO-CAR cells infected with AdC68 encoding SgD-rhEBNA1 show enhanced HVEM binding (vs. AdC68-NBEFSgD-rhEBNA1, $p = 0.0036$; vs. AdC68-rhEBNA1, $p = 0.0035$; Comparing AUC by one-way Anova). A p-value < 0.05 was considered significant. All multiple comparisons were Bonferroni-adjusted to control for type I errors.

Vaccination does not induce rhEBNA1-specific T cells in mice

We tested the ability of our Ad-based rhEBNA1 vaccines to induce rhEBNA1-specific T cell responses in mice. Rhesus LCV does not naturally infect mice, and we were unable to find any reports of rhLCV-specific vaccines tested within the murine immune system. Because mouse epitopes were unknown, we began with a dose escalation study in a small group of BALB/c mice. We used AdC vectors expressing either truncated rhEBNA1 alone or fused to HSV-1 gD from which the transmembrane domain had been deleted. Four animals per group received either 10^9 , 10^{10} , or 10^{11} vps per mouse of AdC68-rhEBNA1 or AdC68-gD-rhEBNA1 administered intramuscularly (i.m.). As a control, four animals were vaccinated with 10^{11} vps per mouse of AdC68-HIV-gag. T cells were tested for IFN- γ production by ICS after PBMCs were stimulated with an overlapping rhEBNA1 peptide pool at 2 and 4 weeks after vaccination. As shown in **Figure 3-3**, frequencies and numbers of rhEBNA1-specific IFN- γ^+ CD8 $^+$ T cells were all low, but looked most promising at the 10^{11} dosage. All rhEBNA1-specific T cell responses were significantly lower than HIV-gag-specific T cell responses ($p < 0.05$), as shown at week 4. Using the highest dose of 10^{11} vps per mouse, we repeated the same study through week 12 and compared responses to vaccine-naïve animals, which were not significantly different than animals vaccinated with either Ad-rhEBNA1-expressing vaccine (**Figure 3-4**). Peptide-specific CD4 $^+$ T cell responses were also undetectable (data not shown). These results indicate that BALB/c mice do not recognize epitopes within rhEBNA1.

A similar series of experiments using C57/Bl6 ($n = 5$) and ICR ($n = 10$) mice produced the same results despite staining for three different cytokines in order to broaden our detection of vaccine-induced responses (**Figure 3-5**). Mice were vaccinated with 10^{11} vp of AdC68-rhEBNA1 or AdC68-gD-rhEBNA1, and PMBCs were stained for IFN- γ , IL-2, and TNF- α . The lack of substantial responses led us to conclude that mice are not capable of recognizing epitopes within rhEBNA1, even when they are outbred (such as ICR mice).

Alternatively, the lack of rhEBNA1-specific T cell responses in mice could be a result of the high degree of stability of rhEBNA1, which is a DNA-binding protein that is not very well degraded. To address this, we destabilized rhEBNA1 by introducing various mutations within the

protease-resistant DNA binding domain (rhEBNA1-M and gD-rhEBNA1-M) to interfere with protein folding and increase degradation and antigen presentation of rhEBNA1. Thus, if mice are capable of responding to rhEBNA1, then immunization with AdC vaccines expressing rhEBNA1-M or gD-rhEBNA1-M would induce larger rhEBNA1-specific T cell responses. However, we were still unable to detect rhEBNA1-specific T cells after vaccination with mutated rhEBNA1 vaccines (data not shown).

To confirm that the lack of rhEBNA1-specific T cell responses was not caused by experimental error, we tested for the induction of gD-specific antibodies by serum ELISA. All animals that received gD-expressing vaccines developed antibodies against gD, which confirms that mice appropriately responded to vaccination (data not shown).

Figure 3-3: Frequency and number of IFN- γ ⁺ CD8⁺ T cells following dose-escalation study

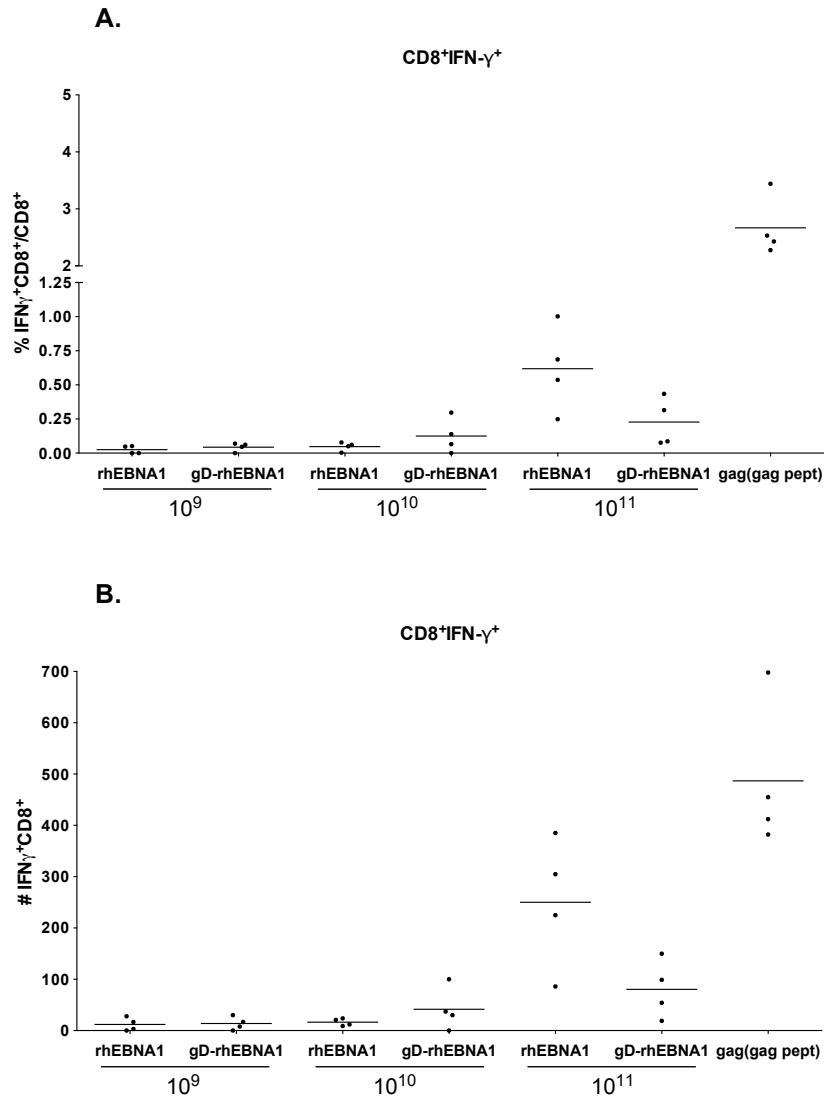


Figure 3-3: The frequency (**A**) and number (**B**) of IFN- γ ⁺ CD8⁺ T cells following a dose-escalation study of BALB/c mice ($n = 4$ per group) that received 10^9 , 10^{10} , or 10^{11} vp of AdC68 vectors expressing either rhEBNA1 or gD-rhEBNA1. As a control, animals were vaccinated with 10^{11} vp of AdC68 expressing HIV-gag. Responses were measured by production of IFN- γ after PBMCs were stimulated with overlapping rhEBNA1 or gag peptide pools. Representative data is shown here at week 4. Responses are shown after subtraction of background values. Bars indicate the mean.

Figure 3-4: Kinetics of peptide-specific CD8⁺ T cells after vaccination

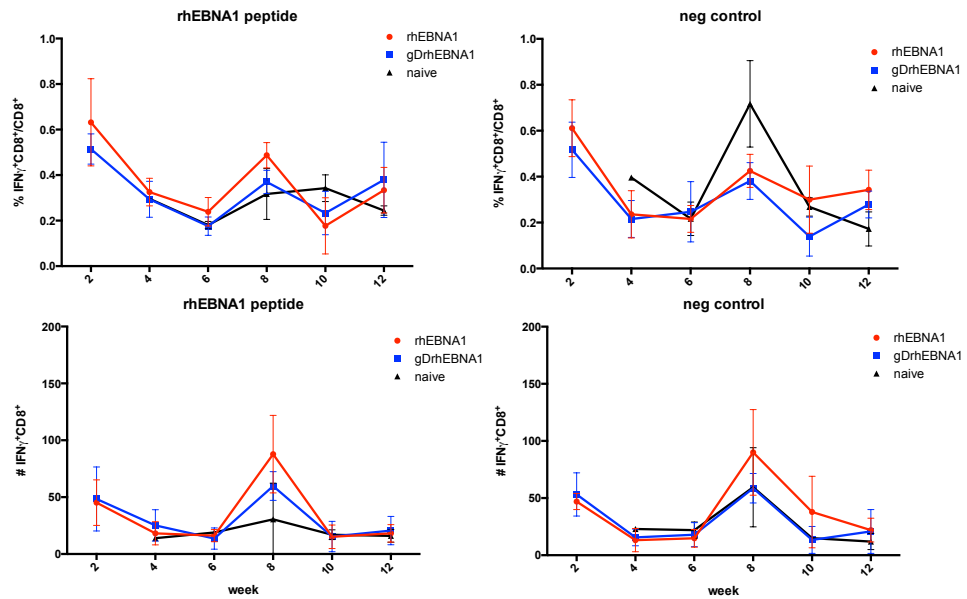


Figure 3-4: BALB/c mice ($n = 5$) were immunized with 10^{11} vp of AdC68-expressing rhEBNA1 (red circle) or gD-rhEBNA1 (blue square) to study the kinetics of peptide-specific T cells. PMBCs were collected every other week after vaccination and were stimulated with overlapping rhEBNA1 (left column) or HIV-gag (right column) peptide pools (labeled here as negative control). Responses are reported as the frequency (top row) or number (bottom row) of IFN- γ ⁺ CD8⁺ T cells after a five hour incubation. Vaccine-naïve mice (black triangle) were included as an additional control starting at week 4 in order to measure general immune fluctuation.

Figure 3-5: Peptide-specific CD8⁺ T cells after vaccination of C57/Bl6 and ICR mice

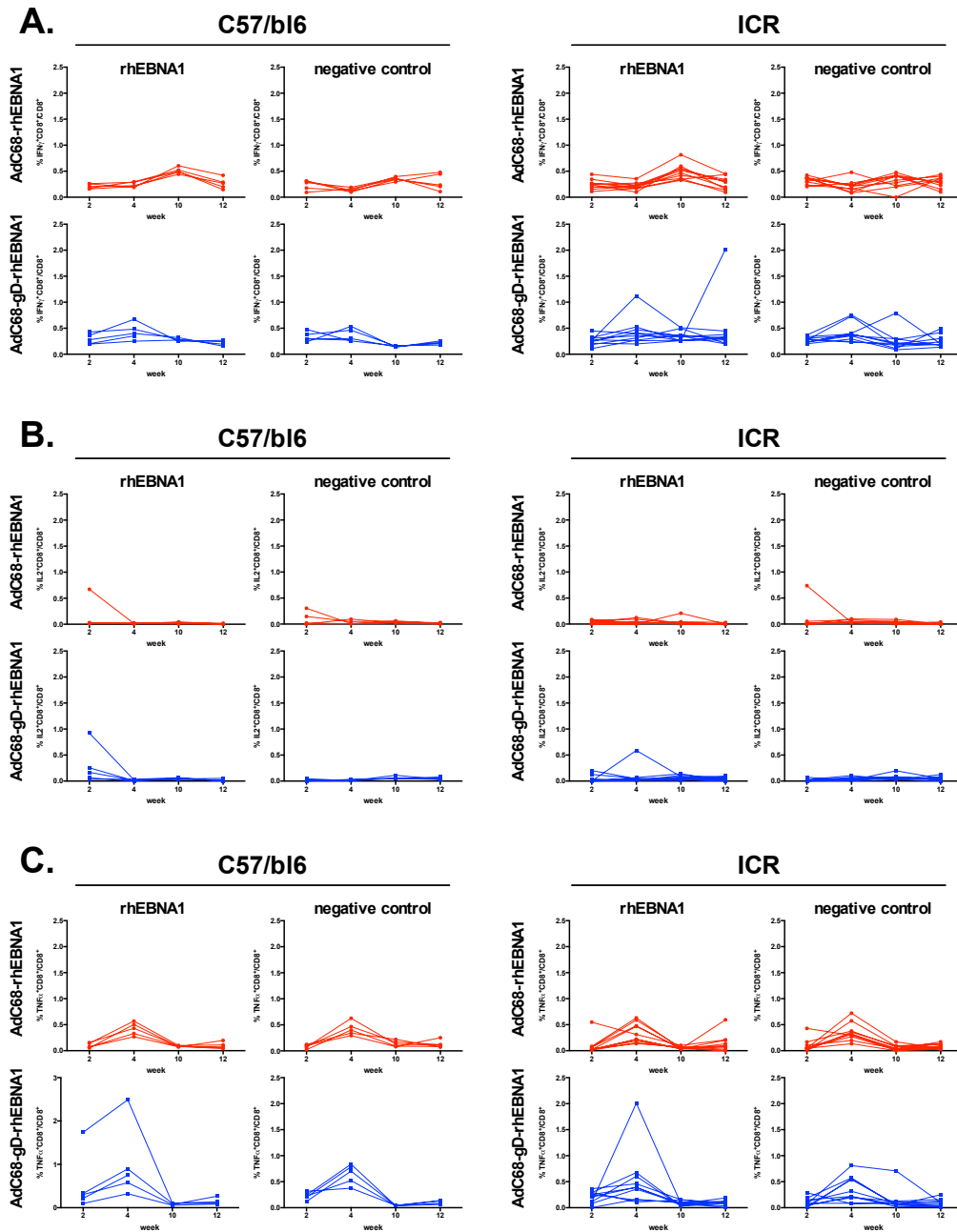


Figure 3-5: C57/Bl6 (left; $n = 5$) and ICR (right; $n = 10$) mice were immunized with 10^{11} vp of AdC68-expressing rhEBNA1 (red circle) or gD-rhEBNA1 (blue square). PMBCs were collected at weeks 2, 4, 10, and 12 after vaccination and were stimulated with overlapping rhEBNA1 or HIV-gag (labeled here as negative control) peptide pools. Responses are reported as the frequency of IFN- γ^+ (A), IL-2 $^+$ (B), or TNF- α^+ (C) CD8 $^+$ T cells after a five-hour incubation.

Vaccination induces rhEBNA1-specific T cells *in vitro*

To test if our vaccines could stimulate rhEBNA1-specific effector T cells *in vitro*, rhesus macaque DCs were infected with the AdC68-rhEBNA1 or AdC68-gD-rhEBNA1 viral vectors and cultured with autologous rhEBNA1-specific CD8⁺ T cells. T cell responses were measured by an IFN- γ ELISPOT assay. As shown in **Figure 3-6**, the rhEBNA1 antigen could be efficiently processed and presented to rhEBNA1-specific CD8⁺ T cells. DCs infected with the AdC68-gD-rhEBNA1 vector were able to induce IFN- γ secretion by rhEBNA1-specific T cells, and responses were comparable to those elicited by an AdC68-rhEBNA1 vector, which lacked gD. Empty vector or non-infected DCs did not induce responses. IFN- γ was produced by responding T cells, since cultures containing only infected DCs failed to produce IFN- γ .

Figure 3-6: *In vitro* stimulation of rhEBNA1-specific T cells

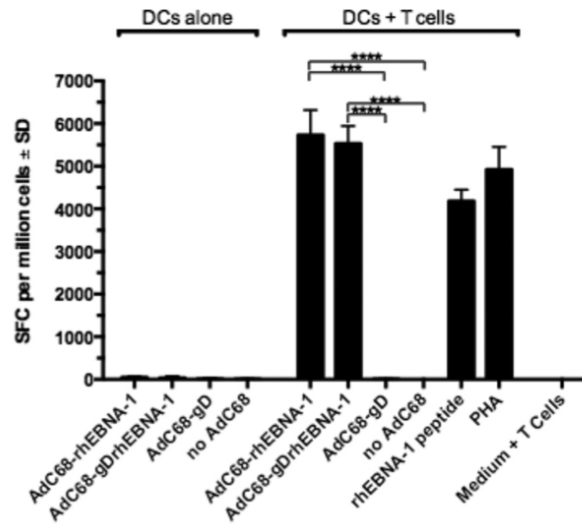


Figure 3-6: Mature DCs from an rhLCV-seropositive rhesus macaque were infected with the indicated Ad vectors or pulsed with rhEBNA1 peptide and then co-cultured with autologous rhEBNA1-specific CD4⁺-depleted CD8⁺ T cells. rhEBNA1-specific responses were measured by an IFN- γ ELISPOT assay after 16 hours and results are shown as average spots per 10⁶ CD8⁺ T cells based on quadruple experiments of the DC + T cells and triplicate experiments of the other samples. Asterisk denotes significant differences: all p-values < 0.0001 except for peptide vs. AdC68-rhEBNA1 (p = 0.0009) and AdC68-gD-rhEBNA1 (p = 0.0036). P-values were calculated using one-way ANOVA, with a p-value < 0.05 considered significant. All multiple comparisons were Bonferroni-adjusted to control for type I errors.

DISCUSSION

EBV infection causes a significant amount of morbidity and mortality within both immune competent and immune compromised populations throughout the world, but there is currently no approved prophylactic or therapeutic EBV vaccine. Using the rhLCV animal model of EBV infection, we constructed AdC-based vaccines that target rhEBNA1, the only antigen of rhLCV (and EBV) expressed during lytic and latent infection and in all associated malignancies. Ad vectors derived from chimpanzee serotypes are highly immunogenic^{159, 251, 253}, have low prevalence rates in human cohorts²⁵⁴, and are well suited for clinical development²⁵⁵. Vaccines expressed a GAR-deleted form of rhEBNA1 that was fused to the HVEM-binding HSV-1 gD to further promote T cell responses. We had originally planned to use AdC vaccines expressing rhEBNA1 without HSV-1 gD as a control, but rhEBNA1 protein expression as detected via western blot was at least 100-fold higher than gD-rhEBNA1. This likely reflects either differences in protein stability caused by fusion to HSV-1 gD or differences in the rates of transcription/translation between shorter versus longer sequences. Therefore, to better control for the adjuvant effect of HSV-1 gD, rhEBNA1 was fused to an HVEM-non-binding form of gD. *In vitro* studies confirmed that vaccines expressed similar levels of gD-rhEBNA1 fusion products so that potential differences after vaccination could be attributed to HVEM binding of gD rather than to differences in antigenic load. Additional *in vitro* studies confirmed that the two forms of gD exhibited the expected HVEM binding patterns.

We initially attempted to confirm vaccine immunogenicity by testing their ability to induce rhEBNA1-specific T cell responses in several different strains of mice, including BALB/c, C57/Bl6, and ICR mice, which are outbred. Mice were vaccinated with AdC68-rhEBNA1 or AdC68-gD-rhEBNA1. We were unable to detect rhEBNA1-specific T cells regardless of the strain of mouse, vaccine received, or dose of vaccination. A dose-escalation study followed by a kinetic analysis of rhEBNA1-specific responses after immunization at the highest dose (10^{11} vps/mouse) did not elicit any clear rhEBNA1-specific T cell responses. While we later learned that levels of transgene expression by AdC-rhEBNA1 and AdC-gD-rhEBNA1 vaccines differed, this was

inconsequential since neither vaccine elicited responses. This is perhaps because there are no rhEBNA1-specific mouse epitopes. An alternative explanation is that rhEBNA1 is an extremely stable protein that is not very well degraded. To address this question, we generated additional vaccines with mutated rhEBNA1 DNA-binding domains to destabilize rhEBNA1 and increase its degradation. However, we were still unable to detect responses in mice upon vaccination with modified vaccines. We assume this reflects a lack of suitable epitopes within rhEBNA1 that can bind to mouse MHC molecules.

While mice were vaccinated with a TMR-deleted vaccine, it is not likely that inclusion of the TMR would have significantly altered the results given that we were unable to detect responses against rhEBNA1 alone, which was expressed at a much higher rate than gD-rhEBNA1. Furthermore, all gD-rhEBNA1 transgene products were expressed at similar levels regardless of the version of HSV-1 gD (data not shown). Thus, mouse studies were not repeated with our TMR-containing vaccines. It is possible that without the TMR, the gD-rhEBNA1 fusion protein was redirected to the nucleus, which would have minimized the adjuvant effect of HSV-1 gD. However, if this were the case, then the magnitude of rhEBNA1-specific T cells would have increased after vaccination with rhEBNA1 (-M) and gD-rhEBNA1 (-M) vaccines.

We confirmed the immunogenicity of our rhEBNA1-expressing vaccines by an *in vitro* assay in which rhesus macaque DCs were co-cultured with autologous peptide-induced rhEBNA1-specific CD8⁺ T cells. Vaccines stimulated IFN- γ production, which demonstrates their ability to induce transgene product-specific T cell responses. These experiments do not exhibit a clear adjuvant effect of HSV-1 gD, which could be due to the high level of rhEBNA1 expression (compared to gD-rhEBNA1) as detected by western blots. A dose titration would have been useful for testing the difference between AdC-rhEBNA1 and AdC-gD-rhEBNA1 vectors and also for confirming the adjuvant effect of HSV-1 gD. Nevertheless, these experiments confirm vector immunogenicity and specificity, which was necessary in order to begin testing in rhesus macaques.

CHAPTER 4:

ADENOVIRUS-BASED VACCINES TO RHESUS LYMPHOCRYPTOVIRUS EBNA1 INDUCE EXPANSION OF CD8⁺ AND CD4⁺ T CELLS IN PERSISTENTLY INFECTED RHESUS MACAQUES

ABSTRACT

Latent EBNA1 is a promising target for a therapeutic vaccine, as it is the only antigen expressed in all EBV-associated malignancies. We have designed and tested two therapeutic EBV vaccines that target the rhesus LCV EBNA1 to determine if ongoing T cell responses during persistent rhLCV infection in rhesus macaques can be expanded upon vaccination. Vaccines were based on two serotypes of E1-deleted simian adenovirus and were administered in a prime-boost regimen. We found that vaccines expressing rhEBNA1 induced expansion of rhEBNA1-specific CD8⁺ and CD4⁺ T cells in 33% and 83% of the vaccinated animals, respectively. Additional animals developed significant changes within T cell subsets without changes in total numbers. Vaccination did not increase T cell responses to rhBZLF1, an immediate early lytic phase antigen of rhLCV, thus indicating that increases of rhEBNA1-specific responses were a direct result of vaccination. Vaccine-induced rhEBNA1-specific T cells were highly functional and

produced various combinations of cytokines as well as the cytolytic molecule granzyme B. These results serve as an important proof-of-principle that functional EBNA1-specific T cells can be expanded by vaccination.

Portions of this chapter were adapted from:
Leskowitz R, Fogg MH, Zhou XY, Kaur A, Silveira ELV, Villinger F, Lieberman PM, Wang F, and Ertl HC. Adenovirus-based vaccines to rhesus lymphocryptovirus EBNA1 induce expansion of specific CD8⁺ and CD4⁺ T cells in persistently infected rhesus macaques. *Journal of Virology* 2014; 88(9): 4721-4735.

INTRODUCTION

EBV is a common human pathogen that establishes a persistent infection through latency in B cells, where it occasionally reactivates. EBV infection is typically benign and is well controlled by the host adaptive immune system; however, it is considered carcinogenic due to its strong association with lymphoid and epithelial cell malignancies. The EBV protein EBNA1 is a promising target for a therapeutic vaccine, as it is the only antigen expressed in all types of latency and in EBV-associated malignancies.

We designed and tested vaccines that target the rhLCV EBNA1 (described in detail in Chapter 3). Rhesus macaques are naturally infected with rhLCV, a gamma-1 herpesvirus that is closely related to EBV^{191, 256}. Most rhesus macaques become infected during infancy, and rhLCV persists for life in a latent form in B cells. Like EBV, rhLCV has been associated with virus-positive B cell lymphomas upon immunosuppression¹⁹¹. EBV and rhLCV share a high degree of sequence homology, they have identical repertoires of lytic and latent genes¹⁸⁹, and they elicit similar immune responses²⁵⁷. We characterized rhEBNA1-specific T cell responses in a cohort of seropositive rhesus macaques and found that most animals have rhEBNA1-specific CD4⁺ and CD8⁺ T cells that resemble human T cell responses in many aspects (Chapter 2). The rhLCV model is therefore ideal for preclinical testing of EBV vaccines.

The goal of this study was to test if prototype vaccines expressing rhEBNA1 could expand ongoing rhEBNA1-specific CD8⁺ and CD4⁺ T cell responses in adult rhesus macaques with persistent rhLCV infections. We developed and tested two vaccine regimens based on replication-defective adenovirus (Ad) vectors derived from chimpanzee serotypes (AdC). Vaccines expressed a GAR-deleted form of rhEBNA1. To further modulate the response, rhEBNA1 was fused to herpes simplex virus glycoprotein D (gD), which binds the herpes virus entry mediator (HVEM) and blocks its interaction with the immunoinhibitory B and T lymphocyte attenuator (BTLA) during T cell activation. HVEM-binding and -non-binding versions of HSV-gD were tested. Vaccination increased the number of circulating rhEBNA1-specific CD8⁺ and CD4⁺ T cells in rhesus macaques with persistent rhLCV infections regardless of gD binding ability.

Responses were highly functional, and T cells produced various combinations of the cytokines IFN- γ , IL-2, and TNF- α . T cells also produced granzyme B, which indicates that vaccination increased the cytolytic potential of rhEBNA1-specific T cells. These preliminary studies confirm that rhEBNA1 is a suitable target for therapeutic rhLCV and presumably EBV vaccines.

RESULTS

Characteristics of NHPs

Fifteen female adult, healthy, and SIV-uninfected rhesus macaques aged 6 to 20 years were enrolled in this study at the Yerkes National Primate Research Center (YNPRC). Animals were negative for neutralizing antibodies to AdC68 and AdC6 and positive for antibodies to rhLCV. **Table 4-3** shows the basic characteristics of animals enrolled in this study.

Vaccination increases the frequency of rhEBNA1-specific T cell responses

To test if our vaccines could induce or expand rhEBNA1-specific T cell responses *in vivo*, animals were injected i.m. with 10^{11} vp of AdC68 vectors expressing SgD-rhEBNA1 (group 1, $n = 6$), NBEFSgD-rhEBNA1 (group 2, $n = 6$), or gD-NP (group 3, $n = 3$). They were boosted 15 weeks later with the same doses of AdC6 vectors expressing the same inserts. Vaccines are described in detail in the previous chapter. Responses were measured from blood collected two months prior to and on the day of vaccination to determine baseline responses and at 2, 4, and 8 weeks after priming and 2, 4, and 6 weeks after boosting (weeks 17, 19, and 21) to test for vaccine-induced changes (**Figure 4-1**). RhEBNA1-specific CD8⁺ and CD4⁺ T cell responses were measured by ICS for IFN- γ , IL-2, and TNF- α ¹⁹⁸. We also analyzed the effects of vaccination on T cell subsets, i.e., effector (T_{EFF}), effector memory (T_{EM}) and central memory (T_{CM}) cells identified by additional stains for CD95, CD28, and CCR7. Results obtained by ICS were normalized to numbers of responding cells per 10^6 live CD3⁺ cells, and background data were subtracted. We used two criteria to define vaccine-induced increases of rhLCV-specific T cell responses. First, average normalized numbers of specific T cells from 5 rhLCV seronegative animals were used to determine the detection limit of the assay; numbers of total cytokine-producing T cells (after background subtraction) had to be two standard deviations (SDs) above this limit. Second, animals were classified as vaccine responders if rhEBNA1-specific cytokine responses increased 2 SDs or more above mean baseline responses for at least 3 time points after vaccination. Animals that met these criteria only within T cell subsets were also viewed as responders, as the

additional stains used to identify T_{EFF}, T_{EM}, and T_{CM} cells increase staining sensitivity by reducing background noise. Details on individual immune responses can be found in **Table 4-1** (CD8⁺ T cell responses) and **Table 4-2** (CD4⁺ T cell responses).

Based on these criteria, 50% (6/12) of the animals were identified as vaccine responders for rhEBNA1-specific CD8⁺ T cells, and 92% (11/12) were vaccine responders for rhEBNA1-specific CD4⁺ T cells (summarized in **Table 4-3**; primary data are provided in **Table 4-1** and **Table 4-2**). The one vaccine non-responder was from group 1. Increases in rhEBNA1-specific T cell responses were driven by the rhEBNA1 vaccines, as none of the group 3 animals who received the control vectors qualified as vaccine responders. Additionally, none of the animals qualified as responders when T cells were tested against an irrelevant rhLCV antigen, i.e., no animals in any group developed sustained T cell increases against rhBZLF1, a highly immunogenic immediate-early antigen of rhLCV (**Table 4-1** and **Table 4-2**).

Figure 4-1: Schedule of vaccinations and blood collection

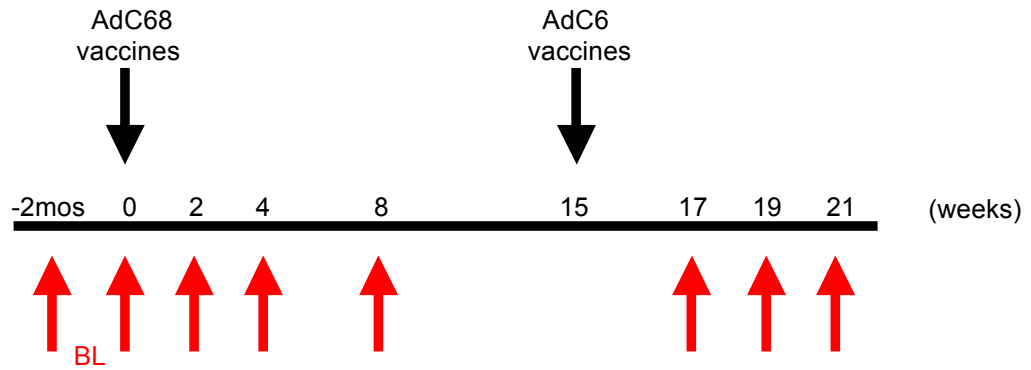


Figure 4-1 shows the vaccination (black arrows) and blood collection (red arrows) schedule. Numbers along the axis display the timing in weeks after the first vaccination (at week 0). Baseline responses for each animal reflect the average between week 0 and 2 months prior to vaccination. BL, baseline; mos, months.

Table 4-1: Number of CD8⁺ T cells/10⁶ live CD3⁺ cells

Specific T cell target	AdC-SgD-rhBNA1 (group 1)										AdC-NBEFSgD-rhBNA1 (group 2)										AdC-gD-NP (group 3)									
	Time after vaccination					Time after vaccination					Time after vaccination					Time after vaccination					Time after vaccination									
	NHP ID	Subset	BL	2	4	8	17	19	21	NHP ID	Subset	BL	2	4	8	17	19	21	NHP ID	Subset	BL	2	4	8	17	19	21			
rhEBNA1	RYa6 (B17)	CD8	284	2583	1201	706	394	1935	1670	RNw9	CD8	260	1316	644	651	545	NT	455	RYc3	CD8	324	—	—	—	520	NT	—	236		
		CD8CM	196	623	562	155	94	460	1165		CD8CM	111	462	265	219	220	NT	252		CD8CM	44	—	—	—	91	NT	—	157		
		CD8EM	102	1625	600	402	306	1232	520		CD8EM	18	772	344	240	247	NT	250		CD8EM	27	—	—	—	0	NT	—	0		
		CD8EFF	60	116	18	81	67	175	24		CD8EFF	161	37	8	183	84	NT	40		CD8EFF	275	—	—	—	469	NT	—	63		
	PH1019 (B17)	CD8	454	608	—	389	711	844	NT	RZ17 (B17)	CD8	—	271	—	—	—	—	1178	1138	RC17	CD8	693	486	230	—	—	—	—	488	
		CD8CM	152	217	—	0	104	261	NT		CD8CM	—	87	—	—	—	—	0	0		CD8CM	72	152	33	—	—	—	—	63	
		CD8EM	19	84	—	285	59	117	NT		CD8EM	—	32	—	—	—	—	0	0		CD8EM	26	12	0	—	—	—	—	15	
		CD8EFF	336	235	—	319	415	281	NT		CD8EFF	—	157	—	—	—	—	1178	1138		CD8EFF	532	222	191	—	—	—	—	363	
	RTn5	CD8	—	—	—	536	—	—	—	RVw6	CD8	435	312	449	360	644	NT	NT	NT	RLz5	CD8	457	—	—	—	—	—	—	225	
		CD8CM	—	—	—	146	—	—	—		CD8CM	203	97	158	122	193	NT	NT	NT		CD8	95	—	—	—	—	—	—	20	
		CD8EM	—	—	—	—	—	—	—		CD8EM	119	245	267	239	252	NT	NT	NT		CD8CM	26	—	—	—	—	—	—	104	
		CD8EFF	—	—	—	—	—	—	—		CD8EFF	126	17	28	15	183	NT	NT	NT		CD8EFF	305	—	—	—	—	—	—	28	
	RC15	CD8	233	—	—	441	—	—	—	RTp4	CD8	360	610	265	436	—	—	—	—	NT	CD8	—	—	—	—	—	—	—	129	
		CD8CM	26	—	—	103	—	—	—		CD8CM	43	265	93	97	—	—	—	—	NT	CD8	—	—	—	—	—	—	—	182	
		CD8EM	34	—	—	16	—	—	—		CD8EM	47	102	41	48	—	—	—	—	NT	CD8	—	—	—	—	—	—	—	—	
	CD8EFF	189	—	—	165	—	—	—		CD8EFF	273	165	127	242	—	—	—	—	NT	CD8	—	—	—	—	—	—	—	—		
RR9	CD8	—	—	—	—	—	—	—	PWw	CD8	347	—	—	—	—	—	—	—	NT	CD8	—	—	—	—	—	—	—	—		
	CD8CM	—	—	—	—	—	—	—		CD8CM	104	—	—	—	—	—	—	—	NT	CD8	—	—	—	—	—	—	—	—		
	CD8EM	—	—	—	—	—	—	—		CD8EM	69	—	—	—	—	—	—	—	NT	CD8	—	—	—	—	—	—	—	—		
	CD8EFF	—	—	—	—	—	—	—		CD8EFF	113	—	—	—	—	—	—	—	NT	CD8	—	—	—	—	—	—	—	—		
RLy9	CD8	—	—	—	—	—	—	—	RCv5	CD8	—	—	—	—	—	—	—	—	NT	CD8	—	—	—	—	—	—	—	—		
	CD8CM	—	—	—	—	—	—	—		CD8CM	—	—	—	—	—	—	—	—	NT	CD8	—	—	—	—	—	—	—	—		
	CD8EM	—	—	—	—	—	—	—		CD8EM	—	—	—	—	—	—	—	—	NT	CD8	—	—	—	—	—	—	—	—		
	CD8EFF	—	—	—	—	—	—	—		CD8EFF	—	—	—	—	—	—	—	—	NT	CD8	—	—	—	—	—	—	—	—		
rhBZLF1	RYa6 (B17)	CD8	408	264	—	—	—	—	244	RNw9	CD8	2184	1876	1279	2888	2213	NT	1460	RYc3	CD8	495	—	—	—	—	—	—	—		
		CD8CM	268	166	—	—	—	—	—		CD8CM	1120	852	815	1363	1266	NT	688		CD8CM	103	—	—	—	—	—	—	—		
		CD8EM	116	25	—	—	—	—	—		CD8EM	575	761	276	1158	619	NT	586		CD8EM	28	—	—	—	—	—	—	—		
		CD8EFF	84	47	—	—	—	—	—		CD8EFF	168	86	70	145	57	NT	29		CD8EFF	370	—	—	—	—	—	—	—		
	PH1019 (B17)	CD8	1473	902	1274	—	—	—	1242	NT	CD8	315	629	254	344	—	—	—	—	RC17	CD8	413	847	759	240	—	—	—	—	
		CD8CM	295	226	168	—	—	—	—		CD8CM	110	239	43	—	—	—	—	—		CD8CM	80	188	43	0	—	—	—	—	
		CD8EM	65	76	10	—	—	—	—		CD8EM	196	148	139	80	—	—	—	—		CD8EM	21	74	13	0	—	—	—	—	
		CD8EFF	1005	484	1063	—	—	—	—		CD8EFF	108	181	77	0	—	—	—	—		CD8EFF	255	563	634	120	—	—	—	—	
	RTn5	CD8	586	390	511	660	—	—	—	586	NT	CD8	590	332	361	386	261	NT	NT	RLz5	CD8	314	—	—	—	—	—	—	281	
		CD8CM	215	147	214	325	—	—	—		CD8CM	262	133	200	133	123	NT	NT	NT		CD8CM	58	—	—	—	—	—	—	14	
		CD8EM	133	84	128	71	—	—	—		CD8EM	184	141	146	121	67	NT	NT	NT		CD8EM	13	—	—	—	—	—	—	0	
		CD8EFF	53	48	52	142	—	—	—		CD8EFF	80	17	0	34	75	NT	NT	NT		CD8EFF	277	—	—	—	—	—	—	—	
	RC15	CD8	285	241	—	—	—	—	—	563	NT	CD8	774	913	1603	765	NT	NT	NT		CD8	—	—	—	—	—	—	—	—	
		CD8CM	19	28	—	—	—	—	—	0	NT	CD8CM	136	235	247	0	NT	NT	NT		CD8	—	—	—	—	—	—	—	—	
		CD8EM	10	0	—	—	—	—	—	563	NT	CD8EM	405	428	615	612	NT	NT	NT		CD8	—	—	—	—	—	—	—	—	
	CD8EFF	207	213	—	—	—	—	—	—	CD8EFF	54	125	499	153	NT	NT	NT	NT		CD8	—	—	—	—	—	—	—	—		
RR9	CD8	973	340	918	964	NT	NT	NT	—	NT	CD8	461	507	446	561	—	—	—	—	NT	CD8	—	—	—	—	—	—	—	—	
	CD8CM	184	207	347	210	NT	NT	NT	—	NT	CD8CM	84	122	110	96	—	—	—	—	NT	CD8	—	—	—	—	—	—	—		
	CD8EM	134	40	84	175	NT	NT	NT	—	NT	CD8EM	165	244	170	267	—	—	—	—	NT	CD8	—	—	—	—	—	—	—		
	CD8EFF	151	0	84	53	NT	NT	NT	—	NT	CD8EFF	48	29	6	9	—	—	—	—	NT	CD8	—	—	—	—	—	—	—		
RLy9	CD8	—	—	—	—	—	—	—	—	NT	CD8	362	—	—	—	—	—	—	—	NT	CD8	—	—	—	—	—	—	—		
	CD8CM	—	—	—	—	—	—	—	—	NT	CD8CM	73	—	—	—	—	—	—	—	NT	CD8	—	—	—	—	—	—	—		
	CD8EM	—	—	—	—	—	—	—	—	NT	CD8EM	14	—	—	—	—	—	—	—	NT	CD8	—	—	—	—	—	—	—		
	CD8EFF	—	—	—	—	—	—	—	—	NT	CD8EFF	304	—	—	—	—	—	—	—	NT	CD8	—	—	—	—	—	—	—		

Table 4-1: rhEBNA1-specific (top) and rhBZLF1-specific (bottom) CD8⁺ T cell responses are shown at all pre- and post-vaccination time points. Responses are normalized to 10⁶ live CD3⁺ T cells after subtraction of background data for individual animals. —, values below the detection limit (based on rhILCV-seronegative rhesus macaques); data for time points at which the parental CD8⁺ T cell response was below the detection limit are not shown in the table (and were also omitted from the graphs). Peptide-specific vaccine responses greater than 2SDs from the mean baseline are highlighted in grey. BL, baseline; NT, not tested; NHP, non-human primate; ID, identification number.

Table 4-2: Number of CD4⁺ T cells/10⁶ live CD3⁺ cells

Specific T cell target	AdC-SgD-rhEBNA1 (group 1)										AdC-NBEFSgD-rhEBNA1 (group 2)										AdC-gd-NP (group 3)									
	Time after vaccination										Time after vaccination										Time after vaccination									
	NHP ID	Subset	BL	2	4	8	17	19	21		NHP ID	Subset	BL	2	4	8	17	19	21		NHP ID	Subset	BL	2	4	8	17	19	21	
rhEBNA1	RYa6 (B17)	CD4	373	1050	551	654	403	819	1597		RNw9	CD4	479	1116	801	1119	900	n.t.	322		RYc3	CD4	699	—	663	614	n.t.	—	942	
		CD4CM	328	796	450	337	272	649	1527			CD4CM	367	752	572	640	582	n.t.	223			CD4CM	534	—	314	707	n.t.	—	875	
		CD4EM	74	367	97	367	179	148	86			CD4EM	86	372	246	380	309	n.t.	104			CD4EM	48	—	76	58	n.t.	—	90	
		CD4EFF	12	0	0	0	14	0	0			CD4EFF	21	4	9	0	0	0	n.t.	0			CD4EFF	27	—	34	0	n.t.	—	63
		CD4	—	488	198	358	369	353	n.t.			CD4	—	557	—	561	—	—	974	620		RCJ7	CD4	547	776	—	869	—	256	n.t.
		CD4CM	—	261	108	360	358	279	n.t.			CD4CM	—	275	—	396	—	—	0	622			CD4CM	346	569	—	518	—	147	n.t.
		CD4EM	—	167	78	182	70	63	n.t.			CD4EM	—	295	—	43	—	—	0	0			CD4EM	116	118	—	78	—	126	n.t.
		CD4EFF	—	0	92	0	16	11	n.t.			CD4EFF	—	0	—	0	—	—	626	0			CD4EFF	20	6	—	156	—	0	n.t.
		CD4	238	465	404	223	—	267	—			CD4	2190	3446	2527	3654	3844	n.t.	n.t.	n.t.			CD4	1070	1017	1036	n.t.	574	1304	971
		CD4CM	208	304	324	403	—	307	—			CD4CM	1358	1736	1346	2066	2140	n.t.	n.t.	n.t.			CD4CM	447	411	398	n.t.	269	502	459
	CD4EM	78	157	110	80	—	98	—			CD4EM	565	1524	1043	1366	1683	n.t.	n.t.	n.t.			CD4EM	307	522	340	n.t.	200	502	362	
	CD4EFF	0	0	0	0	—	0	—			CD4EFF	50	12	47	65	29	n.t.	n.t.	n.t.			CD4EFF	118	0	31	n.t.	59	46	85	
	CD4	428	713	569	352	n.t.	928	n.t.			CD4	449	1913	2437	675	n.t.	n.t.	n.t.	n.t.			CD4	—	—	—	—	—	—	—	
	CD4CM	272	200	293	475	n.t.	274	n.t.			CD4CM	166	830	778	436	n.t.	n.t.	n.t.	n.t.			CD4CM	—	—	—	—	—	—	—	
	CD4EM	94	365	313	5	n.t.	380	n.t.			CD4EM	238	991	1452	291	n.t.	n.t.	n.t.	n.t.			CD4EM	—	—	—	—	—	—	—	
	CD4EFF	3	0	0	0	n.t.	274	n.t.			CD4EFF	70	59	102	0	n.t.	n.t.	n.t.	n.t.			CD4EFF	—	—	—	—	—	—	—	
	CD4	342	389	621	424	n.t.	n.t.	n.t.			CD4	—	594	680	558	252	n.t.	n.t.	n.t.			CD4	—	—	—	—	—	—	—	
	CD4CM	303	262	333	256	n.t.	n.t.	n.t.			CD4CM	—	374	583	324	129	n.t.	n.t.	n.t.			CD4CM	—	—	—	—	—	—	—	
	CD4EM	17	124	167	84	n.t.	n.t.	n.t.			CD4EM	—	264	107	58	111	n.t.	n.t.	n.t.			CD4EM	—	—	—	—	—	—	—	
	CD4EFF	0	20	0	0	n.t.	n.t.	n.t.			CD4EFF	—	0	16	0	0	n.t.	n.t.	n.t.			CD4EFF	—	—	—	—	—	—	—	
	CD4	248	—	430	544	n.t.	537	n.t.			CD4	591	1459	359	730	1053	191	258			CD4	—	—	—	—	—	—	—		
	CD4CM	223	—	245	336	n.t.	310	n.t.			CD4CM	571	1349	289	908	879	396	176			CD4CM	—	—	—	—	—	—	—		
	CD4EM	100	—	164	0	n.t.	94	n.t.			CD4EM	55	137	115	11	242	0	110			CD4EM	—	—	—	—	—	—	—		
	CD4EFF	0	—	36	0	n.t.	20	n.t.			CD4EFF	15	6	5	0	0	0	0			CD4EFF	—	—	—	—	—	—	—		
rhZLF1	RYa6 (B17)	CD4	929	1048	1046	302	484	239	1266		RNw9	CD4	226	—	245	—	194	n.t.	—		RYc3	CD4	962	—	890	243	n.t.	207	744	
		CD4CM	772	979	956	49	293	183	1210			CD4CM	175	—	245	—	194	n.t.	—			CD4CM	811	—	576	231	n.t.	106	614	
		CD4EM	89	55	25	55	187	53	0			CD4EM	32	7	—	39	n.t.	—	—			CD4EM	24	—	45	0	n.t.	35	167	
		CD4EFF	18	16	0	55	0	0	0			CD4EFF	0	—	20	—	13	n.t.	—	—			CD4EFF	17	—	15	0	n.t.	19	0
		CD4	275	372	—	—	—	315	n.t.			CD4	—	268	—	—	—	—	531			RCJ7	CD4	298	430	591	360	468	n.t.	n.t.
		CD4CM	292	288	—	—	—	310	n.t.			CD4CM	—	223	—	—	—	—	0				CD4CM	268	398	496	360	362	n.t.	n.t.
		CD4EM	30	50	—	—	—	11	n.t.			CD4EM	—	57	—	—	—	—	0				CD4EM	25	16	0	0	18	—	n.t.
		CD4EFF	0	8	—	—	—	0	n.t.			CD4EFF	—	11	—	—	—	—	531				CD4EFF	7	0	0	0	27	—	n.t.
		CD4	291	252	420	—	—	—	—			CD4	369	—	—	421	366	n.t.	n.t.	n.t.			CD4	308	458	494	n.t.	213	286	342
		CD4CM	381	297	506	—	—	—	—			CD4CM	254	—	243	224	n.t.	n.t.	n.t.	n.t.			CD4CM	243	360	291	n.t.	158	169	172
	CD4EM	18	13	18	—	—	—	—			CD4EM	35	—	37	58	n.t.	n.t.	n.t.	n.t.			CD4EM	47	76	45	n.t.	28	35	98	
	CD4EFF	2	0	4	—	—	—	—			CD4EFF	48	—	25	42	n.t.	n.t.	n.t.	n.t.			CD4EFF	27	0	22	n.t.	46	39	35	
	CD4	375	213	824	188	n.t.	281	n.t.			CD4	203	—	1102	367	n.t.	n.t.	n.t.	n.t.			CD4	—	—	—	—	—	—	—	
	CD4CM	198	144	746	235	n.t.	0	n.t.			CD4CM	174	—	540	306	n.t.	n.t.	n.t.	n.t.			CD4CM	—	—	—	—	—	—	—	
	CD4EM	124	56	108	0	n.t.	0	n.t.			CD4EM	22	—	177	0	n.t.	n.t.	n.t.	n.t.			CD4EM	—	—	—	—	—	—	—	
	CD4EFF	13	0	27	47	n.t.	0	n.t.			CD4EFF	12	—	278	61	n.t.	n.t.	n.t.	n.t.			CD4EFF	—	—	—	—	—	—	—	
	CD4	639	—	645	421	n.t.	n.t.	n.t.			CD4	470	553	1120	814	—	n.t.	296				CD4	—	—	—	—	—	—	—	
	CD4CM	374	—	394	228	n.t.	n.t.	n.t.			CD4CM	445	334	1019	678	—	n.t.	210				CD4CM	—	—	—	—	—	—	—	
	CD4EM	68	—	46	70	n.t.	n.t.	n.t.			CD4EM	86	175	39	131	—	n.t.	86				CD4EM	—	—	—	—	—	—	—	
	CD4EFF	46	—	0	35	n.t.	n.t.	n.t.			CD4EFF	37	0	7	0	—	n.t.	0				CD4EFF	—	—	—	—	—	—	—	
	CD4	1206	—	427	544	n.t.	n.t.	n.t.			CD4	1147	906	320	820	582	—	—				CD4	—	—	—	—	—	—	—	
	CD4CM	1113	—	300	362	n.t.	n.t.	n.t.			CD4CM	1045	833	335	1197	544	—	—				CD4CM	—	—	—	—	—	—	—	
	CD4EM	18	—	0	52	n.t.	n.t.	n.t.			CD4EM	61	21	1	0	42	—	—				CD4EM	—	—	—	—	—	—	—	
	CD4EFF	0	—	4	26	n.t.	n.t.	n.t.			CD4EFF	7	12	5	0	0	—	—				CD4EFF	—	—	—	—	—	—	—	

Table 4-2: RHEBNA1-specific (top) and rhZLF1-specific (bottom) CD4⁺ T cell responses are shown at all pre- and post-vaccination time points. Responses are normalized to 10⁶ live CD3⁺ T cells after subtraction of background data for individual animals. —, values below the detection limit (based on rhLCV-seronegative rhesus macaques); data for time points at which the parental CD4⁺ T cell response was below the detection limit are not shown in the table (and were also omitted from the graphs). Peptide-specific vaccine responses greater than 2SDs from the mean baseline are highlighted in grey. BL, baseline; NT, not tested; NHP, non-human primate; ID, identification number.

Table 4-3: Characteristics and responsiveness of rhesus macaques enrolled in this study

Group	NHP ID	Age (yr)	MHC alleles	Response to vaccination	
				CD8 ⁺	CD4 ⁺
Group 1: SgD-rhEBNA1	RYa6	12	A.04, A.25 B.01, B.17	R	R
	PH1019	10	A.08, A.18b B.17, B.83	R	R
	RTn5	15	A.01, A.08 B.12b, B.47	NR	R
	RQt5	13	A.04, A.12 B.43a	NR	R
	RRi9	7	A.03, A.04 B.01, B.12b	NR	R
	RLy9	6	A.04 B.28b, B.47	NR	NR
	RNw9	6	A.04, A.08 B.12b, B.15a	R	R
Group 2: NBEFSgD-rhEBNA1	RZi7	9	A.01, A.07/19 B.17, B.55, B.69a	R	R
	RVw6	10	A.01, A.08 B.01, B.02	R	R
	RTp4	15	A.04 B.12b, B.28b	R	R
	PWw	13	A.02, A.08 B.12b, B.28b	NR	R
	RCv5	13	A.04 B.02, B.12b	NR	R
Group 3: gD-NP	RYc3	19	A.01, A.03 B.12b, B.47	NR	NR
	RCj7	9	A.07, A.224 B.15a, B.23	NR	NR
	RLz5	12	A.04 B.12b, B.69a	NR	NR

Abbreviations: NHP, non-human primate; ID, identification number; MHC, major histocompatibility complex; R, responders; NR, non-responders.

Magnitude and differentiation status of rhLCV-specific CD8⁺ T cells after vaccination

Numbers of rhEBNA1-specific CD8⁺ T cells increased after vaccination. Increases were most pronounced and sustained within the CD8⁺ T_{EM} cell subset, while numbers of rhEBNA1-specific CD8⁺ T_{CM} and CD8⁺ T_{EFF} cells increased only transiently (**Figure 4-2A**). Increases of rhEBNA1-specific T cells as measured by area under the curve (AUC) were significantly larger than the corresponding rhBZLF1-specific responses for overall CD8⁺ T ($P = 0.048$ by Mann-Whitney) and CD8⁺ T_{EM} ($P = 0.039$) cells (**Figure 4-2B**). Increases of rhEBNA1-specific T cells were also significantly larger than those of controls (for overall and T_{EM} cells, $P = 0.048$, 0.024 , respectively). For all vaccine responders, rhEBNA1-specific CD8⁺ T cells increased about 4-fold from baseline, with an average increase of 474 total T cells and 277 T_{EM} cells (6.5-fold change) per 10⁶ live CD3⁺ cells after vaccination. Corresponding rhBZLF1-specific responses and rhEBNA1-specific responses within the control group remained stable or contracted, which indicates that increases in rhEBNA1-specific CD8⁺ T cells were a result of vaccination.

There were no significant differences in rhEBNA1-specific CD8⁺ T cell responses between groups 1 and 2. However, the number of rhEBNA1-specific CD8⁺ T_{EM} cell responses of group 1, but not group 2, increased significantly more after vaccination than the corresponding rhBZLF1 responses ($P = 0.0081$) or rhEBNA1 responses of control animals ($P = 0.012$).

The selective increases of rhEBNA1-specific CD8⁺ T_{EM} cells caused shifts in the proportions of the three CD8⁺ T cell subsets (**Figure 4-3A**), while the proportions of rhBZLF1-specific subsets did not change following vaccination (not shown). At baseline, most rhEBNA1-specific CD8⁺ responses were T_{CM} or T_{EFF} cells. After vaccination, the proportion of rhEBNA1-specific CD8⁺ T_{EM} cells increased to nearly double the proportion at baseline for every time point (**Figure 4-3A**, white bars). This shift, which clearly indicates that vaccination preferentially induced or expanded CD8⁺ T_{EM} cells, became significant by week 8 ($P = 0.035$).

Magnitude and differentiation status of rhLCV-specific CD4⁺ T cells after vaccination

RhEBNA1-specific CD4⁺ T cell responses increased after vaccination. These increases were pronounced within both CD4⁺ T_{CM} and T_{EM} cell subsets, while CD4⁺ effector responses

remained stable (**Figure 4-4A**). Increases of rhEBNA1-specific T cells as measured by AUC were significantly larger than the corresponding rhBZLF1-specific responses for overall CD4⁺ T ($P = 0.0003$), CD4⁺ T_{CM} ($P = 0.0019$), and CD4⁺ T_{EM} ($P = 0.02$) cells (**Figure 4-4B**). Increases of rhEBNA1-specific T cells were also significantly larger than the same responses among animals that received the control vaccine (for overall and T_{CM} cells, $P = 0.02$, 0.039 , respectively). Numbers of rhEBNA1-specific CD4⁺ T cells increased about 3-fold from baseline, with an average increase of 424 total T cells, 212 T_{CM} cells, and 191 T_{EM} cells per 10⁶ live CD3⁺ cells. Corresponding rhBZLF1-specific responses and rhEBNA1-specific responses within the control group remained stable or contracted, therefore indicating that increases in rhEBNA1-specific CD4⁺ T cells were a result of vaccination.

RhEBNA1-specific overall CD4⁺ T cell responses were significantly larger for group 2 responders than for group 1 ($P = 0.0173$, AUC, by the Mann-Whitney test); however, subset responses between the same groups were not significantly different. The number of rhEBNA1-specific T cells within group 2 but not group 1 also increased significantly more after vaccination than corresponding rhBZLF1 responses (for overall, T_{CM}, and T_{EM} cells, $P = 0.002$, 0.0009 , 0.021 , respectively) or rhEBNA1 responses of control animals (for overall, T_{CM}, and T_{EM} cells, $P = 0.024$, 0.047 , 0.038 , respectively). This may suggest that vaccines expressing rhEBNA1 with a non-HVEM-binding version of gD induced more potent CD4⁺ T cell responses than did the SgD-rhEBNA1 vaccines.

The distribution of rhEBNA1-specific CD4⁺ T_{CM} and T_{EM} cell subsets shifted after vaccination (**Figure 4-3B**), while rhBZLF1-specific CD4⁺ T cell subsets remained stable (not shown). The shift in rhEBNA1-specific subset proportions, which was significant at week 2 ($P = 0.045$), was caused by pronounced increases of CD4⁺ T_{EM} cells, which resulted in a relative reduction in the percentage of CD4⁺ T_{CM} cells.

Figure 4-2: Magnitude of peptide-specific CD8⁺ T cell responses upon vaccination

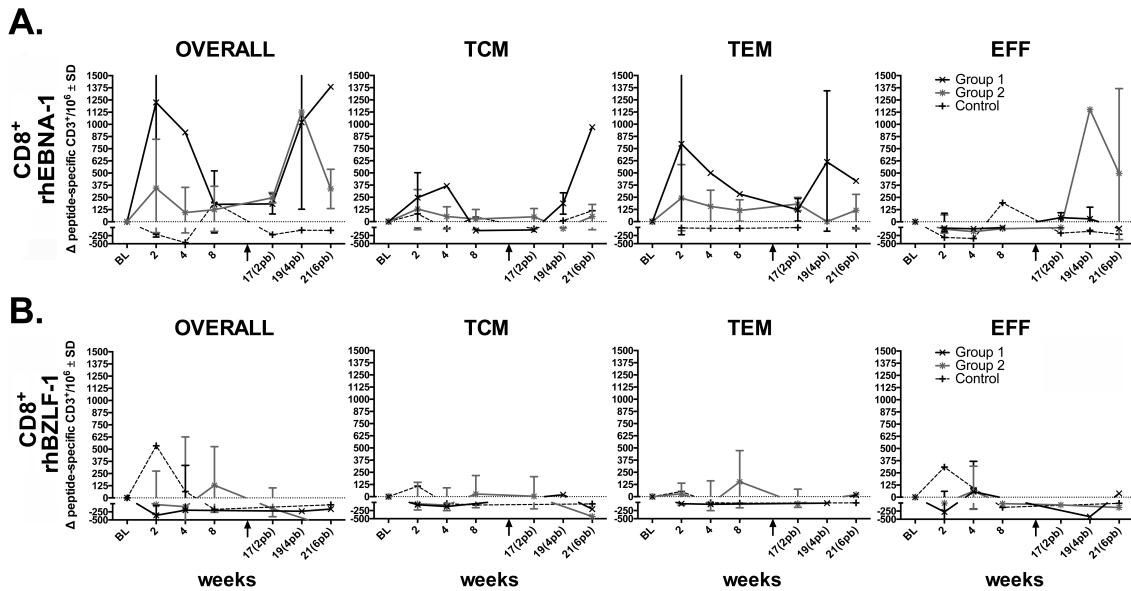


Figure 4-2: PBMCs were stimulated with specific peptide pools and ICS was used to measure production of IFN- γ , IL-2, and TNF- α . Mean counts of rhEBNA1-specific (**A**) and rhBZLF1-specific (**B**) total cytokine-producing CD8⁺ T cells \pm SD are plotted as a change from baseline (BL) for all vaccine responders of groups 1 (X, black line) and 2 (*, grey line) and all animals of group 3 (+, dashed line). Peptide-specific CD8⁺ T cell responses are shown for overall, T_{CM}, T_{EM}, and T_{EFF} subsets (left to right). Raw data were used to calculate changes from baseline, and any values below the limit of detection were excluded from the calculation of the mean. All values are presented as numbers of responding cells per 10⁶ live CD3⁺ cells. To calculate the sum of the peptide-specific response, we subtracted normalized background activity and then summed the 7 possible different combinations of functions. Significant differences were determined by comparing areas under the curve (AUC) and are as follows. For rhEBNA1 versus rhBZLF1 for all vaccine responders, CD8⁺ overall, $P = 0.048$, and T_{EM}, $P = 0.039$. For rhEBNA1 for all vaccine responders versus controls, CD8⁺ overall, $P = 0.048$; T_{EM}, $P = 0.024$. RhEBNA1 CD8⁺ T_{EM} responses were also significant for vaccine responders within group 1 (rhEBNA1 versus rhBZLF1, $P = 0.0081$; rhEBNA1 responders versus controls, $P = 0.012$). P values were calculated using two-sided Mann-Whitney tests (all responders grouped) or ANOVA (comparisons between all three groups), with a P value of <0.05 considered significant.

Figure 4-3: Proportions of peptide-specific CD8⁺ and CD4⁺ T cell subsets upon vaccination

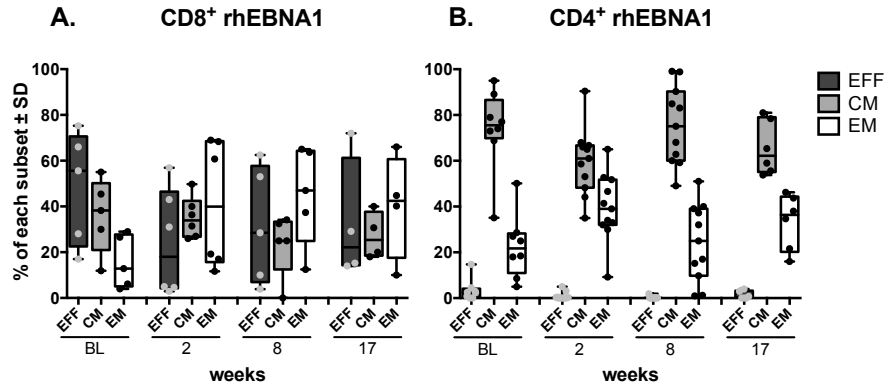


Figure 4-3: The proportions of rhEBNA1-specific CD8⁺ (**A**) and CD4⁺ (**B**) T_{EFF} (dark gray), T_{CM} (light gray), and T_{EM} (white) subsets are shown as a percentage of the total response at baseline and weeks 2, 8, and 17 after vaccination. For each subset, normalized counts were divided by the sum of all three subsets to determine the relative proportions. Results for individual animals are shown as filled circles, and responses for all vaccine responders are displayed as floating bars (5th to 95th percentiles) with lines at the median. Significant differences were determined by comparing the percentage of a given subset after vaccination to the percentage at baseline and are as follows: rhEBNA1-specific CD8⁺ T_{EM} and CD4⁺ T_{EM} cells at week 2, $P = 0.035$ and 0.045 , respectively. P values were calculated using the two-sided Mann-Whitney test, with a P value of <0.05 considered significant.

Figure 4-4: Magnitude of peptide-specific CD4⁺ T cell responses upon vaccination

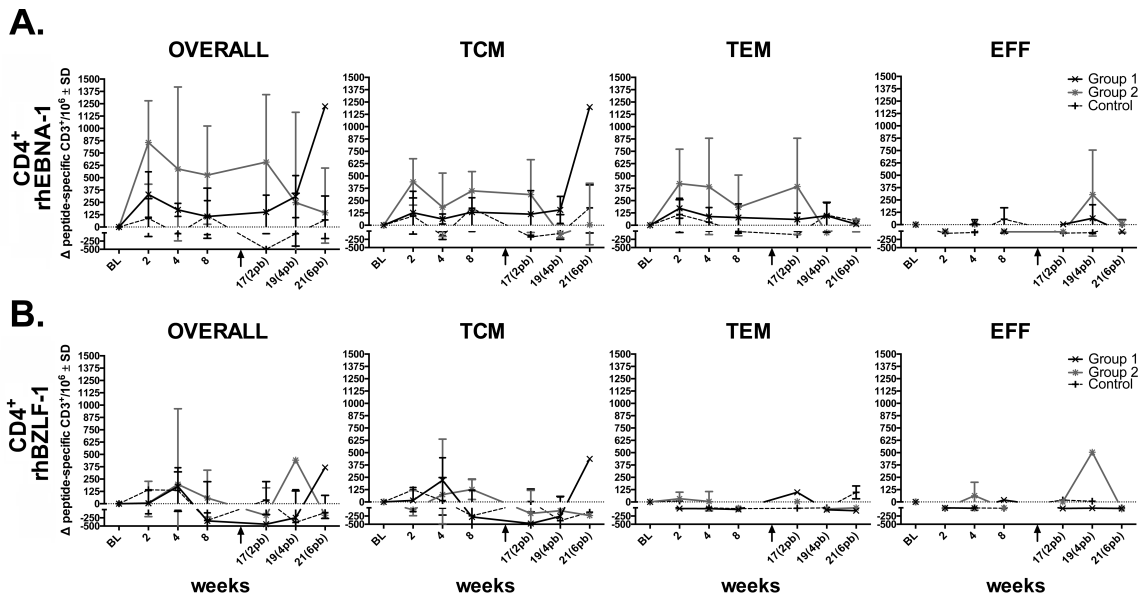


Figure 4-4: Mean counts of rhEBNA1-specific (A) and rhBZLF1-specific (B) total cytokine-producing CD4⁺ T cells \pm SD are plotted as a change from baseline (BL). This figure is organized in the same fashion as Figure 4-2. Significant differences are as follows. For rhEBNA1 versus rhBZLF1 for all vaccine responders, CD4⁺ overall, $P = 0.0003$; T_{CM}, $P = 0.0019$; T_{EM}, $P = 0.02$. For rhEBNA1 for all vaccine responders versus controls, CD4⁺ overall, $P = 0.02$; T_{CM}, $P = 0.039$. RhEBNA1 responses were also significant for vaccine responders within group 2 (for group 2 versus group 1, CD4⁺ overall, $P = 0.0173$; for group 2 rhEBNA1 versus group 2 rhBZLF1, CD4⁺ overall, $P = 0.002$; T_{CM}, $P = 0.0009$; T_{EM}, $P = 0.021$; for group 2 rhEBNA1 versus control rhEBNA1, CD4⁺ overall, $P = 0.024$; T_{CM}, $P = 0.047$; T_{EM}, $P = 0.038$). Responses of rhEBNA1 CD4⁺ T_{EFF} cells were significantly lower than those of both CD4⁺ T_{CM} ($P = 0.0058$) and CD4⁺ T_{EM} ($P = 0.019$) cells. P values were calculated using two-sided Mann-Whitney tests (all responders grouped) or ANOVA (comparisons between all three groups), with a P value of <0.05 considered significant.

Cytokine profile of rhLCV-specific T cells after vaccination

We assessed T cell functions after vaccination using Boolean gating to analyze seven possible different combinations of IFN- γ , IL-2, and TNF- α production²⁵⁷. Cytokine profiles following vaccination were analyzed at weeks 2 and 8 after priming and at week 2 after the boost.

Vaccination caused transient shifts in the cytokine profile of rhEBNA1-specific CD8⁺ T cells (**Figure 4-5A**). At baseline, most rhEBNA1-specific CD8⁺ T cells produced IFN- γ (light blue; EFF, 65%; CM, 25%; EM, 36%) or IL-2 alone (pink; EFF, 26%; CM, 34%; EM, 22%). The percentage of CD8⁺ T_{CM} and T_{EM} cells producing IFN- γ increased significantly by 2 weeks after priming (week 2; CM, 56%, $P = 0.0006$; EM, 71%, $P = 0.0006$) and 2 weeks after boosting (week 17; CM, 59%, $P = 0.0005$; EM, 71%, $P = 0.0018$). The average percentage of CD8⁺ T_{CM} cells producing IL-2 alone, a cytokine generally associated with more resting T cells, significantly decreased at weeks 2 (11%, $P = 0.011$), 8 (10%, $P = 0.0049$), and 17 (11%, $P = 0.02$) after vaccination. In addition, there was a transient increase in the percentage of IFN- γ ⁺ IL-2⁺ CD8⁺ T_{CM} cells at week 8 (BL, 12%; week 8, 45%; $P = 0.012$). As a result, the proportion of polyfunctional CD8⁺ T_{CM} responses increased at week 8. The proportion of cells producing single-, double-, and triple- cytokine responses did not change at any time point for CD8⁺ T_{EFF} or T_{EM} cells. Overall, these results confirm that AdC vectors preferentially expanded rhEBNA1-specific T cell responses that produced IFN- γ , a cytokine with potent anti-viral activity.

As expected, the cytokine profile of rhBZLF1-specific CD8⁺ T cells did not markedly change after vaccination. Most rhBZLF1-specific CD8⁺ T cells produced IFN- γ alone (light blue; EFF, 54%; CM, 47%; EM, 51%) or in combination with IL-2 (yellow; EFF, 11%; CM, 20%; EM, 20%) at baseline and at weeks 2, 8, and 17 after vaccination (**Figure 4-5B**). The only significant change was a decrease in the percentage of IFN- γ ⁺ CD8⁺ T_{EM} cells at week 8 (26%, $P = 0.017$) and therefore a transient decrease in the proportion of single-cytokine-producing cells. This shift was most likely caused by decreases in the magnitude of rhBZLF1 responses after vaccination.

Vaccination increased the absolute numbers of polyfunctional rhEBNA1-specific CD4⁺ T cells without changing the cytokine pattern. RhEBNA1-specific CD4⁺ T cells were highly polyfunctional at baseline and at weeks 2, 8, and 17 after vaccination (**Figure 4-5C**). At each of

these time points, large proportions of cells produced two or three cytokines (baseline CM, 44%; EM, 49%) as well as IFN- γ (CM, 19%; EM, 28%) and IL-2 alone (CM, 25%; EM, 8%). The only significant change after vaccination was an increase in the proportion of IFN- γ ⁺ CD4⁺ T_{EM} cells at week 17 (50%, $P = 0.037$), however, the ratio of triple, double, and single responses did not change. Thus, vaccine-induced CD4⁺ T cell responses remained highly polyfunctional.

Subtle changes in the cytokine profile of rhBZLF1-specific CD4⁺ T cells over time indicate that these cells may have shifted toward a response closer to resting memory. CD8⁺ T_{CM} cells produced mostly IL-2 (pink, 47%) or TNF- α (purple, 18%) at baseline and at weeks 2, 8, and 17 after vaccination (**Figure 4-5D**). However, the proportion of IL-2⁺ CD8⁺ T_{CM} cells increased significantly at week 17 (73%) compared to all other time points before and after vaccination (versus baseline, $P = 0.0047$; versus week 2, $P < 0.0001$; versus week 8, $P = 0.0004$). Additionally, the large proportion of CD8⁺ T_{EM} cells that produced IFN- γ at baseline (30%) and at week 2 after vaccination (27%) decreased significantly by week 8 (8%, $P = 0.0013$). IFN- γ is typically associated with cells that are fully activated, and therefore such decreases further support the notion that rhBZLF1 CD4⁺ T cells were transitioning toward a response closer to resting memory.

Figure 4-5: Cytokine profiles of rhLCV-specific T cells upon vaccination

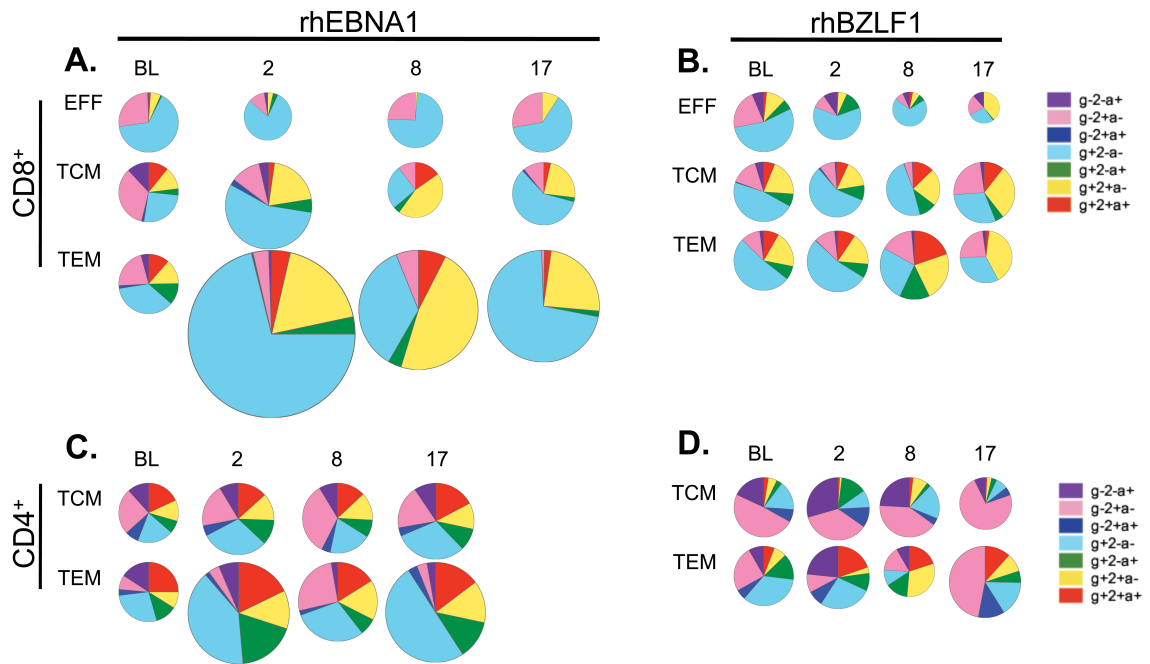


Figure 4-5: Pies represent the average percentage of CD8⁺ and CD4⁺ T cells making each combination of IFN- γ (g), IL-2 (2), and TNF- α (a) following stimulation with specific peptides. RhEBNA1-specific (**A**) and rhBZLF1-specific (**B**) CD8⁺ T_{EFF}, T_{CM}, and T_{EM} responses are shown at baseline and at weeks 2, 8, and 17 after vaccination. The same time points are shown for rhEBNA1-specific (**C**) and rhBZLF1-specific (**D**) CD4⁺ T_{CM}, and T_{EM} responses. Numbers of peptide-specific CD4⁺ T_{EFF} responses were all very low and are therefore not shown. For all responding animals, normalized cell counts were calculated for each function within every subset. Values for each of the seven possible combinations of functions were then divided by the sum of all seven, and pie charts reflect the ratio of those means. Changes in the size of the pie charts reflect proportional changes in the magnitude of total cytokine responses relative to baseline. Significant differences are described in the results section.

Vaccination expands rhEBNA1-specific T cells with cytolytic potential

Target cell lysis is one of the most crucial T cell functions involved in clearing virus-infected cells. While cytokine production provides information on the T cells' functional capacity, it does not directly assess their ability to lyse target cells. We therefore measured production of granzyme B, a lytic enzyme that promotes target cell apoptosis. Granzyme B was measured in CD8⁺ and CD4⁺ T cells for all of the vaccine responders and two animals from the control group using the same methods as those described above. Because granzyme B is stored in cytolytic granules regardless of activation status, peptide-specific responses were considered positive only if granzyme B was produced in combination with one or more cytokines.

We found that vaccine-induced rhEBNA1-specific CD8⁺ T cells produced granzyme B. Although the proportion of granzyme B⁺ CD8⁺ memory T cells was largest at baseline (**Figure 4-6A**), absolute numbers of granzyme B-producing CD8⁺ T cells tended to increase after vaccination. At baseline, most cells produced granzyme B together with TNF- α (purple). After vaccination, there was an increase in the number of cells producing granzyme B with IFN- γ (light blue) (week 2, $P < 0.0001$; week 17/19, $P = 0.05$) and a decrease in the number of cells producing granzyme B with TNF- α (week 8, $P = 0.05$; week 17/19, $P = 0.046$). There was also a transient increase in the number of cells producing all four functions (red), which reached significance at week 8 ($P = 0.048$). Granzyme B-negative responses after vaccination were composed largely of IFN- γ alone, followed by IFN- γ with IL-2 (not shown). In contrast, numbers of rhBZLF1-specific memory CD8⁺ T cells producing granzyme B tended to decrease after vaccination (**Figure 4-6B**). At baseline, the most common cytokines produced with granzyme B were TNF- α followed by IFN- γ . Numbers of granzyme B⁺ TNF- α ⁺ T cells decreased significantly from baseline at week 2 ($P = 0.0003$), week 8 ($P = 0.0021$), and week 17/19 ($P = 0.0003$). As a result, the proportion of rhBZLF1-specific granzyme B⁺ responses decreased significantly at weeks 8 ($P = 0.04$) and 17/19 ($P = 0.003$). Granzyme B-negative responses before and after vaccination were composed largely of IFN- γ alone, followed by relatively equal proportions of T cells that produced all remaining cytokine combinations except IL-2 with TNF- α ; none of which changed after vaccination (not shown).

As expected, the majority of granzyme B⁺ rhEBNA1-specific CD8⁺ T cells were low in CCR7, a homing marker for lymphatic tissues, as is typical for CD8⁺ T_{EM} cells (**Figure 4-7**). Expression of CCR7 on granzyme B⁺ rhEBNA1-specific CD8⁺ T cells was compared to expression of CCR7 on effector CD8⁺ T cells, memory CD8⁺ T cells, and naïve CD8⁺ T cells. As expected, CCR7 expression on effector CD8⁺ T cells (orange) was similar to that on granzyme B⁺ rhEBNA1-specific CD8⁺ T cells, both of which were reduced in comparison to CCR7 expression on CD8⁺ memory (blue) and CD8⁺ naïve (green) T cells.

There were no significant changes in rhEBNA1-specific or rhBZLF1-specific CD8⁺ effector T cell responses after vaccination. RhEBNA1-specific effector T cell responses were all low, and granzyme B⁺ TNF-α⁺ as well as granzyme B⁺ IL-2⁺ were detected most frequently (**Figure 4-6C**). The rhBZLF1-specific CD8⁺ T cell responses detected most frequently with granzyme B were TNF-α or IFN-γ (**Figure 4-6D**). RhBZLF1-specific granzyme B-negative T cell responses were composed largely of IFN-γ alone, and the magnitude of this response decreased at every time point after vaccination (not shown).

Vaccination induced a sustained increase in numbers of rhEBNA1-specific memory CD4⁺ T cells that produced granzyme B—mostly with TNF-α and/or IFN-γ (**Figure 4-6E**). The numbers of granzyme B⁺ IFN-γ⁺ and granzyme B⁺ IFN-γ⁺ TNF-α⁺ memory CD4⁺ T cells increased more than 6 and 10 times from baseline, respectively. Responses were significantly larger than baseline by 2 weeks (B⁺γ⁺, *P* = 0.0025), 8 weeks (B⁺γ⁺α⁺, *P* = 0.0042), and 17/19 weeks (B⁺γ⁺α⁺, *P* = 0.031) after vaccination. Despite these changes, the average proportion of granzyme B⁺ responses did not significantly change from baseline, where more than one-quarter of specific CD4⁺ memory T cells produced granzyme B in combination with other factors. Granzyme B-negative responses were also highly polyfunctional, and there were significant increases in the magnitude of cells producing various cytokine combinations compared to baseline (week 2, γ⁺; week 8, γ⁺2⁺α⁺, γ⁺α⁺, γ⁺; week 17/19, α⁺; *P* < 0.05) (not shown). In contrast, total numbers of granzyme B⁺ rhBZLF1-specific memory CD4⁺ T cells did not change following vaccination (**Figure 4-6F**). At baseline, the most common cytokines produced with granzyme B were TNF-α or IL-2, and there was a significant decrease in the number of rhBZLF1-specific memory CD4⁺ T

cells that produced granzyme B with TNF- α at week 8 ($P = 0.0096$) and week 17/19 ($P = 0.0089$). Most granzyme B-negative CD4⁺ T cell responses were composed of either IFN- γ alone or IL-2 alone, and the number of cells producing IL-2 alone increased significantly at week 17/19 ($P = 0.0001$, data not shown). This decrease in rhBZLF1-specific granzyme B⁺ TNF- α ⁺ CD4⁺ T cells and increase in rhBZLF1-specific IL-2⁺ CD4⁺ T cells further indicates differentiation towards a more resting phenotype. RhLCV-specific cytolytic T cells are crucial for controlling the outgrowth of virus-infected cells^{258, 259}, and we have shown that rhEBNA1-specific T cells expanded through vaccination produce the cytolytic molecule granzyme B.

Figure 4-6: Granzyme B production by rhLCV-specific T cells

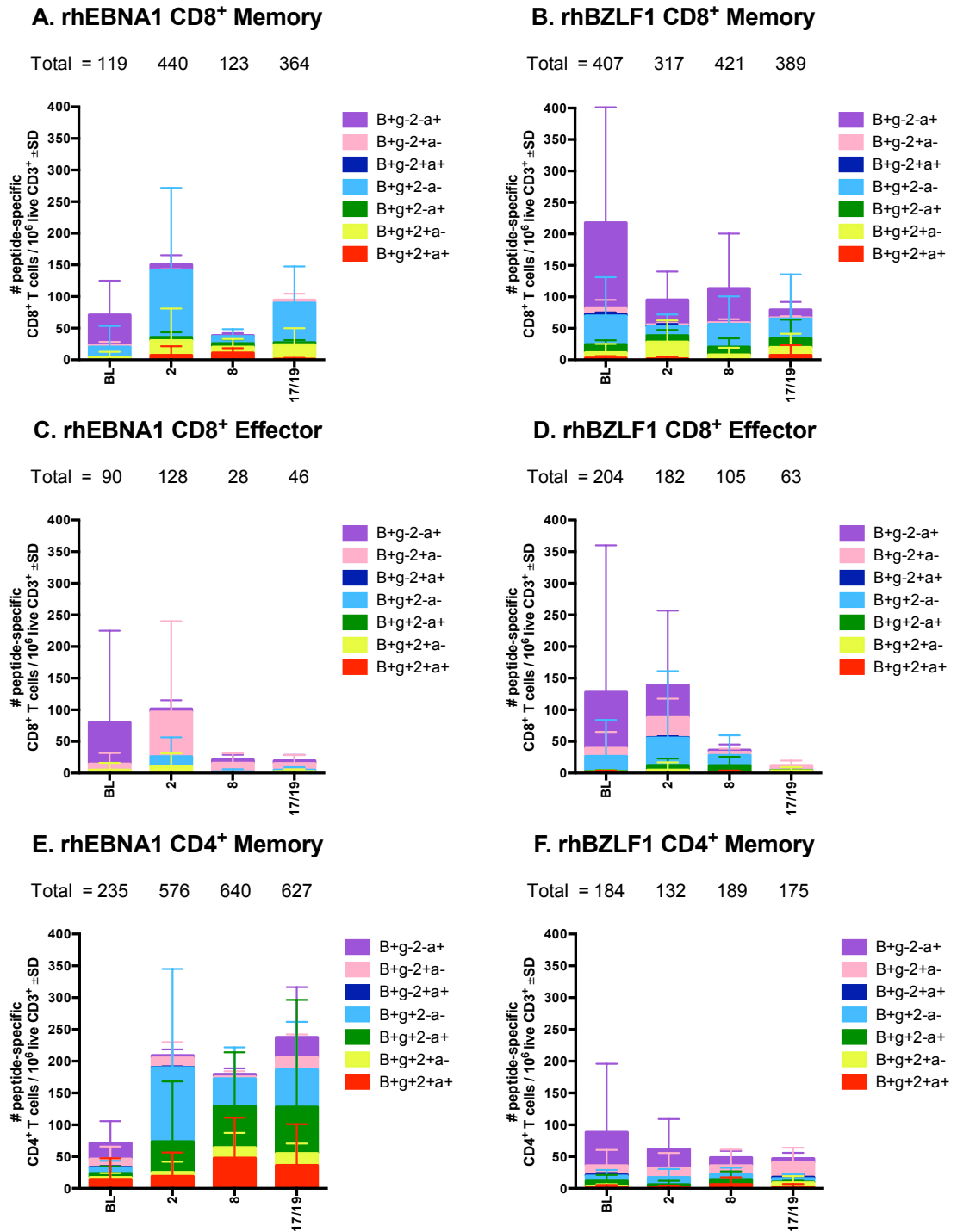


Figure 4-6: Vaccine responders were evaluated for granzyme B-producing T cells. PBMCs were stimulated with overlapping peptide pools, and ICS was used to measure production of granzyme B (denoted B), IFN- γ (g), IL-2 (2), and TNF- α (a). Bars reflect the average magnitudes of granzyme B⁺ T cells producing each combination of cytokines after stimulation with specific peptides. RhEBNA1-specific CD8⁺ memory (A) and effector (C) cell responses as well as rhBZLF1-specific CD8⁺ memory (B) and effector (D) cell responses are shown. RhEBNA1-specific CD4⁺ memory (E) and rhBZLF1-specific CD4⁺ memory (F) cell responses (Continued on page 118)

Figure 4-7: Expression of CCR7 before and after vaccination

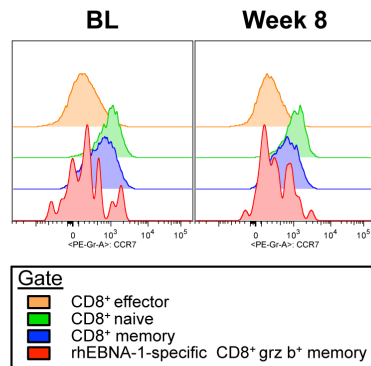


Figure 4-7: CCR7 expression by rhEBNA1-specific memory CD8⁺ T cells that produce granzyme B with all combinations of cytokines (red) is shown in comparison to total non-specific memory (blue), naïve (green), and effector (orange) populations. Responses are shown at baseline and week 8 for one representative vaccine responder. Responses at weeks 2 and 17/19 were the same as week 8 and are therefore not shown. Significant differences are described in the results section.

(Continued from page 117)

are also shown. The total sums of all peptide-specific cytokine responses at each time point are listed above the bars. Total values reflect the sum of every combination of the four functions tested; cells that produced only granzyme B were excluded. Responses are shown at baseline (BL) and at weeks 2, 8, and 17/19 after vaccination. All responses were normalized and background values were subtracted. Significant differences are described in the results section.

DISCUSSION

The development of a vaccine to prevent EBV infection or treat EBV-associated diseases is of high priority¹⁰⁴, but therapeutic vaccines that aim to expand ongoing immune responses to persisting viruses like EBV face a unique set of challenges. Neutralizing antibodies are generally ill suited to clear cells that have already been infected, and T cells may be difficult to expand if recurrent antigen exposure by viral reactivations has caused terminal differentiation and functional T cell impairments²⁶⁰. EBNA1 is an important target for immune responses that aim to reduce EBV reservoirs in latently infected cells because it is the only antigen synthesized during all stages of latency and in all EBV-associated malignancies. Despite its importance, the ability to boost rhEBNA1-specific T cell responses in rhesus macaques has never been tested. In this proof-of-concept study, we are the first to report that ongoing rhEBNA1-specific T cell responses during persistent rhLCV infection in rhesus macaques can be expanded upon vaccination.

We tested two prime-boost vaccine regimens based on replication-defective AdC vectors that express rhEBNA1. Vaccines expressed a GAR-deleted form of rhEBNA1 fused to HSV-gD to potentially further promote T cell recall responses. The N-terminus of HSV-gD binds to the bimodal HVEM²⁴⁹ and prevents inhibitory molecules like BTLA from binding and signaling during T cell activation²⁵⁰. To control for this effect, an HVEM-non-binding version of HSV-gD was also tested. Animals were distributed as evenly as possible between vaccine groups based on age, Mamu phenotype, and rhLCV-specific T cell responses. Because T cells to persisting viruses tend to fluctuate in response to reactivations, we enumerated and characterized rhEBNA1- and rhBZLF1-specific T cell responses at two time points prior to vaccination²⁵⁷ and set stringent criteria to assess if vaccination expanded rhEBNA1-specific T cells. We found that vaccination increased numbers of circulating rhEBNA1-specific CD8⁺ and CD4⁺ T cells regardless of gD binding ability and that booster immunization was relatively ineffective. Vaccination augmented mainly CD8⁺ T_{EM}, CD4⁺ T_{CM}, and CD4⁺ T_{EM} cells. Responses were highly functional, and T cells produced various combinations of the cytokines IFN- γ , IL-2, and TNF- α and the cytolytic molecule

granzyme B. Furthermore, responses were vaccine-specific, as T cell responses to the lytic antigen rhBZLF1 did not increase following vaccination.

The ability to increase both CD8⁺ and CD4⁺ T cell responses through vaccination was an important finding of this study. While CD8⁺ T cells can eliminate virus-infected cells, CD4⁺ T cells can also target virus that persists in MHC class II⁺ cells. RhLCV-infected B cells and also some EBV-associated malignancies express both MHC class I and II²⁶¹, and EBNA1-specific CD8⁺ and CD4⁺ T cells are both capable of lysing target cells *in vitro*^{199, 209}. Vaccination expanded specific CD8⁺ T cell responses in 2/6 animals from group 1 and 4/6 animals from group 2. Two of the vaccine responders from group 2 (RVw6, RTp4) developed significant changes within T cell subsets (EM and CM, respectively) without changes in total numbers. This indicates a vaccine-specific effect on the phenotype of rhEBNA1-specific T cells. One animal (RZi7) developed a response after vaccination that was not detected at baseline, which indicates that vaccination may have induced new responses, although it is also possible that vaccination increased the magnitude of ongoing responses from below to above our limit of detection in this animal. Interestingly, the Mamu genotype may have influenced responsiveness, as all three of the Mamu B*17⁺ animals developed vaccine-specific CD8⁺ T cell responses. In comparison, a larger number of animals (11/12) developed specific CD4⁺ T cell responses to vaccination, including all three that did not have detectable rhEBNA1-specific CD4⁺ T cells at baseline. About one-half of the vaccine responders from each group (group 1, 3/5; group 2, 3/6) developed significant changes within T cell subsets without changes in total numbers. It is perhaps not surprising that vaccination stimulated more CD4⁺ versus CD8⁺ T cell responses, as EBNA1-specific CD4⁺ T cell epitopes are more immunodominant in both humans^{1, 67} and in rhesus macaques²⁵⁷.

RhLCV-specific cytolytic T cells are crucial for controlling the outgrowth of virus-infected cells^{93, 258, 259}, and utilization of the perforin/granzyme pathway is largely dependent on T cell specificity^{262, 263}. Importantly, we found that numbers of rhEBNA1-specific CD8⁺ T cells producing granzyme B increased after vaccination. We also found large and sustained increases in numbers of granzyme B-producing CD4⁺ T cells. By just 2 weeks after vaccination, numbers of specific CD8⁺ and CD4⁺ T cells producing granzyme B had increased about 3 times over baseline

levels. Most granzyme B was produced in combination with IFN- γ and/or TNF- α , which is typical for cytolytic T_{EFF}/T_{EM} cells. While *in vitro* killing assays would have provided the most direct functional analysis, granzyme B expression by flow cytometry serves as a surrogate assay that provides a more quantitative assessment of numbers of potentially lytic cells. Our findings suggest that both CD8⁺ and CD4⁺ rhEBNA1-specific T cells may participate in the elimination of rhLCV-infected cells.

It is also interesting that numbers of granzyme B⁺ rhBZLF1-specific T cells decreased after vaccination. Within the same population, numbers of TNF- α ⁺ cells decreased and IL-2⁺ cells increased. Together, this indicates that rhBZLF1-specific T cells were differentiating towards a more resting phenotype. Such differentiation could reflect a vaccine-induced reduction in rhLCV reactivation events. It would have been of interest to measure rhLCV loads before and after vaccination, as this would have provided the most direct evidence of vaccine efficacy or lack thereof. Only 1 in 10⁵ to 10⁶ peripheral B cells carries EBV in healthy subjects^{264, 265}. Because the viral genome is present at such low levels, it is difficult to detect viral load fluctuations in live animal studies, in which peripheral blood samples are limited.

We were intrigued to find that differences in immune responses between animals vaccinated with either rhEBNA1 vaccine regimen were too subtle to clearly demonstrate an effect of HSV-gD. This is because we have previously shown that expression of antigen within HSV-gD augments primary antigen-specific CD8⁺ T cell responses in mice, and such responses were larger than with antigen alone or when expressed within a non-binding HSV-gD²⁴⁷. This study was the first to test the same approach for the expansion of ongoing T cell responses during a persistent viral infection in rhesus macaques. While differences in T cell responses to rhEBNA1 expressed within the binding (group 1) or non-binding (group 2) version of gD were not significant, it is interesting that only animals who received the vaccine with binding gD developed increased CD8⁺ T_{EM} cell responses that were significantly larger than corresponding rhBZLF1 responses as well as rhEBNA1-specific responses of control animals. The opposite was found for CD4⁺ responses, whereby only animals that received the non-binding version of gD developed significant increases in T_{CM} and T_{EM} cell responses.

To determine if additional factors influenced whether or not an animal responded to vaccination, we compared baseline immune responses between responders and non-responders. Total numbers of rhEBNA1-specific CD8⁺ or CD4⁺ T cells were largely comparable at baseline (data not shown), so it is unlikely that differences in pre-vaccination T cell responses influenced whether or not an animal responded. In terms of cytokine production, vaccine responders tended to have a higher proportion of polyfunctional rhEBNA1-specific CD8⁺ T_{CM} cells at baseline than did non-responders (data not shown, $P = 0.048$), which could suggest a higher proliferative capacity of polyfunctional T cells than of those with a more restricted functional profile.

To determine whether vaccination with AdC-SgD-rhEBNA1 or AdC-NBEFSgD-rhEBNA1 augmented pre-existing or *de-novo* responses, our collaborators generated T cell lines with overlapping rhEBNA1 peptides and then measured IFN- γ production by ELISPOT after re-stimulating cells with pools, subpools, or single peptides derived from rhEBNA1²⁶⁶. They found that vaccination expanded new and existing responses. They detected responses in 4 of 12 animals before vaccination and in 8 of 12 animals after vaccination. All of the responses detected prior to vaccination were still detected after vaccination, but at much higher levels, and one animal also developed a new response. Vaccination stimulated *de-novo* CD4⁺ or CD8⁺ T cell responses in four additional animals. Again, it is difficult to interpret trends due to the small number of animals in each group. Fewer animals were described as vaccine responders using this approach compared to ICS, which highlights the importance of choosing appropriate assays to study different aspects of the immune response. IFN- γ ELISPOT is an invaluable tool for defining epitope-specific responses, but it does not account for additional cytokines or cytolytic molecules that are produced in response to vaccination. Furthermore, extended stimulation can change T cell functions and deplete T cells to sub-dominant epitopes.

A previous study explored the feasibility of EBNA1-specific immunotherapy for treatment of EBV-associated cancer²⁶⁷. In this study, an Ad-based vaccine expressing a GAR-depleted sequence of EBNA1 fused to epitopes of latent membrane protein (LMP) of EBV was tested for *in vitro* expansion of T cells obtained from patients with EBV-associated recurrent metastatic nasopharyngeal carcinoma. More than one-half of the T cell lines contained EBNA1-specific CD8⁺

T cells following *in vitro* expansion, demonstrating that humans develop EBNA1-specific CD8⁺ T cells, which can be expanded upon further antigenic stimulation. While adoptive transfer of *ex vivo*-expanded EBV-specific T cells has resulted in sustained clinical responses in some patients²⁶⁸, adoptive immunotherapy is costly, requires access to highly specialized health care facilities, and is therefore an impractical solution for the thousands of patients diagnosed annually with EBV-associated diseases. Another study showed that EBNA1-specific CD8⁺ T cells could be isolated from healthy human adults as well as from patients with post-transplantation lymphoproliferative disease²⁶⁹. These results are in agreement with our studies, which showed not only that rhLCV-infected rhesus macaques mount an rhEBNA1-specific CD8⁺ T cell response upon natural infection, but also that these CD8⁺ T cells can be expanded *in vivo* upon vaccination. Responses were sufficiently robust to allow for their detection directly *ex vivo* without further expansion through extended *in vitro* culture.

Our study is the first to assess rhEBNA1-based vaccines in seropositive non-human primates. We showed that rhEBNA1-specific T cells can be expanded through vaccination and also that these T cells are highly functional. The main limitation of the vaccines was that only one-half of the animals showed increases in CD8⁺ T cell responses, and responsiveness appeared to be influenced by the Mamu genotype. This suggests that the numbers of potentially MHC class I-binding epitopes are limited within rhEBNA1²⁶⁶. Our stringent criteria for responsiveness, which stipulated that T cell counts had to increase significantly over baseline at three of the tested time points, combined with the limited numbers of animals, may have prevented us from identifying weak responders.

In summary, the results presented here confirm that rhEBNA1 is a valid target for a T cell vaccine to rhLCV. Vaccination led to the expansion of rhEBNA1 immune cells that exhibited functions fit for controlling viral infection. Future studies should aim at generating more robust rhEBNA1-specific T cell responses through modified vaccines. It would be of interest to monitor the effect of vaccination on viral load or on the frequency of virus-infected cells as a potential readout for a positive vaccine response²⁶⁴. Additional testing of modified vaccines in rhLCV-

seropositive and -seronegative rhesus macaques is also warranted to further explore rhEBNA1-based vaccines for prevention and treatment of EBV-associated diseases.

CHAPTER 5: DISCUSSION

SIGNIFICANCE

EBV was the first human tumor-associated virus to be discovered. This common human pathogen infects more than 95% of the human adult population worldwide and establishes a persistent infection through latency in B cells. Although EBV infection is typically benign and is well controlled by the host adaptive immune system, it can sometimes cause chronic disease and malignant transformation. Thus, EBV is considered a carcinogen due to its strong association with various lymphoid and epithelial cell malignancies. Despite the large range of EBV-associated diseases, neither prophylactic vaccines that block primary EBV infection nor therapeutic vaccines that eliminate virus-positive lesions are currently available.

EBV's ability to enter latency and avoid recognition by host immune cells is one of the factors that makes designing an effective vaccine quite challenging, as it is unclear exactly what type of immunity would provide the best protection against primary infection, IM, and associated malignancies. Because a different repertoire of genes is expressed during EBV's lytic and latent phases, the selection of appropriate vaccine targets is contingent on a thorough understanding of EBV, its life cycle, and associated pathogenesis. Considerable progress has been made towards reaching such goals, beginning with an improved understanding of EBV biology and associated diseases. The development of a successful vaccine largely depends on this knowledge.

EBV vaccines could be used to prevent infection, modify infection and reduce disease, prevent disease, or treat disease. Most preventative vaccine efforts focus on decreasing acquisition or reducing the burden of IM through neutralizing antibodies or T cells. It has been speculated that by re-defining virus-specific immune responses, vaccines that reduce the incidence of IM may ultimately reduce the rate of some EBV-associated malignancies. In the only phase II trial of an EBV vaccine, the rate of IM but not the rate of acquisition was reduced in

healthy seronegative subjects who received soluble gp350 plus adjuvant²⁷⁰. Similar findings resulted from a peptide vaccine corresponding to EBV latency proteins¹⁸¹, which highlights the importance of T cells for controlling infection. Therapeutic EBV vaccines aim to prevent or treat EBV-associated malignancies by correcting for the selective loss of EBV-specific T cells, which can target tumor cells and prevent or delay tumor progression. For this approach to be effective, tumor cells must maintain viable antigen processing and presentation. The success of passive immunization by adoptive transfer of EBV-specific T cells to treat PTLD highlights the importance of this concept, as PTLD lesions maintain normal antigen processing and presentation. However, the same approach has been less successful as treatment for NPC, BL, and HL, where antigen expression is more restricted and local tumor environments differ²⁷¹. The infusion of epitope-specific CTLs is one method for overcoming restricted antigen expression, and this has demonstrated promising results, even following immunosuppressive treatments^{136, 268, 272}. Antigen-loaded DCs have also been tested, and have shown mixed results in the clinic^{200, 201, 273}. A therapeutic EBV vaccine could similarly be used to restore or enhance EBV-specific T cell-mediated immunity directly *in vivo*. The impact of such a vaccine could be staggering, as vaccines are more accessible and less costly than adoptive transfer techniques.

EBNA1 is the only EBV antigen consistently expressed in all forms of latency and in all known EBV-associated malignancies, and it is therefore an attractive target for vaccine development. However, EBNA1 has only recently begun to be viewed as an appropriate vaccine antigen. It was originally believed that EBNA1-specific CTL responses were either non-existent or non-functional due to an internal repeat domain that had been shown to interfere with antigen presentation by MHC class I molecules¹⁹⁴⁻¹⁹⁶. It has since been shown that functional EBNA1-specific T cells are frequently detected in EBV-infected humans^{197, 198}, and a loss of EBNA1-specific CD4⁺ and/or CD8⁺ T cells has been correlated with numerous EBV-associated diseases, including HL, NPC, and BL^{62, 132-134}. These findings suggest that immune responses to EBNA1 play an important role in controlling EBV infection. In support of its potential as a vaccine target, EBNA1 and other sub-dominant latent EBV T cell responses from both healthy and EBV-positive tumor-bearing individuals have been recovered *ex vivo*^{182, 184, 269}. The overarching goal

throughout this dissertation was to determine if EBNA1 is a suitable target for vaccine development.

SUMMARY AND CONCLUSIONS

An improved understanding of EBNA1 T cell responses will benefit the preclinical development of EBV vaccines. Herpesviruses generally drive T cell differentiation towards highly activated effector-like cells rather than towards exhaustion, but this is highly variable and depends on the quantity, location, and duration of a specific antigen^{274, 275}. Using the EBV homolog rhLCV, I characterized T cell responses to rhEBNA1 in naturally infected rhesus macaques to determine the effect of low-level, persistent antigen on the magnitude, phenotype, and function of rhEBNA1-specific T cells. These studies also served to evaluate the capacity of rhEBNA1-specific T cells to respond to vaccination, as T cells affected by persistent antigen exposure may be difficult to expand, T_{CM} cell pools are often depleted, and T_{EFF}/T_{EM} cells do not function optimally²⁷⁶⁻²⁷⁸. In Chapter 2, we used ICS and flow cytometry to measure rhEBNA1-specific responses directly *ex vivo*, which allowed us to quantitate responses and to directly analyze their functional nature without expansion. In contrast, methods frequently used to study EBV-specific T cell responses utilize EBV-specific T cell lines expanded *in vitro* after repetitive antigenic stimulation, which can change T cell function and lead to selective proliferation of specific clones.

By comparing our results to studies conducted in humans, we demonstrated that the rhLCV animal model faithfully reproduces EBNA1-specific T cell responses and provides a powerful tool for preclinical vaccine studies. Despite the small sample size of 15 animals, rhEBNA1-specific T cells were detected at a frequency of 93%, which is strikingly similar to the global seroprevalence of EBV. Furthermore, trends in the magnitudes of these responses are also similar to what has been observed in humans; numbers of rhEBNA1-specific CD4⁺ T cells were larger than CD8⁺ T cells, and the opposite was observed for rhBZLF1. The relatively equal proportions of rhEBNA1-specific CD4⁺ T_{CM} and T_{EM} cells that we detected could be due to low-

level expression of rhEBNA1 during latent rhLCV infection, since persistent antigen promotes the differentiation of T_{EM} and T_{EFF} cells. RhEBNA1-specific $CD4^+$ T cell responses were also highly functional and produced IFN- γ , IL-2, and TNF- α in various combinations. This indicates that cells are not under constant TCR stimulation. Their ability to produce IL-2, which stimulates cell growth, survival, and proliferation and is a function lost during early stages of exhaustion, may indicate that rhEBNA1-specific $CD4^+$ T cells maintain a proliferative capacity. However, proliferation assays would be needed to test this hypothesis. On the other hand, rhEBNA1-specific $CD8^+$ T cells were primarily IFN- γ -producing effector cells that expressed low levels of the inhibitory molecule PD-1. Cell surface expression of PD-1 is a measure of T cell activation. High levels of PD-1 expression coupled with low functional capacity indicate T cell exhaustion and are consistently correlated to poor proliferation and increased sensitivity to apoptosis. Thus, while the majority of rhEBNA1-specific $CD8^+$ T cells displayed an effector phenotype, rhEBNA1-specific $CD8^+$ T cells were not persistently activated. Interestingly, PD-1 expression was higher on rhEBNA1-specific $CD4^+$ memory T cells, which indicates that these T cells probably see antigen more often. Since rhBZLF1 is only expressed during lytic replication, rhBZLF1-specific T cells exhibited characteristics that more closely resembled responses to an acute infection with occasional re-exposure, as expected. RhBZLF1-specific $CD4^+$ T cells maintained a resting phenotype of central memory and primarily produced single-cytokine responses. As with rhEBNA1, the $CD8^+$ T cell response against rhBZLF1 was more activated than the $CD4^+$ T cell response, but contained a large proportion of memory cells as well.

The presence of rhEBNA1-specific T_{CM} cells with the capacity for expansion of more activated subsets indicates the potential to successfully target and expand rhEBNA1-specific T cells by vaccination. Evidence of their capacity to expand and contract was described in the first part of Chapter 2, where initially large numbers of rhEBNA1-specific T_{EFF}/T_{EM} cells decreased and stabilized over time. We speculated that rhLCV reactivation could have caused the initial peaks in T cell numbers. Data on viral loads might have allowed us to draw more solid conclusions, although peak viral loads probably occurred prior to our first time point. It is also possible that the initial large numbers of rhEBNA1-specific T cells were caused by cross-reactivity or general

inflammation in animals with ongoing unrelated infections. Unfortunately, these studies were conducted prior to our acquisition of the rhBZLF1 peptide pool, which would have provided further insight into whether rhLCV had reactivated in some animals. Data from these early time points were not used to characterize responses.

In Chapters 3 and 4, we designed and tested novel AdC-based prototype vaccines that target rhEBNA1. To be effective, such a vaccine needs to elicit both protective CTL responses as well as a strong central memory component. Ad vectors have been shown to induce potent, multi-specific, and sustained transgene product-specific T cell responses, which is important for targeting cells already infected with virus. Animals received AdC68-prime followed by AdC6-booster vaccines that expressed rhEBNA1 fused to functional (group 1) and non-functional (group 2) versions of HSV-gD. HVEM-binding forms of HSV-gD have been shown to enhance transgene product-specific CD8⁺ T cell responses during vaccination by inhibiting the HVEM-BTLA immune inhibitory signaling pathway. To facilitate antigen processing, we also removed the GAR domain from the coding sequence of rhEBNA1. Using ICS and flow cytometry, we conducted in-depth analyses to examine the effect of vaccination on T cell phenotype and function.

Our study is the first to assess rhEBNA1-based vaccines in a seropositive non-human primate study, where we show that highly functional rhEBNA1-specific CD8⁺ and CD4⁺ T cells can be expanded *in vivo* through vaccination. The results presented in Chapter 4 confirm that rhEBNA1 is a valid target for a therapeutic T cell vaccine to rhLCV, as vaccination led to the expansion of rhEBNA1 immune cells that exhibited functions fit for controlling viral infection.

To avoid misinterpreting viral reactivation or general immune fluctuations as vaccine responses, we set stringent criteria to define vaccine-driven responses. While this may have ultimately excluded animals with weaker responses to vaccination, total CD8⁺ and CD4⁺ T cells increased in 33% and 83% of vaccinated animals, respectively. Two additional animals from group 2 developed increases in CD8⁺ T_{CM} or T_{EM} cells and one animal from group 1 developed an increase in CD4⁺ T_{EM} cells without any changes in total numbers. This indicates vaccine-induced shifts in cell phenotypes. The ability to expand both CD8⁺ and CD4⁺ T cell responses through vaccination was an important finding of this study, since both T cell subtypes can target and lyse

EBV-infected cells^{199, 209}. It is perhaps not surprising that vaccination stimulated higher CD4⁺ than CD8⁺ T cell responses, as EBNA1-specific CD4⁺ T cell epitopes are more immunodominant in both humans^{1, 67} and in rhesus macaques²⁵⁷. Vaccination augmented mainly CD8⁺ T_{EM}, CD4⁺ T_{CM}, and CD4⁺ T_{EM} cells. Responses were highly functional, and T cells produced various combinations of the cytokines IFN- γ , IL-2, and TNF- α and the lytic enzyme granzyme B, which is important for controlling outgrowth of virus-infected cells.

This was the first study to utilize the immune-stimulating effect of HSV-gD to expand ongoing T cell responses in non-human primates. We were intrigued to find that vaccine-driven immune responses were similar regardless of gD binding ability, since our laboratory has consistently shown that vaccines that express antigens as fusion proteins with HSV-gD elicit more potent T cell responses compared to vaccines that express antigens alone. HSV-gD has also displayed an adjuvant-like effect under conditions of T cell stress in tumor-bearing²⁴⁷ and aged²⁷⁹ mice. However, these experiments utilized the HSV-gD adjuvant effect during priming of T cell responses. In contrast, our results indicate that blockade of the HVEM signaling pathway fails to augment T cell expansion of previously primed, ongoing responses. Alternatively, the small sample size of each vaccine group (n = 6) may not have provided enough power to assess significant differences between groups. There were some intriguing differences in post-vaccination frequencies of rhBZLF1-specific T cells, which contracted more in animals that received functional versions of HSV-gD. This could potentially reflect a reduction in viral load, which in turn would suggest functionally superior T cell responses. Additional studies that include measurements of viral loads before and after vaccination would be needed to confirm or reject this hypothesis.

Expression of gD-rhEBNA1 fusion proteins *in vitro* was more than 100-fold lower than rhEBNA1 alone. Since antigenic load influences the immune response, our recombinant Ad-based vaccine that expressed rhEBNA1 alone was not an appropriate control for the Ad-gDrhEBNA1 vaccine. Instead, we chose to compare binding and non-binding versions of HSV-gD. It would be interesting to test the Ad-rhEBNA1 vaccine in the presence or absence of additional adjuvants to determine if higher levels of rhEBNA1 transgene expression generate higher responses or responses in a larger number of animals.

Another unexpected outcome was that peak responses occurred after the first vaccination, rather than after boosting. However, the peak immune response after boosting typically occurs faster than after priming, and we waited the same length of time (2 weeks) to collect blood after each administration. Thus, responses may have peaked before they were measured. Furthermore, numbers of rhEBNA1-specific T cells after 21 weeks were still larger than at baseline in many animals. There were also significant increases in PD-1 expression by week 2 after vaccination, which slowly declined by week 8 and were maintained at a similar percentage through conclusion of the study (data not shown). The percentage of PD-1-expressing cells at these later points in time still appeared higher than at baseline, although differences did not reach significance. Finally, the reduced proliferative capacity of T_{EM} cells compared to T_{CM} cells could be another factor that contributed to the low response following the second vaccination, as T_{EM} cell responses were still relatively high shortly before boosting.

It is important to note that our studies only assessed responses in peripheral blood, but activated T cells can also reside in the lymph nodes, the spleen, or in the periphery. This is especially true at locations where tissues express cognate antigen. As a result, there may have been a more definitive effect of HSV-gD that was not detected by our employed assays. This could also explain the lack of a significant increase following boost, as T cells may have already been mobilized from the circulation. Animals were released back to YNPC upon completion of the study and necropsies were therefore not an option. This is definitely something that is important to consider when designing future studies.

FUTURE DIRECTIONS

Ad vectors are capable of stimulating both CD4⁺ and CD8⁺ T cell responses, and their inherent immunogenicity has the potential to elicit strong responses, but overall there is still a need for more effective strategies that induce larger and more sustained responses. Future studies should aim at generating more robust T cell responses through modified vaccines. This can be accomplished through epitope vaccines that expand T cell responses against sub-

dominant EBV T cell epitopes. However, because epitope recognition depends on MHC genotype, this approach is challenging for human vaccines that aim to target large populations. Cytokines and signaling molecules can also be used to help shape and promote immune cell responses. Vaccines can be designed to encode growth factors such as IL-2 and GM-CSF. They can also be administered in the presence of cytokines such as IL-7, IL-10, and IL-21, which have been shown to promote large central memory responses in some studies²⁸⁰. Chemotherapeutic agents that effect signaling pathways during cell differentiation can be used in a similar manner²⁸¹.

Alternative antigen delivery systems for use in heterologous prime-boost regimens can also be explored as a means of inducing larger and/or more sustained responses. For example, a CMV-based SIV vaccine has been shown to induce potent, sustained, and broad T_{EM} cell responses that were able to suppress SIV viral loads to undetectable levels in 50% of rhesus macaques after challenge²⁸². It is noteworthy that CMV-vaccinated animals with SIV breakthrough infections did not achieve a lowering of viral loads, which presumably reflects that CMV-based vaccines fail to induce T_{CM} cells, which have a higher proliferative capacity than T_{EM} cells. Among animals unable to rapidly control viral load, those that were boosted with an Ad-based vaccine had significantly reduced peak viremia, which was most likely due to SIV-specific T_{CM} cell responses induced by the Ad-based vaccines. A similar approach may be best suited to prevent EBV acquisition. In a therapeutic context, the strong T_{EM} cell responses induced by a CMV-based vaccine could potentially be used to clear EBV viral reservoirs by inducing latent virus reactivation after vaccination. This could be used as a preventative measure to eliminate virus-infected cells among individuals at high risk of developing EBV-associated malignancies. Ad-prime followed by poxvirus-based boost is another approach to explore, since pox vectors have been shown to act as potent boosts in NHPs and humans²⁸³.

Additional factors to consider when designing vaccines to treat or prevent EBV-associated malignancies are deficiencies within the tumor site itself. For example, local immune suppression in the tumor tissue may dampen the outcome of a therapeutic EBV vaccine, and we may need to develop approaches that can overcome this. As one example, anti-PD-1 or anti-

CTLA-4 treatment can sometimes be used to overcome local immune suppression for tumors that express relevant ligands.

Optimal EBV vaccine targets are still unknown, and the continued testing of candidate vaccines is fundamental for advancing the field. The ideal formulation is still unclear and may depend on the desired application. One method for increasing overall vaccine effectiveness is to include epitopes from additional EBV latency proteins such as LMP1 and/or LMP2, which are expressed by tumors such as NPC, GC, and HL. Although neither LMP1 nor LMP2 are dominant targets during natural infection, they contain subdominant CD8⁺ T cell epitopes, and studies suggest that vaccinating against these responses may have clinical benefit. For example, an Ad-based vaccine expressing random overlapping peptides from EBNA1, LMP1, and LMP2 stimulated epitope-specific responses that inhibited LCL outgrowth in cell lines generated from both healthy EBV seropositive individuals as well as NPC patients¹⁸⁴. This indicates that infected cells in diseases such as NPC may be accessible targets for activated EBV-specific T cells. Hui et al. expanded upon this concept and designed a recombinant modified vaccinia Ankara (MVA) vaccine that expressed portions of EBNA1 and LMP2. The objective of this phase I study was to measure safety and immunogenicity and not to test clinical effect, but results were promising, as vaccination increased numbers of circulating CD4⁺ and CD8⁺ T cell responses to EBNA1 and/or LMP2 in 15 of 18 recent NPC chemotherapy patients in remission²⁸⁴. The size of responses generated by their vaccine was similar to or higher than effector frequencies following adoptive transfer. However, responses were only sustained in half of the highest dose group. Thus, more durable and lasting responses are needed. It is possible that virus-neutralizing antibodies limited the effectiveness of their MVA-based vaccine, whereas our use of two distinct chimpanzee-based Ad vectors avoids this limitation.

As demonstrated in this thesis, the rhLCV model has proven to be a highly relevant and useful tool for the preclinical testing of EBV-related rhLCV vaccines. Recently, virus-like replicon particle vaccines expressing rhEBNA3A, B and/or gp350 of rhLCV were tested in rhLCV seronegative rhesus macaques, where gp350 was shown to induce antibodies, while the immunodominant rhEBNA3 latency proteins induced detectable CD4⁺ and CD8⁺ T cell

responses^{183, 285}. In comparison, immunization with soluble rhLCV gp350 alone induced a larger antibody response, animals were better protected from infection, and those that did become infected had reduced viral loads in the blood compared to animals that received the VRP vaccines. A vaccine that induces NAb against gp350 and T cell responses against important latency proteins is an interesting concept that merits further exploration, as this approach could be more effective than vaccines that target either one alone. Adenovirus-based vaccines would be an interesting platform for exploring this approach since they can induce potent B cell and antibody responses in addition to transgene product-specific CD4⁺ and CD8⁺ T cells.

As the field progresses, we need to define better markers of disease and correlates of protection. Levels of EBV DNA in the blood can be predictive of some types of lymphomas, and a vaccine that reduces viral DNA load may ultimately reduce the incidence of certain cancers. As discussed previously, data on rhLCV loads before and after vaccination would have provided the most direct evidence of vaccine efficacy or lack thereof. However, direct measurement of EBV replication in the oropharynx through saliva is difficult, and very low levels of viral genome in the peripheral blood of healthy individuals make it difficult to detect viral load fluctuations in live animal studies with limited samples. A more thorough analysis of viral loads would provide clarity, but this hinges on the development of more sensitive assays. Alternatively, larger cohorts can provide more samples for testing viral loads. It will be important to explore correlations between viral load and specific immune responses or between viral load and PD-1 expression in order to define prognostic markers and correlates or surrogates of protection. Larger cohorts would also provide more statistical power for interpreting results.

The field of therapeutic EBV vaccines is still relatively young, and there are many questions that need answers before such vaccines will have success in a clinical setting. We have shown that rhEBNA1-specific T cells can be expanded through vaccination, but we do not yet know whether they confer protection or can be used to target tumor cells. Future studies using SIV-infected rhesus macaques or tumor challenge models can be used to address some of these questions, but the absence of good surrogate markers for the development of most EBV-associated tumors, the long length of time between primary acquisition and development of most

tumors, and the lack of immune correlates of protection make clinical trials difficult to conduct. Furthermore, it is not yet clear what combination of viral antigens would be needed for a vaccine to effectively prevent or treat EBV-associated malignancies, but it will likely be a combination of relevant CD4⁺ and CD8⁺ T cell antigens expressed in a variety of tumors. By continuing to study the intricacies of different EBV-associated malignancies and testing various candidate vaccines in animals and humans, we can begin to answer the aforementioned questions, and we can use this information to design more effective vaccines.

CHAPTER 6: MATERIALS AND METHODS

6.1 T CELL RESPONSES TO LATENT ANTIGEN EBNA1 AND LYTIC ANTIGEN BZLF1 DURING PERSISTENT RHLCV INFECTION OF RHESUS MACAQUES

Non-Human Primates (NHPs)

Adult, healthy, and simian immunodeficiency virus (SIV)-uninfected Indian-origin *Macaca mulatta* animals were housed at the Yerkes National Primate Research Center (YNPRC; Atlanta, GA). Most animals with the exception of PH1019 and PWw were born at YNPRC. Animals were either housed at a field station or at the main station. All animals were female adults ranging from 5-19 years of age at the start of the study. Animals were tested for Mamu-A*01, -A*02, -A*08, -B*01, -B*04, -B*08, and -B*17. All animals included in the analyses tested positive for rhLCV infection by serologic testing for serum antibodies against the rhLCV small viral capsid antigen²⁶⁵. Characteristics are shown in **Table 2-1**. Additional samples were obtained from five rhLCV-seronegative rhesus macaques in the extended specific-pathogen-free colony housed at the New England National Primate Research Center, Harvard Medical School, Southborough, MA. All procedures involving handling of animals were performed according to approved protocols and upon review by the Institutional Animal Care and Usage Committees.

Isolation and Preservation of Lymphocytes

Peripheral blood mononuclear cells (PBMCs) were isolated from blood as described¹⁵⁸. Briefly, whole blood collected in CPT tubes was centrifuged at 2600 rpm for 30 minutes. The clear plasma layer (top layer) was transferred to cryo tubes (about 1 ml per tube) and frozen at -80°C. The remaining plasma layer was then gently mixed with the cloudy lymphocyte layer below and transferred to a new 50 ml conical tube. Remnants of the mixed cell layer within the CPT tube

were gently washed twice with 5 ml of HBSS and transferred to the same 50 mL conical tube. The tube was topped with HBSS and spun at 1200 rpm for 10 minutes. After discarding supernatant, cells were resuspended in 5 ml ACK lysis buffer and incubated for 5 minutes at room temperature. Cells were washed twice with HBSS and resuspended in RPMI complete medium (RPMI 1640 supplemented with 10% fetal bovine serum [FBS; Tissue Culture Biological], 10 mM HEPES, penicillin-streptomycin, and gentamicin [Cellgro]). Samples were tested immediately after isolation or 1×10^7 cells per ml were frozen in 90% fetal bovine serum (FBS) and 10% dimethyl sulfoxide (DMSO) (Sigma, St. Louis, MO) at -80°C until testing.

Intracellular Cytokine Staining (ICS)

The function of rhEBNA1- and rhBZLF1-specific T cells was assessed by intracellular cytokine staining (ICS) after stimulation with peptide pools²⁸⁶. RhEBNA1 was used at a final concentration of 2 μg of each peptide per ml, and rhBZLF1 was used at a final concentration of 1 μg of each peptide per ml. Frozen cells were thawed and immediately washed with Hank's balanced salt solution (HBSS; Mediatech Inc., Herndon, VA) supplemented with 2 units/ml DNase I, resuspended with RPMI medium and stimulated for 6 h with anti-CD28, anti-CD49d, and Brefeldin A. Cells were stained with violet-fluorescent reactive dye Pacific Blue, anti-CD14-Pacific Blue, anti-CD16-Pacific Blue, anti-CD20-Pacific Blue, anti-CD8-allophycocyanin (APC)-H7, anti-CD4-Alexa 700, anti-CD95-phycoerythrin (PE)-Cy5, and anti-CD28-PE-Texas Red (ECD) for 30 min at 4°C (solution prepared in PBS). Additionally, cells were stained with anti-CCR7-PE. After fixation and permeabilization with Cytotfix/Cytoperm (BD Biosciences, San Jose, CA) for 30 min at 4°C , cells were stained with anti-interferon gamma (IFN- γ)-APC, anti-interleukin-2-fluorescein isothiocyanate (anti-IL-2-FITC), anti-tumor necrosis factor alpha (TNF- α)-PE-Cy7, and anti-CD3-peridinin chlorophyll protein (PerCp)-Cy5.5 for 30 min at 4°C (solution prepared in 1x perm wash). Cells were washed twice, fixed with BD Stabilizing Fixative (BD Biosciences, San Jose, CA), and then analyzed by fluorescence-activated cell sorting (FACS) using an LSRII instrument (BD Biosciences, San Jose, CA) and DiVa software. Flow cytometric acquisition and analysis of samples were performed on at least 500,000 events. Single-color controls used CompBeads Anti-

Mouse Igk (BD Biosciences, San Jose, CA) for compensation. The same protocol was repeated for cell surface staining of PD-1, except cells were stained for 30 minutes with anti human CD279-brilliant violet (BV) 605 and washed prior to the 6 h stimulation. **Table 6-1** is a comprehensive list of all antibodies used in these studies, including item numbers, clones, and concentrations used for staining.

Postacquisition analyses were performed with FlowJo software (TreeStar, Ashland, OR). **Figure 6-1A** shows the gating strategy. Briefly, single cells were gated from PBMCs (a) followed by lymphocytes (b), live CD3⁺ T cells (c), CD4⁺ versus CD8⁺ T cells (d), and differentiation within each T cell population (e). **Figures 6-1B** and **6-1C** show responses to the rhEBNA1 peptide pool exemplified by one rhLCV-seropositive (B) and one rhLCV-seronegative (C) animal. Results were normalized to numbers of responding cells per 10⁶ live CD3⁺ cells. Data shown on graphs represent values of peptide-stimulated cells from which background values have been subtracted. To calculate the sum of peptide-specific responses, we subtracted normalized background activity and then summed the seven possible different combinations of functions. We define a positive response as any value greater than the mean plus two standard deviations of total CD4⁺ (183 CD4⁺ cells per 10⁶ CD3⁺ T cells) or CD8⁺ (216 CD8⁺ cells per 10⁶ CD3⁺ T cells) cytokine responses from five seronegative subjects from the New England Primate Research Center. In part II, peptide-specific responses were measured at two time points spaced two months apart, and analyses were based on the average response of each subject. RhEBNA1- and rhBZLF1-specific total cytokine responses for each time point can be seen in **Tables 2-3A** and **2-3B**, respectively. Polyfunctionality pie-chart graphs were generated using SPICE software (NIH, Bethesda, MD).

Synthetic peptides

Two different rhEBNA1 peptide pools were used in the ICS experiments conducted in this chapter. The rhEBNA1 peptide pool used in part I consists of 51 15-mer peptides that overlap by 5 amino acids (Genemed Syn, San Antonio, TX). The rhEBNA1 peptide pool used in part II consists of 85 15-mer peptides that overlap by 10 amino acids except for the GA repeat domain,

which overlaps by 5 amino acids. Additional rhEBNA1 peptides used in part II were purchased from NeoBioSci (Cambridge, MA). **Table 6-2** shows a list of the rhEBNA1 peptides used in parts I and II. To account for its large size, rhEBNA1 was divided into two pools for all ICS experiments conducted in part II: pool one with peptides 1-42 and pool two with peptides 43-85. Responses were combined after normalization and subtraction of background values. The rhBZLF1 peptide pool consists of 60 15-mer peptides with an 11 amino acid overlap and was provided by A. Kaur. Peptides were reconstituted in DMSO.

Statistical analysis:

RhEBNA1- and rhBZLF1-specific immune responses were compared between CD4⁺ and CD8⁺ T cells. IFN- γ , IL-2, and TNF- α cytokine production as well as effector, central memory (T_{CM}), and effector memory (T_{EM}) cell subset analyses within both CD4⁺ and CD8⁺ T cell populations was also compared. All comparisons were performed using a two-tailed Wilcoxon's signed-rank test unless otherwise noted. A Bonferroni adjustment was applied to all multiple comparisons in order to control for a type I error rate. A *P*-value <0.05 was considered statistically significant. Graphpad Prism version 6 (La Jolla, CA) and SPICE version 5.22 (NIH, Bethesda, MD) were used for calculations and illustrations.

Table 6-1: List of antibodies

Antibody	Clone	Company	Catalog number	Ratio used
Mouse anti-human CD28	CD28.2	BD Biosciences, San Jose, CA	555725	1µl/ml
Mouse anti-human CD49d	9F10	BD Biosciences, San Jose, CA	555501	1µl/ml
violet-fluorescent reactive dye PacBlue		Invitrogen, Carlsbad, CA	L34955	1:400
Mouse anti-human CD14-PacBlue	M5E2	BD Biosciences, San Jose, CA	558121	1:50
Mouse anti-human CD16-PacBlue	3G8	BD Biosciences, San Jose, CA	558122	1:50
Mouse anti-human CD20-PacBlue	2H7	AbD Serotec, Raleigh, NC	MCA1710PB	1:50
Mouse anti-human CD8-APC-H7	SK1	BD Biosciences, San Jose, CA	560179	1:25
Mouse anti-human CD4-Alexa 700	OKT4	BD Biosciences, San Jose, CA	557922	1:20
Mouse anti-human CD95-PE-Cy5	DX2	BD Biosciences, San Jose, CA	559773	1:10
Mouse anti-human CD28-ECD	CD28.2	Beckman Coulter, Fullerton, CA	6607111	1:20
Mouse anti-human CCR7-PE	150503	R&D Systems, Minneapolis, MN	FAB197P	1:50
Mouse anti-human IFN-γ-APC	B27	BD Biosciences, San Jose, CA	554702	1:50
Mouse anti-human IL-2-FITC	MQ1-17H12	BD Biosciences, San Jose, CA	554566	1:50
Mouse anti-human TNF-α-PE-Cy7	MAb11	BD Biosciences, San Jose, CA	557647	1:20
Mouse anti-human CD3-PerCp-Cy5.5	SP34-2	BD Biosciences, San Jose, CA	552852	1:50
Mouse anti-human CD279 (PD-1)-BV 605	EH12.2H7	BioLegend, San Diego, CA	329923	1:20

Figure 6-1: Gating strategy and representative examples

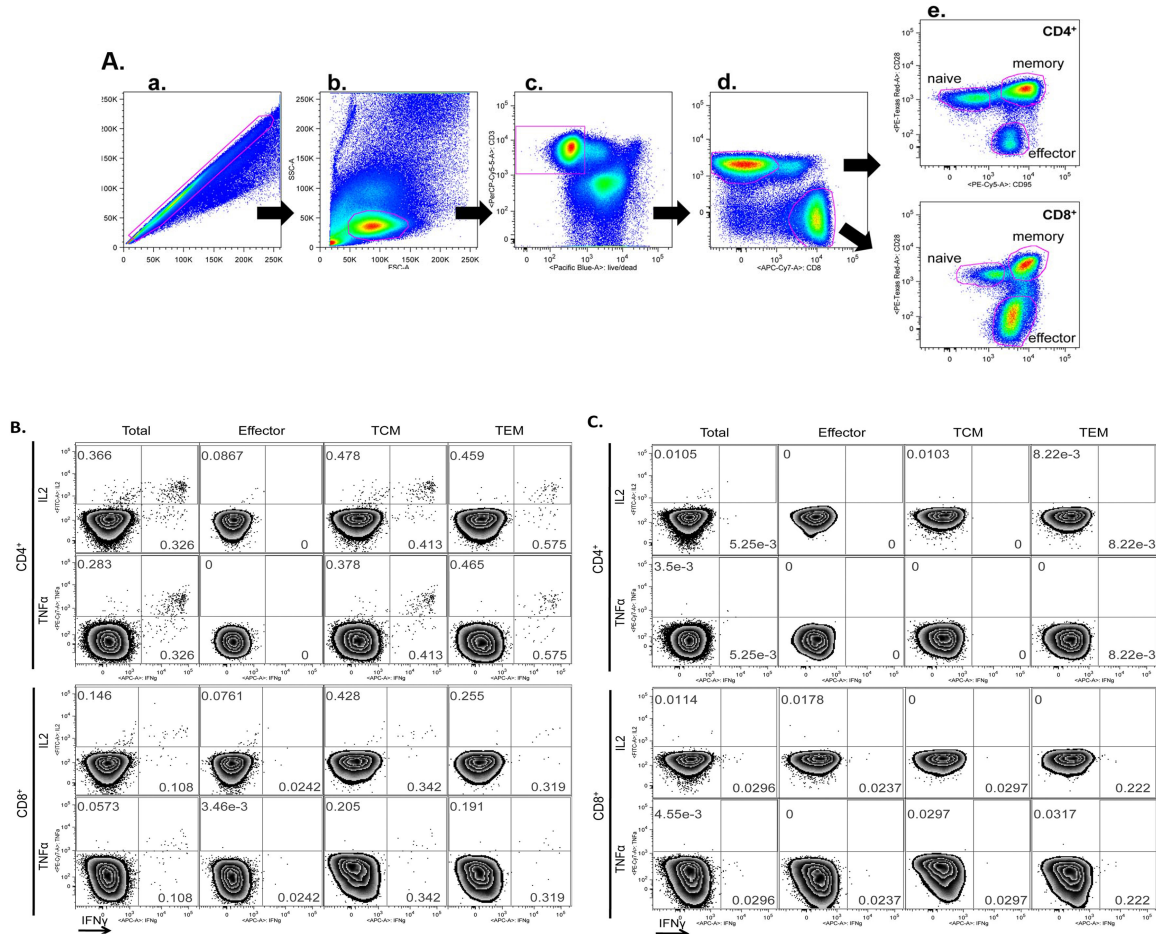


Figure 6-1: Gating strategy for multiparameter flow cytometry and representative examples

(A) The following gating strategy was used to identify rhEBNA1-specific T cells: Cells were initially gated on the basis of their forward scatter (FSC) area versus FSC height profile to remove doublets (a), followed by a lymphocyte gate based on FSC area versus side scatter (SSC) area profile (b). Dead cells were then excluded by gating CD3 versus a live-cell stain (Pacific blue). The amine reactive live/dead stain was in the same channel as CD14⁺, CD16⁺ and/or CD20⁺, so that non-T cell populations were also gated out at this step (c). CD4⁺ and CD8⁺ T cell differentiation (d) was based on CD28 and CD95 expression (effector, CD95^{hi}CD28^{lo}; memory, CD95^{hi}CD28^{hi}) (e). Memory cells were further differentiated into central memory and effector memory with CCR7 (central memory, CCR7^{hi}; effector memory, CCR7^{lo})[♦]. A gate was then set for each stain identifying intracellular-accumulated IFN-γ, IL-2, or TNF-α. RhEBNA1-specific CD4⁺ and CD8⁺ T cell multi-subset analysis from the peripheral blood of one seropositive (B) and one seronegative (C) animal was performed. The analyses were performed with samples immediately frozen after blood collection and PBMC isolation. Phorbol myristate acetate and ionomycin were used as positive controls, and medium with DMSO was used as a negative control (data not shown). Numbers represent the frequency of cytokine-producing cells in the corresponding quadrant. Samples were analyzed by FACS using LSRII and DiVa software. Post-acquisition analyses were performed with FlowJo.

[♦]Some groups refer to the CD95^{hi}CD28^{hi}CCR7^{lo} population as transitional effector memory (T_{TEM}) cells²⁸⁷, which differ from other CD28^{lo} T_{EM} cells by showing superior homing to peripheral sites and increased production of IL-2.

Table 6-2: rhEBNA1 peptide sequences

Position	#	Sequence	Part I	Part II	Molecular Weight
1-15	1	MSDGRGPGNGLGYTG	1		1438.53
6-20	2	GPGNGLGYTGPGLLES		1	1375.45
11-25	3	LGYTGPGLSRPCCA	2		1431.57
16-30	4	PGLESRPCCASGSGS		2	1315.36
21-35	5	RPGGASGSGSGGNRG	3		1273.27
26-40	6	SGSGSGGNRGRGAHG		3	1313.29
31-45	7	GGNRGRGAHGRGRGR	4		1520.62
36-50	8	RGAHGRGRGRGRGRG		4	1562.71
41-55	9	RGRGRGRGRGRGGGG	5		1468.59
46-60	10	GRGRGRGGGGVLGET		5	1385.49
51-65	11	RGGGGVLGETGFEFGG	6		1349.41
56-70	12	VLGETGFEFGHGSES		6	1462.49
61-75	13	GEFGHGSESETRHG	7		1543.53
66-80	14	HGSESETRHGNGHRD		7	1675.65
71-85	15	ETRHGNGHRDKKRRS	8		1833.98
76-90	16	NGHRDKKRRSCVGCK		8	1744
81-95	17	KKRRSCVGCKGGTGG	9		1493.74
86-100	18	CVGCKGGTGGSSAGG		9	1197.28
91-105	19	GGTGGSSAGGAGGNS	10		1093.01
101-115	20	AGGNSRGGGGAGVGS	11		1160.14
111-125	21	AGVGSGRGAGGSGGA	12		1117.12
121-135	22	GSGGAGGGAGGSLGG	13		1017.98
131-145	23	GSLGGGAGGSSGGSG	14		1064.01
141-155	24	SGGSGAGGSGAGGSG	15		1021.93
151-165	25	AGGSGAGGSGAGGSR	16		1105.07
161-175	26	AGGSRGRGRGRGSA	17		1358.43
171-185	27	RGGSAGGRGGRGGGG	18		1215.23
181-195	28	RGGGGGGSRGRGRG	19		1300.34
191-205	29	GRGRGRGGGSRGRGR	20		1498.62
201-215	30	RGRGRGRGRGRGRGE	21		1639.8
211-225	31	RGRGEGPSKGEKRPR	22		1666.86
221-235	32	EKRPRSPSGRSSSSQS	23		1645.76
231-245	33	SSSQSSSRSSSSRS	24		1503.47
241-255	34	SSSRSSSNGSDSSDF	25		1506.42
251-265	35	DSSDFPGFPGHRPLP	26		1625.77
256-270	36	PGFPGHRPLTSFPG		10	1563.79
261-275	37	HRPLTSFPGSPLGG	27		1519.73
266-280	38	TSFPGSPLGGYRGTD		11	1511.62
271-285	39	SPLGGYRGTDTGDDG	28		1409.43
276-290	40	YRGTDTGDDGDEQPP		12	1564.55
281-295	41	GTDGDEQPPGAVEQ	29		1456.44
286-300	42	DEQPPGAVEQGPED		13	1524.52
291-305	43	GAVEQGPEDPGEGP	30		1395.4
296-310	44	GPGEDPGEGPSRQTT		14	1484.51
301-315	45	PGEGPSRQTTSSGGR	31		1487.56
306-320	46	SRQTTSSGGRGSGKK		15	1507.62
311-325	47	TSGGRGSGKKGWFG	32		1438.54
316-330	48	GSGKKGWFGRRRGE		16	1634.8
321-335	49	GGWFGRRRGEGRGF	33		1651.8
326-340	50	RRRGEGGRGFKKFEN		17	1794
331-345	51	GGRGFKKFENMAKNL	34		1696.97
336-350	52	KKFENMAKNLKVLLA		18	1747.15
341-355	53	MAKNLKVLLARCQAE	35		1688.07
346-360	54	KVLLARCQAERTNTT		19	1703.98

351-365	55	RCQAERTNTTGNWPF	36		1780.94
356-370	56	RTNTTGNWPFVGVVY		20	1758.95
361-375	57	GNWPFVGVVYGPKTS	37		1655.86
366-380	58	GVFVYGPKTSCYNLR		21	1703.97
371-385	59	GPKTSCYNLRRCIAC	38		1685.01
376-390	60	CYNLRRCIACCIPEC		22	1760.16
381-395	61	RCIACCIPECRLTPL	39		1691.13
386-400	62	CIPECRLTPLGRLPF		23	1715.12
391-405	63	RLTPLGRLPFGYAPE	40		1686.99
396-410	64	GRLPFGYAPEPGPQP		24	1582.79
401-415	65	GYAPEPGPQPGPMRE	41		1582.77
406-420	66	PGPQPGPMRESTDCY		25	1634.82
411-425	67	GPMRESTDCYFIVFL	42		1778.09
416-430	68	STDCYFIVFLQTMIF		26	1828.19
421-435	69	FIVFLQTMIFAECVK	43		1789.23
426-440	70	QTMIFAECVKDALRD		27	1740.03
431-445	71	AECVKDALRDYIMTK	44		1756.07
436-450	72	DALRDYIMTKPLPTS		28	1721.02
441-455	73	YIMTKPLPTSSVQVT	45		1664.99
446-460	74	PLPTSSVQVTVITFE		29	1617.87
451-465	75	SVQVTVITFEDPVML	46		1677.98
456-470	76	VITFEDPVMLPVFFP		30	1751.13
461-475	77	DPVMLPVFFPPHLP	47		1677.05
466-480	78	PVFFPPHLPAAAVAA		31	1504.8
471-485	79	PHLPAAAVAAEGGEG	48		1346.46
476-490	80	AAVAAEGGEGAEGDD		32	1318.27
481-495	81	EGGEGAEGDDGDEGG	49		1350.18
486-500	82	AEGDDGDEGGEGGDG		33	1336.15
491-505	83	GDEGGEGGDNEGDE	50		1393.2
496-510	84	EGGDNEGDEGAAGQ		34	1362.23
501-511	85	NEGDEGAAGQE	51		1075.99

Table 6-2: The rhEBNA1 overlapping peptide library contains a total of 85 peptides synthesized at 85-90% purity. Peptides are 15 aa in length and overlap by 5 or 10 amino acids. The 51 peptides used in part I were ordered from Genemed Synthesis (San Antonio, TX) and overlap by 10 amino acids. An additional 34 peptides were ordered from NeoBio Sciences (Cambridge, MA) so that the complete peptide library used in part II was composed of 85 peptides that overlapped by 5 amino acids except for the GAR domain, which overlapped by 10 amino acids. The GAR region is highlighted in grey, and colors represent the hydrophobic classification of each amino acid: red, very hydrophobic; orange, hydrophobic; green, hydrophilic; blue, very hydrophilic. Figure was generated using the Sigma-Aldrich PEPscreen® library design tool.

6.2 ADENOVIRUS-BASED VACCINES TO RHEBNA1: VECTOR DESIGN, MOUSE STUDIES, IN VITRO TESTING

Vaccine vectors

The rhEBNA1 gene was deleted of the GAR domain and a flag epitope was inserted using conventional cloning techniques as described²⁸⁸. Start and stop codons were also removed, and the final gene product was amplified by PCR with the following primers: Fw5'- ACCGGT AGGGAGGGTGGTTTGGGAGG-3' and Rv5'- ACGCGTCGACCTCCTGCCCCGCCGCGTCGAC -3'. Primers were purchased from Integrated DNA Technologies (Coralville, IA). DNA fragments were cloned into the Apal site of the pRE4 vector as described²⁴⁸. The correct in frame cloning of the rhEBNA1 encoding gene was confirmed by restriction enzyme digest followed by visualization of bands by gel electrophoresis and DNA sequencing. To generate pSh-SgD-rhEBNA1 and pSh-NBEFSgD-rhEBNA1 vectors, the GAR-deleted rhEBNA1 gene was ligated into pShuttle vectors containing sequences encoding the previously described²⁴⁷ mutated versions of HSV-1 gD, which either showed increased (SgD) or reduced (NBEFSgD) binding to HVEM²⁴⁸. Transgenes were under control by the CMV enhancer and promoter. Restriction enzyme digests followed by gel electrophoresis and nucleotide sequencing confirmed correct insertion of the rhEBNA1 sequences into pShuttle.

We then cloned the inserts including the regulatory elements from the pShuttle vectors into the E1 domain of molecular clones of E1-deleted AdC vectors of simian serotype 25 (SAdV-25; AdC68) and serotype 23 (SAdV-23; AdC6) used for primary and booster immunizations, respectively, as described²⁸⁹.

Recombinant AdC vectors were rescued and propagated on HEK 293 cells as described²⁸⁹. Virus was purified and titrated as previously described²⁸⁹. Vector batches were quality controlled by determining virus particle (vp) to infectious units (moi) ratios. They were tested for replication-competent Ad and endotoxin contaminations. Genetic integrity of AdC vectors was determined by

restriction enzyme digest of purified viral DNA. AdC-gD-NP and AdC-gD vectors have been described previously^{247, 279}.

Vectors used in mouse experiments were cloned as described above, except rhEBNA1 was first ligated into an empty pShuttle vector (to generate AdC-rhEBNA1) or a pShuttle that contained wild-type HSV-1 gD without the transmembrane domain (to generate AdC-gD-rhEBNA1).

Immunoblotting

Expression of the different forms of rhEBNA1 from recombinant AdC vectors was confirmed upon infection of CHO cells stably transfected to express the coxsackie adenovirus receptor (CAR) by Western Blot analysis. An AdC68 vector expressing gD was used as a control vector. Briefly, CHO-CAR cells were grown in Dulbecco's modified Eagle's medium (DMEM) supplemented with 10% fetal calf serum (FBS), 1% penicillin/streptomycin, 1% pyruvate and 1% non-essential amino acids at 37°C in 5% CO₂ until 80% confluence in wells of a 6-well plate. Medium was then replaced with 1ml of serum-free DMEM, and about 10⁶ cells were infected with either 10¹¹, 10¹⁰, or 10⁹ vp of vector per well or 10¹⁰, 10⁹, or 10⁸ vp of vector per well. After 2 hours, 1ml complete DMEM was added to each well, and cells were harvested after 48 hours.

Total cellular protein was prepared by washing cells 2x with phosphate-buffered saline (PBS). They were then suspended in RIPA buffer (Invitrogen, Grand Island, NY) supplemented with Complete Protease Inhibitor (Roche, Indianapolis, IN). Cells were transferred to a new tube and incubated for 1 hour on ice. Tubes were spun for 30 minutes at 4°C to pellet debris, and lysate was transferred to new tubes. 10ul of lysate was mixed with 10ul 2X loading buffer (Laemmli blue dye, 2-mercaptoethanol) and boiled for 5 minutes. Protein samples were then separated with 4-15% gradient sodium dodecyl sulfate-polyacrylamide gel electrophoresis (SDS-PAGE) and proteins were transferred to a 0.45 um PVDF transfer membrane (Millipore, Billerica, MA). The membranes were blocked for 1 hour at room temperature in 5% fat-free milk dissolved in PBS containing 0.1% Tween-20. After washing, expression of chimeric rhEBNA1 proteins was detected with a mouse monoclonal antibody specific for the Flag epitope (M2; Sigma, St Louis,

MO), diluted 1:1,000 in 5% milk, PBS, 0.1% Tween 20 and incubated at 4°C overnight. Blots were then washed, incubated for 1 hour with a horseradish peroxidase-conjugated goat anti-mouse IgG antibody (1:30,000, KPL), and developed with Super Signal West Pico chemiluminescence substrate (Thermo Scientific, Waltham, MA). Membranes were washed extensively between all steps. Some membranes were treated with stripping buffer (Thermo Scientific) for 15 minutes, washed in PBS-Tween, blocked and re-probed as described above. To detect gD, membranes were probed with a polyclonal anti-gD serum R6 (R45) diluted 1:500. Donkey anti-rabbit IgG horseradish peroxidase (HRP) (Amersham Biosciences, Little Chalfont, Buckinghamshire, UK) was used as a secondary antibody at 1:10,000. For loading control, we stripped and re-probed with a 1:20,000 dilution of a β -actin-specific antibody (AC-15; Sigma, St Louis, MO), and then 1:30,000 goat anti-mouse IgG-HRP as described above.

Immunofluorescence

Expression of transgene products by AdC vectors was further measured by immunofluorescence. Cells (10^6) were infected as described above with 10^{10} or 10^9 vp of vector and washed. PBS (1 ml) supplemented with 10 mM EDTA was added to each well, and cells were incubated at 37°C for 5 minutes. Cells were harvested, washed, and transferred to a 96-well plate where they were stained with mouse anti-Flag antibody for 30 minutes, washed, and probed with goat anti-mouse IgG-Alexa700 (Molecular Probes, Eugene, OR). Cells were washed twice more, fixed with BD Stabilizing Fixative (BD Biosciences, San Jose, CA), and then analyzed by FACS using LSRII (BD Biosciences, San Jose, CA) and DiVa software.

HVEM binding assay

CHO-CAR cells (10^6) were infected with 10^{10} vps of AdC vectors as described above. After 48 hours, cells were harvested and total cellular protein was prepared as described above. Protein extracts were kept at -80°C until use. Western blotting and densitometry (AlphaEaseFC software version 3.3.0; Alpha Innotech, San Leandro, CA) were used to normalize the amount of chimeric protein in the extracts.

To measure the gD fusion proteins' ability to bind HVEM, ELISA plates were coated with 50 μ l per well of a 5 μ g/ml concentration of HVEM²⁴⁷ diluted in 0.1 M carbonate coating buffer (pH 9.6) and incubated overnight at 4°C. Plates were washed 5 times and then blocked for 1.5 hours in 5% milk-PBST (0.05% Tween20) at room temperature. After washing, normalized protein extract was serially diluted in blocking solution and added to the plates for 1.5 hours. To detect captured chimeric protein, 50 μ l mouse anti-Flag antibody diluted 1:1,000 in 5% milk-PBST was added for 1 hour, followed by 50 μ l goat anti-mouse IgG-HRP diluted 1:1,000 for 30 minutes with washings after each step. TMB substrate solution (Calbiochem, San Diego, CA) was then added to each well, plates were stored in the dark for 15 minutes, and the reaction was stopped by adding 2N HCl. The optical density at 450 nm was determined using a microtiter plate reader.

Electrophoretic mobility shift assays (EMSA)

Adenovirus vaccines expressing gD, rhEBNA1, or gD-rhEBNA1 were used to infect CHO/CAR cells at 10^{10} VPS in order to measure DNA-binding ability of rhEBNA1 transgenes. Infected cells were harvested and then prepared as total cell lysates. Lysates were assayed by electrophoretic mobility shift assays (EMSA) with a ³²P labeled probe for rhEBNA1 binding sites at rhLCV OriP. as previously described²⁹⁰.

Animals and immunization regimen

Dose-escalation study: Four to six week old female BALB/c mice were purchased from the National Cancer Institute. Groups of 4 mice each received 10^9 , 10^{10} , or 10^{11} vp of AdC68 vaccines that expressed either rhEBNA1 or gD-rhEBNA1. As a control, animals were vaccinated with 10^{11} vp of AdC68 expressing HIV-gag. Blood was collected at weeks 2 and 4 after vaccination.

Kinetics studies: Groups of 5 female BALB/c mice received 10^{11} vp of AdC68-expressing rhEBNA1 or gD-rhEBNA1. Blood was collected every other week after vaccination. Vaccine-naïve mice were included as an additional control starting at week 4 in order to measure general immune fluctuation. Similar experiments were conducted with C57/bl6 mice and ICR mice. Three to four week old female C57/bl6 mice were purchased from Taconic labs (NY, Hudson),

and 6-8 week old female ICR mice were purchased from ACE Animals Inc. (Boyertown, PA). Groups of 5 C57/bl6 mice and 10 ICR mice received 10^{11} vp of AdC68-expressing rhEBNA1 or gD-rhEBNA1. Blood was collected at weeks 2, 4, 10, and 12 after vaccination. The same studies were repeated with AdC68-rhEBNA1-M vaccines. All vaccines were diluted in PBS and administered intramuscularly to the tibialis anterior muscle of each hindlimb (50 μ L per leg). Animals were housed at the Wistar Institute Animal Facility (Philadelphia, PA), and all procedures were performed according to institutionally approved protocols.

Isolation of lymphocytes

Blood was collected in 1mL of 4% sodium citrate, and 1mL of L-15 media (Cellgro, Herndon, VA) was then added. Lymphocytes were purified through a Histopaque (Sigma-Aldrich, St. Louis, MO) gradient solution and washed in PBS supplemented with 1% FBS. Cells were then treated with 1mL lysis buffer (ebioscience, San Diego, CA) for 5 min on ice to rupture red blood cells. 1% FBS in PBS was added and cells were centrifuged at 1500 rpm for 10 minutes. Pellets were washed again and cells were resuspended in 2% MLC/DMEM (DMEM, 2% heat-inactivated FBS, 1% Pen–Strep, 10 mM Hepes, 1 mM sodium pyruvate, 0.1 mM non-essential amino acids, 10^6 M 2-mercaptoethanol)(Cellgro, Herndon, VA) to a final volume of 200 μ l.

Intracellular cytokine staining (ICS)

Induction of rhEBNA1-specific T cells was assessed by intracellular cytokine staining (ICS) after stimulation of PBMCs with overlapping peptide pools. RhEBNA1 was used at a final concentration of 2 μ g of each peptide per ml. As a control, cells were stimulated with an HIV-gag peptide pool at the same concentration. PBMCs (10^6 cells/well) were incubated with peptide pools and Brefeldin A (1 ml/ml; GolgiPlug; BD Biosciences, San Jose, CA) for 5 hrs at 37 °C in a 96-well round bottom microtiter plate at a final volume of 200 μ l/well in 2%MLC/DMEM. After washing, cells were incubated for 30 min at 4°C in 50 μ l/well of staining solution (in PBS) composed of LIVE/DEAD fixable aqua dead cell stain (AmCyan), anti-CD8-PercP-Cy5.5, and in some experiments either anti-CD4-FITC and anti-CD44-APC or anti-CD44-Alexa700, anti-CD62L-FITC, and anti-CD127-PacBlue. After several washings, cells were fixed and

permeabilized with Cytofix/Cytoperm (BD Biosciences, San Jose, CA) for 20 min at 4°C, and then stained with 50µl/well of staining solution (in 1x Perm Wash) composed of anti-IFN-γ-PE, and in some experiments with anti-IL-2-APC and anti-TNF-α-PE-Cy7. Cells were washed twice, fixed with BD Stabilizing Fixative (BD Biosciences, San Jose, CA), and then analyzed by FACS using LSRII (BD Biosciences, San Jose, CA) and DiVA software. Flow cytometric acquisition and analysis of samples was performed on at least 500,000 events. Post-acquisition analyses were performed with FlowJo (TreeStar, Ashland, OR). Data shown on graphs represent values of peptide-stimulated cells from which background values have been subtracted, unless negative control data is shown. Single color controls used CompBeads anti-rat and anti-hamster Igk (BD Biosciences, San Jose, CA) for compensation. **Table 6-3** is a comprehensive list of all antibodies used in these studies, including item numbers, clones, and concentrations used for staining.

***In vitro* stimulation**

Dendritic cells (DCs) were generated from peripheral blood mononuclear cells (PBMCs) of a rhLCV seropositive rhesus macaque by culturing in the presence of GM-CSF and IL-4 (R&D Systems, Minneapolis, MN). They were subsequently matured in the presence of monocyte-conditioned medium as previously described²⁹¹. Matured DCs were infected with recombinant AdC vectors at 50 moi per cell and cultured overnight. Effector CD8⁺ T cells were generated by stimulating PBMCs from the same animal with a rhEBNA1 peptide pool followed by depletion of CD4⁺ T cells as described²¹⁵. Twenty thousand AdC vector- or rhEBNA1 peptide-pulsed DCs were used as APCs in the presence or absence of 50,000 CD8⁺ T cells in an IFN-γ ELISPOT assay. After a 16h incubation, IFN-γ-secreting cells were visualized following the manufacturer's instructions (Mabtech, Cincinnati, OH) as described previously²¹⁵. The number of activated CD8⁺ T cells was enumerated by counting the number of spots using an automated reader and analysis software (Zellnet, Fort Lee, NJ) and the results were expressed as the number of spot forming cells per 10⁶ CD8⁺ T cells. Positive and negative controls were CD8⁺ T cells cultured in the presence of PHA or medium alone.

Synthetic peptides

The rhEBNA1 peptide pool consists of 85 15-mer peptides overlapping by 10 amino acids (Genemed Synthesis Inc. San Antonio, TX). The peptide pools used for testing of pre-vaccination samples contained peptides to the GAR domain and we continued to use these pools although the vaccine does not carry these sequences of rhEBNA1. The HIV-gag peptide pool consists of (123) 15-mer peptides overlapping by 11 amino acids (National Institutes of Health AIDS Research and Reference Reagent Program). All peptides were reconstituted in DMSO.

Statistical analysis

Experiments were conducted repeatedly using 4-5 mice per group. Results show the means \pm SD. Significances between two groups were analyzed by one-tailed Student's t-test or a one-way ANOVA, depending on the number of comparisons made. A p-value <0.05 was considered significant. All multiple comparisons were Bonferroni-adjusted to control for type I errors.

Table 6-3: List of antibodies for ICS (mouse studies)

Antibody	Clone	Company	Catalog number	Ratio used
LIVE/DEAD fixable aqua dead cell stain		Invitrogen, Carlsbad, CA	L34957	1:500
Rat anti-mouse CD8-PerCp-Cy5.5	53-6.7	BioLegend, San Diego, CA	100734	1:100
Rat anti-mouse CD4-FITC	RM4-4	BD Biosciences, San Jose, CA	553055	1:100
Rat anti-mouse CD44-APC	IM7	BioLegend, San Diego, CA	103011	1:100
Rat anti-mouse CD44-Alexa 700	IM7	BioLegend, San Diego, CA	103026	1:100
Rat anti-mouse CD62L-FITC	MEL-14	BD Biosciences, San Jose, CA	553150	1:100
Rat anti-mouse CD127-PacBlue	A7R34	eBioScience, San Diego, CA	48-1271-82	1:100
Rat anti-mouse IFN- γ -PE	XMG1.2	BD Biosciences, San Jose, CA	554412	1:100
Rat anti-mouse IL-2-APC	JES6-5H4	BD Biosciences, San Jose, CA	554429	1:100
Rat anti-mouse TNF- α -PE-Cy7	MP6- XT22	BioLegend, San Diego, CA	506324	1:100

6.3 ADENOVIRUS-BASED VACCINES TO RHEBNA1 INDUCE EXPANSION OF CD8⁺ AND CD4⁺ T CELLS IN PERSISTENTLY INFECTED RHESUS MACAQUES

Microneutralization assay for Ad virus-specific neutralizing antibodies (NA)

NA titers were determined as described previously¹⁶⁷ on HEK 293 cells infected with AdC vectors expressing green fluorescent protein (GFP).

Non-human primates

Fifteen female adult, healthy, and SIV-uninfected rhesus macaques (*Macaca mulatta*) of Indian origin aged 6 to 20 years were enrolled into the study. Animals were housed at the Yerkes National Primate Research Center (YNPRC, Atlanta, GA) at either the field station or the main station. All animals except PH1019 and PWw were born at YNPRC. Animals were negative for NAs to AdC68 and AdC6, except for one animal (RZi7) with a low titer (1:10) to AdC6. All animals tested positive for rhLCV infection by serologic testing for serum antibodies against the rhLCV small viral capsid antigen²⁶⁵. Mamu phenotypes were also determined. A detailed analysis of baseline rhEBNA1- and rhBZLF1-specific immune responses was conducted and is discussed in chapter 2.

Additional samples were obtained from five rhLCV-seronegative rhesus macaques housed in the extended specific-pathogen-free colony at the New England Primate Research Center, Harvard Medical School, Southborough, MA. All procedures involving handling of animals were performed according to approved protocols and upon review by the respective Institutional Animal Care and Usage Committees.

Immunization regimen of rhesus macaques

Fifteen animals were divided into 3 groups with similar age distribution and rhEBNA1 immune response status. Group 1 animals ($n = 6$) received 10^{11} vps of AdC68-SgD-rhEBNA1, group 2

animals ($n = 6$) received 10^{11} vps of AdC68-NBEFSgD-rhEBNA1, and group 3 animals ($n = 3$) received 10^{11} vps of an AdC68 vector expressing an irrelevant antigen (i.e., nucleoprotein of influenza A virus) fused into gD (AdC68-gD-NP). Animals were boosted 15 weeks after priming with 10^{11} vps of the corresponding AdC6 vectors expressing the same antigens used for priming. All vaccines were given intramuscularly (i.m.). See **Table 4-3** for basic characteristics of the animals enrolled in the study and the vaccines they received.

Isolation and preservation of lymphocytes

Peripheral blood mononuclear cells (PBMCs) were isolated from blood as described²⁵⁷. Briefly, whole blood collected in CPT tubes was centrifuged at 2600 rpm for 30 minutes. The clear plasma layer (top layer) was transferred to cryo tubes (about 1 ml per tube) and frozen at -80°C . The remaining plasma layer was then gently mixed with the cloudy lymphocyte layer below and transferred to a new 50 ml conical tube. Remnants of the mixed cell layer within the CPT tube were gently washed twice with 5 ml of HBSS and transferred to the same 50 mL conical tube. The tube was topped with HBSS and spun at 1200 rpm for 10 minutes. After discarding supernatant, cells were resuspended in 5 ml ACK lysis buffer and incubated for 5 minutes at room temperature. Cells were washed twice with HBSS and resuspended in RPMI complete medium. Samples were tested immediately after isolation or 1×10^7 cells per ml were frozen in 90% FBS and 10% dimethyl sulfoxide (Sigma, St. Louis, MO) at -80°C until testing.

Intracellular cytokine staining (ICS)

The magnitude and function of rhEBNA1- and rhBZLF1-specific T cells was assessed by intracellular cytokine staining (ICS) after stimulation with peptide pools²⁵⁷. Samples collected at different time points were tested in parallel for each animal to minimize variability. RhEBNA1 was used at a final concentration of $2\mu\text{g}$ of each peptide per ml, and rhBZLF1 was used at a final concentration of $1\mu\text{g}$ of each peptide per ml. Frozen cells were thawed and immediately washed with HBSS supplemented with 2 units/ml DNase I, resuspended with RPMI medium, and stimulated for 6 hrs with anti-CD28, anti-CD49d, and Brefeldin A. Cells were stained with violet-fluorescent reactive dye-Pacific Blue, anti-CD14-Pacific Blue, anti-CD16-Pacific Blue, anti CD20-

Pacific Blue, anti-CD8-APC-H7, anti-CD4-Alexa700, anti-CD95-PE-Cy5, and anti-CD28-Texas Red for 30 min at 4°C (solution prepared in PBS). Additionally, cells were stained with anti-CCR7-PE. After fixation and permeabilization with Cytofix/Cytoperm (BD Biosciences, San Jose, CA) for 30 min at 4°C, cells were stained with anti-IFN- γ -APC, anti-IL-2-FITC, anti-TNF- α -PE-Cy7, and anti-CD3-PerCp-Cy5.5 for 30 min at 4°C (solution prepared in 1x perm wash). Cells were washed twice, fixed with BD Stabilizing Fixative (BD Biosciences, San Jose, CA), and then analyzed by FACS using LSRII (BD Biosciences, San Jose, CA) and DiVA software. Flow cytometric acquisition and analysis of samples were performed on at least 500,000 events. Post-acquisition analyses were performed with FlowJo (TreeStar, Ashland, OR). Data shown on graphs represent values of peptide-stimulated cells from which background values have been subtracted. Polyfunctionality pie chart graphs were generated using SPICE software (NIH, Bethesda MD, <http://exon.niaid.nih.gov/spice/>). Single-color controls used CompBeads Anti-Mouse Igk (BD Biosciences, San Jose, CA) for compensation. See **Table 6-1** for a comprehensive list of all antibodies used in these studies, including item numbers, clones, and concentrations used for staining.

The above-described experiment was repeated for 11 of the 12 animals (excluding RLz5) with the addition of an antibody for staining of intracellular granzyme B. Anti-granzyme B PE-Cy5.5 (clone GB11; Life Science Products, Chestertown, MD) was added after the fixation and permeabilization steps at a dilution of 1:40 (determined by titration). Responses were tested at weeks 0, 2, 8, and either week 17 or week 19 after vaccination, depending on sample availability.

Synthetic peptides

The rhEBNA1 peptide pool consists of 85 15-mer peptides overlapping by 10 amino acids except for the GAR domain, where peptides overlap by 5 amino acids (Genemed Synthesis Inc., San Antonio, TX; NeoBioSci, Cambridge, MA). The peptide pools used for testing of pre-vaccination samples contained peptides to the GAR domain and we continued to use these pools although the vaccine does not carry these sequences of rhEBNA1. To account for its large size, the rhEBNA1 peptide pool was divided into two pools, one with peptides 1 to 42 and the other with peptides 43

to 85. Responses were combined after normalization and subtraction of background values. The rhBZLF1 peptide pool consists of 60 15-mer peptides with 11 amino acid overlap and was provided by A. Kaur. Peptides were reconstituted in DMSO.

Statistical analysis

For statistical analyses of data several comparisons were made. To assess the overall magnitude of vaccine responses, areas under the curve (AUC) using increases of cytokine producing T cells (normalized after subtraction of background responses) over baseline counts (normalized after subtraction of background responses) were calculated. For these calculations negative values were set at 0. The AUCs for animals belonging to both rhEBNA1 vaccine groups were compared to the AUCs of control animals by using unpaired Mann-Whitney tests. Comparisons between all three groups or between the three types of T cell subsets were conducted by analysis of variance (ANOVA). Comparisons for individual patterns of functions were made by Fischer's least significant difference test by ANOVA. All multiple comparisons were Bonferroni adjusted to control for type I error rate, and *P* values of < 0.05 were considered significant. Data were analyzed using Prism version 6a software.

CHAPTER 7: REFERENCES

1. Landais E, Saulquin X, Houssaint E. The human T cell immune response to Epstein-Barr virus. *Int J Dev Biol* 2005;49:285-92.
2. Parkin DM. The global health burden of infection-associated cancers in the year 2002. *Int J Cancer* 2006;118:3030-44.
3. Schooley RT, Arbit DI, Henle W, Hirsch MS. T-lymphocyte subset interactions in the cell-mediated immune response to Epstein-Barr virus. *Cell Immunol* 1984;86:402-12.
4. Burkitt D. A sarcoma involving the jaws in African children. *Br J Surg* 1958;46:218-23.
5. Burkitt D. A tumour syndrome affecting children in tropical Africa. *Postgrad Med J* 1962;38:71-9.
6. Epstein MA, Achong BG, Barr YM. Virus Particles in Cultured Lymphoblasts from Burkitt's Lymphoma. *Lancet* 1964;1:702-3.
7. Henle G, Henle W, Diehl V. Relation of Burkitt's tumor-associated herpes-type virus to infectious mononucleosis. *Proc Natl Acad Sci U S A* 1968;59:94-101.
8. Nilsson K, Klein G, Henle W, Henle G. The establishment of lymphoblastoid lines from adult and fetal human lymphoid tissue and its dependence on EBV. *Int J Cancer* 1971;8:443-50.
9. Sixbey JW, Nedrud JG, Raab-Traub N, Hanes RA, Pagano JS. Epstein-Barr virus replication in oropharyngeal epithelial cells. *N Engl J Med* 1984;310:1225-30.
10. Fields BN, Knipe DM, Howley PM. *Fields virology*, 6th ed. Philadelphia: Wolters Kluwer Health/Lippincott Williams & Wilkins, 2013.
11. Tselis AC, Jenson HB. *Epstein-Barr virus*. New York: Taylor & Francis, 2006.
12. Straus SE, Cohen JI, Tosato G, Meier J. NIH conference. Epstein-Barr virus infections: biology, pathogenesis, and management. *Ann Intern Med* 1993;118:45-58.
13. Young LS, Rickinson AB. Epstein-Barr virus: 40 years on. *Nat Rev Cancer* 2004;4:757-68.
14. Thomas JA, Allday MJ, Crawford DH. Epstein-Barr virus-associated lymphoproliferative disorders in immunocompromised individuals. *Adv Cancer Res* 1991;57:329-80.
15. Jenson HB. Epstein-Barr virus. *Pediatr Rev* 2011;32:375-83; quiz 84.
16. Naher H, Gissmann L, Freese UK, Petzoldt D, Helfrich S. Subclinical Epstein-Barr virus infection of both the male and female genital tract--indication for sexual transmission. *J Invest Dermatol* 1992;98:791-3.
17. Borza CM, Hutt-Fletcher LM. Alternate replication in B cells and epithelial cells switches tropism of Epstein-Barr virus. *Nat Med* 2002;8:594-9.
18. Laichalk LL, Hochberg D, Babcock GJ, Freeman RB, Thorley-Lawson DA. The dispersal of mucosal memory B cells: evidence from persistent EBV infection. *Immunity* 2002;16:745-54.
19. Babcock GJ, Decker LL, Volk M, Thorley-Lawson DA. EBV persistence in memory B cells in vivo. *Immunity* 1998;9:395-404.
20. Rose C, Green M, Webber S, Kingsley L, Day R, Watkins S, Reyes J, Rowe D. Detection of Epstein-Barr virus genomes in peripheral blood B cells from solid-organ transplant recipients by fluorescence in situ hybridization. *J Clin Microbiol* 2002;40:2533-44.
21. Khan G, Miyashita EM, Yang B, Babcock GJ, Thorley-Lawson DA. Is EBV persistence in vivo a model for B cell homeostasis? *Immunity* 1996;5:173-9.
22. Babcock GJ, Hochberg D, Thorley-Lawson AD. The expression pattern of Epstein-Barr virus latent genes in vivo is dependent upon the differentiation stage of the infected B cell. *Immunity* 2000;13:497-506.

23. Tierney RJ, Steven N, Young LS, Rickinson AB. Epstein-Barr virus latency in blood mononuclear cells: analysis of viral gene transcription during primary infection and in the carrier state. *J Virol* 1994;68:7374-85.
24. Kuppers R. B cells under influence: transformation of B cells by Epstein-Barr virus. *Nat Rev Immunol* 2003;3:801-12.
25. Abbot SD, Rowe M, Cadwallader K, Ricksten A, Gordon J, Wang F, Rymo L, Rickinson AB. Epstein-Barr virus nuclear antigen 2 induces expression of the virus-encoded latent membrane protein. *J Virol* 1990;64:2126-34.
26. Fahraeus R, Jansson A, Ricksten A, Sjoblom A, Rymo L. Epstein-Barr virus-encoded nuclear antigen 2 activates the viral latent membrane protein promoter by modulating the activity of a negative regulatory element. *Proc Natl Acad Sci U S A* 1990;87:7390-4.
27. Cordier M, Calender A, Billaud M, Zimmer U, Rousselet G, Pavlish O, Banchereau J, Tursz T, Bornkamm G, Lenoir GM. Stable transfection of Epstein-Barr virus (EBV) nuclear antigen 2 in lymphoma cells containing the EBV P3HR1 genome induces expression of B-cell activation molecules CD21 and CD23. *J Virol* 1990;64:1002-13.
28. Kaiser C, Laux G, Eick D, Jochner N, Bornkamm GW, Kempkes B. The proto-oncogene c-myc is a direct target gene of Epstein-Barr virus nuclear antigen 2. *J Virol* 1999;73:4481-4.
29. Knutson JC. The level of c-fgr RNA is increased by EBNA-2, an Epstein-Barr virus gene required for B-cell immortalization. *J Virol* 1990;64:2530-6.
30. Nitsche F, Bell A, Rickinson A. Epstein-Barr virus leader protein enhances EBNA-2-mediated transactivation of latent membrane protein 1 expression: a role for the W1W2 repeat domain. *J Virol* 1997;71:6619-28.
31. Waltzer L, Perricaudet M, Sergeant A, Manet E. Epstein-Barr virus EBNA3A and EBNA3C proteins both repress RBP-J kappa-EBNA2-activated transcription by inhibiting the binding of RBP-J kappa to DNA. *J Virol* 1996;70:5909-15.
32. Tomkinson B, Kieff E. Use of second-site homologous recombination to demonstrate that Epstein-Barr virus nuclear protein 3B is not important for lymphocyte infection or growth transformation in vitro. *J Virol* 1992;66:2893-903.
33. Lee MA, Diamond ME, Yates JL. Genetic evidence that EBNA-1 is needed for efficient, stable latent infection by Epstein-Barr virus. *J Virol* 1999;73:2974-82.
34. Kaye KM, Izumi KM, Kieff E. Epstein-Barr virus latent membrane protein 1 is essential for B-lymphocyte growth transformation. *Proc Natl Acad Sci U S A* 1993;90:9150-4.
35. Eliopoulos AG, Rickinson AB. Epstein-Barr virus: LMP1 masquerades as an active receptor. *Curr Biol* 1998;8:R196-8.
36. Kaye KM, Devergne O, Harada JN, Izumi KM, Yalamanchili R, Kieff E, Mosialos G. Tumor necrosis factor receptor associated factor 2 is a mediator of NF-kappa B activation by latent infection membrane protein 1, the Epstein-Barr virus transforming protein. *Proc Natl Acad Sci U S A* 1996;93:11085-90.
37. Liu ZG, Hsu H, Goeddel DV, Karin M. Dissection of TNF receptor 1 effector functions: JNK activation is not linked to apoptosis while NF-kappaB activation prevents cell death. *Cell* 1996;87:565-76.
38. Longnecker R, Miller CL, Miao XQ, Marchini A, Kieff E. The only domain which distinguishes Epstein-Barr virus latent membrane protein 2A (LMP2A) from LMP2B is dispensable for lymphocyte infection and growth transformation in vitro; LMP2A is therefore nonessential. *J Virol* 1992;66:6461-9.
39. Longnecker R, Kieff E. A second Epstein-Barr virus membrane protein (LMP2) is expressed in latent infection and colocalizes with LMP1. *J Virol* 1990;64:2319-26.
40. Miller CL, Lee JH, Kieff E, Longnecker R. An integral membrane protein (LMP2) blocks reactivation of Epstein-Barr virus from latency following surface immunoglobulin crosslinking. *Proc Natl Acad Sci U S A* 1994;91:772-6.
41. Portis T, Longnecker R. Epstein-Barr virus LMP2A interferes with global transcription factor regulation when expressed during B-lymphocyte development. *J Virol* 2003;77:105-14.

42. Swaminathan S, Tomkinson B, Kieff E. Recombinant Epstein-Barr virus with small RNA (EBER) genes deleted transforms lymphocytes and replicates in vitro. *Proc Natl Acad Sci U S A* 1991;88:1546-50.
43. Fu Q, He C, Mao ZR. Epstein-Barr virus interactions with the Bcl-2 protein family and apoptosis in human tumor cells. *J Zhejiang Univ Sci B* 2013;14:8-24.
44. Kitagawa N, Goto M, Kurozumi K, Maruo S, Fukayama M, Naoe T, Yasukawa M, Hino K, Suzuki T, Todo S, Takada K. Epstein-Barr virus-encoded poly(A)(-) RNA supports Burkitt's lymphoma growth through interleukin-10 induction. *EMBO J* 2000;19:6742-50.
45. Smith PR, de Jesus O, Turner D, Hollyoake M, Karstegl CE, Griffin BE, Karran L, Wang Y, Hayward SD, Farrell PJ. Structure and coding content of CST (BART) family RNAs of Epstein-Barr virus. *J Virol* 2000;74:3082-92.
46. Marshall WL, Yim C, Gustafson E, Graf T, Sage DR, Hanify K, Williams L, Fingerroth J, Finberg RW. Epstein-Barr virus encodes a novel homolog of the bcl-2 oncogene that inhibits apoptosis and associates with Bax and Bak. *J Virol* 1999;73:5181-5.
47. Nevels M, Nitzsche A, Paulus C. How to control an infectious bead string: nucleosome-based regulation and targeting of herpesvirus chromatin. *Rev Med Virol*;21:154-80.
48. Anagnostopoulos I, Hummel M, Kreschel C, Stein H. Morphology, immunophenotype, and distribution of latently and/or productively Epstein-Barr virus-infected cells in acute infectious mononucleosis: implications for the interindividual infection route of Epstein-Barr virus. *Blood* 1995;85:744-50.
49. Thorley-Lawson DA. Epstein-Barr virus: exploiting the immune system. *Nat Rev Immunol* 2001;1:75-82.
50. Kurth J, Hansmann ML, Rajewsky K, Kuppers R. Epstein-Barr virus-infected B cells expanding in germinal centers of infectious mononucleosis patients do not participate in the germinal center reaction. *Proc Natl Acad Sci U S A* 2003;100:4730-5.
51. Chaganti S, Ma CS, Bell AI, Croom-Carter D, Hislop AD, Tangye SG, Rickinson AB. Epstein-Barr virus persistence in the absence of conventional memory B cells: IgM+IgD+CD27+ B cells harbor the virus in X-linked lymphoproliferative disease patients. *Blood* 2008;112:672-9.
52. Thorley-Lawson DA, Gross A. Persistence of the Epstein-Barr virus and the origins of associated lymphomas. *N Engl J Med* 2004;350:1328-37.
53. Amon W, Farrell PJ. Reactivation of Epstein-Barr virus from latency. *Rev Med Virol* 2005;15:149-56.
54. Coskun O, Sener K, Kilic S, Erdem H, Yaman H, Besirbellioglu AB, Gul HC, Eyigun CP. Stress-related Epstein-Barr virus reactivation. *Clin Exp Med* 2009;10:15-20.
55. Pierson DL, Stowe RP, Phillips TM, Lugg DJ, Mehta SK. Epstein-Barr virus shedding by astronauts during space flight. *Brain Behav Immun* 2005;19:235-42.
56. Grinde B. Herpesviruses: latency and reactivation - viral strategies and host response. *J Oral Microbiol* 2013;5.
57. Odumade OA, Hogquist KA, Balfour HH, Jr. Progress and problems in understanding and managing primary Epstein-Barr virus infections. *Clin Microbiol Rev*;24:193-209.
58. Long HM, Taylor GS, Rickinson AB. Immune defence against EBV and EBV-associated disease. *Curr Opin Immunol* 2011;23:258-64.
59. Murphy KP, Travers P, Walport M, Janeway C. *Janeway's immunobiology*, 7th ed. New York: Garland Science, 2008.
60. Moss DJ, Burrows SR, Silins SL, Misko I, Khanna R. The immunology of Epstein-Barr virus infection. *Philos Trans R Soc Lond B Biol Sci* 2001;356:475-88.
61. Thorley-Lawson DA, Geilinger K. Monoclonal antibodies against the major glycoprotein (gp350/220) of Epstein-Barr virus neutralize infectivity. *Proc Natl Acad Sci U S A* 1980;77:5307-11.
62. Heller KN, Arrey F, Steinherz P, Portlock C, Chadburn A, Kelly K, Munz C. Patients with Epstein Barr virus-positive lymphomas have decreased CD4(+) T-cell responses to the viral nuclear antigen 1. *Int J Cancer* 2008;123:2824-31.
63. Henle G, Henle W. Epstein-Barr virus-specific IgA serum antibodies as an outstanding feature of nasopharyngeal carcinoma. *Int J Cancer* 1976;17:1-7.

64. Iizasa H, Nanbo A, Nishikawa J, Jinushi M, Yoshiyama H. Epstein-Barr Virus (EBV)-associated gastric carcinoma. *Viruses* 2012;4:3420-39.
65. Seder RA, Ahmed R. Similarities and differences in CD4+ and CD8+ effector and memory T cell generation. *Nat Immunol* 2003;4:835-42.
66. Kaech SM, Wherry EJ. Heterogeneity and cell-fate decisions in effector and memory CD8+ T cell differentiation during viral infection. *Immunity* 2007;27:393-405.
67. Hislop AD, Taylor GS, Sauce D, Rickinson AB. Cellular responses to viral infection in humans: lessons from Epstein-Barr virus. *Annu Rev Immunol* 2007;25:587-617.
68. Parish IA, Kaech SM. Diversity in CD8(+) T cell differentiation. *Curr Opin Immunol* 2009;21:291-7.
69. Hislop AD, Gudgeon NH, Callan MF, Fazou C, Hasegawa H, Salmon M, Rickinson AB. EBV-specific CD8+ T cell memory: relationships between epitope specificity, cell phenotype, and immediate effector function. *J Immunol* 2001;167:2019-29.
70. Hislop AD, Annels NE, Gudgeon NH, Leese AM, Rickinson AB. Epitope-specific evolution of human CD8(+) T cell responses from primary to persistent phases of Epstein-Barr virus infection. *J Exp Med* 2002;195:893-905.
71. Woodberry T, Suscovich TJ, Henry LM, Davis JK, Frahm N, Walker BD, Scadden DT, Wang F, Brander C. Differential targeting and shifts in the immunodominance of Epstein-Barr virus-specific CD8 and CD4 T cell responses during acute and persistent infection. *J Infect Dis* 2005;192:1513-24.
72. Chattopadhyay PK, Betts MR, Price DA, Gostick E, Horton H, Roederer M, De Rosa SC. The cytolytic enzymes granzyme A, granzyme B, and perforin: expression patterns, cell distribution, and their relationship to cell maturity and bright CD57 expression. *J Leukoc Biol* 2009;85:88-97.
73. Harari A, Bellutti Enders F, Cellera C, Bart PA, Pantaleo G. Distinct profiles of cytotoxic granules in memory CD8 T cells correlate with function, differentiation stage, and antigen exposure. *J Virol* 2009;83:2862-71.
74. Catalina MD, Sullivan JL, Brody RM, Luzuriaga K. Phenotypic and functional heterogeneity of EBV epitope-specific CD8+ T cells. *J Immunol* 2002;168:4184-91.
75. Steven NM, Annels NE, Kumar A, Leese AM, Kurilla MG, Rickinson AB. Immediate early and early lytic cycle proteins are frequent targets of the Epstein-Barr virus-induced cytotoxic T cell response. *J Exp Med* 1997;185:1605-17.
76. Callan MF, Fazou C, Yang H, Rostron T, Poon K, Hatton C, McMichael AJ. CD8(+) T-cell selection, function, and death in the primary immune response in vivo. *J Clin Invest* 2000;106:1251-61.
77. Hoshino Y, Morishima T, Kimura H, Nishikawa K, Tsurumi T, Kuzushima K. Antigen-driven expansion and contraction of CD8+-activated T cells in primary EBV infection. *J Immunol* 1999;163:5735-40.
78. Callan MF, Tan L, Annels N, Ogg GS, Wilson JD, O'Callaghan CA, Steven N, McMichael AJ, Rickinson AB. Direct visualization of antigen-specific CD8+ T cells during the primary immune response to Epstein-Barr virus in vivo. *J Exp Med* 1998;187:1395-402.
79. Pudney VA, Leese AM, Rickinson AB, Hislop AD. CD8+ immunodominance among Epstein-Barr virus lytic cycle antigens directly reflects the efficiency of antigen presentation in lytically infected cells. *J Exp Med* 2005;201:349-60.
80. Murray RJ, Kurilla MG, Brooks JM, Thomas WA, Rowe M, Kieff E, Rickinson AB. Identification of target antigens for the human cytotoxic T cell response to Epstein-Barr virus (EBV): implications for the immune control of EBV-positive malignancies. *J Exp Med* 1992;176:157-68.
81. Ning RJ, Xu XQ, Chan KH, Chiang AK. Long-term carriers generate Epstein-Barr virus (EBV)-specific CD4(+) and CD8(+) polyfunctional T-cell responses which show immunodominance hierarchies of EBV proteins. *Immunology* 2011;134:161-71.
82. Saulquin X, Ibisch C, Peyrat MA, Scotet E, Hourmant M, Vie H, Bonneville M, Houssaint E. A global appraisal of immunodominant CD8 T cell responses to Epstein-Barr virus and cytomegalovirus by bulk screening. *Eur J Immunol* 2000;30:2531-9.

83. Blake N, Haigh T, Shaka'a G, Croom-Carter D, Rickinson A. The importance of exogenous antigen in priming the human CD8+ T cell response: lessons from the EBV nuclear antigen EBNA1. *J Immunol* 2000;165:7078-87.
84. Lee SP, Tierney RJ, Thomas WA, Brooks JM, Rickinson AB. Conserved CTL epitopes within EBV latent membrane protein 2: a potential target for CTL-based tumor therapy. *J Immunol* 1997;158:3325-34.
85. Ouyang Q, Wagner WM, Walter S, Muller CA, Wikby A, Aubert G, Klatt T, Stevanovic S, Dodi T, Pawelec G. An age-related increase in the number of CD8+ T cells carrying receptors for an immunodominant Epstein-Barr virus (EBV) epitope is counteracted by a decreased frequency of their antigen-specific responsiveness. *Mech Ageing Dev* 2003;124:477-85.
86. Wan YY. Multi-tasking of helper T cells. *Immunology* 2010;130:166-71.
87. Adhikary D, Behrends U, Moosmann A, Witter K, Bornkamm GW, Mautner J. Control of Epstein-Barr virus infection in vitro by T helper cells specific for virion glycoproteins. *J Exp Med* 2006;203:995-1006.
88. Amyes E, Hatton C, Montamat-Sicotte D, Gudgeon N, Rickinson AB, McMichael AJ, Callan MF. Characterization of the CD4+ T cell response to Epstein-Barr virus during primary and persistent infection. *J Exp Med* 2003;198:903-11.
89. Long HM, Leese AM, Chagoury OL, Connerty SR, Quarcoopome J, Quinn LL, Shannon-Lowe C, Rickinson AB. Cytotoxic CD4+ T cell responses to EBV contrast with CD8 responses in breadth of lytic cycle antigen choice and in lytic cycle recognition. *J Immunol* 2011;187:92-101.
90. Precopio ML, Sullivan JL, Willard C, Somasundaran M, Luzuriaga K. Differential kinetics and specificity of EBV-specific CD4+ and CD8+ T cells during primary infection. *J Immunol* 2003;170:2590-8.
91. Leen A, Meij P, Redchenko I, Middeldorp J, Bloemena E, Rickinson A, Blake N. Differential immunogenicity of Epstein-Barr virus latent-cycle proteins for human CD4(+) T-helper 1 responses. *J Virol* 2001;75:8649-59.
92. Munz C, Bickham KL, Subklewe M, Tsang ML, Chahroudi A, Kurilla MG, Zhang D, O'Donnell M, Steinman RM. Human CD4(+) T lymphocytes consistently respond to the latent Epstein-Barr virus nuclear antigen EBNA1. *J Exp Med* 2000;191:1649-60.
93. Long HM, Haigh TA, Gudgeon NH, Leen AM, Tsang CW, Brooks J, Landais E, Houssaint E, Lee SP, Rickinson AB, Taylor GS. CD4+ T-cell responses to Epstein-Barr virus (EBV) latent-cycle antigens and the recognition of EBV-transformed lymphoblastoid cell lines. *J Virol* 2005;79:4896-907.
94. Landais E, Saulquin X, Scotet E, Trautmann L, Peyrat MA, Yates JL, Kwok WW, Bonneville M, Houssaint E. Direct killing of Epstein-Barr virus (EBV)-infected B cells by CD4 T cells directed against the EBV lytic protein BHRF1. *Blood* 2004;103:1408-16.
95. Wallace LE, Wright J, Ulaeto DO, Morgan AJ, Rickinson AB. Identification of two T-cell epitopes on the candidate Epstein-Barr virus vaccine glycoprotein gp340 recognized by CD4+ T-cell clones. *J Virol* 1991;65:3821-8.
96. White CA, Cross SM, Kurilla MG, Kerr BM, Schmidt C, Misko IS, Khanna R, Moss DJ. Recruitment during infectious mononucleosis of CD3+CD4+CD8+ virus-specific cytotoxic T cells which recognise Epstein-Barr virus lytic antigen BHRF1. *Virology* 1996;219:489-92.
97. Mackay LK, Long HM, Brooks JM, Taylor GS, Leung CS, Chen A, Wang F, Rickinson AB. T cell detection of a B-cell tropic virus infection: newly-synthesised versus mature viral proteins as antigen sources for CD4 and CD8 epitope display. *PLoS Pathog* 2009;5:e1000699.
98. Levin LI, Munger KL, O'Reilly EJ, Falk KI, Ascherio A. Primary infection with the Epstein-Barr virus and risk of multiple sclerosis. *Ann Neurol* 2010;67:824-30.
99. Chen DY, Chen YM, Lan JL, Chen HH, Hsieh CW, Wey SJ, Lu JJ. Polymyositis/dermatomyositis and nasopharyngeal carcinoma: the Epstein-Barr virus connection? *J Clin Virol* 2010;49:290-5.
100. Ferrell PB, Aitchison CT, Pearson GR, Tan EM. Seroepidemiological study of relationships between Epstein-Barr virus and rheumatoid arthritis. *J Clin Invest* 1981;67:681-7.
101. Harley JB, Harley IT, Guthridge JM, James JA. The curiously suspicious: a role for Epstein-Barr virus in lupus. *Lupus* 2006;15:768-77.

102. Lossius A, Johansen JN, Torkildsen O, Vartdal F, Holmoy T. Epstein-Barr virus in systemic lupus erythematosus, rheumatoid arthritis and multiple sclerosis-association and causation. *Viruses* 2013;4:3701-30.
103. Pender MP. Infection of autoreactive B lymphocytes with EBV, causing chronic autoimmune diseases. *Trends Immunol* 2003;24:584-8.
104. Cohen JI, Fauci AS, Varmus H, Nabel GJ. Epstein-Barr virus: an important vaccine target for cancer prevention. *Sci Transl Med* 2011;3:107fs7.
105. Carbone A, Tirelli U, Gloghini A, Volpe R, Boiocchi M. Human immunodeficiency virus-associated systemic lymphomas may be subdivided into two main groups according to Epstein-Barr viral latent gene expression. *J Clin Oncol* 1993;11:1674-81.
106. Thomas JA, Hotchin NA, Allday MJ, Amlot P, Rose M, Yacoub M, Crawford DH. Immunohistology of Epstein-Barr virus-associated antigens in B cell disorders from immunocompromised individuals. *Transplantation* 1990;49:944-53.
107. Sullivan JL, Woda BA. X-linked lymphoproliferative syndrome. *Immunodef Rev* 1989;1:325-47.
108. LaCasce AS. Post-transplant lymphoproliferative disorders. *Oncologist* 2006;11:674-80.
109. Martorelli D, Muraro E, Merlo A, Turrini R, Fae DA, Rosato A, Dolcetti R. Exploiting the interplay between innate and adaptive immunity to improve immunotherapeutic strategies for Epstein-Barr-virus-driven disorders. *Clin Dev Immunol* 2011;2012:931952.
110. Rochford R, Cannon MJ, Moormann AM. Endemic Burkitt's lymphoma: a polymicrobial disease? *Nat Rev Microbiol* 2005;3:182-7.
111. Brady G, MacArthur GJ, Farrell PJ. Epstein-Barr virus and Burkitt lymphoma. *J Clin Pathol* 2007;60:1397-402.
112. Thorley-Lawson DA, Allday MJ. The curious case of the tumour virus: 50 years of Burkitt's lymphoma. *Nat Rev Microbiol* 2008;6:913-24.
113. Guerreiro-Cacais AO, Li L, Donati D, Bejarano MT, Morgan A, Masucci MG, Hutt-Fletcher L, Levitsky V. Capacity of Epstein-Barr virus to infect monocytes and inhibit their development into dendritic cells is affected by the cell type supporting virus replication. *J Gen Virol* 2004;85:2767-78.
114. de-The G, Geser A, Day NE, Tukei PM, Williams EH, Beri DP, Smith PG, Dean AG, Bronkamm GW, Feorino P, Henle W. Epidemiological evidence for causal relationship between Epstein-Barr virus and Burkitt's lymphoma from Ugandan prospective study. *Nature* 1978;274:756-61.
115. Rowe M, Kelly GL, Bell AI, Rickinson AB. Burkitt's lymphoma: the Rosetta Stone deciphering Epstein-Barr virus biology. *Semin Cancer Biol* 2009;19:377-88.
116. Guttensohn N, Cole P. Epidemiology of Hodgkin's disease. *Semin Oncol* 1980;7:92-102.
117. Levine PH, Ablashi DV, Berard CW, Carbone PP, Waggoner DE, Malan L. Elevated antibody titers to Epstein-Barr virus in Hodgkin's disease. *Cancer* 1971;27:416-21.
118. Anagnostopoulos I, Herbst H, Niedobitek G, Stein H. Demonstration of monoclonal EBV genomes in Hodgkin's disease and Ki-1-positive anaplastic large cell lymphoma by combined Southern blot and in situ hybridization. *Blood* 1989;74:810-6.
119. Rowe M, Rickinson A. Epstein-Barr Virus and Cancer Encyclopedia of life sciences: Nature Publishing Group, 2001.
120. Chang ET, Adami HO. The enigmatic epidemiology of nasopharyngeal carcinoma. *Cancer Epidemiol Biomarkers Prev* 2006;15:1765-77.
121. Akiba S, Koriyama C, Herrera-Goepfert R, Eizuru Y. Epstein-Barr virus associated gastric carcinoma: epidemiological and clinicopathological features. *Cancer Sci* 2008;99:195-201.
122. Raab-Traub N. Epstein-Barr virus in the pathogenesis of NPC. *Semin Cancer Biol* 2002;12:431-41.
123. Junker AK. Epstein-Barr virus. *Pediatr Rev* 2005;26:79-85.
124. Uozaki H, Fukayama M. Epstein-Barr virus and gastric carcinoma--viral carcinogenesis through epigenetic mechanisms. *Int J Clin Exp Pathol* 2008;1:198-216.

125. Lo KW, Chung GT, To KF. Deciphering the molecular genetic basis of NPC through molecular, cytogenetic, and epigenetic approaches. *Semin Cancer Biol* 2012;22:79-86.
126. Tao Q, Young LS, Woodman CB, Murray PG. Epstein-Barr virus (EBV) and its associated human cancers--genetics, epigenetics, pathobiology and novel therapeutics. *Front Biosci* 2006;11:2672-713.
127. Kennedy G, Komano J, Sugden B. Epstein-Barr virus provides a survival factor to Burkitt's lymphomas. *Proc Natl Acad Sci U S A* 2003;100:14269-74.
128. Yasuda A, Noguchi K, Minoshima M, Kashiwazaki G, Kanda T, Katayama K, Mitsuhashi J, Bando T, Sugiyama H, Sugimoto Y. DNA ligand designed to antagonize EBNA1 represses Epstein-Barr virus-induced immortalization. *Cancer Sci* 2011;102:2221-30.
129. Kaul R, Murakami M, Choudhuri T, Robertson ES. Epstein-Barr virus latent nuclear antigens can induce metastasis in a nude mouse model. *J Virol* 2007;81:10352-61.
130. Murakami M, Lan K, Subramanian C, Robertson ES. Epstein-Barr virus nuclear antigen 1 interacts with Nm23-H1 in lymphoblastoid cell lines and inhibits its ability to suppress cell migration. *J Virol* 2005;79:1559-68.
131. Westhoff Smith D, Sugden B. Potential cellular functions of Epstein-Barr Nuclear Antigen 1 (EBNA1) of Epstein-Barr Virus. *Viruses* 2013;5:226-40.
132. Fogg MH, Wirth LJ, Posner M, Wang F. Decreased EBNA-1-specific CD8+ T cells in patients with Epstein-Barr virus-associated nasopharyngeal carcinoma. *Proc Natl Acad Sci U S A* 2009;106:3318-23.
133. Piriou E, van Dort K, Nanlohy NM, van Oers MH, Miedema F, van Baarle D. Loss of EBNA1-specific memory CD4+ and CD8+ T cells in HIV-infected patients progressing to AIDS-related non-Hodgkin lymphoma. *Blood* 2005;106:3166-74.
134. Moormann AM, Heller KN, Chelimo K, Embury P, Ploutz-Snyder R, Otieno JA, Oduor M, Munz C, Rochford R. Children with endemic Burkitt lymphoma are deficient in EBNA1-specific IFN-gamma T cell responses. *Int J Cancer* 2009;124:1721-6.
135. Rooney CM, Smith CA, Ng CY, Loftin S, Li C, Krance RA, Brenner MK, Heslop HE. Use of gene-modified virus-specific T lymphocytes to control Epstein-Barr-virus-related lymphoproliferation. *Lancet* 1995;345:9-13.
136. Heslop HE, Rooney CM. Adoptive cellular immunotherapy for EBV lymphoproliferative disease. *Immunol Rev* 1997;157:217-22.
137. Straathof KC, Savoldo B, Heslop HE, Rooney CM. Immunotherapy for post-transplant lymphoproliferative disease. *Br J Haematol* 2002;118:728-40.
138. Haque T, McAulay KA, Kelly D, Crawford DH. Allogeneic T-cell therapy for Epstein-Barr virus-positive posttransplant lymphoproliferative disease: long-term follow-up. *Transplantation* 2010;90:93-4.
139. Ghosh SK, Perrine SP, Williams RM, Faller DV. Histone deacetylase inhibitors are potent inducers of gene expression in latent EBV and sensitize lymphoma cells to nucleoside antiviral agents. *Blood* 2012;119:1008-17.
140. Finco O, Rappuoli R. Designing Vaccines for the Twenty-First Century Society. *Front Immunol* 2013;5:12.
141. Kang SM, Compans RW. Host responses from innate to adaptive immunity after vaccination: molecular and cellular events. *Mol Cells* 2009;27:5-14.
142. Nabel GJ. Designing tomorrow's vaccines. *N Engl J Med* 2013;368:551-60.
143. Morgan AJ. Epstein-Barr virus vaccines. *Vaccine* 1992;10:563-71.
144. Harrop R, John J, Carroll MW. Recombinant viral vectors: cancer vaccines. *Adv Drug Deliv Rev* 2006;58:931-47.
145. Lukashok SA, Horwitz MS. New perspectives in adenoviruses. *Curr Clin Top Infect Dis* 1998;18:286-305.
146. Haj-Ahmad Y, Graham FL. Development of a helper-independent human adenovirus vector and its use in the transfer of the herpes simplex virus thymidine kinase gene. *J Virol* 1986;57:267-74.
147. Wilson JM. Adenoviruses as gene-delivery vehicles. *N Engl J Med* 1996;334:1185-7.

148. Kootstra NA, Verma IM. Gene therapy with viral vectors. *Annu Rev Pharmacol Toxicol* 2003;43:413-39.
149. Yang Y, Jooss KU, Su Q, Ertl HC, Wilson JM. Immune responses to viral antigens versus transgene product in the elimination of recombinant adenovirus-infected hepatocytes in vivo. *Gene Ther* 1996;3:137-44.
150. Raper SE, Chirmule N, Lee FS, Wivel NA, Bagg A, Gao GP, Wilson JM, Batshaw ML. Fatal systemic inflammatory response syndrome in a ornithine transcarbamylase deficient patient following adenoviral gene transfer. *Mol Genet Metab* 2003;80:148-58.
151. Yang Y, Su Q, Wilson JM. Role of viral antigens in destructive cellular immune responses to adenovirus vector-transduced cells in mouse lungs. *J Virol* 1996;70:7209-12.
152. Molinier-Frenkel V, Lengagne R, Gaden F, Hong SS, Choppin J, Gahery-Segard H, Boulanger P, Guillet JG. Adenovirus hexon protein is a potent adjuvant for activation of a cellular immune response. *J Virol* 2002;76:127-35.
153. Tatsis N, Fitzgerald JC, Reyes-Sandoval A, Harris-McCoy KC, Hensley SE, Zhou D, Lin SW, Bian A, Xiang ZQ, Iparraguirre A, Lopez-Camacho C, Wherry EJ, et al. Adenoviral vectors persist in vivo and maintain activated CD8+ T cells: implications for their use as vaccines. *Blood* 2007;110:1916-23.
154. Xiang ZQ, Yang Y, Wilson JM, Ertl HC. A replication-defective human adenovirus recombinant serves as a highly efficacious vaccine carrier. *Virology* 1996;219:220-7.
155. Tatsis N, Ertl HC. Adenoviruses as vaccine vectors. *Mol Ther* 2004;10:616-29.
156. Casimiro DR, Chen L, Fu TM, Evans RK, Caulfield MJ, Davies ME, Tang A, Chen M, Huang L, Harris V, Freed DC, Wilson KA, et al. Comparative immunogenicity in rhesus monkeys of DNA plasmid, recombinant vaccinia virus, and replication-defective adenovirus vectors expressing a human immunodeficiency virus type 1 gag gene. *J Virol* 2003;77:6305-13.
157. Farina SF, Gao GP, Xiang ZQ, Rux JJ, Burnett RM, Alvira MR, Marsh J, Ertl HC, Wilson JM. Replication-defective vector based on a chimpanzee adenovirus. *J Virol* 2001;75:11603-13.
158. McCoy K, Tatsis N, Koriath-Schmitz B, Lasaro MO, Hensley SE, Lin SW, Li Y, Giles-Davis W, Cun A, Zhou D, Xiang Z, Letvin NL, et al. Effect of preexisting immunity to adenovirus human serotype 5 antigens on the immune responses of nonhuman primates to vaccine regimens based on human- or chimpanzee-derived adenovirus vectors. *J Virol* 2007;81:6594-604.
159. Tatsis N, Lasaro MO, Lin SW, Haut LH, Xiang ZQ, Zhou D, Dimenna L, Li H, Bian A, Abdulla S, Li Y, Giles-Davis W, et al. Adenovirus vector-induced immune responses in nonhuman primates: responses to prime boost regimens. *J Immunol* 2009;182:6587-99.
160. Holterman L, Vogels R, van der Vlugt R, Sieuwerts M, Grimbergen J, Kaspers J, Geelen E, van der Helm E, Lemckert A, Gillissen G, Verhaagh S, Custers J, et al. Novel replication-incompetent vector derived from adenovirus type 11 (Ad11) for vaccination and gene therapy: low seroprevalence and non-cross-reactivity with Ad5. *J Virol* 2004;78:13207-15.
161. Vogels R, Zuijdsgeest D, van Rijnsoever R, Hartkoorn E, Damen I, de Bethune MP, Kostense S, Penders G, Helmus N, Koudstaal W, Cecchini M, Wetterwald A, et al. Replication-deficient human adenovirus type 35 vectors for gene transfer and vaccination: efficient human cell infection and bypass of preexisting adenovirus immunity. *J Virol* 2003;77:8263-71.
162. Tatsis N, Tesema L, Robinson ER, Giles-Davis W, McCoy K, Gao GP, Wilson JM, Ertl HC. Chimpanzee-origin adenovirus vectors as vaccine carriers. *Gene Ther* 2006;13:421-9.
163. Fitzgerald JC, Gao GP, Reyes-Sandoval A, Pavlakis GN, Xiang ZQ, Wlazlo AP, Giles-Davis W, Wilson JM, Ertl HC. A simian replication-defective adenoviral recombinant vaccine to HIV-1 gag. *J Immunol* 2003;170:1416-22.
164. Pinto AR, Fitzgerald JC, Giles-Davis W, Gao GP, Wilson JM, Ertl HC. Induction of CD8+ T cells to an HIV-1 antigen through a prime boost regimen with heterologous E1-deleted adenoviral vaccine carriers. *J Immunol* 2003;171:6774-9.
165. Sridhar S, Reyes-Sandoval A, Draper SJ, Moore AC, Gilbert SC, Gao GP, Wilson JM, Hill AV. Single-dose protection against *Plasmodium berghei* by a simian adenovirus vector using a human cytomegalovirus promoter containing intron A. *J Virol* 2008;82:3822-33.

166. Zhou D, Cun A, Li Y, Xiang Z, Ertl HC. A chimpanzee-origin adenovirus vector expressing the rabies virus glycoprotein as an oral vaccine against inhalation infection with rabies virus. *Mol Ther* 2006;14:662-72.
167. Chen H, Xiang ZQ, Li Y, Kurupati RK, Jia B, Bian A, Zhou DM, Hutnick N, Yuan S, Gray C, Serwanga J, Auma B, et al. Adenovirus-based vaccines: comparison of vectors from three species of adenoviridae. *J Virol* 2010;84:10522-32.
168. Hjalgrim H, Askling J, Rostgaard K, Hamilton-Dutoit S, Frisch M, Zhang JS, Madsen M, Rosdahl N, Konradsen HB, Storm HH, Melbye M. Characteristics of Hodgkin's lymphoma after infectious mononucleosis. *N Engl J Med* 2003;349:1324-32.
169. Sauce D, Larsen M, Curnow SJ, Leese AM, Moss PA, Hislop AD, Salmon M, Rickinson AB. EBV-associated mononucleosis leads to long-term global deficit in T-cell responsiveness to IL-15. *Blood* 2006;108:11-8.
170. Hjalgrim H, Askling J, Sorensen P, Madsen M, Rosdahl N, Storm HH, Hamilton-Dutoit S, Eriksen LS, Frisch M, Ekbom A, Melbye M. Risk of Hodgkin's disease and other cancers after infectious mononucleosis. *J Natl Cancer Inst* 2000;92:1522-8.
171. North JR, Morgan AJ, Thompson JL, Epstein MA. Purified Epstein-Barr virus Mr 340,000 glycoprotein induces potent virus-neutralizing antibodies when incorporated in liposomes. *Proc Natl Acad Sci U S A* 1982;79:7504-8.
172. Haque T, Johannessen I, Dombagoda D, Sengupta C, Burns DM, Bird P, Hale G, Mieli-Vergani G, Crawford DH. A mouse monoclonal antibody against Epstein-Barr virus envelope glycoprotein 350 prevents infection both in vitro and in vivo. *J Infect Dis* 2006;194:584-7.
173. Cui X, Cao Z, Sen G, Chattopadhyay G, Fuller DH, Fuller JT, Snapper DM, Snow AL, Mond JJ, Snapper CM. A novel tetrameric gp350 1-470 as a potential Epstein-Barr virus vaccine. *Vaccine* 2013;31:3039-45.
174. Ragot T, Finerty S, Watkins PE, Perricaudet M, Morgan AJ. Replication-defective recombinant adenovirus expressing the Epstein-Barr virus (EBV) envelope glycoprotein gp340/220 induces protective immunity against EBV-induced lymphomas in the cottontop tamarin. *J Gen Virol* 1993;74 (Pt 3):501-7.
175. Emini EA, Schleif WA, Silberklang M, Lehman D, Ellis RW. Vero cell-expressed Epstein-Barr virus (EBV) gp350/220 protects marmosets from EBV challenge. *J Med Virol* 1989;27:120-3.
176. Epstein MA, Morgan AJ, Finerty S, Randle BJ, Kirkwood JK. Protection of cottontop tamarins against Epstein-Barr virus-induced malignant lymphoma by a prototype subunit vaccine. *Nature* 1985;318:287-9.
177. Morgan AJ, Mackett M, Finerty S, Arrand JR, Scullion FT, Epstein MA. Recombinant vaccinia virus expressing Epstein-Barr virus glycoprotein gp340 protects cottontop tamarins against EB virus-induced malignant lymphomas. *J Med Virol* 1988;25:189-95.
178. Gu SY, Huang TM, Ruan L, Miao YH, Lu H, Chu CM, Motz M, Wolf H. First EBV vaccine trial in humans using recombinant vaccinia virus expressing the major membrane antigen. *Dev Biol Stand* 1995;84:171-7.
179. Rees L, Tizard EJ, Morgan AJ, Cubitt WD, Finerty S, Oyewole-Eletu TA, Owen K, Royed C, Stevens SJ, Shroff RC, Tanday MK, Wilson AD, et al. A phase I trial of Epstein-Barr virus gp350 vaccine for children with chronic kidney disease awaiting transplantation. *Transplantation* 2009;88:1025-9.
180. Sokal EM, Hoppenbrouwers K, Vandermeulen C, Moutschen M, Leonard P, Moreels A, Haumont M, Bollen A, Smets F, Denis M. Recombinant gp350 vaccine for infectious mononucleosis: a phase 2, randomized, double-blind, placebo-controlled trial to evaluate the safety, immunogenicity, and efficacy of an Epstein-Barr virus vaccine in healthy young adults. *J Infect Dis* 2007;196:1749-53.
181. Elliott SL, Suhrbier A, Miles JJ, Lawrence G, Pye SJ, Le TT, Rosenstengel A, Nguyen T, Allworth A, Burrows SR, Cox J, Pye D, et al. Phase I trial of a CD8+ T-cell peptide epitope-based vaccine for infectious mononucleosis. *J Virol* 2008;82:1448-57.

182. Liu G, Yao K, Wang B, Zhou F, Chen Y, Li L, Chi J, Peng G. Reconstituted complexes of mycobacterial HSP70 and EBV LMP2A-derived peptides elicit peptide-specific cytotoxic T lymphocyte responses and anti-tumor immunity. *Vaccine* 2011;29:7414-23.
183. Ruiss R, Jochum S, Wanner G, Reisbach G, Hammerschmidt W, Zeidler R. A virus-like particle-based Epstein-Barr virus vaccine. *J Virol* 2011;85:13105-13.
184. Lutzky VP, Corban M, Heslop L, Morrison LE, Crooks P, Hall DF, Coman WB, Thomson SA, Moss DJ. Novel approach to the formulation of an Epstein-Barr virus antigen-based nasopharyngeal carcinoma vaccine. *J Virol* 2010;84:407-17.
185. Akkina R. New generation humanized mice for virus research: comparative aspects and future prospects. *Virology* 2013;435:14-28.
186. Wang F. Nonhuman primate models for Epstein-Barr virus infection. *Curr Opin Virol* 2013;3:233-7.
187. Wang F. A new animal model for Epstein-Barr virus pathogenesis. *Curr Top Microbiol Immunol* 2001;258:201-19.
188. Orlova N, Wang F, Fogg MH. Persistent infection drives the development of CD8+ T cells specific for late lytic infection antigens in lymphocryptovirus-infected macaques and Epstein-Barr virus-infected humans. *J Virol* 2011;85:12821-4.
189. Ruf IK, Moghaddam A, Wang F, Sample J. Mechanisms that regulate Epstein-Barr virus EBNA-1 gene transcription during restricted latency are conserved among lymphocryptoviruses of Old World primates. *J Virol* 1999;73:1980-9.
190. Carville A, Mansfield KG. Comparative pathobiology of macaque lymphocryptoviruses. *Comp Med* 2008;58:57-67.
191. Rivaller P, Carville A, Kaur A, Rao P, Quink C, Kutok JL, Westmoreland S, Klumpp S, Simon M, Aster JC, Wang F. Experimental rhesus lymphocryptovirus infection in immunosuppressed macaques: an animal model for Epstein-Barr virus pathogenesis in the immunosuppressed host. *Blood* 2004;104:1482-9.
192. Rivaller P, Jiang H, Cho YG, Quink C, Wang F. Complete nucleotide sequence of the rhesus lymphocryptovirus: genetic validation for an Epstein-Barr virus animal model. *J Virol* 2002;76:421-6.
193. Wang F, Rivaller P, Rao P, Cho Y. Simian homologues of Epstein-Barr virus. *Philos Trans R Soc Lond B Biol Sci* 2001;356:489-97.
194. Dantuma NP, Sharipo A, Masucci MG. Avoiding proteasomal processing: the case of EBNA1. *Curr Top Microbiol Immunol* 2002;269:23-36.
195. Levitskaya J, Sharipo A, Leonchiks A, Ciechanover A, Masucci MG. Inhibition of ubiquitin/proteasome-dependent protein degradation by the Gly-Ala repeat domain of the Epstein-Barr virus nuclear antigen 1. *Proc Natl Acad Sci U S A* 1997;94:12616-21.
196. Tellam JT, Lekieffre L, Zhong J, Lynn DJ, Khanna R. Messenger RNA sequence rather than protein sequence determines the level of self-synthesis and antigen presentation of the EBV-encoded antigen, EBNA1. *PLoS Pathog* 2012;8:e1003112.
197. Tellam J, Connolly G, Green KJ, Miles JJ, Moss DJ, Burrows SR, Khanna R. Endogenous presentation of CD8+ T cell epitopes from Epstein-Barr virus-encoded nuclear antigen 1. *J Exp Med* 2004;199:1421-31.
198. Voo KS, Fu T, Wang HY, Tellam J, Heslop HE, Brenner MK, Rooney CM, Wang RF. Evidence for the presentation of major histocompatibility complex class I-restricted Epstein-Barr virus nuclear antigen 1 peptides to CD8+ T lymphocytes. *J Exp Med* 2004;199:459-70.
199. Lee SP, Brooks JM, Al-Jarrah H, Thomas WA, Haigh TA, Taylor GS, Humme S, Schepers A, Hammerschmidt W, Yates JL, Rickinson AB, Blake NW. CD8 T cell recognition of endogenously expressed Epstein-Barr virus nuclear antigen 1. *J Exp Med* 2004;199:1409-20.
200. Chia WK, Wang WW, Teo M, Tai WM, Lim WT, Tan EH, Leong SS, Sun L, Chen JJ, Gottschalk S, Toh HC. A phase II study evaluating the safety and efficacy of an adenovirus-DeltaLMP1-LMP2 transduced dendritic cell vaccine in patients with advanced metastatic nasopharyngeal carcinoma. *Ann Oncol* 2011;23:997-1005.
201. Lin CL, Lo WF, Lee TH, Ren Y, Hwang SL, Cheng YF, Chen CL, Chang YS, Lee SP, Rickinson AB, Tam PK. Immunization with Epstein-Barr Virus (EBV) peptide-pulsed dendritic

- cells induces functional CD8+ T-cell immunity and may lead to tumor regression in patients with EBV-positive nasopharyngeal carcinoma. *Cancer Res* 2002;62:6952-8.
202. Sivachandran N, Wang X, Frappier L. Functions of the Epstein-Barr virus EBNA1 protein in viral reactivation and lytic infection. *J Virol* 2012;86:6146-58.
203. Munz C. Epstein-barr virus nuclear antigen 1: from immunologically invisible to a promising T cell target. *J Exp Med* 2004;199:1301-4.
204. Kariya Y, Hamatake M, Urano E, Yoshiyama H, Shimizu N, Komano J. Dominant-negative derivative of EBNA1 represses EBNA1-mediated transforming gene expression during the acute phase of Epstein-Barr virus infection independent of rapid loss of viral genome. *Cancer Sci* 2009.
205. Nasimuzzaman M, Kuroda M, Dohno S, Yamamoto T, Iwatsuki K, Matsuzaki S, Mohammad R, Kumita W, Mizuguchi H, Hayakawa T, Nakamura H, Taguchi T, et al. Eradication of Epstein-Barr virus episome and associated inhibition of infected tumor cell growth by adenovirus vector-mediated transduction of dominant-negative EBNA1. *Mol Ther* 2005;11:578-90.
206. Yin Q, Flemington EK. siRNAs against the Epstein Barr virus latency replication factor, EBNA1, inhibit its function and growth of EBV-dependent tumor cells. *Virology* 2006;346:385-93.
207. Apcher S, Komarova A, Daskalogianni C, Yin Y, Malbert-Colas L, Fahraeus R. mRNA translation regulation by the Gly-Ala repeat of Epstein-Barr virus nuclear antigen 1. *J Virol* 2009;83:1289-98.
208. Schubert U, Anton LC, Gibbs J, Norbury CC, Yewdell JW, Bennink JR. Rapid degradation of a large fraction of newly synthesized proteins by proteasomes. *Nature* 2000;404:770-4.
209. Nikiforow S, Bottomly K, Miller G, Munz C. Cytolytic CD4(+)-T-cell clones reactive to EBNA1 inhibit Epstein-Barr virus-induced B-cell proliferation. *J Virol* 2003;77:12088-104.
210. Yi JS, Cox MA, Zajac AJ. T-cell exhaustion: characteristics, causes and conversion. *Immunology* 2010;129:474-81.
211. Mueller SN, Ahmed R. High antigen levels are the cause of T cell exhaustion during chronic viral infection. *Proc Natl Acad Sci U S A* 2009;106:8623-8.
212. Wherry EJ, Blattman JN, Murali-Krishna K, van der Most R, Ahmed R. Viral persistence alters CD8 T-cell immunodominance and tissue distribution and results in distinct stages of functional impairment. *J Virol* 2003;77:4911-27.
213. Obar JJ, Fuse S, Leung EK, Bellfy SC, Usherwood EJ. Gammaherpesvirus persistence alters key CD8 T-cell memory characteristics and enhances antiviral protection. *J Virol* 2006;80:8303-15.
214. Blackburn SD, Shin H, Haining WN, Zou T, Workman CJ, Polley A, Betts MR, Freeman GJ, Vignali DA, Wherry EJ. Coregulation of CD8+ T cell exhaustion by multiple inhibitory receptors during chronic viral infection. *Nat Immunol* 2009;10:29-37.
215. Fogg MH, Kaur A, Cho YG, Wang F. The CD8+ T-cell response to an Epstein-Barr virus-related gammaherpesvirus infecting rhesus macaques provides evidence for immune evasion by the EBNA-1 homologue. *J Virol* 2005;79:12681-91.
216. Elliott SL, Pye SJ, Schmidt C, Cross SM, Silins SL, Misko IS. Dominant cytotoxic T lymphocyte response to the immediate-early trans-activator protein, BZLF1, in persistent type A or B Epstein-Barr virus infection. *J Infect Dis* 1997;176:1068-72.
217. Fogg MH, Garry D, Awad A, Wang F, Kaur A. The BZLF1 homolog of an Epstein-Barr-related gamma-herpesvirus is a frequent target of the CTL response in persistently infected rhesus macaques. *J Immunol* 2006;176:3391-401.
218. Kannanganat S, Ibegbu C, Chennareddi L, Robinson HL, Amara RR. Multiple-cytokine-producing antiviral CD4 T cells are functionally superior to single-cytokine-producing cells. *J Virol* 2007;81:8468-76.
219. Precopio ML, Betts MR, Parrino J, Price DA, Gostick E, Ambrozak DR, Asher TE, Douek DC, Harari A, Pantaleo G, Bailer R, Graham BS, et al. Immunization with vaccinia virus induces polyfunctional and phenotypically distinctive CD8(+) T cell responses. *J Exp Med* 2007;204:1405-16.

220. Hong JJ, Amancha PK, Rogers K, Ansari AA, Villinger F. Re-evaluation of PD-1 expression by T cells as a marker for immune exhaustion during SIV infection. *PLoS One* 2013;8:e60186.
221. Greenough TC, Campellone SC, Brody R, Jain S, Sanchez-Merino V, Somasundaran M, Luzuriaga K. Programmed Death-1 expression on Epstein Barr virus specific CD8+ T cells varies by stage of infection, epitope specificity, and T-cell receptor usage. *PLoS One* 2010;5:e12926.
222. Stuber G, Dillner J, Modrow S, Wolf H, Szekely L, Klein G, Klein E. HLA-A0201 and HLA-B7 binding peptides in the EBV-encoded EBNA-1, EBNA-2 and BZLF-1 proteins detected in the MHC class I stabilization assay. Low proportion of binding motifs for several HLA class I alleles in EBNA-1. *Int Immunol* 1995;7:653-63.
223. Subklewe M, Chahroudi A, Bickham K, Larsson M, Kurilla MG, Bhardwaj N, Steinman RM. Presentation of epstein-barr virus latency antigens to CD8(+), interferon-gamma-secreting, T lymphocytes. *Eur J Immunol* 1999;29:3995-4001.
224. Bickham K, Munz C, Tsang ML, Larsson M, Fonteneau JF, Bhardwaj N, Steinman R. EBNA1-specific CD4+ T cells in healthy carriers of Epstein-Barr virus are primarily Th1 in function. *J Clin Invest* 2001;107:121-30.
225. Houssaint E, Saulquin X, Scotet E, Bonneville M. Immunodominant CD8 T cell response to Epstein-Barr virus. *Biomed Pharmacother* 2001;55:373-80.
226. Tan LC, Gudgeon N, Annels NE, Hansasuta P, O'Callaghan CA, Rowland-Jones S, McMichael AJ, Rickinson AB, Callan MF. A re-evaluation of the frequency of CD8+ T cells specific for EBV in healthy virus carriers. *J Immunol* 1999;162:1827-35.
227. Heller KN, Upshaw J, Seyoum B, Zebroski H, Munz C. Distinct memory CD4+ T-cell subsets mediate immune recognition of Epstein Barr virus nuclear antigen 1 in healthy virus carriers. *Blood* 2007;109:1138-46.
228. Guerreiro M, Na IK, Letsch A, Haase D, Bauer S, Meisel C, Roemhild A, Reinke P, Volk HD, Scheibenbogen C. Human peripheral blood and bone marrow Epstein-Barr virus-specific T-cell repertoire in latent infection reveals distinct memory T-cell subsets. *Eur J Immunol* 2010;40:1566-76.
229. Rosignoli G, Lim CH, Bower M, Gotch F, Imami N. Programmed death (PD)-1 molecule and its ligand PD-L1 distribution among memory CD4 and CD8 T cell subsets in human immunodeficiency virus-1-infected individuals. *Clin Exp Immunol* 2009;157:90-7.
230. Salisch NC, Kaufmann DE, Awad AS, Reeves RK, Tighe DP, Li Y, Piatak M, Jr., Lifson JD, Evans DT, Pereyra F, Freeman GJ, Johnson RP. Inhibitory TCR coreceptor PD-1 is a sensitive indicator of low-level replication of SIV and HIV-1. *J Immunol* 2010;184:476-87.
231. Hokey DA, Johnson FB, Smith J, Weber JL, Yan J, Hirao L, Boyer JD, Lewis MG, Makedonas G, Betts MR, Weiner DB. Activation drives PD-1 expression during vaccine-specific proliferation and following lentiviral infection in macaques. *Eur J Immunol* 2008;38:1435-45.
232. Petrovas C, Price DA, Mattapallil J, Ambrozak DR, Geldmacher C, Cecchinato V, Vaccari M, Trzyniszewska E, Gostick E, Roederer M, Douek DC, Morgan SH, et al. SIV-specific CD8+ T cells express high levels of PD1 and cytokines but have impaired proliferative capacity in acute and chronic SIVmac251 infection. *Blood* 2007;110:928-36.
233. Day CL, Kaufmann DE, Kiepiela P, Brown JA, Moodley ES, Reddy S, Mackey EW, Miller JD, Leslie AJ, DePierres C, Mncube Z, Duraiswamy J, et al. PD-1 expression on HIV-specific T cells is associated with T-cell exhaustion and disease progression. *Nature* 2006;443:350-4.
234. Petrovas C, Casazza JP, Brenchley JM, Price DA, Gostick E, Adams WC, Precopio ML, Schacker T, Roederer M, Douek DC, Koup RA. PD-1 is a regulator of virus-specific CD8+ T cell survival in HIV infection. *J Exp Med* 2006;203:2281-92.
235. Sugano N, Ikeda K, Oshikawa M, Idesawa M, Tanaka H, Sato S, Ito K. Relationship between *Porphyromonas gingivalis*, Epstein-Barr virus infection and reactivation in periodontitis. *J Oral Sci* 2004;46:203-6.
236. Angelini DF, Serafini B, Piras E, Severa M, Coccia EM, Rosicarelli B, Ruggieri S, Gasperini C, Buttari F, Centonze D, Mechelli R, Salvetti M, et al. Increased CD8+ T Cell

- Response to Epstein-Barr Virus Lytic Antigens in the Active Phase of Multiple Sclerosis. *PLoS Pathog*;9:e1003220.
237. Glaser R, Pearl DK, Kiecolt-Glaser JK, Malarkey WB. Plasma cortisol levels and reactivation of latent Epstein-Barr virus in response to examination stress. *Psychoneuroendocrinology* 1994;19:765-72.
238. Stowe RP, Pierson DL, Feedback DL, Barrett AD. Stress-induced reactivation of Epstein-Barr virus in astronauts. *Neuroimmunomodulation* 2000;8:51-8.
239. Minhas V, Brayfield BP, Crabtree KL, Kankasa C, Mitchell CD, Wood C. Primary gamma-herpesviral infection in Zambian children. *BMC Infect Dis*;10:115.
240. Scherrenburg J, Piriou ER, Nanlohy NM, van Baarle D. Detailed analysis of Epstein-Barr virus-specific CD4+ and CD8+ T cell responses during infectious mononucleosis. *Clin Exp Immunol* 2008;153:231-9.
241. Chattopadhyay PK, Chelimo K, Embury PB, Mulama DH, Sumba PO, Gostick E, Ladell K, Brodie TM, Vulule J, Roederer M, Moormann AM, Price DA. Holoendemic malaria exposure is associated with altered Epstein-Barr virus-specific CD8(+) T-cell differentiation. *J Virol*;87:1779-88.
242. Cao SM, Simons MJ, Qian CN. The prevalence and prevention of nasopharyngeal carcinoma in China. *Chin J Cancer* 2011;30:114-9.
243. Henle W, Henle G. The Epstein-Barr Virus (EBV) in Burkitt's lymphoma and nasopharyngeal carcinoma. *Ann Clin Lab Sci* 1974;4:109-14.
244. Tempera I, Klichinsky M, Lieberman PM. EBV latency types adopt alternative chromatin conformations. *PLoS Pathog* 2011;7:e1002180.
245. Leight ER, Sugden B. EBNA-1: a protein pivotal to latent infection by Epstein-Barr virus. *Rev Med Virol* 2000;10:83-100.
246. Frappier L. Contributions of Epstein-Barr nuclear antigen 1 (EBNA1) to cell immortalization and survival. *Viruses* 2012;4:1537-47.
247. Lasaro MO, Tatsis N, Hensley SE, Whitbeck JC, Lin SW, Rux JJ, Wherry EJ, Cohen GH, Eisenberg RJ, Ertl HC. Targeting of antigen to the herpesvirus entry mediator augments primary adaptive immune responses. *Nat Med* 2008;14:205-12.
248. Connolly SA, Landsburg DJ, Carfi A, Wiley DC, Cohen GH, Eisenberg RJ. Structure-based mutagenesis of herpes simplex virus glycoprotein D defines three critical regions at the gD-HveA/HVEM binding interface. *J Virol* 2003;77:8127-40.
249. Rajcani J, Vojvodova A. The role of herpes simplex virus glycoproteins in the virus replication cycle. *Acta Virol* 1998;42:103-18.
250. Stiles KM, Whitbeck JC, Lou H, Cohen GH, Eisenberg RJ, Krummenacher C. Herpes simplex virus glycoprotein D interferes with binding of herpesvirus entry mediator to its ligands through downregulation and direct competition. *J Virol* 2010;84:11646-60.
251. Reyes-Sandoval A, Fitzgerald JC, Grant R, Roy S, Xiang ZQ, Li Y, Gao GP, Wilson JM, Ertl HC. Human immunodeficiency virus type 1-specific immune responses in primates upon sequential immunization with adenoviral vaccine carriers of human and simian serotypes. *J Virol* 2004;78:7392-9.
252. Schneider J, Gilbert SC, Hannan CM, Degano P, Prieur E, Sheu EG, Plebanski M, Hill AV. Induction of CD8+ T cells using heterologous prime-boost immunisation strategies. *Immunol Rev* 1999;170:29-38.
253. Lasaro MO, Ertl HC. New insights on adenovirus as vaccine vectors. *Mol Ther* 2009;17:1333-9.
254. Xiang Z, Li Y, Cun A, Yang W, Ellenberg S, Switzer WM, Kalish ML, Ertl HC. Chimpanzee adenovirus antibodies in humans, sub-Saharan Africa. *Emerg Infect Dis* 2006;12:1596-9.
255. Barnes E, Folgori A, Capone S, Swadling L, Aston S, Kurioka A, Meyer J, Huddart R, Smith K, Townsend R, Brown A, Antrobus R, et al. Novel adenovirus-based vaccines induce broad and sustained T cell responses to HCV in man. *Sci Transl Med* 2012;4:115ra1.
256. Moghaddam A, Rosenzweig M, Lee-Parritz D, Annis B, Johnson RP, Wang F. An animal model for acute and persistent Epstein-Barr virus infection. *Science* 1997;276:2030-3.

257. Leskowicz RM, Zhou XY, Villinger F, Fogg MH, Kaur A, Lieberman PM, Wang F, Ertl HC. CD4+ and CD8+ T-Cell Responses to Latent Antigen EBNA-1 and Lytic Antigen BZLF-1 during Persistent Lymphocryptovirus Infection of Rhesus Macaques. *J Virol* 2013;87:8351-62.
258. Khanolkar A, Yagita H, Cannon MJ. Preferential utilization of the perforin/granzyme pathway for lysis of Epstein-Barr virus-transformed lymphoblastoid cells by virus-specific CD4+ T cells. *Virology* 2001;287:79-88.
259. Gudgeon NH, Taylor GS, Long HM, Haigh TA, Rickinson AB. Regression of Epstein-Barr virus-induced B-cell transformation in vitro involves virus-specific CD8+ T cells as the principal effectors and a novel CD4+ T-cell reactivity. *J Virol* 2005;79:5477-88.
260. Shin H, Wherry EJ. CD8 T cell dysfunction during chronic viral infection. *Curr Opin Immunol* 2007;19:408-15.
261. Haigh TA, Lin X, Jia H, Hui EP, Chan AT, Rickinson AB, Taylor GS. EBV latent membrane proteins (LMPs) 1 and 2 as immunotherapeutic targets: LMP-specific CD4+ cytotoxic T cell recognition of EBV-transformed B cell lines. *J Immunol* 2008;180:1643-54.
262. Sun Q, Burton RL, Lucas KG. Cytokine production and cytolytic mechanism of CD4(+) cytotoxic T lymphocytes in ex vivo expanded therapeutic Epstein-Barr virus-specific T-cell cultures. *Blood* 2002;99:3302-9.
263. Paludan C, Bickham K, Nikiforow S, Tsang ML, Goodman K, Hanekom WA, Fonteneau JF, Stevanovic S, Munz C. Epstein-Barr nuclear antigen 1-specific CD4(+) Th1 cells kill Burkitt's lymphoma cells. *J Immunol* 2002;169:1593-603.
264. Ohashi M, Fogg MH, Orlova N, Quink C, Wang F. An Epstein-Barr virus encoded inhibitor of Colony Stimulating Factor-1 signaling is an important determinant for acute and persistent EBV infection. *PLoS Pathog* 2012;8:e1003095.
265. Rao P, Jiang H, Wang F. Cloning of the rhesus lymphocryptovirus viral capsid antigen and Epstein-Barr virus-encoded small RNA homologues and use in diagnosis of acute and persistent infections. *J Clin Microbiol* 2000;38:3219-25.
266. Silveira EL, Fogg MH, Leskowicz RM, Ertl HC, Wiseman RW, O'Connor DH, Lieberman P, Wang F, Villinger F. Therapeutic vaccination against rhEBNA-1 elicits T cell responses to novel epitopes in rhesus macaques. *J Virol* 2013.
267. Smith C, Tsang J, Beagley L, Chua D, Lee V, Li V, Moss DJ, Coman W, Chan KH, Nicholls J, Kwong D, Khanna R. Effective treatment of metastatic forms of Epstein-Barr virus-associated nasopharyngeal carcinoma with a novel adenovirus-based adoptive immunotherapy. *Cancer Res* 2012;72:1116-25.
268. Louis CU, Straathof K, Bollard CM, Ennamuri S, Gerken C, Lopez TT, Huls MH, Sheehan A, Wu MF, Liu H, Gee A, Brenner MK, et al. Adoptive transfer of EBV-specific T cells results in sustained clinical responses in patients with locoregional nasopharyngeal carcinoma. *J Immunother* 2010;33:983-90.
269. Jones K, Nourse JP, Morrison L, Nguyen-Van D, Moss DJ, Burrows SR, Gandhi MK. Expansion of EBNA1-specific effector T cells in posttransplantation lymphoproliferative disorders. *Blood* 2010;116:2245-52.
270. Moutschen M, Leonard P, Sokal EM, Smets F, Haumont M, Mazzu P, Bollen A, Denamur F, Peeters P, Dubin G, Denis M. Phase I/II studies to evaluate safety and immunogenicity of a recombinant gp350 Epstein-Barr virus vaccine in healthy adults. *Vaccine* 2007;25:4697-705.
271. Kanakry JA, Ambinder RF. EBV-related lymphomas: new approaches to treatment. *Curr Treat Options Oncol* 2013;14:224-36.
272. Comoli P, Pedrazzoli P, Maccario R, Basso S, Carminati O, Labirio M, Schiavo R, Secondino S, Frasson C, Perotti C, Moroni M, Locatelli F, et al. Cell therapy of stage IV nasopharyngeal carcinoma with autologous Epstein-Barr virus-targeted cytotoxic T lymphocytes. *J Clin Oncol* 2005;23:8942-9.
273. Li F, Song D, Lu Y, Zhu H, Chen Z, He X. Delayed-type hypersensitivity (DTH) immune response related with EBV-DNA in nasopharyngeal carcinoma treated with autologous dendritic cell vaccination after radiotherapy. *J Immunother* 2013;36:208-14.

274. Mackay LK, Wakim L, van Vliet CJ, Jones CM, Mueller SN, Bannard O, Fearon DT, Heath WR, Carbone FR. Maintenance of T cell function in the face of chronic antigen stimulation and repeated reactivation for a latent virus infection. *J Immunol* 2012;188:2173-8.
275. Seckert CK, Griessl M, Buttner JK, Scheller S, Simon CO, Kropp KA, Renzaho A, Kuhnappel B, Grzimek NK, Reddehase MJ. Viral latency drives 'memory inflation': a unifying hypothesis linking two hallmarks of cytomegalovirus infection. *Med Microbiol Immunol* 2012;201:551-66.
276. Joshi NS, Kaech SM. Effector CD8 T cell development: a balancing act between memory cell potential and terminal differentiation. *J Immunol* 2008;180:1309-15.
277. Masopust D, Ha SJ, Vezys V, Ahmed R. Stimulation history dictates memory CD8 T cell phenotype: implications for prime-boost vaccination. *J Immunol* 2006;177:831-9.
278. Geginat J, Lanzavecchia A, Sallusto F. Proliferation and differentiation potential of human CD8+ memory T-cell subsets in response to antigen or homeostatic cytokines. *Blood* 2003;101:4260-6.
279. DiMenna L, Latimer B, Parzych E, Haut LH, Topfer K, Abdulla S, Yu H, Manson B, Giles-Davis W, Zhou D, Lasaro MO, Ertl HC. Augmentation of primary influenza A virus-specific CD8+ T cell responses in aged mice through blockade of an immunoinhibitory pathway. *J Immunol* 2010;184:5475-84.
280. Kurtulus S, Tripathi P, Hildeman DA. Protecting and rescuing the effectors: roles of differentiation and survival in the control of memory T cell development. *Front Immunol* 2013;3:404.
281. Takai S, Sabzevari H, Farsaci B, Schlom J, Greiner JW. Distinct effects of saracatinib on memory CD8+ T cell differentiation. *J Immunol* 2012;188:4323-33.
282. Hansen SG, Piatak M, Jr., Ventura AB, Hughes CM, Gilbride RM, Ford JC, Oswald K, Shoemaker R, Li Y, Lewis MS, Gilliam AN, Xu G, et al. Immune clearance of highly pathogenic SIV infection. *Nature* 2013;502:100-4.
283. Quinn KM, Da Costa A, Yamamoto A, Berry D, Lindsay RW, Darrach PA, Wang L, Cheng C, Kong WP, Gall JG, Nicosia A, Folgori A, et al. Comparative analysis of the magnitude, quality, phenotype, and protective capacity of simian immunodeficiency virus gag-specific CD8+ T cells following human-, simian-, and chimpanzee-derived recombinant adenoviral vector immunization. *J Immunol* 2013;190:2720-35.
284. Hui EP, Taylor GS, Jia H, Ma BB, Chan SL, Ho R, Wong WL, Wilson S, Johnson BF, Edwards C, Stocken DD, Rickinson AB, et al. Phase I trial of recombinant modified vaccinia ankara encoding Epstein-Barr viral tumor antigens in nasopharyngeal carcinoma patients. *Cancer Res* 2013;73:1676-88.
285. Sashihara J, Hoshino Y, Bowman JJ, Krogmann T, Burbelo PD, Coffield VM, Kamrud K, Cohen JL. Soluble rhesus lymphocryptovirus gp350 protects against infection and reduces viral loads in animals that become infected with virus after challenge. *PLoS Pathog* 2011;7:e1002308.
286. Lasaro MO, Haut LH, Zhou X, Xiang Z, Zhou D, Li Y, Giles-Davis W, Li H, Engram JC, Dimenna LJ, Bian A, Sazanovich M, et al. Vaccine-induced T cells provide partial protection against high-dose rectal SIVmac239 challenge of rhesus macaques. *Mol Ther* 2011;19:417-26.
287. Fukazawa Y, Park H, Cameron MJ, Lefebvre F, Lum R, Coombes N, Mahyari E, Hagen SI, Bae JY, Reyes MD, 3rd, Swanson T, Legasse AW, et al. Lymph node T cell responses predict the efficacy of live attenuated SIV vaccines. *Nat Med* 2012;18:1673-81.
288. Blake NW, Moghaddam A, Rao P, Kaur A, Glickman R, Cho YG, Marchini A, Haigh T, Johnson RP, Rickinson AB, Wang F. Inhibition of antigen presentation by the glycine/alanine repeat domain is not conserved in simian homologues of Epstein-Barr virus nuclear antigen 1. *J Virol* 1999;73:7381-9.
289. Zhou D, Zhou X, Bian A, Li H, Chen H, Small JC, Li Y, Giles-Davis W, Xiang Z, Ertl HC. An efficient method of directly cloning chimpanzee adenovirus as a vaccine vector. *Nat Protoc* 2011;5:1775-85.
290. Lu F, Wikramasinghe P, Norseen J, Tsai K, Wang P, Showe L, Davuluri RV, Lieberman PM. Genome-wide analysis of host-chromosome binding sites for Epstein-Barr Virus Nuclear Antigen 1 (EBNA1). *Virol J* 2010;7:262.

291. Messmer D, Ignatius R, Santisteban C, Steinman RM, Pope M. The decreased replicative capacity of simian immunodeficiency virus SIVmac239Delta(nef) is manifest in cultures of immature dendritic cells and T cells. *J Virol* 2000;74:2406-13.